Synthesis, Characterisation and Reactivity Studies of Low Oxidation State Main Group Element Complexes

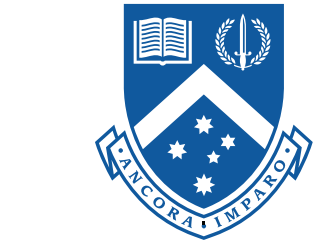

MONASH University

By

Palak Garg

Thesis presented to The School of Chemistry, Monash University
For the degree of Doctor of Philosophy
April 2021

Copyright Notice

Declaration

This thesis contains no material which has been accepted for the award of any other degree or diploma at any university or equivalent institution and that, to the best of my knowledge and belief, this thesis contains no material previously published or written by another person, except where due reference is made in the text of the thesis.

Print Name: Palak Garg

Date: 19-April-2021

To my family whose constant support made it possible

&

in loving memory of my grandfather

Acknowledgements

The past four years, en route my PhD in Melbourne, have been immensely enriching in both academic and personal fronts. It has been a great pleasure to carry out cutting edge research in one of the leading research groups in main group chemistry. This experience has blessed me with several learnings that will stay with me in the journey ahead.

First and foremost, I would like to thank Prof. Cameron Jones for giving me the opportunity to conduct research in his group. His guidance and support throughout the course of my PhD journey has made it a fruitful experience. Hopefully, I will be an expert in the usage of 'THE' after this.

I convey my sincere thanks to Dr. Deepak Dange for introducing me to the lab techniques, his generous assistance in various lab activities and spending time to proof read this thesis.

To Cory (MOPFM), your assistance with the computational chemistry part for chapter 2 and conducting the theoretical studies in chapter 5 which have given valuable insights. I wish to extend my thanks to Dr. Albert Paparo and Dr. Yuvaraj K for always keeping their ears open for all my research queries and weird chemistry ideas, and Dafydd for being always available for my writing queries. Also, a big cheer to the present and former Jones group members (Jacques, Casper, Chris, Martin, Sneha, Michael, Arif, Veronika and Sam) for all the help and the good times we had.

I want to offer my thanks to Monash University for awarding me the scholarships to study in Australia. I also wish to thank the technical staff in the chemistry department for their impromptu help over the years.

A special acknowledgment to my family, 6326 miles away, for their constant encouragement, love and support during the bright days as well as the difficult times. And finally, to all the friends I have made along the way who made life enjoyable in Australia.

Abstract

This thesis appertains to the synthesis and reactivity of low oxidation state main group element complexes through various methods. As such, it is an exploration of the utility of different ligand systems in the stabilisation of low oxidation state especially the group 14 element complexes.

Chapter 1 briefly introduces the origin of low oxidation state main group chemistry. It then focuses on bonding, oxidation state and general synthetic routes to low oxidation state group 14 element complexes.

Chapter 2 focuses on the utilisation of monodentate ligands in group 14 chemistry. The introduction discusses reported monodentate ligands, group 14 element complexes and their reactivity towards small molecules. This is followed by the design and synthesis of novel monodentate pro-ligands, using a theoretical approach. Finally, the synthesis of various germanium(II) halides, germanium(II) alkoxides and germanium(I) dimers is discussed.

Chapter 3 presents the synthesis of bifunctional bis(amidinate) ligands and their use in stabilisation of several main group element complexes. The synthesis of group 2, 13 and 14 element halide precursors are presented utilising the bis(amidinate) ligands bridged by several linker groups. The latter part of the chapter focuses on various attempts to reduce the aforementioned group 2, 13 and 14 element complexes in order to synthesise low oxidation state $[\text{-E-X-E-}]_n$ type species.

Chapter 4 discusses the synthesis and complexation of bulky bis(monodentate) and bis (bidentate) ligand frameworks. The synthesis of multiple linker based bis(amide) and nitrogen bridged bis(amidinate) ligand systems are presented. These ligands are then compared for the stabilisation of alkali metal salts, group 2 and 14 element halide complexes, which however, resulted in the formation of corresponding novel heavier cyclophanes.

Chapter 5 details the reactivity of silicon(I) and germanium(I) dimer complexes. There is a review of the reactivity of low oxidation state silicon(I), silicon(II) and germanium(I) complexes that have been previously reported. Following from this, the reactions of a

silicon(I) dimer toward small molecules CO, CO_2 and N_2O and unsaturated substrates (Bu^tNC and C_2H_4) are explored. The isolation of a diradicaloid species using Bu^tNC has also been demonstrated. The final section covers the investigation of the reactivity of a germanium(I) dimer with H_2, CO and C_2H_4.

Table of Contents

Acknowledgements ..... **i**

Abstract ..... **ii**

Table of Contents ..... **iv**

Abbreviations ..... **ix**

Chapter 1 General Trends in Main Group Chemistry **1**

1.1 Introduction 1

1.2 Low Oxidation State Main Group Chemistry 1

1.2.1 Oxidation States 1

1.2.2 Inert Pair Effect 2

1.2.3 Double Bond Rule 3

1.2.4 Breaking the Double Bond Rule 3

1.2.5 Triple Bond 5

1.2.6 Heavier Carbene Analogues 6

1.2.7 Kinetic Stabilisation 6

1.3 Bonding and Geometry in Low Oxidation State Complexes 7

1.3.1 Heavier Alkene and Alkyne Analogues 7

1.3.2 Heavier Carbene Analogues 12

1.3.3 Substituent Effects on the Ground States of Tetrelenes 13

1.4 Synthetic Strategies Towards Low Oxidation State Group 14 Element Complexes 16

1.4.1 Synthesis of Low Oxidation State Group 14 Element(II) Complexes 16

1.4.2 Reduction to Form Heavier Low Oxidation State Group 14 Element(I) and (II) Complexes 17

1.5 Reactivity of Low Oxidation State Group 14 Element Heavier Tetrelenes and Ditetrelynes 18

1.6 References 20

Chapter 2 Development of Monodentate Bulky Amide Ligands for Synthesis of Germanium(II) Halides and Heavier Ditetrelynes 23

2.1 Introduction 23

2.1.1 Monodentate Ligands 23

2.1.1.1 Terphenyl Ligands 24

2.1.1.2 $(Me_3Si)_2CH$- Substituted Ligands 24

2.1.1.3 Rind-Br 25

2.1.1.4 Aryl-Silyl Amide Ligands 26

2.1.1.5 Boryl-Silyl Amides 27

2.1.1.6 Bis(aryl) Amides and Terphenyl Amides 28

2.1.2 Use of Monodentate Ligands in the Synthesis of Group 14 Element(II) Halides 29

2.1.3 Heavier Group 14 Alkyne Analogues 31

2.1.3.1 Digermynes 31

2.1.3.2 Distannynes 34

2.1.3.3 Diplumbynes 36

2.1.4 Small Molecule Activation using Group 14 Element(I) Dimers 37

2.1.4.1 Reaction with H_2 37

2.1.4.2 Reactions with CO_2, CS_2, N_2O 41

2.1.5 Monomeric two-Coordinate Hydride Complexes 42

2.1.5.1 Synthesis of Group 14 Element(II) Hydride Complexes 42

2.1.5.2 Reactivity of two-Coordinate Group 14 Element(II) Hydride Complexes 44

2.2 Research Proposal 46

2.3 Results and Discussion 47

2.3.1 Synthesis of Bulky Aryl-Silyl Amine Pro-Ligands 47

2.3.2 Synthesis of Aryl-Silyl Amido Group 14 Element(II) Halide Complexes 50

2.3.3 Steric Profile 54

2.3.4 Attempted Reductions of Amido Germanium(II) Chloride Complexes 59

2.3.5 Attempted Synthesis of Monomeric two-Coordinate Germanium(II) Hydride Complexes 63

2.4 Conclusion 65

2.5 Experimental 65

2.6 References 76

Chapter 3 Utilisation of Bidentate Bis(amidinate) Ligands for Stabilisation of Dinuclear Main Group Element Complexes 81

3.1 Introduction 81

3.1.1 Bidentate Ligands 81

3.1.1.1 β-Diketiminate (Nacnac) Ligands 82

3.1.1.2 Amidinate and Guanidinate Ligands 83

3.1.2 Bis(bidentate) Ligands 85

3.1.2.1 Bis(amidinate) Ligands 86

3.1.3 Amidinate and Bis(amidinate) Ligands in Main Group Chemistry 87

3.1.3.1 Group 2 and 13 Element Complexes 88

3.1.3.2 Group 14 Element Complexes 90

3.2 Research Proposal 94

3.3 Results and Discussion 95

3.3.1 Synthesis of Bulky Bidentate Bis(amidinate) Ligands 95

3.3.2 Synthesis of Main Group Element Complexes 96

3.3.2.1 Bis(amidinato) Alkali Metal Salts 96

3.3.2.2 Synthesis of Groups 2 and 13 Complexes 99

3.3.2.3 Synthesis of Group 14 Element Complexes 103

3.3.3 Reduction Attempts 109

3.3.3.1 Attempted Reductions of Group 2 and 13 Element Halide Complexes 109

3.3.3.2 Reductions of Group 14 Element Halide Complexes 110

3.4 Conclusion 115

3.5 Experimental 115

3.6 References 124

Chapter 4 Use of Bis(amide) and (amidinate) Ligands to Stabilise Low Oxidation State Heavier N-donor Bis(tetrelenes) 129

4.1 Introduction 129

4.1.1 Bis(amide) Ligands 129

4.1.2 N-Bridged Bis(amidinate) Ligands 132
4.1.3 Bis(amide) and Bis(amidinate) Coordinated Group 14 Element(II) Tetrelenes 133
4.1.4 Reactivity of Heavier Tetrelenes and Bis(tetrelenes) 138
4.1.4.1 Reactions with σ-bonds 139
4.1.4.2 Reactions with Chalcogens 140
4.1.4.3 Reactions of Tetra(amido) Bis(teterelenes) 140
4.2 Research Proposal 141
4.3 Results and Discussion 142
4.3.1 Synthesis of Ligands 142
4.3.1.1 Aryl Bridged Bis(amines) 143
4.3.1.2 Alkyl/Aryl-Silyl Bis(amines) 144
4.3.1.3 N-Bridged Bis(amidines) 148
4.3.2 Synthesis of Main Group Element Complexes 150
4.3.2.1 Lithiation of Synthesised Pro-Ligands 150
4.3.2.2 Synthesis of Amido Group 14 Element Complexes 151
4.3.2.3 Synthesis of Amidinato Group 2 and Group 14 Element Complexes 156
4.3.3 Reactivity of Synthesised Bis(tetrelenes) 160
4.4 Conclusion 160
4.5 Experimental 161
4.6 References 171
Chapter 5 Reactivity Studies of Amidinate Stabilised Singly Bonded Silicon(I) and Germanium(I) Dimers 176
5.1 Introduction 176
5.1.1 Reactivity of Silicon(I) and Germanium(I) Dimers 176
5.1.1.1 Activation of Small Molecules 176
5.1.1.2 Reactivity Towards Unsaturated Substrates 180
5.1.1.3 Reactivity Towards Transition Metals 183
5.2 Research Proposal 185
5.3 Results and Discussion 186

5.3.1 Reactivity of Silicon(I) Dimer 186
5.3.1.1 Reaction with Carbon Monoxide 186
5.3.1.2 Reaction with Bu^tNC 195
5.3.1.3 Reactions with H_2, CO_2 and N_2O 200
5.3.1.4 Reaction with C_2H_4 203
5.3.2 Reactivity of Germanium(I) Dimer 204
5.4 Conclusion 206
5.5 Experimental 207
5.6 References 213
Appendix I 217
General Synthetic Considerations 217
Appendix II 218
Crystallographic Data 218
Appendix III 219
Computational Studies 219
Appendix IV 220
Publications in Support of this Thesis 220

Abbreviations

δ	Chemical shift in NMR spectroscopy (ppm)
η^n	Hapticity, designates coordination to the metal centre in a "side-on" fashion through n atoms
K	Designates a chelate ring that includes one or more dative bonds
$\Delta_{s\text{-}t}$	Singlet-triplet energy gap
ΔE_{sp}	The energy separating the valence s- and p-orbitals
ΔG	Gibbs free energy
ΔH	Enthalpy
ΔS	Entropy
μ	Designates a bridging ligand
ν/cm^{-1}	Wavenumber
$\Delta_{HOMO\text{-}LUMO}$	HOMO-LUMO energy gap
% bV	Percentage buried volume
Å	Ångström, 1×10^{-10} m
Ar	A general aryl substituent
Ar*	2,6-$(Ph_2CH)_2$-4-MePh
Ar*DAB	$[\{N(Ar^*)C(H)\}_2]^{2-}$
Ar***	2,6-$\{(3,5\text{-}Bu^t{}_2Ph)_2CH\}_2$-4-MePh
Ar†	2,6-$(Ph_2CH)_2$-4-Pr^iPh
Ar#	2,6-$(Ph_2CH)_2$-4-Bu^tPh
Ar"	2,6-$Pr^i{}_2$-4-(CPh_3)-Ph
Ar^N	2,6-$\{(2\text{-Nap})_2CH\}_2$-4-MePh
Bbp	2,6-$\{(Me_3Si)_2CH\}_2$Ph
Bbt	2,6-$\{(Me_3Si)_2CH\}_2$-4-$\{(Me_3Si)_3C\}$Ph
br	Broad
Bu^i	Isobutyl/Me_2CHCH_2
Bu^n	Primary butyl
Bu^s	Secondary butyl
Bu^t	Tertiary butyl, $(CH_3)_3C$
Bu^tO	$(CH_3)_3CO$

C	Celsius
ca.	Circa/approximately
cal	Calorie (1 kcal = 4.184 J)
cat	Catecholato/1,2-O_2-Ph
cat.	A catalytic amount
cf.	Confer/compare with
Cp	Cyclopentadienyl/C_5H_5
Cy	Cyclohexyl
$^{Cy}L^{*}$	$\{(Cy_3Si)Ar^{*}N\}^{-}$
$^{Cy}L^{\dagger}$	$\{(Cy_3Si)Ar^{\dagger}N\}^{-}$
$^{Cy}L^{N}$	$\{(Cy_3Si)Ar^{N}N\}^{-}$
C_6D_6	Deuterated benzene
d	Doublet
DAB	Diazobutadiene/$\{CHN(R)\}_2$
DBF	Dibenzofurandiyl
DCM	Dichloromethane/CH_2Cl_2
decomp.	Decomposition
Dep	2,6-Et_2Ph
DFT	Density Funcitonal Theory
DIBAL-H	Diisobutylaluminium hydride/Bu^{i}_2AlH
Dip	2,6-diisopropylphenyl/2,6-Pr^{i}_2Ph
Dip^{+}	2,6-Pr^{i}_2-4-Bu^{t}Ph
^{Dip}Ar	2,6-$(Dip)_2$Ph
$^{Dip}Ar^{Cl}$	2,6-$(Dip)_2$-4-ClPh
$^{Dip}Ar^{F}$	2,6-$(Dip)_2$-4-FPh
$^{Dip}Ar^{OMe}$	2,6-$(Dip)_2$-4-OMePh
$^{Dip}Ar^{tBu}$	2,6-$(Dip)_2$-4-Bu^{t}Ph
$^{Dip}Ar^{TMS}$	2,6-$(Dip)_2$-4-TMSPh
^{Dip}DAB	$[\{N(Dip)C(H)\}_2]^{2-}$
^{Dip}Nacnac	$[\{N(Dip)C(Me)\}_2HC]^{-}$
Dip^{Y}	2,6-Pr^{i}_2-4-Pr^{i}Ph
DMAP	*p*-dimethylaminopyridine/4-Me_2NPy
E	Element

e^-	Electron
Et	Ethyl/C_2H_5
e.g.	*Exemplī grătiā*/for example
E_{hybrid}	The energy of hybridisation
EHT	Extended Hückel theory
Eind	1,1,3,3,5,5,7,7-octaethyl-s-hydrindacen-4-yl
EMind	1,1,7,7-tetraethyl-3,3,5,5-tetramethyl-s-hydrindacen-4-yl
en	Ethylenediamine
g	Gram
HB_{cat}	Catechol borane
HB_{pin}	Pinacol borane
HMDS	Hexamethyldisilazane/$(Me_3Si)_2NH$
HOMO	Highest Occupied Molecular Orbital
Hz	Hertz, s^{-1}
i.e.	*id est*/it is, in other words
IPr	$\{C(H)N(Dip)_2\}C:$
$^{i\text{Pr}}L^*$	$\{(Pr^i_3Si)(Ar^*)N\}^-$
$^{i\text{Pr}}L^\dagger$	$\{(Pr^i_3Si)(Ar^\dagger)N\}^-$
IPrIMe	$:C(Pr^iNCMe)_2$
$^{i\text{Pr}}L^N$	$\{(Pr^i_3Si)(Ar^N)N\}^-$
IR	Infrared
in vacuo	In a vacuum/under vacuum
J	Joule
K	Kelvin
KC_8	Potassium graphite
K-Selectride	$(Bu^s)_3BHK$
L	A ligand
LDA	Lithium diisopropyl amide/Pr^i_2NLi
$LiBu^n$	n-Butyllithium

$LiAlH_4$	Lithium aluminium hydride
L-Selectride	$(Bu^s)_3BHLi$
LUMO	Lowest Unoccupied Molecular Orbital
m	Mulitplet (NMR), medium (IR)
M	A metal
M	Molar (mol L^{-1})
M^+	A molecular ion (MS)
Me	Methyl, CH_3
Mes	2,4,6-Me_3Ph
Mes^*	2,4,6-Bu^t_3Ph
^{Mes}Ar	2,6-$(Mes)_2$Ph
^{Mes}Nacnac	$[\{N(Mes)C(Me)\}_2CH]^-$
Mg(I)	$\{(^{Mes}Nacnac)Mg\}_2$
MG	Main Group
MHz	Megahertz, 10^6 Hz
mL	Millilitre/1×10^{-3} L
MO	Molecular Orbital
mol	Mole
M.p.	Melting Point
MS	Mass Spectrometry
$NaBH_4$	Sodium borohydride
Nacnac	A general β-diketiminate ligand
NaH	Sodium hydride
nbd	Norbornadiene
NBO	Natural Bond Order
NBS	N-bromosuccinimide
NHC	N-heterocyclic carbene
$^nJ_{EE'}$	Coupling constant between nuclei E and E' separated by n bonds
NMR	Nuclear Magnetic Resonance
OA	Oxidative Addition
p	Principle (orbital)

p-Bu^{t}Ph/4-Bu^{t}Ph	Para-tertiary butyl phenyl
^{PhBo}L	$\{(^{Dip}DAB)B(SiPh_3)N\}^-$
^{Ph}L*	$\{(Ph_3Si)Ar^*N\}^-$
^{Ph2Me}L*	$\{(MePh_2Si)Ar^*N\}^-$
Ph	Phenyl/C_6H_5
pin	Pinacolato
ppm	parts per million
Pr^i	Isopropyl/$(CH_3)_2HC$
Py	Pyridine
q	Quartet
R/R’	general organic moiety
Rind	1,1,3,3,5,5,7,7-octa-R-substituted s-hydrindacenyl
s	Singlet (NMR); Strong (IR)
s	Sharp (orbital)
sept	Septet
SOJT	Second-Order Jahn-Teller effect
t	Triplet (NMR)
T	Temperature
Tbb	2,6-$\{(Me_3Si)_2CH\}_2$-4-Bu^{t}Ph
^{TBo}L	$\{(^{Dip}DAB)B(TMS)N\}^-$
Tbt	2,6-$\{(Me_3Si)_2CH\}_2$-4-$\{(Me_3Si)_2CH\}$Ph
^{tBu6}Ar	2,6-(2,4,6-Bu$^t{}_3$Ph)$_2$Ph
^{tBuMes}Nacnac	$[HC\{N(Mes)C(Bu^t)\}_2]^-$
^{tBuPh}L*	$\{(4\text{-}Bu^tPh)_3Si\}(Ar^*)N\}^-$
^{tBuPh}L†	$\{(4\text{-}Bu^tPh)_3Si\}(Ar^\dagger)N\}^-$
^{tBuPh}L^N	$\{(4\text{-}Bu^tPh)_3Si\}(Ar^N)N\}^-$
^{tBuO}L*	$[\{(Bu^tO)_3Si\}Ar^*N]^-$
^{tBuO}L†	$[\{(Bu^tO)_3Si\}Ar^\dagger N]^-$
THF	Tetrahydrofuran/$(C_2H_4)_2O$
THF-d_8	Deuterated toluene/$(C_2D_4)2O$
TMC	Tetramethyl carbene/$\{:C(MeNCMe)_2\}$

TMEDA	Tetramethylethylenediamine/$(Me_2NCH_2)_2$
TMS	Trimethylsilyl/Me_3Si
$^{TMS}L^{*}$	$\{(TMS)Ar^{*}N\}^{-}$
$^{TMS}L^{***}$	$\{(TMS)Ar^{*}N\}^{-}$
$^{TMS}L^{\#}$	$\{(TMS)Ar^{\#}N\}^{-}$
$^{TMS}L^{N}$	$\{(TMS)Ar^{N}N\}^{-}$
Trip	2,4,6-Pr^{i}_3Ph
^{Trip}Ar	2,6-$(Trip)_2Ph$
$^{Trip}Ar^{i}Pr2$	2,6-$(Trip)_2$-3,5-Pr^{i}_2Ph
Toluene-d_8	Deuterated toluene/C_7D_8
tosyl	4-MePh-SO
UV	Ultra Violet
UV-Vis	Ultraviolet-visible
v	Very
viz.	Videlicet/namely
VT	Variable Temperature
WB indices	Wiberg Bond indices
w	Weak (IR)
X	A halide/F, Cl, Br or I
Xyl	2,6-Me_2-Ph

Chapter 1
General Trends in Main Group Chemistry

1.1 Introduction

For a long time, metal complex chemistry was dominated by transition metals (d-block elements) as they could be isolated in multiple oxidation states. In contrast, the stability of main group element complexes was limited to only a few oxidation states, hence, their chemistry considered largely underdeveloped. However, the past three decades have seen an enormous growth in accessibility of several oxidation states in such main group elements, specifically towards the development of low oxidation state main group element complex chemistry and reactivity.

The introduction and the subsequent chapters in this thesis will focus on bonding, synthesis and reactivity aspects of low oxidation main group element complexes, particularly those of heavier group 14 elements.

1.2 Low Oxidation State Main Group Chemistry

1.2.1 Oxidation States

The significant recent interest in main group (s- and p-block) element chemistry is not only because of their lesser toxicity and high natural abundance in earth's crust (e.g. Si and Al are 28 % and 8.3 % abundant), but also due to their resemblance to the transition metal counterparts.[1]

As stated above, the observation of multiple oxidation states is a relatively new phenomenon among main group elements. Parkin defined the oxidation state as, "The charge remaining on an atom when all the ligands are removed heterolytically in their closed form, with the electrons being transferred to the more electronegative partner; homonuclear bonds do not contribute to the oxidation state."[2] An element can generally have an oxidation state as per the number of valence electrons in its periodic group, which could also vary according to the electronegativity of the associated ligand.

Unlike transition metals which can exhibit several oxidation states due to partially filled d-orbitals, main group elements are typically found in one or at the most two oxidation

states in their complexes. For example, the s-block elements belonging to groups 1 and 2, can acquire a charge of +1 (alkali metals) and +2 (alkaline earth metals), respectively. The lighter p-block elements follow a similar behaviour in accordance to their group number. However, this changes for the heavier p-block elements due to the inert pair effect.

As the name suggests, the term 'low oxidation' refers to an oxidation state lower than the usual oxidation number of that group or element. For instance, magnesium is most stable in +2 oxidation state, whereas a complex containing magnesium in +1 oxidation state will be stated as a low oxidation state compound.[3]

1.2.2 Inert Pair Effect

The term 'inert pair' was first coined in 1927 by Nevil Sidwick.[4] Inert pair effect defines the tendency of two valence electrons of the outermost s-orbital to remain unshared in bonding (as lone pairs) as they are tightly bound to the nucleus, also called as 'inert pair'. This effect can be observed for heavier groups 13, 14, 15 and 16 elements of the periodic table.

For example, when talking about the group 14 elements, they have a general valence electronic configuration ns^2p^2 and one should expect a +4 oxidation state. The lightest element, carbon, shows variable oxidation states from -4 to +4. Silicon mostly favours +4 state, germanium and tin show both +2 and +4 oxidation states, while the heaviest element, lead prefers +2 oxidation state. These observations can be well explained by the inert pair effect. In case of germanium and tin, this effect is attributed to the 'd-block contraction' owing to the poor shielding of d-orbitals which increases the effective nuclear charge on the outer s-electrons. This leads to a stronger binding and leaves the valence s-electron pair inert.[5,6] For lead, both f-block contraction (similar to d-block contraction but results in greater effective nuclear charge due to the more diffused f-orbitals) and the relativistic effect make the 6s electron pair inert.[6] The relativistic effect states that the faster an object moves the heavier it becomes, and approaches the speed of light at infinite mass. On moving down the group (towards lead), the velocity of the 1s electrons increases so that they do not 'fall-into' the nucleus. This results in a slight increase in their mass and induces a contraction of 1s-orbital as well as the higher s-orbitals. The p-orbitals in the inner shells with higher angular momentum remain unaffected, hence there are larger energy level separations between *n*s- and *n*p-orbitals,

which also gives rise to an increase in the energy of hybridisation (E_{hybrid}) between these orbitals. Therefore, the formation of an s-character unshared electron pair on the element centre is more likely. Thus, in the heaviest congener, the energy of hybridisation is comparatively large.

1.2.3 Double Bond Rule

In case of lighter main group elements, the ability to form multiple bonds is ubiquitous, e.g. alkene, alkyne and carbonyls. However, for heavier main group elements the multiple bonding was considered to be impossible. This phenomenon was proposed as "Classical Double Bond Rule". Pitzer suggested that "elements having a principle quantum number greater than two should not be able to form the pπ-pπ bonds with themselves or with other elements".[7] Mulliken explained this lack of π-bonding by considering the greater strength of σ-bond over π-bond for heavier elements.[8] He showed that the energy for pσ-pσ bond formation ($E_{p\sigma\text{-}p\sigma}$) for the second row elements was greater than the sum of $E_{s\sigma\text{-}s\sigma}$ and $E_{p\pi\text{-}p\pi}$ bonds.

1.2.4 Breaking the Double Bond Rule

The double bond rule was continuously proved by experimental evidence until 1976, when Lappert and co-workers isolated and characterised a tin(II) species $[\{(Me_3Si)_2CH\}_2Sn]_2$.[9] This divalent tin species was also termed a 'distannene' and exists as a dimer in the solid-state. However, it dissociates to a monomeric singlet heavier carbene analogue $[\{(Me_3Si)_2CH\}Sn:]$ in cyclohexane or in benzene solution (**Scheme 1.1**).[10]

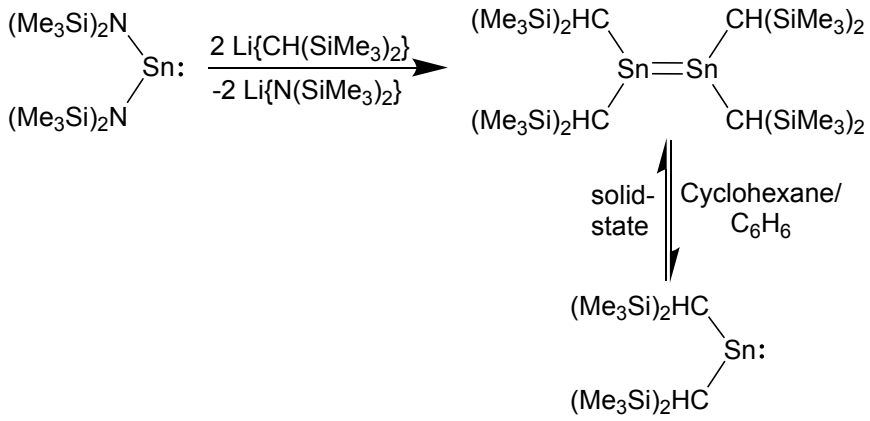

Scheme 1.1. Synthesis of the first "distannene" and its equilibrium with a heavier carbene analogue.

This tin dimer was structurally characterised and comprises a weak double (Sn=Sn) bond in solid-state. The Sn-Sn distance was 2.764(2) Å, which was found to be similar to that reported for hexaphenyldistanane [$(Ph_3Sn)_2$] (cf. 2.770(4)).[11] Unlike alkenes, the heavier tin analogue featured a bent geometry with C-Sn-C unit at a dihedral angle of 112° to the double bond. Due to its dissociation into monomeric species in solution, the double bond rule was not completely dissatisfied at this point.

However, the double bond theory was completely invalidated with the isolation of first thermally stable disilene by West et al.[12] and disphsophene by Yoshifuji and co-workers in 1981.[13] West reported a multiply bonded silicon(II) compound [$\{(Mes)_2Si\}_2$] (Mes = 2,4,6-Me_3Ph) which was synthesised by the photolysis of [$(Mes)_2Si(SiMe_3)_2$] in hexane at room temperature (**Scheme 1.2**). The disilene featured a double bond between the two silicon centres.[14,15] The Si=Si bond distance was 2.16 Å, which is 0.2 Å shorter than the Si-Si single bond in the dihydro compound (cf. $Ph_2HSiSiHPh_2$),[16] indicating the presence of a pπ-pπ bond. Each silicon centre showed a moderately pyramidal arrangement of atoms.

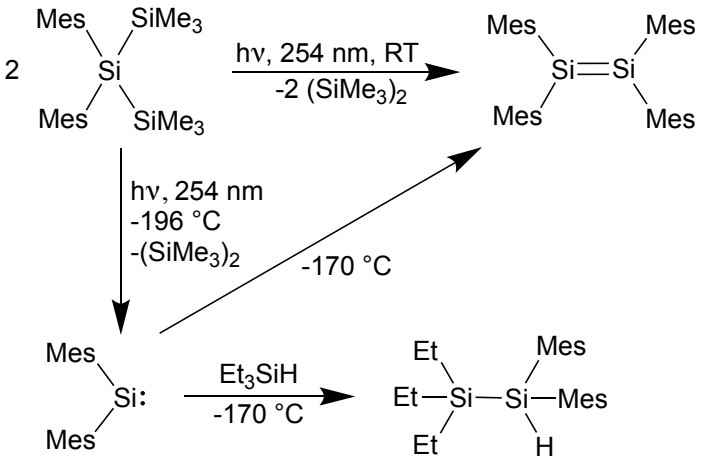

Scheme 1.2. Synthesis of the first disilene [$(Mes)_2Si=Si(Mes)_2$].

West et al. found that this disilene was stable at room temperature (in absence of air) and formed in highest yield (80 % conversion) at -100 °C. They also observed that when the photolysis of the starting material was done at -196 °C, a blue coloured compound was observed rather than a yellow solution. They proposed the blue compound to be the monomeric silylene [$(Mes)_2Si$:]. This silylene could not be isolated at that time, although, the reaction with triethyl silane resulted in a Si-H bond insertion. Further, warming up the solution to -170 °C gave rise to the dimerisation product, i.e., disilene (**Scheme 1.2**).

The first diphosphene synthesis involved the reduction of [(Mes*)PCl_2] (Mes* = 2,4,6-Bu^t_3Ph) with magnesium metal under argon (**Scheme 1.3**).[13] The resulting orange coloured compound [(Mes*)P=P(Mes*)] was surprisingly thermally stable and could be handled in air. The P-P double bond (2.034 Å) was considerably shorter than in singly bonded phenyl phosphanes (e.g. $(PhP)_5$ = 2.217 Å, $(PhP)_6$ = 2.237 Å).[17,18] This indicated the presence of π-bonding character in diphosphene, despite the strong steric hindrance of the Mes* group.

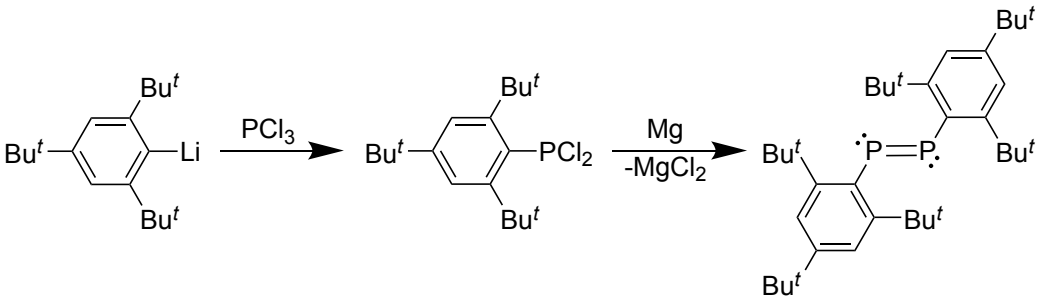

Scheme 1.3. Synthesis of the first diphosphene [(Mes*)P=P(Mes*)].

1.2.5 Triple Bond

Following the discovery of double bonded compounds, the first triple bonded compound with two heavier main group elements was isolated much later, in 1997.[19] This first triply bonded species a 'digallyne' [{(^{Trip}Ar)Ga}$_2$$Na_2$] (^{Trip}Ar = 2,6-$(Trip)_2$Ph, Trip = 2,4,6-$Pr^i_3$Ph) was synthesised by Robinson and co-workers. The synthesis involved the reduction of [(^{Trip}Ar)$GaCl_2$] over sodium metal (**Scheme 1.4**). The Ga-Ga bond distance (2.319(3) Å) was much shorter than the reported digallium species ([{$(Me_3Si)_2CH$}$_2$Ga]$_2$, Ga-Ga = 2.541(1) Å).[20] Different from acetylene, the digallyne featured a bent structure around the Ga-Ga bond with average C-Ga-Ga bond angle of 131.0°.

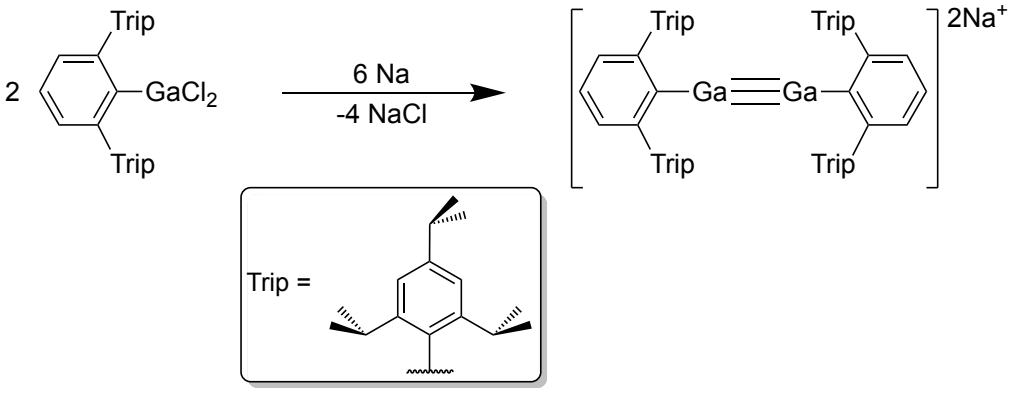

Scheme 1.4. Synthesis of the first "triply" bonded compound 'digallyne'.

However, in 1998, DFT calculations carried out by Cotton et al. proved it to be a double bonded species.[21] They found that the shortening of the Ga-Ga bond distance was a result of non-covalent attractive interactions between sodium atom and substituted phenyl rings branched on the bulky ligand of galliums. That being said, the geometry and bonding in triply bonded heavier congeners were not fully explored until early 2000s.

1.2.6 Heavier Carbene Analogues

Heavier carbenes analogues or tetrelenes are neutral L_2E: (L = ligand, E = Si-Pb) compounds which contain a two-coordinate element centre in +2 oxidation state. However, for a long time, they were only seen as intermediates generated *in situ* during UV radiation and pyrolysis.[22,23] The first isolated stable germanium, tin and lead tetrelenes as well as silylene are given in **Figure 1.1**.[24,25]

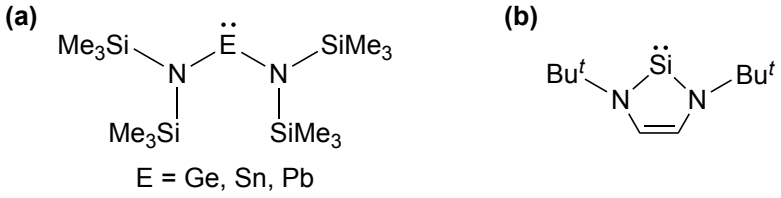

Figure 1.1. The first isolated stable tetrelenes (Ge, Sn, Pb) and silylene.

1.2.7 Kinetic Stabilisation

In theory, it is difficult to prepare low oxidation state main group element complexes. These complexes are thermodynamically unstable, which is why they have a tendency to disproportionate into a compound with the stable oxidation state and the element.[26] Additionally, during synthesis they favour oligomerisation reactions.[27] To overcome such issues, sterically demanding bulky or chelating ligands are employed in order to kinetically stabilise these compounds in lower oxidation states. The kinetic stabilisation increases the activation energy of disproportionation and oligomerisation, thus allowing access to the low oxidation compounds. Since such realisation, a plethora of compounds have been isolated using the kinetic stabilisation method.[28] The ligands used for synthesising these complexes are elaborately discussed in chapter 2 and chapter 3.

1.3 Bonding and Geometry in Low Oxidation State Complexes

1.3.1 Heavier Alkene and Alkyne Analogues

Alkenes ($R_2C{=}CR_2$) and alkynes (RC≡CR) show linear and planar geometries, respectively, which is not the case with the heavier alkene and alkyne analogues. On descending group 14, the donor-acceptor type interaction in heavier ditetrelynes becomes less stable. In ditetrelynes, this feature starts with disilyne which has a strong triple bonding character with relatively smaller Si-Si bond distance and larger R-Si-Si bond angle.[29,30] While diplumbynes show exclusively a Pb-Pb single bond with a non-bonded lone pair of electrons on each lead centre, larger bond length and a nearly 90° trans-bent angle (**Figure 1.2**).[31] The bonding character in digermynes and distannynes varies according to ligand substituents and is largely discussed in chapter 2.[32–34]

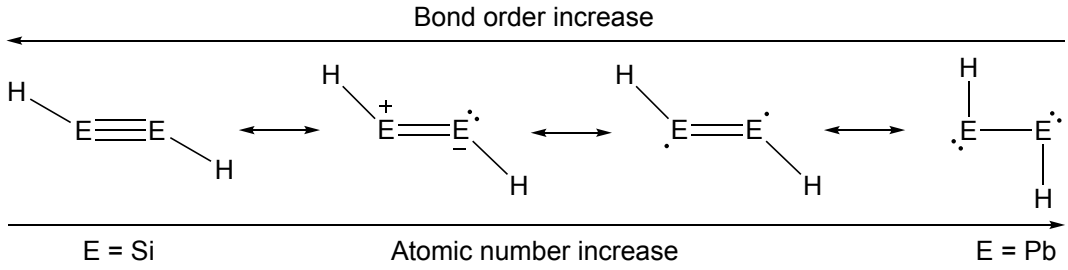

Figure 1.2. Bonding trends in heavier triple bonded ditetrelynes.

A similar trend of shortening of bond distances has also been observed in case of heavier alkene analogues. In short, the bond angle increases with the atomic number and the bending becomes more pronounced in heavier alkynes. This phenomenon is termed as trans-bending and can be seen in heavier group 14 element (Si-Pb) complexes (**Figure 1.3**).

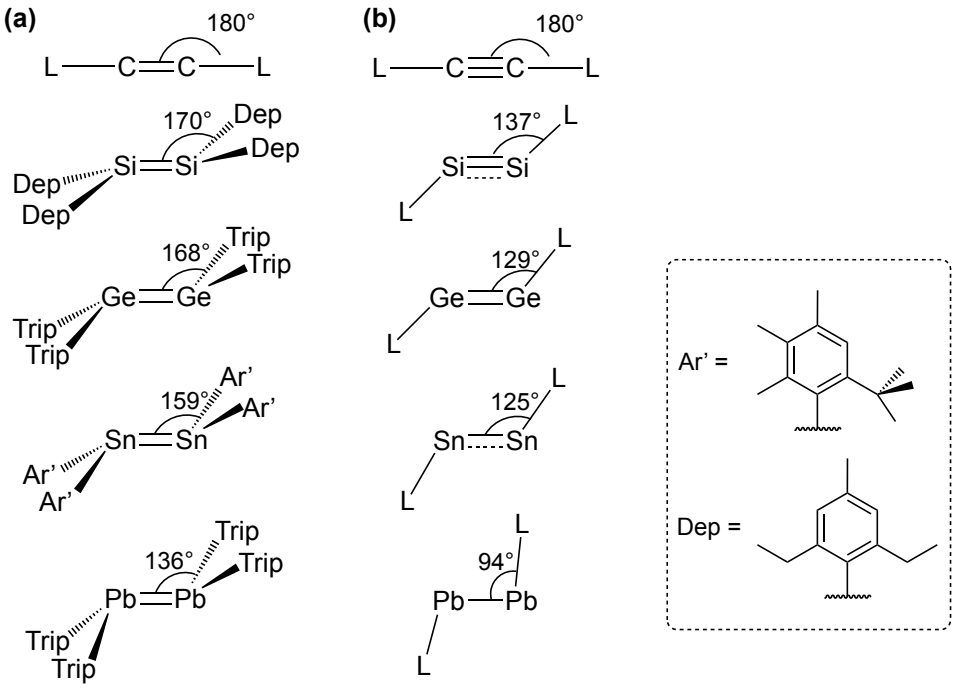

Figure 1.3. L-E-E bond angles in heavier group 14 alkene (**a**)[35–38] and alkyne (**b**) analogues.

Trans-bending can be best explained by considering the **1**) orbital properties, **2**) inert pair effect and **3**) orbital hybridisation. On descending the group, the size of atomic orbitals (*n*s and *n*p) increases as the principle quantum number increases, but this increase in size of s- and p-orbitals is not at the same rate. In fact, the outer p-orbital increases more in size than the corresponding s-orbital for heavier elements.[39] That is why, in case of carbon, similarly sized s- and p-orbitals form 'good' hybrid orbitals. Whereas, for heavier elements the hybridisation becomes difficult and they tend to bond with higher p-orbitals leaving two non-bonding electrons in the higher s-orbital as unshared. This can also be illustrated by the example on comparing the heavier analogues (EH_n, E = Si-Pb, n = 1 or 2) with carbene (CH_2) and carbynes (CH) (**Figure 1.4**).

In case of s- and p-orbital hybridisation, carbenes and carbynes exist in triplet and quartet configurations, respectively. The heavier analogues, on the other hand, prefer EH and EH_2 in their corresponding singlet and doublet configurations, without or with less hybridisation. Additionally, the two valence electrons tend to remain as a lone pair on descending the group due to the 'inert pair effect' (section **1.2.2**). To sum up, the diffusiveness of p-orbitals and poor hybridisation leads to the weak π-bonding in heavier analogues and so called 'trans-bending'. This phenomenon can be explained by considering the valence orbitals, or more precisely by molecular orbital theory.

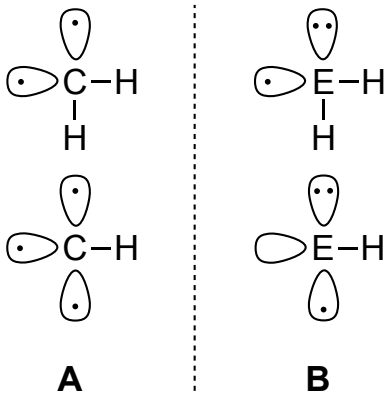

Figure 1.4. Carbene and carbyne in triplet and quartet states, respectively (**A**), heavier group 14 analogues in singlet and doublet states, respectively (**B**).

In case of alkene formation, the two CH_2 monomers in triplet ground state combine to form σ- and π-bonds through sharing of unpaired electrons. This is not the case in heavier alkenes as they prefer the singlet configuration, a lone pair of electrons is present in the valence *n*s-orbital. When EH_2 monomers try to combine, electrostatic repulsion by the lone pairs forces two monomers to rotate divergently in order to alleviate this repulsion. This allows the donation of sp^2 lone pair of one monomer element centre to the empty p-orbital of the neighbouring monomer element centre, resulting in formation of two dative bonds leading to a trans-pyramidal geometry (**Figure 1.5**).

A similar situation occurs during the formation of triple bonds. CH having a quartet state allows the head on overlap of two CH monomers which enables the formation of a σ- and two π-bonds with a linear geometry. While, again, with heavier group 14 elements the repulsion between heavier EH monomers cause a rotation, which results in the formation of two dative bonds. Also, one formal π-bond forms between the unpaired electrons located within p_z-orbitals of each EH monomer, giving an overall trans-bent geometry to the molecule. This observation can also be explained on the basis of molecular orbital theory.

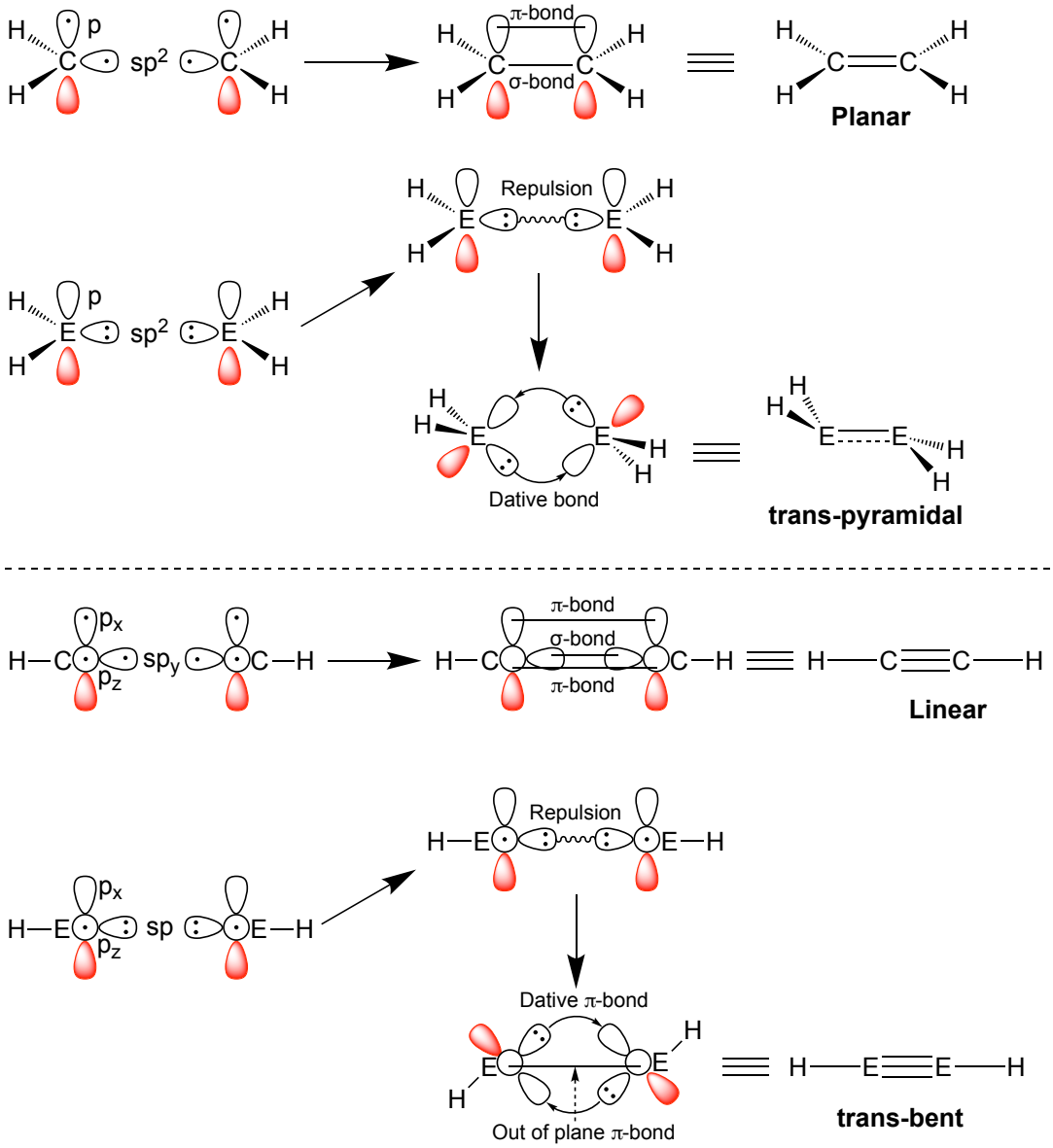

Figure 1.5. Interaction modes for the formation of double (top) and triple (bottom) bonds including carbon and heavier group 14 elements (E = Si, Ge, Sn and Pb).

Molecular orbital theory describes the trans-bending phenomenon on the basis of formation of bonding, anti-bonding orbitals and mixing of these orbitals. The bending in heavier analogues can be explained if we consider the molecular orbitals of ethylene and digermene (bending of 40° through extended Hückel theory (EHT) calculations) (**Figure 1.6**).[40]

In case of the heavier alkene analogues, as it starts to bend, a mixing of π* and σ molecular orbitals (MOs) occurs due to the same a_g symmetry of these orbitals. A similar mixing occurs for both a_u symmetry MOs, π and σ*. Without mixing, the energy of σ* should go down while π should go up. However, as a result of mixing, the energy of

mixed orbitals $1b_u$, $2a_g$ and $2b_u$ decreases whilst that of a_g orbital increases. In ethylene, the $1a_g$ destabilisation is close to digermene (ethylene = +0.38 eV, digermene = +0.32 eV), but the difference lies in b_u stabilisation which is very small in ethylene (-0.19 eV) as compared to digermene (-0.47 eV). Thus, the total energy of the system decreases as a result of mixing in digermene while it increases in ethylene. Consequently, the bent geometry is more favoured over the planar geometry in digermene.

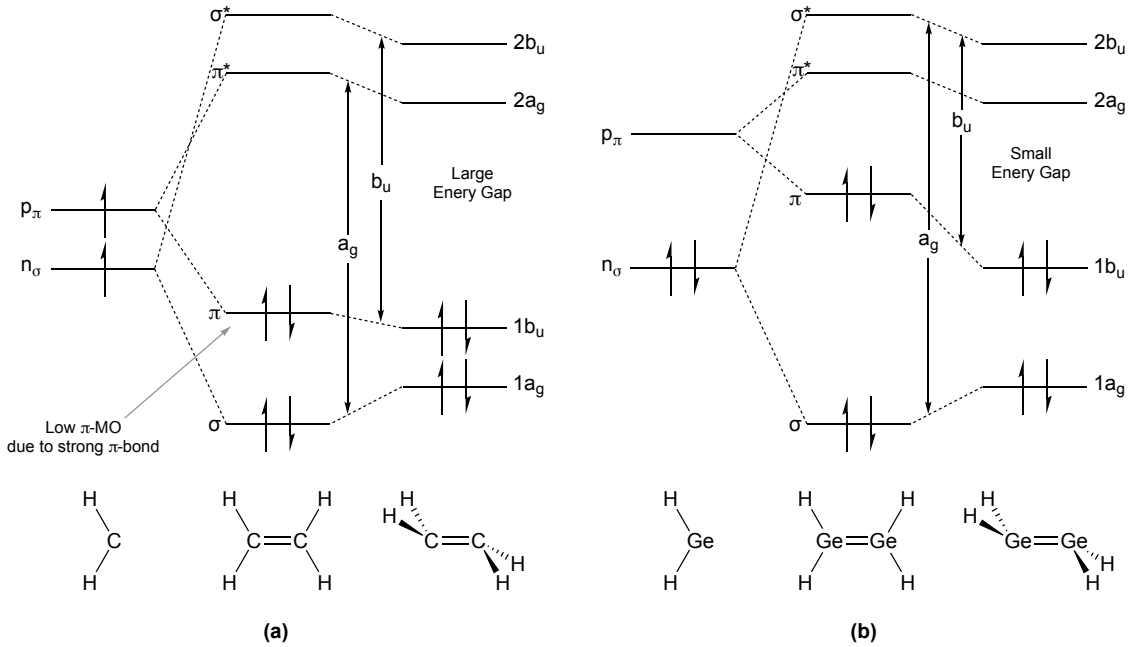

Figure 1.6. Molecular orbital diagram relating ethylene (**a**) and digermene (**b**) conversion from planar to trans-pyramidal geometry.

The more significant b_u mixing in digermene is due to the smaller π- and σ*-separations as compared to ethylene. This shorter separation is a consequence of two factors in digermene **a**) the larger distance between nσ and pπ and **b**) the weaker π-bonding as compared to ethylene, which leads to the higher energy of the π-orbital. These factors work in an opposite way for σ- and π*-separation.

This type of orbital mixing is also called second-order Jahn-Teller effect (SOJT). It involves the symmetry allowed mixing of filled highest occupied molecular orbital (HOMO) and low lying unoccupied molecular orbital (LUMO+1), which are close in energy (π and σ* in this case).[40] This mixing can be used to elucidate the bonding in heavier alkyne analogues. Similar to SOJT mixing in heavier alkene analogues, mixing occurs between in-plane π-bonding orbital and σ*-orbital of b_u symmetry on bending (**Figure 1.7**).[40] It gives rise to a π-bond with significant non-bonded electron pair

character, also referred as 'slipped' π-bond. The mixing of σ and π* weakens the σ-bond. SOJT mixing readily occurs in heavier group 14 elements as the gap between bonding and antibonding is much smaller compared to carbon.[1,41]

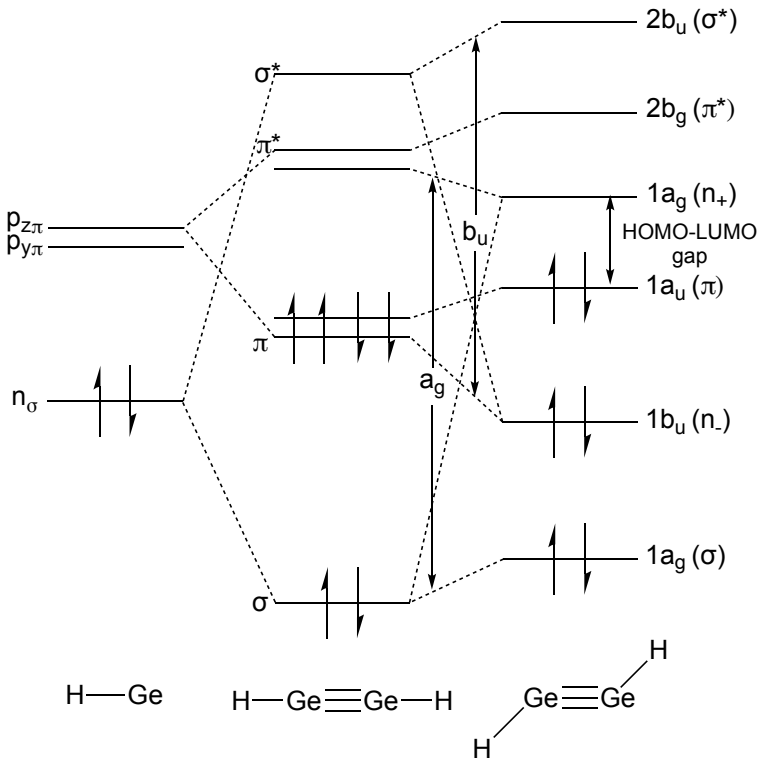

Figure 1.7. Molecular orbital diagram of digermyne in linear and trans-bent geometries.

1.3.2 Heavier Carbene Analogues

Tetrelenes can exist in two electronic configurations, depending on the electron filling arrangement of their orbitals, namely singlet and triplet states (**Figure 1.8**).[42] The singlet state refers to a system in which the valence electrons in n-orbital form a lone pair of electrons and leaves an empty p-orbital. While for triplet state, one electron resides in both n- and p-orbitals. The electronic configuration of tetrelenes is dependent on the n- to p-orbital energy gap. This gap is also called as singlet triplet gap ($\Delta_{s\text{-}t}$), which is nothing, but the energy required to promote an n-orbital electron of the singlet state to the p-orbital for the formation of triplet state. On considering the ground state multiplicity of the EH_2 species (E = C-Pb), methylene CH_2 exhibits a ground state triplet with the singlet state being higher in energy by 9.0 kcal/mol.[43] While in case of the other elements (Si-Pb), they are ground state triplets with significantly higher singlet state energies than triplet state energies (tetrelenes, $\Delta_{s\text{-}t}$ (kcal/mol) = SiH_2 = 21; GeH_2 = 23.1; SnH_2 = 23.8; SnH_2 = 41.0).[44,45]

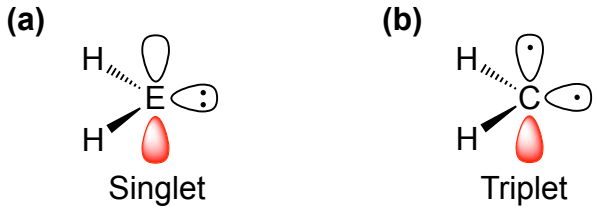

Figure 1.8. Electronic configurations representation of a singlet (**a**) and triplet (**b**) states.

This trend describes that on moving down the group the singlet becomes more stable with increasing molecular weight of group 14 elements.[46] It can be explained by considering three factors: **a**) Pairing energy - in case of singlet state the two paired electrons are in same plane which results in a much greater repulsion as compared to the triplet. Since the orbitals are more diffused on moving down in a group, repulsion becomes lesser, and the pairing energy decreases on moving to silicon form carbon. Hence, the pairing energy required for CH_2 is 12.7 kcal/mol more than SiH_2. **b**) Electrostatic stabilisation and orbital mixing - according to Bent's rule, electronegative substituents bind to the orbital with more p-character while leaving the s-orbital for electropositive substituents like lone pair.[47] In CH_2, the nearly non-polar C-H bonds have similar p- and s-orbital concentrations. On the other hand, in EH_2 (E = Si-Pb) the E-H bonds are relatively more polarised (due to higher electronegativity of H) which results in a lone pair with more s-character and lower energy with a preference towards singlet state. **c**) Orbital mixing - due to the poor hybridisation of elements from second row the s-p mixing becomes less favoured. This contributes to a more s-character lone pair, thus lowering the energy. On comparing the s-character of SiH_2 and CH_2 lone pairs, the former has 89 % s-character while the later has 52 % s-character.[48]

1.3.3 Substituent Effects on the Ground States of Tetrelenes

The singlet triplet energy gaps in heavier carbenes are not fixed and can be altered via steric and electronic effects. The effect of substituents on $\Delta_{s\text{-}t}$ have been studied using UV-vis spectroscopy, by which the absorption of excitation by one electron leading to transition from non-bonding orbital to the vacant p-orbital can be analysed.[49]

In general, the substituents can have a σ- and π-donating or withdrawing effects on the heavier element's n- and p-orbitals. The electropositive substituents (e.g. SiH_3) result in σ-donation through inductive effect, which increases the energy of n-orbital, thus stabilising the triplet state and destabilising the singlet state. In contrast, electronegative

substituents such as F, CF_3 result in withdrawal of the electron density through induction which decreases the energy of n-orbital lone pair and stabilises singlet state. π Substituents also show a similar effect over the p-orbital as the σ-donation shows over n-orbital.

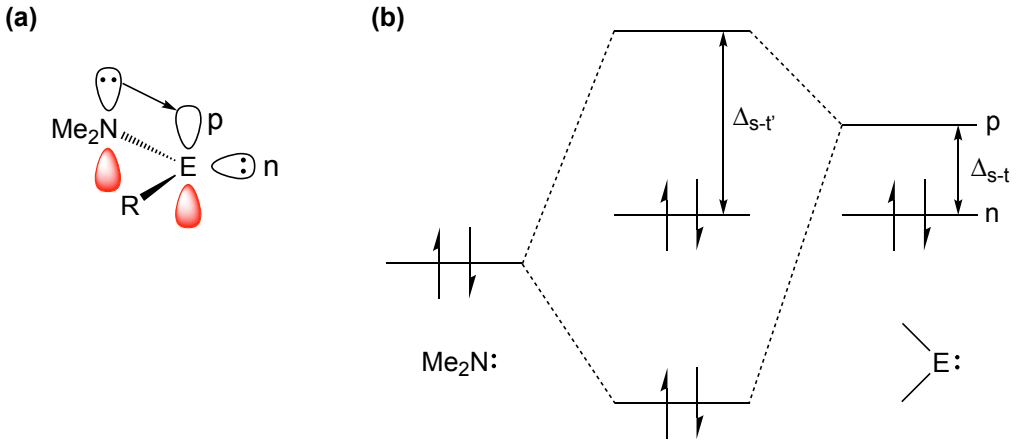

Figure 1.9. Molecular orbital diagram of n-donating substituents effect on heavier tetrelenes.

Substituents with a lone pair are able to donate electron density to empty p-orbital (n-bonding), which results in a hypsochromic (blue) shift in UV-vis spectroscopy. This partial donation of lone pair increases the energy of p-orbital. E.g. in case of **Figure 1.9** the n-donor ligand NMe_2 partially donates its lone pair to empty p-orbital of element centre, which increases the p-orbital energy and affects the $\Delta_{s\text{-}t}$.

From the above observation, one would expect a similar blue shift in case of vinyl/aryl substituents as they also contain π-electron density which can be donated to the empty p-orbital. However, this was not found to be true, instead, a bathochromic shift (red shift) was observed.[50] This difference arises due to the mixing of low lying π*-orbitals of an unsaturated substituent, and the two-step process can also be seen in **Figure 1.10**. When the occupied π-orbital of vinyl group interacts with the 3p-orbital of Si, it results in the formation of bonding and antibonding π-3p orbitals. The formed anti-bonding π-3p orbital further interacts with the low lying π*-orbital of vinyl substituent, which lowers the $\Delta_{s\text{-}t}$ energy and thereby shows a red shift.

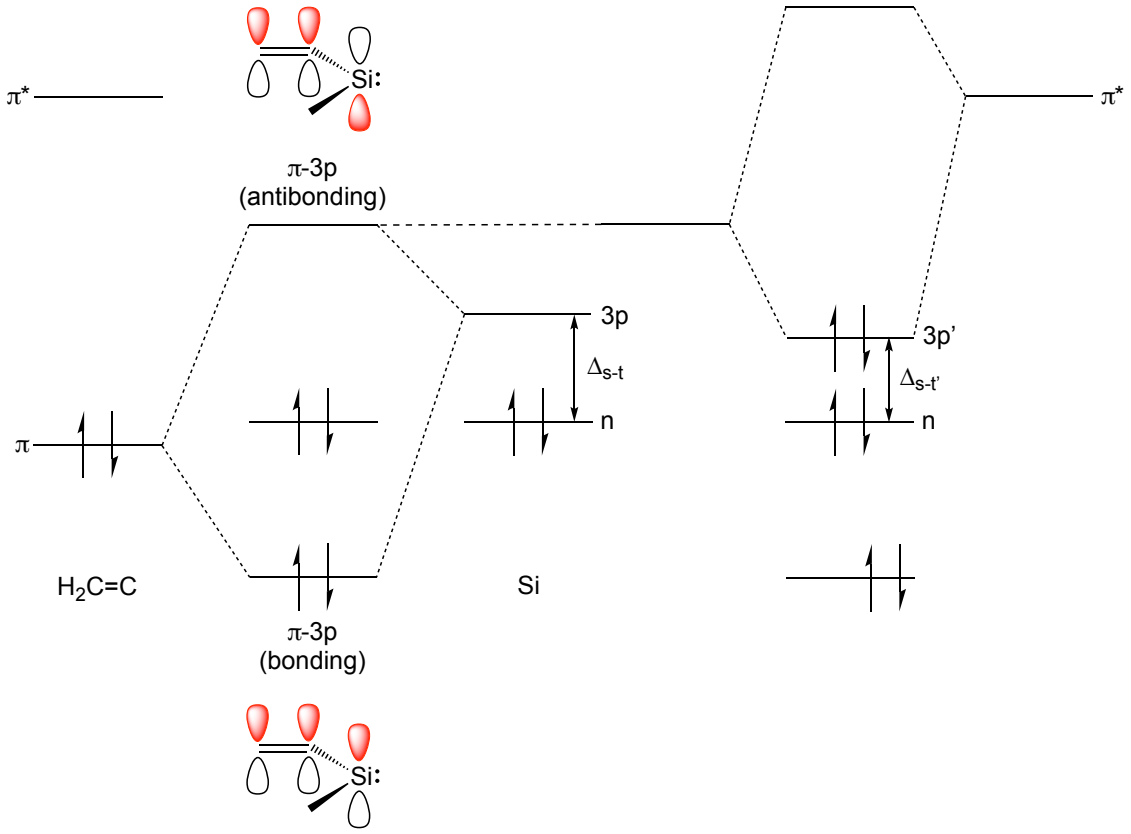

Figure 1.10. Molecular orbital diagram of the effect of vinyl substituent on $\Delta_{s\text{-}t}$.

When talking about the steric effect on $\Delta_{s\text{-}t}$, it is the bond angle which greatly influences the energy of n- and p-orbitals. On increasing the bond angle, the lone pair of electrons gains more p-character, thus the energy of n-orbital increases.[51] This results in a lesser $\Delta_{s\text{-}t}$ and a red shift. An opposite effect has been observed on decreasing the bond angle which shows an increase in $\Delta_{s\text{-}t}$ with a blue shift. This observation has been experimentally seen by altering the steric bulk of substituents for the silicon centres in various silylenes (**Figure 1.11**).[52] On increasing the steric bulk from Ph_2Si to Mes_2Si the α angle increases, thus a red shift was observed. In case of aliphatic substituents, the α angle decreases with cyclisation of the substituent hence a blue shift was observed.

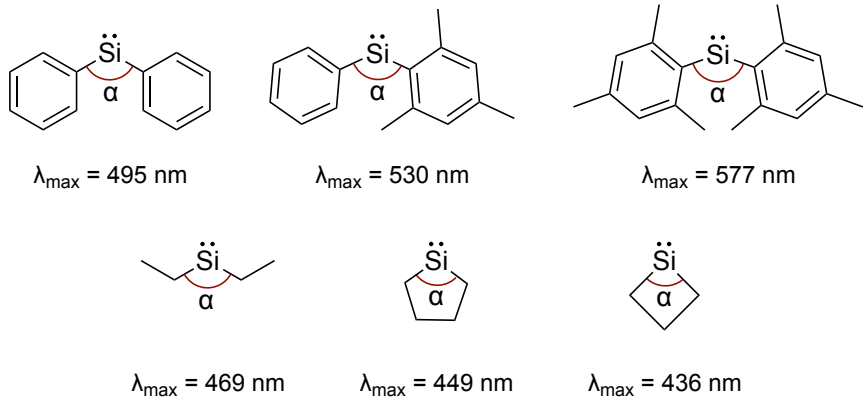

Figure 1.11. Steric effect on $\Delta_{s\text{-}t}$ monitored by UV-vis spectroscopy on series of silylenes.

1.4 Synthetic Strategies Towards Low Oxidation State Group 14 Element Complexes

The synthesis of low oxidation state main group element complexes is a continuously growing area of interest due to their tendency to show "transition metal like reactivity" towards small molecules and catalysis.[1] The routes to access such complexes have seen major development since the isolation of Lappert's 'distannene'. The common synthetic routes to access low oxidation state main group element complexes can be divided in two parts- **i**) synthesis of low oxidation state halide complexes **ii**) reduction of halide complexes to form low oxidation state group 14 element(I) and element(II) complexes.

1.4.1 Synthesis of Low Oxidation State Group 14 Element(II) Complexes

While the compounds in +2 oxidation state are more stable and easily accessible than +1, they are still classified as low oxidation state. The low oxidation state element(II) complexes (Ge-Sn) can be easily synthesised via salt metathesis and protolysis reactions (**Scheme 1.5**).

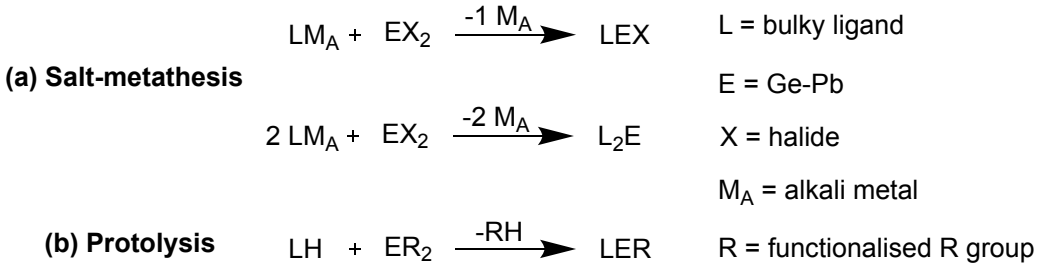

Scheme 1.5. General synthetic routes to group 14 element(II) complexes.

The most commonly used method is the salt metathesis route. It involves the reaction of alkali metal salt of the ligand (alkyl, amides, silyl) with appropriate equivalents of element(II) dihalide. This strategy has been used to stabilise a wide range of group 14 element(II) complexes of types LEX and L_2E (L = ligand, E = Ge-Pb, X = halide).[9,53–56] More specific examples are discussed in chapters 2, 3 and 4. The next route, i.e. protolysis, is basically the exchange of an acidic proton of the ligand with a basic R-functional (alkoxide, amide) group, e.g. the reaction of LH with group 14(II) element bis(diamides) ($E(NR_2)_2$).[57]

In case of silicon, however, the silicon(II) dihalides are not easily available, hence they are generally synthesised by reduction of silicon(IV) trihalide precursors. More recently the silicon(II) dihalide precursor, $IPr.SiCl_2$ (IPr = [{C(H)N(Dip)$_2$}C:]) has been employed as an alternative to silicon(II) dihalide.[58] However, its use in the synthesis of silicon(II) species is still limited to few examples.[59]

1.4.2 Reduction to Form Heavier Low Oxidation State Group 14 Element(I) and (II) Complexes

The other approach, which is well known for accessing group 14 element(I) and element(II) complexes, is reduction. Here, the so-called precursor complexes can be readily reduced using a variety of reducing agents to form the desired low oxidation state group 14 element complexes. Some of the most common reduction pathways for synthesis of group 14 element(II) ditetrelenes via reduction are the dehalogenation of two equivalents of dihalo [L_2EX_2] species or one equivalent of dihalo [L_2EX_2] species with heavier tetrelenes [L_2E:] or compounds of type [$L_2E(X)E(X)L_2$] (**Scheme 1.6**).

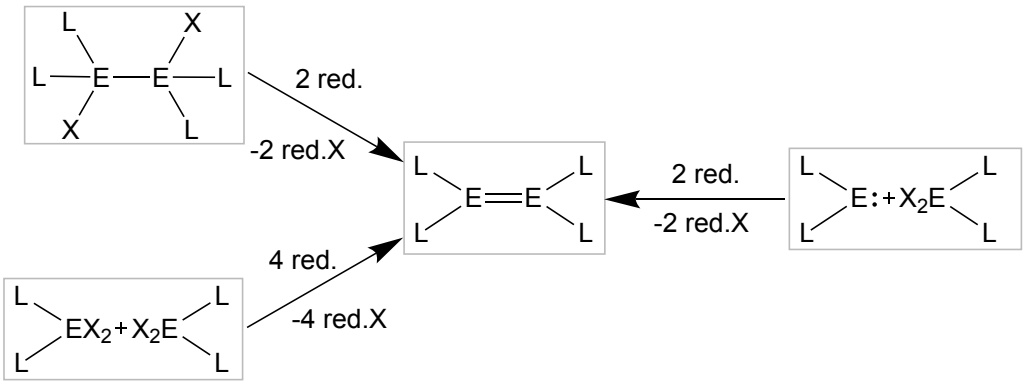

Scheme 1.6. Possible synthetic routes to heavier ditetrelenes (E = Si-Pb, L = Ligand, X = halogen, red. = reducing agent).

The routes to access heavier ditetrelynes involve the reduction of **i**) two equivalents of LEX species or **ii**) the reduction of $[LE(X)_2E(X)_2L]$ or [LE(X)E(X)L] type species. An alternative route uses the elimination of dihydrogen from dihydrido bridged precursor complexes, and are only known for synthesis of distannynes and diplumbynes (**Scheme 1.7**).

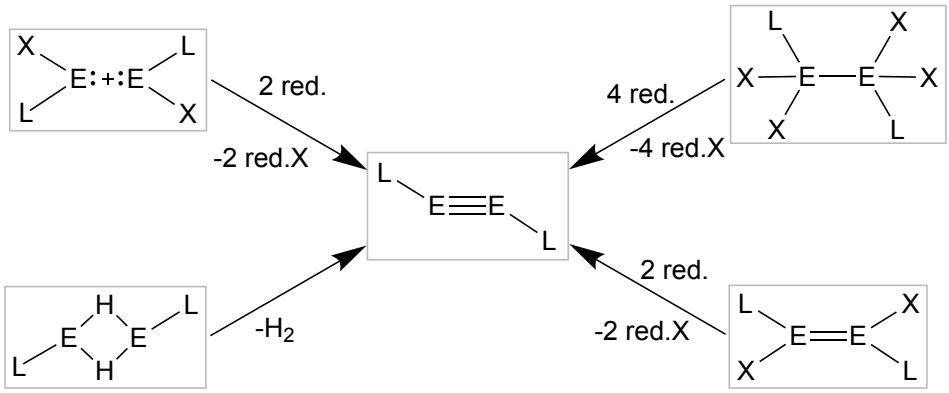

Scheme 1.7. Possible synthetic routes to heavier ditetrelynes (E = Si-Pb, L = Ligand, X = halogen; red. = reducing agent); Hydrogen elimination route is only known for Sn and Pb.

1.5 Reactivity of Low Oxidation State Group 14 Element Heavier Tetrelenes and Ditetrelynes

As mentioned in the above section, low oxidation state main group element complexes tend to show 'transition metal like activity'. This means the main group element complexes also possesses a donor/acceptor (amphiphilic) characteristic. This is similar to transition metal complexes, which contain both occupied and unoccupied orbitals. The general frontier orbital interactions on small molecules activation, bond activation and reductive elimination are depicted in **Figure 1.12**.[1,60] In case of heavier ditetrelynes, these interactions initially involve the donation from the small molecule species' σ/π-orbital into the LUMO of heavier ditetrelynes. Further, a synergistic electron donation occurs from the π-HOMO of ditetrelyne into the σ*/π*-orbital of small molecule. Analogous frontier orbital interactions have also been observed in transition metal complexes and heavier tetrelenes.[60]

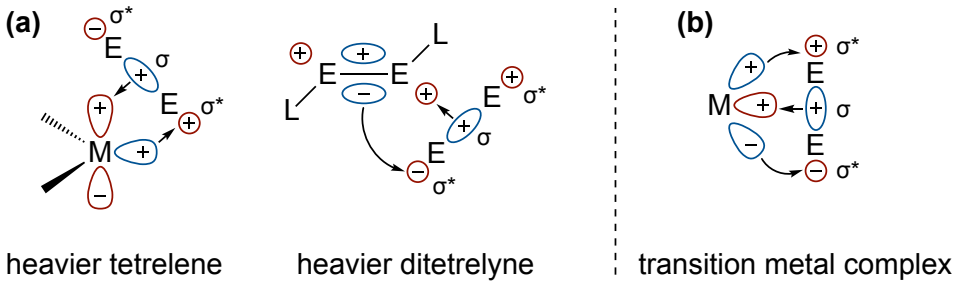

Figure 1.12. Frontier orbital interactions between a small molecule with a heavier tetrelene, ditetrelyne **(a)** and transition metal complexes **(b)**.

The heavier alkyne analogues possess a donor/acceptor orbital pair which forms due to SOJT mixing of orbitals resulting in an empty a_g orbital, capable of accepting electrons and a lone pair containing orbital a_u which can donate the electron pair. The molecular orbital diagram representation of participating donor/acceptor orbitals are given in **Figure 1.13**. During the course of any σ-bond reaction, these orbitals participate in oxidative addition and interact with small molecules and unsaturates. The detailed study and examples of reactivity studies are discussed in chapters 2, 4 and 5.

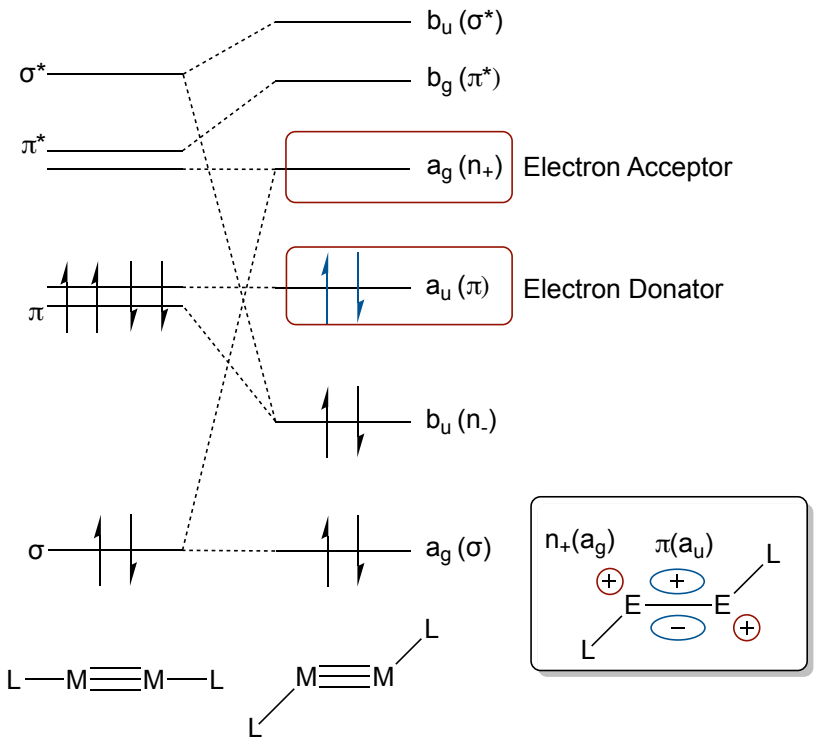

Figure 1.13. Molecular orbital scheme of heavier ditetrelynes, highlighting the donor/acceptor orbitals.

1.6 References

1 P. P. Power, *Nature*, 2010, **463**, 171–177.

2 G. Parkin, *J. Chem. Educ.*, 2006, **83**, 791–799.

3 C. Jones, *Commun. Chem.*, 2020, **3**, 1–4.

4 N. V. Sidwick, *The Electronic Theory of Valency*, Clarendon Press, Oxford, UK., 1927.

5 R. S. Drago, *J. Phys. Chem.*, 1958, **62**, 353–357.

6 P. Pyykkö, *Chem. Rev.*, 1988, **88**, 563–594.

7 P. Jutzi, *Angew. Chem., Int. Ed.*, 1975, **14**, 232–245.

8 R. S. Mulliken, *J. Am. Chem. Soc.*, 1950, **72**, 4493–4503.

9 D. E. Goldberg, D. H. Harris, M. F. Lappert and K. M. Thomas, *J. Chem. Soc., Chem. Commun.*, 1976, **227**, 261–262.

10 J. D. Cotton, P. J. Davidson, M. F. Lappert and M. Sciences, *J. Chem. Soc., Dalton Trans.*, 1976, 2275–2276.

11 V. H. Preut, H. J. Haupt and F. Huber, *Z. Anorg. Allg. Chem*, 1973, **396**, 81–89.

12 R. West, M. J. Fink and J. Michl, *Science*, 1981, **214**, 1343–1344.

13 M. Yoshifuji, I. Shima, N. Inamoto, K. Hirotsu and T. Higuchi, *J. Am. Chem. Soc.*, 1981, **103**, 4587–4589.

14 R. West, *Science*, 1984, **225**, 1109–1114.

15 M. J. Fink, M. J. Michalczyk, K. J. Haller, R. West and J. Michl, *J. Chem.Soc., Chem. Commun.*, 1983, 1010–1011.

16 S. G. Baxter, K. Mislow and J. F. Blount, *Tetrahedran*, 1980, **36**, 605–616.

17 J. J. Daly, *J. Chem. Soc.*, 1965, 4789–4799.

18 J. J. Daly, *J. Chem. Soc.*, 1964, 6147–6166.

19 J. Su, X. W. Li, R. C. Crittendon and G. H. Robinson, *J. Am. Chem. Soc.*, 1997, **119**, 5471–5472.

20 W. Uhl and M. Layh, *J. Organomet. Chem.*, 1989, **364**, 289–300.

21 F. A. Cotton, A. H. Cowley and X. Feng, *J. Am. Chem. Soc.*, 1998, **120**, 1795–1799.

22 W. H. Atwell and D. R. Weyenberg, *Angew. Chem., Int. Ed.*, 1969, **8**, 469–477.

23 H. Gilman, S. G. Cottis and W. H. Atwell, *J. Am. Chem. Soc.*, 1964, **86**, 1596–1599.

24 M. Denk, R. Lennon, R. Hayashi, R. West, A. V. Belyakov, H. P. Verne, A. Haaland, M. Wagner and N. Metzler, *J. Am. Chem. Soc.*, 1994, **116**, 2691–2692.

25 M. J. S. Gynane, D. H. Harris, M. F. Lappert, P. P. Power, P. Riviere and M. Riviere-baudet, *J. Chem. Soc., Dalton Trans.*, 1977, 2004–2009.

26 F. S. Kipping and J. E. Sands, *J. Chem. Soc., Trans.*, 1921, 830–847.

27 A. H. Cowley, *Polyhedron*, 1984, **3**, 389–432.

28 M. Kira, T. Maruyama, C. Kabuto, K. Ebata and H. Sakurai, *Angew. Chem., Int. Ed. Engl.*, 1994, **33**, 1489–1491.

29 K. Kobayashi and S. Nagase, *Organometallics*, 1997, **16**, 2489–2491.

30 M. Takahashi and Y. Kawazoe, *Organometallics*, 2008, **27**, 4829–4832.

31 Y. Chen, M. Hartmann, M. Diedenhofen and G. Frenking, *Angew. Chem., Int. Ed.*, 2001, **40**, 2051–2055.

32 W. Kurlancheek, Y. Jung and M. Head-Gordon, *Dalton Trans.*, 2008, 4428–4435.

33 R. C. Fischer, L. Pu, J. C. Fettinger, M. A. Brynda and P. P. Power, *J. Am. Chem. Soc.*, 2006, **128**, 11366–11367.

34 N. Takagi and S. Nagase, *Organometallics*, 2001, **20**, 5498–5500.

35 M. Weidenbruch, H. Kiliana, K. Petersb, H. G. v. Schneringb and H. Marsmannc, *Chem. Ber.*, 1995, **128**, 983–985.

36 S. Masamune, S. Murakami, J. T. Snow, H. Tobita and D. J. Williams, *Organometallics*, 1984, **3**, 333–334.

37 H. Schäfer, W. Saak and M. Weidenbruch, *Organometallics*, 1999, **18**, 3159–3163.

38 M. Stürmann, W. Saak, H. Marsmann and M. Weidenbruch, *Angew. Chem., Int. Ed.*, 1999, **38**, 187–189.

39 S. Nagase, K. Kobayashi and N. Takagi, *J. Organomet. Chem.*, 2000, **611**, 264–271.

40 G. Trinquier and J.-P. Malrieu, *J. Am. Chem. Soc.*, 1987, **109**, 5303–5315.

41 P. P. Power, *Organometallics*, 2007, **26**, 4362–4372.

42 V. Y. Lee and A. Sekiguchi, in *Organometallic Compounds of Low-Coordinate Si, Ge, Sn and Pb: From Phantom Species to Stable Compounds*, Wiley, New York, 2010, pp. 139–188.

43 Y. Apeloig, R. Pauncz, M. Karni, R. West, W. Steiner and D. Chapman, *Organometallics*, 2003, **22**, 3250–3256.

44 J. Berkowitz, J. P. Greene, H. Cho and B. Ruscis, *J. Chem. Phys.*, 1987, **86**, 1235–1248.

45 K. Balasubramanian, *J. Chem. Phys.*, 1988, **89**, 5731–5738.

46 M. Denk, R. West, R. Hayashi, Y. Apeloig, R. Pauncz and M. Kami, in *Organosilicon Chemistry II: From Molecules to Materials*, Wiley-VCH Verlag GmbH, Weinheim, Germany, 1995, pp. 251–261.

47 H. A. Bent, *Chem. Rev.*, 1961, **61**, 275–311.

48 B. T. Luke, J. A. Pople, M.-B. Krogh-Jespersen, Y. Apeloig, J. Chandrasekhar and P. v. R. Schleyer, *J. Am. Chem. Soc.*, 1986, **108**, 260–269.

49 Y. Apeloig and M. Karni, *J. Chem. Soc., Chem. Commun.*, 1985, 1048–1049.

50 Y. Apeloig, M. Karni, R. West and K. Welsh, *J. Am. Chem. Soc.*, 1994, **116**, 9719–9729.

51 Z. Rappoport and Y. Apeloig, *The Chemistry of Organic Silicon Compounds* Vol. 2, Wiley, New York, 1998.

52 M. J. Michalczyk, M. Fink, D. J. DeYoung, C. W. Carlson, K. Welsh, R. West and J. Michl, *Silicon, Germanium, Tin and Lead Compound*, 1986, **9**, 75.

53 T. Fjeldberg, A. Haaland, B. E. R. Schilling, M. F. Lappert and A. J. Thorne, *J. Chem. Soc., Dalton Trans.*, 1986, 1551–1556.

54 J. Li, A. Stasch, C. Schenk and C. Jones, *Dalton Trans.*, 2011, **40**, 10448–10456.

55 L. Pu, M. M. Olmstead, P. P. Power and B. Schiemenz, *Organometallics*, 1998, **17**, 5602–5606.

56 P. B. Hitchcock, H. A. Jasim, M. F. Lappert, W. P. Leung, A. K. Rai and R. E. Taylor, *Polyhedron*, 1991, **10**, 1203–1213.

57 H. Braunschweig, C. Drost, P. B. Hitchcock, M. F. Lappert and L. J.-M. Pierssens, *Angew. Chem., Int. Ed. Engl.*, 1997, **36**, 261–263.

58 R. S. Ghadwal, H. W. Roesky, S. Merkel, J. Henn and D. Stalke, *Angew. Chem., Int. Ed.*, 2009, **48**, 5683–5686.

59 T. J. Hadlington, J. A. B. Abdalla, R. Tirfoin, S. Aldridge and C. Jones, *Chem. Commun.*, 2016, **52**, 1717–1720.

60 T. J. Hadlington, M. Driess and C. Jones, *Chem. Soc. Rev.*, 2018, **47**, 4176–4197.

Chapter 2
Development of Monodentate Bulky Amide Ligands for Synthesis of Germanium(II) Halides and Heavier Ditetrelynes

2.1 Introduction

From the discussion in chapter 1, it can be seen that ligands play a vital role in the stabilisation of low oxidation state main group element complexes. Use of sterically demanding bulky ligands is crucial for kinetic stability of such main group element centres. Further, these ligands also influence the structure and reactivity of synthesised main group element complexes.

In this chapter, some of the monodentate ligand systems, particularly amide ligands will be discussed. The relevance of monodentate amide ligands in isolating group 14 element halide complexes and heavier ditetrelynes of type LEEL, where L is a bulky monodentate ligand and E is Si-Pb, will also be explored. In addition to that, reactions of these heavier analogues towards small molecules, and the catalytic activity of low-coordinate hydride complexes, will be highlighted.

2.1.1 Monodentate Ligands

The word 'dentate' originates from the Latin word *dentis* meaning tooth, and refers to the number of donor atoms of the ligand. The use of monodentate ligands in low oxidation state main group element chemistry has been widespread in the last 3 decades. Unlike chelating bidentate ligands (described in chapter 3), monodentate ligands are monoanionic Lewis bases characterised by a single donor atom site which links to the element centre. Thus, the resulting main group element complexes need to have sterically demanding bulky ligands to give the extra (kinetic) stabilisation. Moreover, main group complexes utilising monodentate ligands are believed to be more reactive as a result of coordinatively unsaturated element centres. In this section, the carbon donor aryl and nitrogen donor amide monodentate ligands will be discussed.

2.1.1.1 Terphenyl Ligands

A useful class of aryl ligands are the well-known terphenyl ligands which have largely been developed by Power and co-workers in last twenty years. Although, they were firstly synthesised in 1942,[1] a one pot synthetic route was developed in 1986[2] and the full potential of terphenyls in terms of metal complex formation was realised since then.[3] They are 2,6-bis(aryl)-phenyl [2,6-Ar_2Ph-] ligands in which the two ortho aryl groups are bonded to a central aryl ring (**Figure 2.1**).

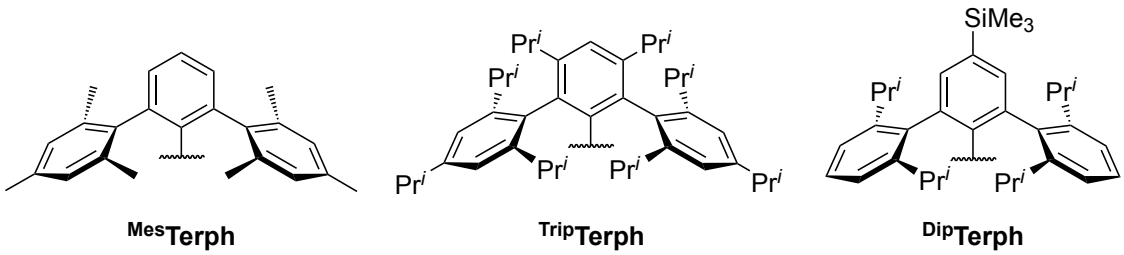

Figure 2.1. Examples of previously reported terphenyl ligands.

The one pot synthesis by Hart and co-workers of terphenyls used 2,6-dibromoiodobenzene in THF as a starting material. To this solution, the desired aryl Grignard reagent in THF was added and the reaction mixture was quenched with dilute acid after stirring for few hours. Later on, a modified Hart route was developed for more efficient synthesis, and was further refined by Power for the synthesis of bulkier terphenyls.[4] The initial step of this route involved lithiation of 1,3-dichlorobenzene using $LiBu^n$, followed by addition of the desired aryl Grignard reagent. Further, this aryl Grignard intermediate was quenched with water or iodine to give an unsubstituted terphenyl or halogen substituted terphenyl pro-ligands (**Scheme 2.1**). Thereafter, to change the steric and electronic properties of the terphenyl ligands, many modifications have been performed and a large variety of terphenyls have been reported to date.[5,6]

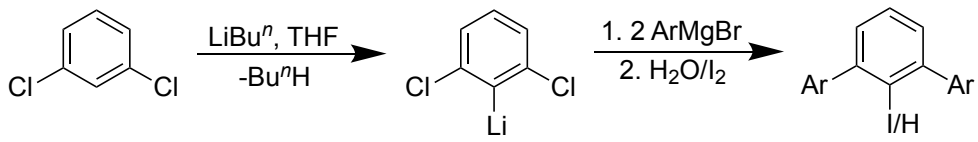

Scheme 2.1. Modified synthesis of terphenyl ligands.

2.1.1.2 $(Me_3Si)_2CH$- Substituted Ligands

Another class of aryl ligands used in low oxidation state main group chemistry are [{$(Me_3Si)_2CH$}$^-$] substituted aryl ligands. They are structurally similar to terphenyl

ligands except [{$(Me_3Si)_2CH$}$^-$] groups are substituted at 2,6-positions of central phenyl ring, which gives them markedly different electronic properties in comparison to terphenyl ligands. These ligands were introduced by Okazaki et al. in 1987 with the synthesis of [2,4,6-{$((Me_3Si)_2CH)_3$-Ph}] (Tbt) ligand.[7] Other examples of these ligands with H, Bu^t and -$C(SiMe_3)_3$ substituted at para positions are known, and shown in **Figure 2.2**.[8–10]

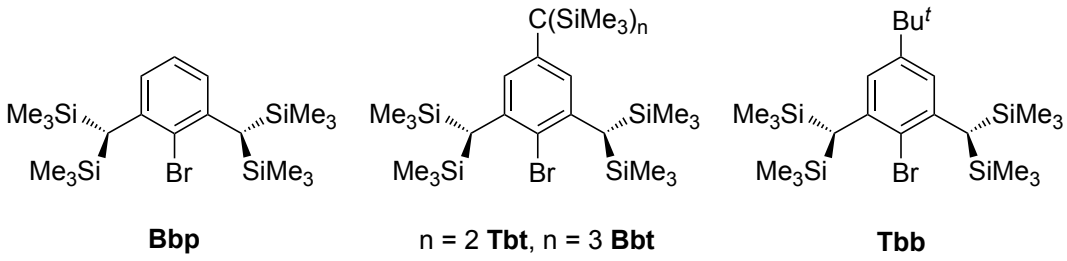

Figure 2.2. Examples of reported silyl substituted aryl pro-ligands.

These substituted pro-ligands were synthesised by reacting the desired 2,6-bis(dibromomethyl)bromobenzene with a large excess of TMSCl (TMS = Me_3Si-) and elemental magnesium in THF (**Scheme 2.2**). The reaction mixture was heated to reflux, and the bromide of ligand was isolated. These ligands have largely been utilised and developed by Tokitoh and Okazaki for synthesis of series of low oxidation state main group element complexes.

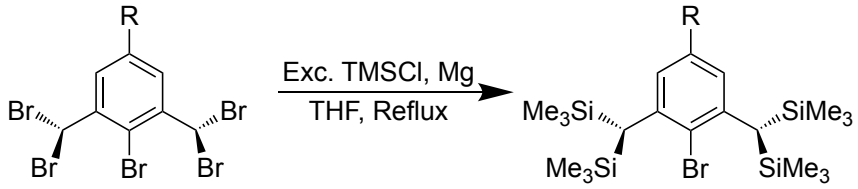

Scheme 2.2. General synthesis of silyl substituted aryls.

2.1.1.3 Rind-Br

A different class of carbon donor ligands are the saturated indacenes reported by Matsuo et al.[11] These ligands involve the 1,1,3,3,5,5,7,7-octa-R-substituted s-hydrindacenyl group fused with two five-membered rings, called 'Rind' groups. The most significant advantage of these ligands when compared to other monodentate ligands is the 'freeze-rotation' of C-C bond of the central phenyl ring and the substituent carbon atoms. On the other hand, aryl and amide ligands have 'free or hindered rotation' of the C-C bond which tends to change the steric bulk in solution due to the possible rotation (**Figure 2.3**).

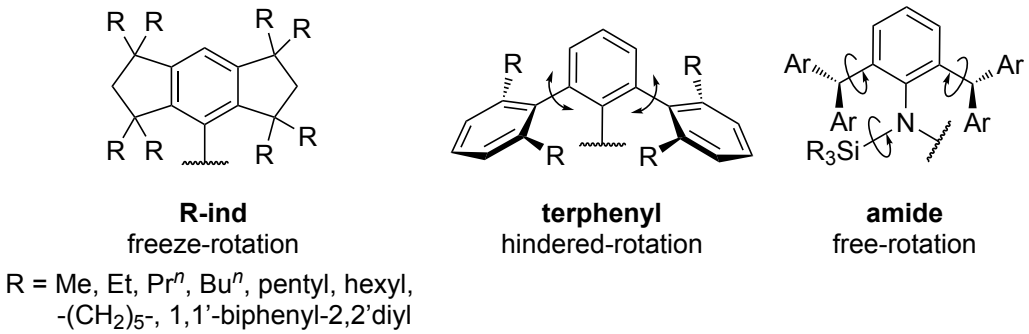

Figure 2.3. Substitutions on R-ind and possible rotations for R-ind, terphenyl and amide ligands.

In general, the synthesis of these ligands involves three to four steps and are not very high yielding. However, the ligand EMind-Br (4-bromo-1,1,7,7-tetraethyl-3,3,5,5-tetramethyl-s-hydrindacene) and xMEind-Br (4-bromo-1,1,5,5-tetraethyl-3,3,7,7-tetramethyl-1,2,3,5,6,7-hexahydro-s-indacene) have been isolated in 97 % and 84 % yields, respectively. The general synthesis of these pro-ligands involves initial formation of 1,3-bis (1-chloro alkyl) benzene compounds.[11] This is followed by an intramolecular double Friedel-Crafts cyclisation and finally a bromination step on the formed Rind-H species to get the Rind-Br pro-ligands (**Scheme 2.3**). The overall steric bulk of these ligand can be modified by changing the position and bulk of the R and R' substituents.

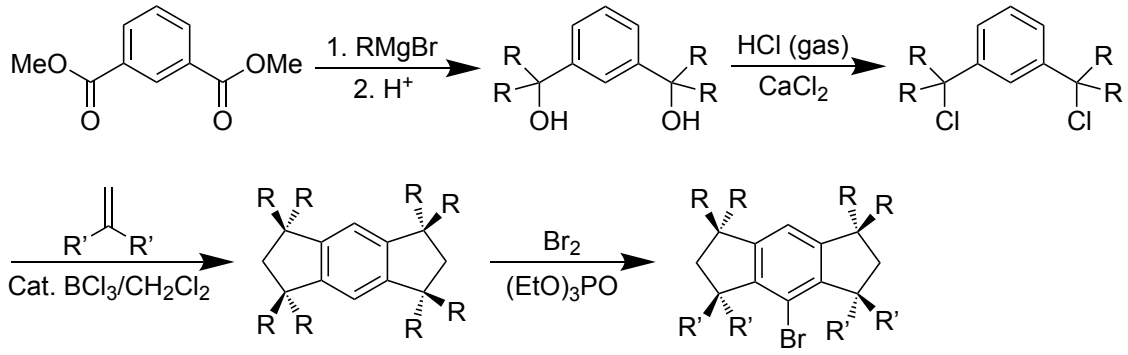

Scheme 2.3. General synthesis of Rind-Br.

2.1.1.4 Aryl-Silyl Amide Ligands

Monodentate amide ligands have been used extensively in main group chemistry. With the use of the bis(trimethylsilyl) amide ligand [{N(SiMe$_3$)$_2$}$^-$] in stabilising various main group element complexes by Lappert and co-workers, the amide ligands achieved substantial attention.[12,13] However, due to the smaller bulk of the silyl ligand system, a bulkier aryl-silyl amide ligand [{N(SiMe$_3$)Dip}$^-$] (Dip = 2,6-Pr$^i_2$Ph) was isolated in 1981 for the stabilisation of low oxidation state main group element complexes.[14] Since then,

this ligand system has been derivatised by increasing bulk at the silyl and phenyl groups, to enhance the bulk of these systems.

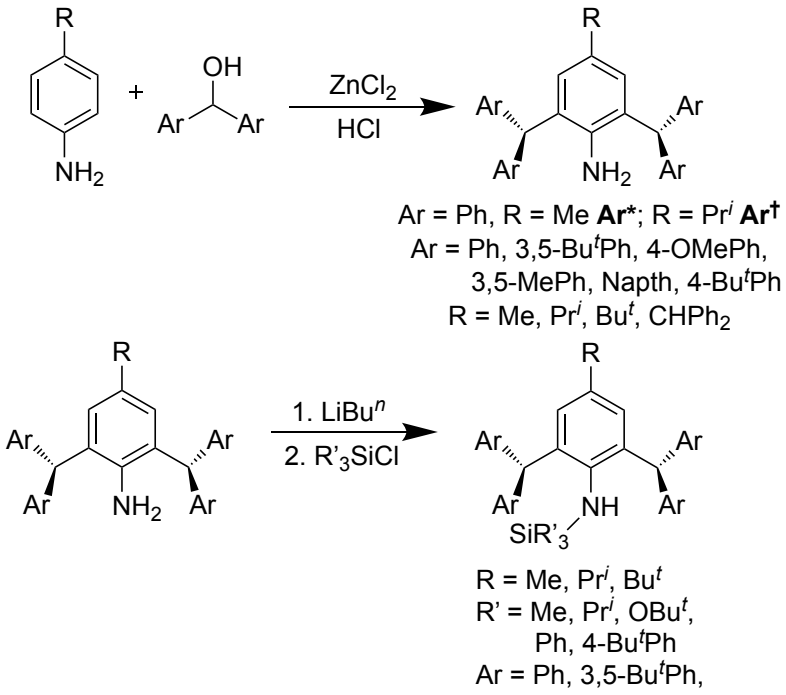

Scheme 2.4. Synthesis of various bulky aryl-silyl pro-ligands.

Our group has developed a series of bulky aryl-silyl amide ligands with the use of bulky anilines. The bulky aniline Ar^*NH_2 (where Ar^* = 2,6-$(Ph_2CH)_2$-4-Me-Ph) was synthesised in 2010 by Berthon-Gelloz et al. by condensation of *p*-toluidine with two equivalents of benzhydrol.[15] Later, these "pentaphenyl" based bulky anilines have been largely explored and modified by our group for the development of monodentate aryl-silyl amide ligands.[16–18] The synthesis of monodentate aryl-silyl amide ligands is quite straightforward. It involves the deprotonation of aniline using $LiBu^n$ to yield the lithium salt of aniline [ArNHLi] which is followed by quenching with various chlorosilane species [R_3SiCl] to yield the respective monodentate amine pro-ligands.[17] **Scheme 2.4** presents the synthetic procedure and examples of monodentate amines reported in the literature.

2.1.1.5 Boryl-Silyl Amides

This class of silyl ligand incorporates a boryl fragment instead of bulky aniline groups. They were firstly synthesised in our group in 2016.[19] The general representation for these ligand class is ([{$N(SiR_3)B(^{Dip}DAB)$}$^-$]; DAB = $(DipNCH)_2$). These ligands offer considerable steric bulk due to presence of the DAB moiety. Further, the boron atom

demonstrates a competing possibility of N→B π-donation, by which the ligands can act as weaker N-donors towards the metal centres.

The synthesis of these ligands involved the initial synthesis of [(^{Dip}DAB)BNH$_2$] moiety via multiple steps.[20] This was then deprotonated using LiBu^n, followed by the quenching of the reaction mixture with R$_3$SiCl (**Scheme 2.5**).[19,21]

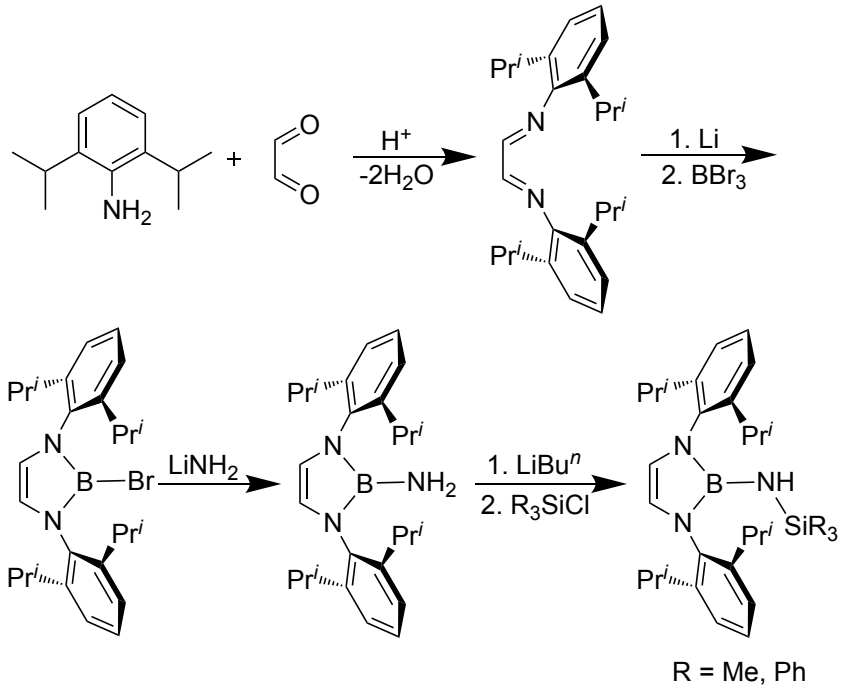

Scheme 2.5. Synthesis of [{N(SiR$_3$)B(^{Dip}DAB)}$^-$].

2.1.1.6 Bis(aryl) Amides and Terphenyl Amides

Other classes of amide ligands are bis(aryl) amides and terphenyl amides. The bis(aryl) ligands were synthesised via a palladium cross coupling reaction of aryl halide with bulky aniline. So far many bis(aryl) amide ligands have been synthesised (**Scheme 2.6**).[22,23]

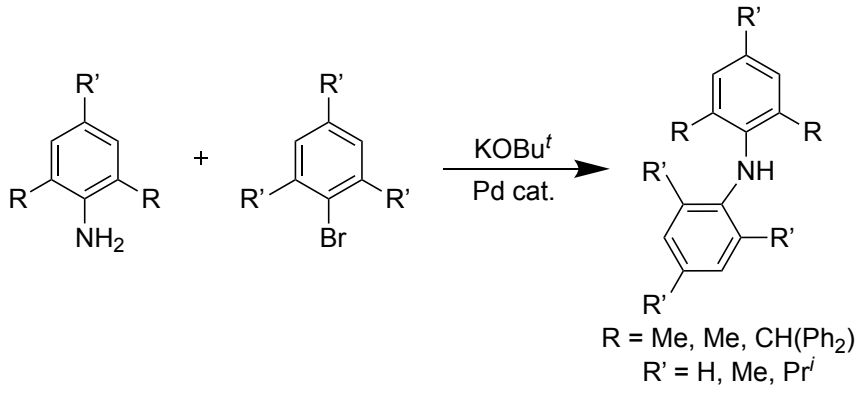

Scheme 2.6. Synthesis of bis(aryl) amine pro-ligands.

The terphenyl amide ligands were synthesised from terphenyl halides. First, the corresponding terphenyl halide was lithiated using LiBu^n. The resulting lithium salt was treated with tosyl azide (tosyl: 4-MePh-SO) to form terphenyl azide. The resulting azide was further reduced with $LiAlH_4$ to yield the terphenyl aniline (**Scheme 2.7**).[4,24] Due to the large steric bulk of the terphenyl groups, substitution of large groups at the N-centre have not been possible for these ligands, and only two examples of these ligands have been reported so far.[4]

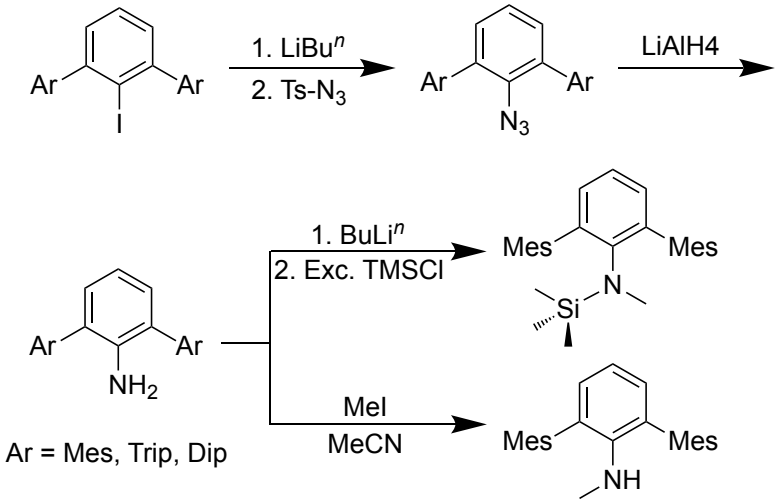

Scheme 2.7. Synthesis of terphenyl anilines and terphenyl amine pro-ligands.

2.1.2 Use of Monodentate Ligands in the Synthesis of Group 14 Element(II) Halides

Several monodentate ligands have been utilised in isolation of group 14 element(II) halide complexes of the type LEX (L = Ligand, E = Ge-Pb, X = Cl, Br, I). In terms of synthesis, the group 14(II) halide complexes were accessed by a salt metathesis route comprising the treatment of the lithium or potassium salt of the ligand with the respective group 14 halide EX_2 (E = Ge, Sn, Pb, X= Cl, Br, I).

Germanium(II) halide complexes derived from terphenyl ligands exhibit both monomeric and dimeric structures. The reported terphenyl complexes [{(Ar)GeCl}$_2$] (Ar = 2,6-(Mes)$_2$Ph (^{Mes}Ar), Mes = 2,4,6-Me$_3$Ph; 2,6-(Trip)$_2$Ph (^{Trip}Ar), Trip = 2,4,6-Pr$^i_3$Ph; 2,6-(Dip)$_2$Ph (^{Dip}Ar), Dip = 2,6-Pr$^i_2$Ph) exist as dimers in solid-state and as monomer in solution.[25–27] The compound [{(^{Trip}Ar)GeCl}$_2$] however exists as both dimer and monomer in the solid-state due to difference in crystallisation conditions. A similar case has been seen for the tin(II) chloride complex, [{(^{Trip}Ar)SnCl}$_2$].[28] Furthermore, all of

the lead(II) halides [{(Ar)PbBr}$_2$] (Ar = ^{Trip}Ar, ^{Mes}Ar, ^{Dip}Ar) exist as dimeric halide bridged complexes (**Scheme 2.8**).[29,30]

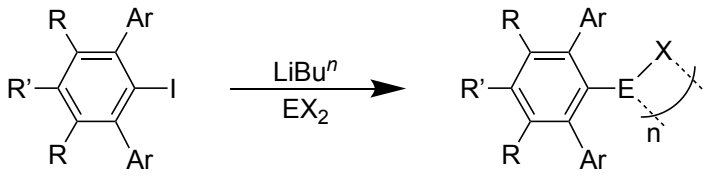

R'/R'= H; Ar = Trip; E = Ge, Sn; X = Cl; n = 1
R' = H, Cl, SiMe$_3$; R = H, Pr^i; Ar = Mes, Dip, Trip; E = Ge, X = Cl, I; n = 2
R' = H, Cl, F, Bu^t, SiMe$_3$, R = H, Pr^i; Ar = Mes, Dip, Trip; E = Sn; X = Cl, I; n = 2
R'/R = H; Ar = Mes, Dip, Trip; E = Pb; X = Br; n = 2

Scheme 2.8. Synthesis of terphenyl ligand stabilised group 14 element(II) halides.

Germanium(II) halide complexes isolated using the other two aryl ligands are [{(Bbt)GeBr}$_2$], [{(Tbb)GeBr}$_2$] (**Scheme 2.9**),[31,32] [(E)-{(Eind)GeX}$_2$] (X= Cl, Br; Eind = 1,1,3,3,5,5,7,7-octaethyl-s-hydrindacen-4-yl), and [{(EMind)GeCl}$_2$] (EMind = 1,1,7,7-tetraethyl-3,3,5,5-tetramethyl-s-hydrindacen-4-yl).[33,34] All of these germanium(II) halide species are dimeric and display a trans-digermene structure. Each germanium centre incorporates a halide with Ge-Ge bond in the range of 2.363-2.5087 Å. No tin(II) and lead(II) halides have been synthesised using these two ligand frameworks to date.

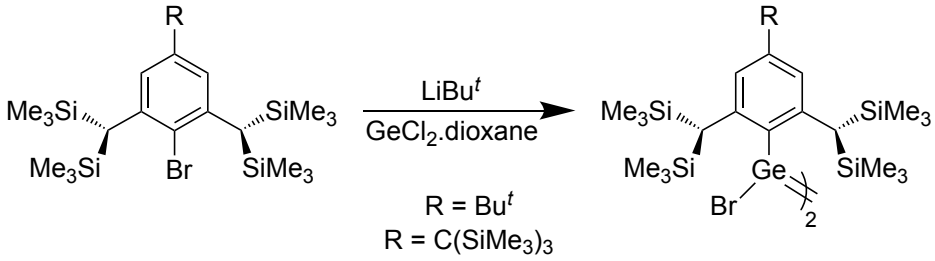

Scheme 2.9. Synthesis of [{(Bbt)GeBr}$_2$] and [{(Tbb)GeBr}$_2$].

Aryl-silyl and boryl-silyl ligands have been utilised in the isolation of a variety of germanium(II) halides in moderate to good yields (**Scheme 2.10**).[17,18,35] The germanium(II) chlorides crystallise as monomers in solid-state with bent N-Ge-Cl units. Similarly, tin(II) halides are also monomeric which also indicates the extreme bulk provided by the monodentate aryl-silyl and boryl-silyl amide ligands. Only two lead(II) chlorides [(^{TMS}L*)PbCl] (^{TMS}L* = TMSAr*N) and [(^{PhMe}L*)PbCl] (^{PhMe}L* = (MePh$_2$Si)Ar*N) have been synthesised to date.[17] Both these complexes have been

isolated in low yields (41 % and 8 %, respectively) and are dimers with bridging halides in solid-state.

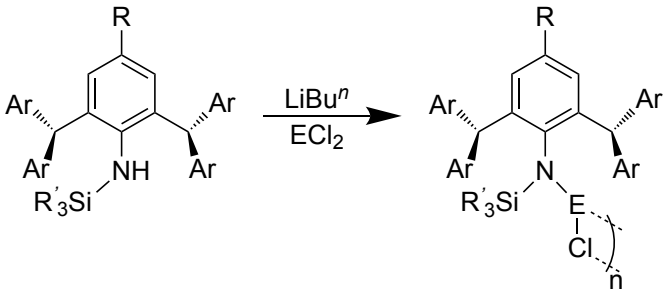

R = Me, Pr^i; R' = Me, Pr^i, Ph, OBu^t; E =Ge; n = 1
R = Me, Pr^i; R' = Me, Pr^i, Ph; E =Ge; n = 1
R = Me; R' = Me, Ph; E = Pb; n = 2

Scheme 2.10. Synthesis of aryl-silyl ligand stabilised group 14 element(II) halides.

The chemistry of bis(aryl) and terphenyl ligands are comparatively less developed.[36] Only limited examples of bis(aryl) ligand stabilised germanium(II) halides and a few tin(II) halides are known.[22,23,37] For the further discussion we will mostly focus on the complexes related to terphenyl and monodentate amide ligands, and other ligand based complexes will only be discussed where it is necessary.

2.1.3 Heavier Group 14 Alkyne Analogues

The heavier group 14 alkyne analogues are of general formula LEEL (L = ligand, E = Ge-Pb). Until 2000, stable group 14 element heavier alkynes were unknown. Unlike the carbon analogues, the synthesis of heavier homologues require extreme steric bulk to isolate the element centre in +1 oxidation state. Their geometry and bond order vary from that of carbon analogues. In fact, heavier alkyne analogues do not show a 'true' triple bond and on descending the group the bond order decreases from carbon analogues' bond order (3). The general synthesis of such complexes is by the reduction of element halide complexes LEX (L = ligand, E = Si-Pb, X = Cl, Br, I).

2.1.3.1 Digermynes

The first heavier germanium(I) dimer was reported in 2002 by Power and co-workers. It was stabilised by bulky ^{Dip}terphenyl ligand [2,6-(Dip)$_2$Ph] and was synthesised via the reduction of [(^{Dip}Ar)GeCl] with elemental potassium in benzene.[38] The product was isolated as orange-red coloured crystals in 38 % yield. Notably, this terphenyl digermyne [{(^{Dip}Ar)Ge}$_2$] possesses a considerably shorter Ge-Ge bond length (2.2850(6) Å) than the covalent radii of Ge-Ge single bond (ca. 2.44 Å), which also highlights the multiple

bond character. The Ge-Ge-C bond angle was 128.67(8)°. The digermyne has a trans-bent structure which indicates the presence of nonbonding electrons on each germanium centre, thus giving it singlet biradicaloid character. On the basis of theoretical studies, the bond order was speculated to be close to two. Despite the bond order being less than an ideal triple bond, these species will be denoted as 'Digermynes' in this chapter.

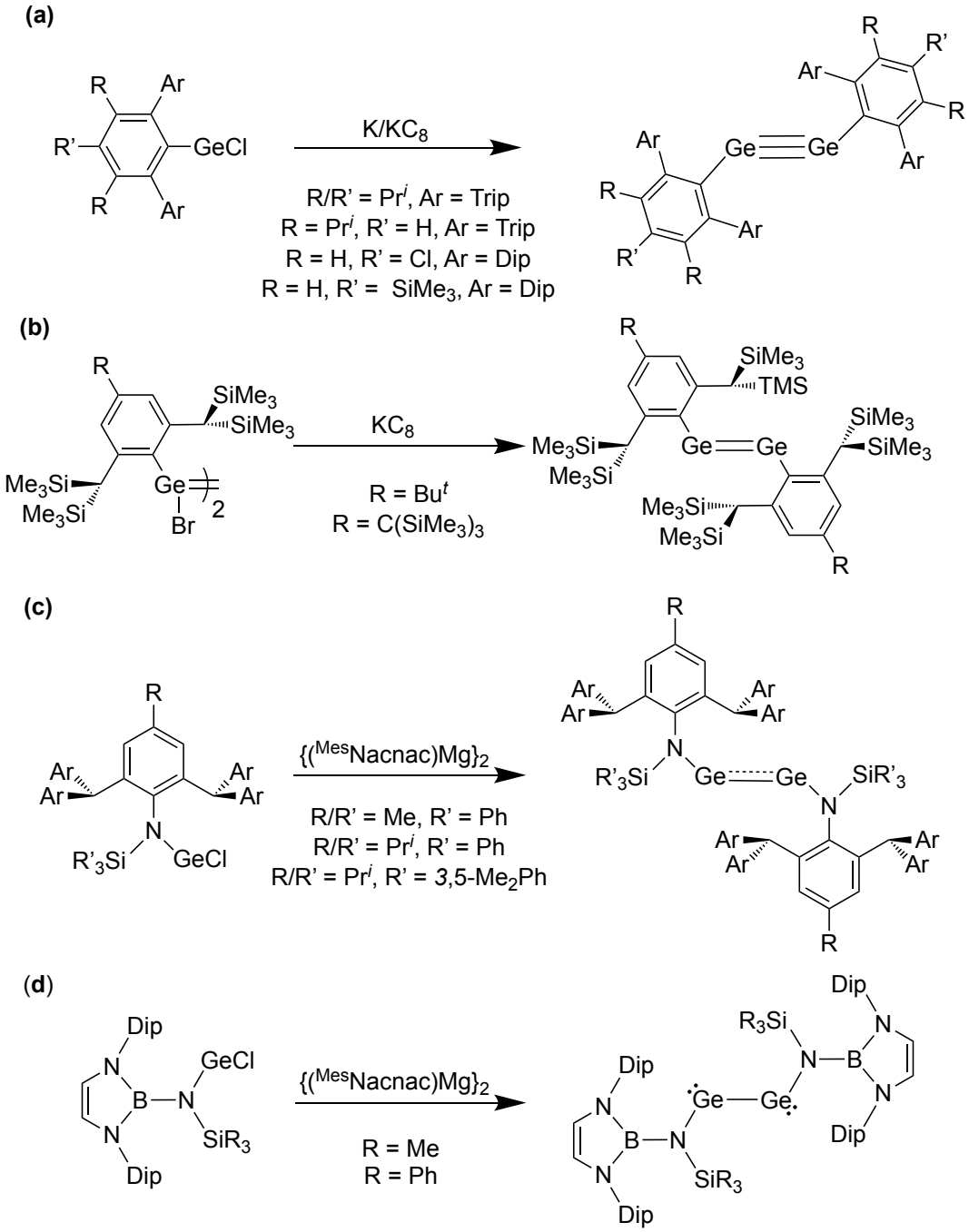

Scheme 2.11. Synthesis of terphenyl stabilised digermynes (**a**), aryl stabilised digermynes (**b**), aryl-silyl amide stabilised digermynes (**c**), and boryl-silyl amide stabilised digermynes (**d**).

Currently, a wide range of terphenyl stabilised digermynes are available which are synthesised by using the potassium or potassium graphite (KC_8) as reducing agents (**Scheme 2.11**).[39] These alkyne analogues also possess a trans-bent geometry with varying bond lengths, depending on the substituent(s) on the terphenyl ligand. Additionally, the digermynes [{($^{Trip}Ar^{iPr2}$)Ge}$_2$] ($^{Trip}Ar^{iPr2}$ = 2,6-(Trip)$_2$-3,5-Pr$^i_2$Ph) (Ge-Ge = 2.2125(13) Å) and [{($^{Dip}Ar^{TMS}$)Ge}$_2$] ($^{Dip}Ar^{TMS}$ = 2,6-(Dip)$_2$-4-TMSPh) (Ge-Ge = 2.2438(8) Å) with the electron releasing groups and $SiMe_3$ on central phenyl rings tend to show shorter bond lengths due to decrease in bending, which also suggests the multiple bonding character. On the other hand, the digermyne [{($^{Dip}Ar^{Cl}$)Ge}$_2$] ($^{Dip}Ar^{Cl}$ = 2,6-(Dip)$_2$-4-ClPh) with electron withdrawing group has an opposite effect and shows a longer Ge-Ge (2.3071(3) Å) bond length. A similar synthetic procedure was used to isolate doubly bonded tbb and tbt ligand stabilised digermynes i.e. the reduction of [LGeBr] with potassium graphite. The average Ge-Ge bond distances in [{(Tbb)Ge}$_2$] and [{(Bbt)Ge}$_2$] are 2.23 Å and 2.22 Å, respectively.[32,40] These shorter bond lengths arise from a lower $E_{D\text{-}Q}$ gap in the LGe (L = Bbt, Tbb) moiety due to presence of electron releasing silyl groups.

Our group made an entry in the field of heavier ditetrelynes with the synthesis of the first amido digermyne in 2011, the synthetic procedure being the reduction of [($^{TMS}L^*$)GeCl] ($^{TMS}L^*$ = (TMS)Ar*N) with half equivalent of [{(^{Mes}Nacnac)Mg}$_2$] (^{Mes}Nacnac = [HC{N(Mes)C(Me)}$_2$]$^-$; Mes = 2,4,6-Me$_3$Ph) affording [{($^{TMS}L^*$)Ge}$_2$] in 55 % yield.[41] Contrary to aryl digermynes, attempts to synthesise [{($^{TMS}L^*$)Ge}$_2$] using reducing agents like K, Na and KC_8 resulted in very low yields. The dimer exhibits a Ge-Ge bond length 2.7093(7) Å and N-Ge-Ge angle 100.09(6)° which are correspondingly much longer and more acute than the earlier reported aryl digermynes. This unexpected lengthening of bond was also supported by theoretical calculations and results from the donation of nitrogen lone pair to germanium's empty p-orbital $N_{lp}\rightarrow$Ge. Due to this donation, the propensity for multiple bonding in Ge-Ge decreases and a planarisation occurs in the Ge_2NSiC fragment, resulting in a weaker single Ge-Ge bond. On the contrary, when the ligand bulk was increased to bulkier $^{iPr}L^\dagger$ from $^{TMS}L^*$, a multiply bonded amido digermyne was isolated in 2014.[42] The multiply bonded amido digermyne [{($^{iPr}L^\dagger$)Ge}$_2$] was accessed similarly as the previous singly bonded amido digermyne. The Ge-Ge bond length (2.3668(6)) Å and N-Ge-Ge bond angle 119.61(1)°) were found to be similar to Power's aryl digermynes. Unlike the $^{TMS}L^*$ group, the $^{iPr}L^\dagger$ group provides

more bulk to element centre, which apparently disallows a N_{lp}→Ge π-interaction and thereby prevents the Ge_2NSiC fragment planarisation. As a result, it forms a stronger multiple Ge-Ge bond. Other amido digermynes are the recently reported boryl-silyl amido digermynes [{(^{TBo}L)Ge}$_2$] (^{TBo}L = [{(^{Dip}DAB)B(TMS)N}$^-$]) and [{(^{PhBo}L)Ge}$_2$] (^{PhBo}L = [{(^{Dip}DAB)B($SiPh_3$)N}$^-$]) (**Scheme 2.11**).[35] Both these digermynes maintain a trans-bent geometry with single Ge-Ge bonds (2.6003(6) Å and 2.602(1) Å) and N-Ge-Ge angles of 103.09(1)° and 107.05(6)°. The single bond here can also be explained by the planarisation of Ge_2NSiB fragment.

2.1.3.2 Distannynes

The first tin(I) dimer [{(^{Dip}Ar)Sn}$_2$] was also isolated by Power in 2002 via the reduction of [(^{Dip}Ar)SnCl] with potassium metal (**Scheme 2.12**).[43] The Sn-Sn bond length was found to be 2.6675(4) Å, which was considerably shorter than the average Sn-Sn single bond length (Sn-Sn = 2.80 Å). The dimer has a planar core structure with a Sn-Sn-C bond angle of 125.24(7)°. Since then, several aryl ligand stabilised tin(I) dimers have been reported in literature, synthesised using potassium or KC_8 as reductants.[39,44,45]

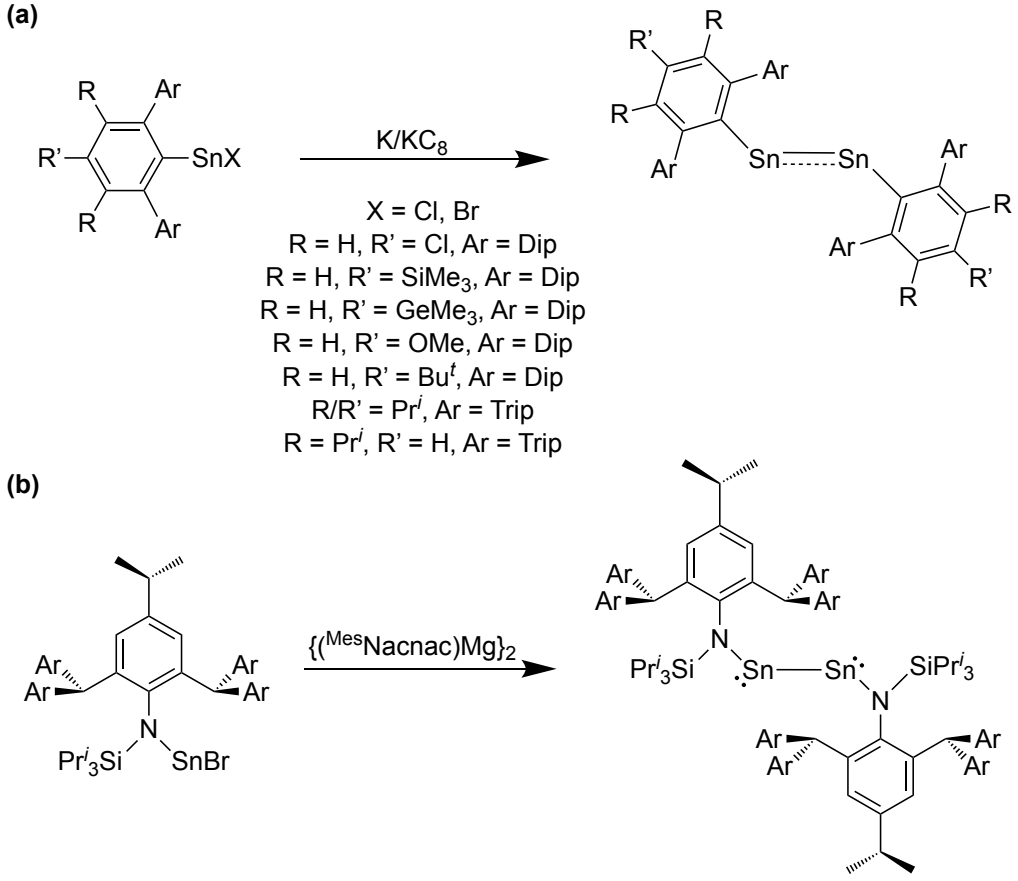

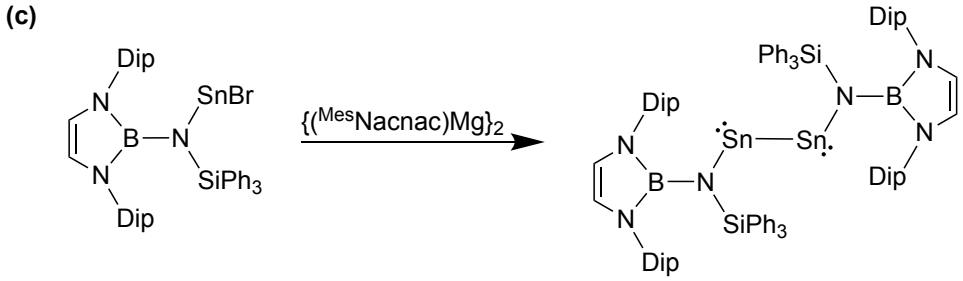

Scheme 2.12. Synthesis of terphenyl stabilised distannynes (**a**), aryl-silyl amide stabilised distannyne (**b**), and boryl-silyl amide stabilised distannyne (**c**).

Two different bonding modes are observed for terphenyl distannynes (**Figure 2.4**). For shorter Sn-Sn distance distannynes (2.6-2.7 Å) ([{(Ar)Sn}$_2$]; Ar = $^{Dip}Ar^{Cl}$, $^{Dip}Ar^{OMe}$, $^{Dip}Ar^{tBu}$, $^{Trip}Ar^{iPr2}$), multiple bonding (bond order = 1.5 and 2.0) was observed with moderate C-Sn-Sn bending angles (121.8-125.24°). The central phenyl ring of the terphenyl units in such dimers was found to lie in plane with the C-Sn-Sn-C core. On the other hand, substitution of $SiMe_3$ and $GeMe_3$ at the para position of the central phenyl ring results in single bonded isomers with longer Sn-Sn distances (3.0 Å and 3.1 Å) and more acute C-Sn-Sn angles (97.7° and 99.1°). The central phenyl ring of the terphenyl unit now lies perpendicular to C-Sn-Sn-C unit.

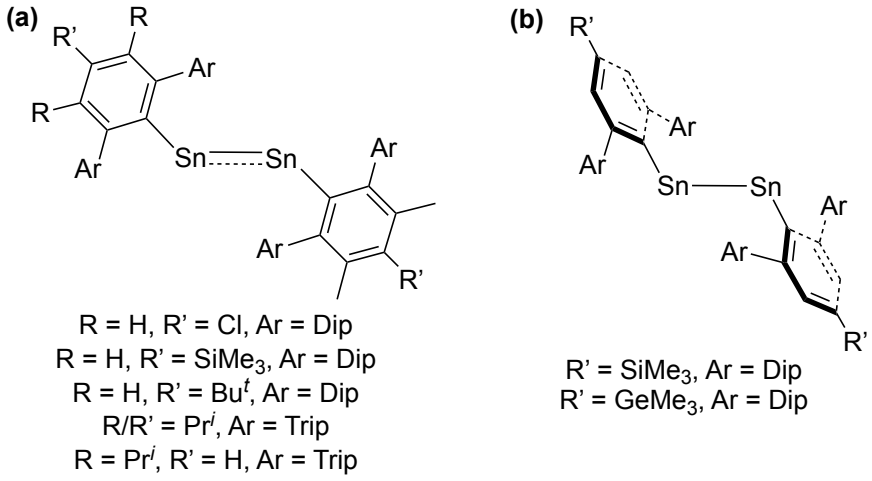

Figure 2.4. Comparison of geometries of multiply bonded (**a**) and singly bonded (**b**) terphenyl distannynes.

The first amido distannyne [{($^{iPr}L^{\dagger}$)Sn}$_2$] was isolated by reducing the [($^{iPr}L^{\dagger}$)SnBr] complex with [{(^{Mes}Nacnac)Mg}$_2$] (**Scheme 2.12**).[46] This dimer is thermally stable in the solid-state but decomposes in solution over two days. It features a Sn-Sn bond length (3.1429(7) Å) longer than the above-mentioned terphenyl distannynes and an N-Sn-Sn bond angle of 104.00°. This further confirms the presence of a single bond, which is due

to planarisation of the Sn_2NSiC fragment, like in the singly bonded amido digermynes (covalent radii Ge = 1.20 Å vs. Sn =1.39 Å). Another amido distannyne [{(^{PhBo}L)Sn}$_2$] was reported utilising the boryl-amide ligand (**Scheme 2.12**).[35] This dimer consists of a single Sn-Sn bond with a distance of 3.0638(7) Å and average N-Sn-Sn angle of 100.42°, which are comparable to the distannyne [{(^{iPr}L†)Sn}$_2$].

2.1.3.3 Diplumbynes

The isolation of the first lead(I) analogue in 2000 marked as the starting point for the heavier ditetrelyne chemistry. The credit for the first lead(I) dimer [{(^{Trip}Ar)Pb}$_2$] is also given to Power and co-workers.[47] It was obtained by treatment of [{^{Trip}ArPb(μ-Br)}$_2$] with $LiAlH_4$ in diethyl ether. It was proposed that the reaction proceeds via formation of a lead hydride intermediate [{(^{Trip}Ar)Pb(μ-H)}$_2$] which eliminates H_2 upon warming the solution. Further, it condenses to result in the [{(^{Trip}Ar)Pb}$_2$] complex in 10 % isolated yield (**Scheme 2.13**). In fact, this hypothesis was found to be true by Lars Wesemann with the isolation and structural characterisation of the dimeric hydride bridged species [{(^{Trip}Ar)Pb(μ-H)}$_2$].[48] Recently, the yields of these diplumbynes have been improved 'greatly', up to 64 % by using [{(^{Mes}Nacnac)Mg}$_2$] as reducing agent. In addition to that, several lead(I) complexes have also been isolated using the [{(^{Mes}Nacnac)Mg}$_2$] or DIBAL-H (DIBAL-H = [(Bu^i_2)AlH]).[49]

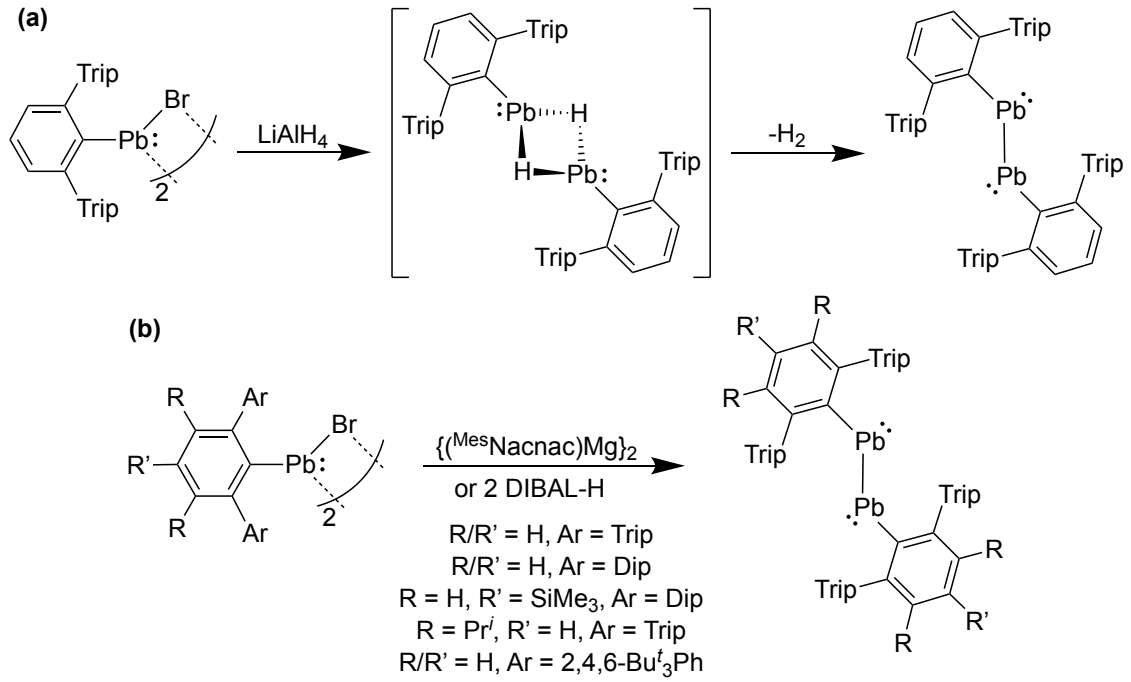

Scheme 2.13. Synthesis of first terphenyl stabilised diplumbyne (**a**) and improved synthesis of terphenyl stabilised diplumbynes (**b**).

The lead(I) complex [{(^{Trip}Ar)Pb}$_2$] features a planar, trans-bent C-Pb-Pb-C unit. The Pb-Pb bond distance is 3.1881(1) Å which is shorter than the interatomic lead element distance (3.49 Å), and longer than in the typical diplumbane [{Ph_3Pb}$_2$] (Pb-Pb = 2.844(4) Å). The Pb-Pb-C angle, 94.26(4)°, being close to a right angle, indicates 'little' hybridisation as well as the presence of a lone pair of electrons at each lead centre, as a result of inert pair effect. The structural parameters of recently reported diplumbynes [{(^{Trip}Ar^{i}^{Pr2})Pb}$_2$] and [{(^{t}^{Bu6}Ar)Pb}$_2$] (^{t}^{Bu6}Ar = 2,6-(2,4,6-Bu^{t}$_3$Ph)$_2$-Ph) are the Pb-Pb bond lengths 3.0382(6) Å and 3.0394(9) Å and Pb-Pb-C bond angles 114.73(7)° and 116.02(6)°, respectively. The Pb-Pb-C bond angles in these diplumbynes are comparatively widened than in other diplumbynes, due to substitution of additional Pr^{i} and Bu^{t} groups on the ligand framework, which increases the steric effect of the ligand. This also explains the shortening of the Pb-Pb bonds in these two dimers relative to the firstly reported diplumbyne. The presence of multiple bonds in these diplumbynes with bond orders of 0.8-1.5 was confirmed by computational studies. That being said, amide ligand stabilised diplumbynes are still unknown.

2.1.4 Small Molecule Activation using Group 14 Element(I) Dimers

2.1.4.1 Reaction with H_2

Since the first report of homolytic cleavage of dihydrogen with terphenyl ligand stabilised digermyne [{(^{Dip}Ar)Ge}$_2$] in 2005, there have been several group 14 element(I) heavier alkyne analogues which can activate dihydrogen. The addition of one, two or three equivalents of dihydrogen to [{(^{Dip}Ar)Ge}$_2$] at room temperature and atmospheric pressure yields a mixture of digermene (germanium(II) hydride), digermane (germanium(III) hydride), and a primary germane (geramanium(IV) hydride) species (**Scheme 2.14**).[50] The three different species were also confirmed by the ^{1}H NMR hydride resonances at δ 3.21, 3.58 and 5.87 ppm, respectively. It is worth noting that the mechanistic study reinforces the formation of mixed hydride species in multiple steps (**Figure 2.5**): (**a**) firstly, the formation of [(^{Dip}Ar)Ge(μ-H)GeHAr^{Dip}] on addition of H_2, which further isomerises to [(^{Dip}Ar)GeGeH$_2$(Ar^{Dip})], (**b**) this intermediate species then reacts with H_2 at single site of Ge or joint Ge-Ge site to give [(^{Dip}Ar)GeH$_3$] and [(^{Dip}Ar)GeH$_2$GeH$_2$(Ar^{Dip})], (**c**) lastly, the initial product [(^{Dip}Ar)Ge(μ-H)GeH(Ar^{Dip})] isomerises to give [(^{Dip}Ar)GeHGeH(Ar^{Dip})].[51]

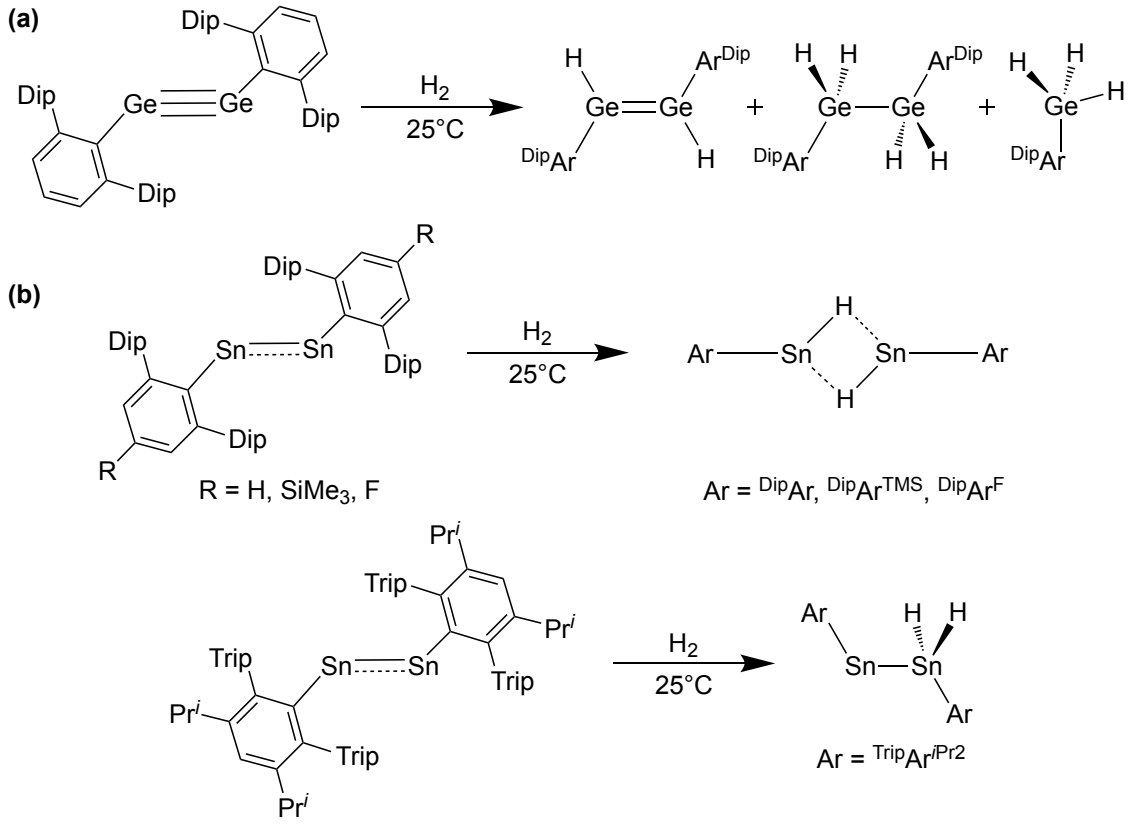

Scheme 2.14. H_2 activation by terphenyl stabilised digermyne (**a**) and terphenyl stabilised distannynes (**b**).

The terphenyl stabilised tin analogues ([{(Ar)Sn}$_2$], Ar = ^{Dip}Ar, ^{Dip}Ar^{TMS}, ^{Dip}Ar^{F} (^{Dip}Ar^{F} = 2,6-(Dip)$_2$-4-FPh), ^{Trip}Ar) were also shown to activate dihydrogen under atmospheric pressure. [{(Ar)Sn}$_2$] dihydrogen activation (^{Dip}Ar, ^{Dip}Ar^{TMS}, ^{Dip}Ar^{F}) resulted in the formation of a bridged hydrido compound at room temperature,[52] while only [{(^{Dip}Ar)Sn(μ-H)}$_2$] released dihydrogen when heated to 80 °C.[53] However, reaction of the bulkier distannyne [{(^{Trip}Ar^{iPr2})Sn}$_2$] gives a non-bridged dihydrostannye, due to greater stability of the formed complex at room temperature. The mechanism of dihydrogen activation by [{(^{Dip}Ar)Sn}$_2$] resembles the earlier mentioned activation for the digermyne [{(^{Dip}Ar)Ge}$_2$]. It proceeds through formation of the species [(^{Dip}Ar)SnSnH$_2$(Ar^{Dip})], followed by isomerisation and dissociation steps to form two [(^{Dip}Ar)Sn:] fragments. These fragments reassemble to form the bridged hydride species [{(^{Dip}Ar)Sn(μ-H)}$_2$].[51]

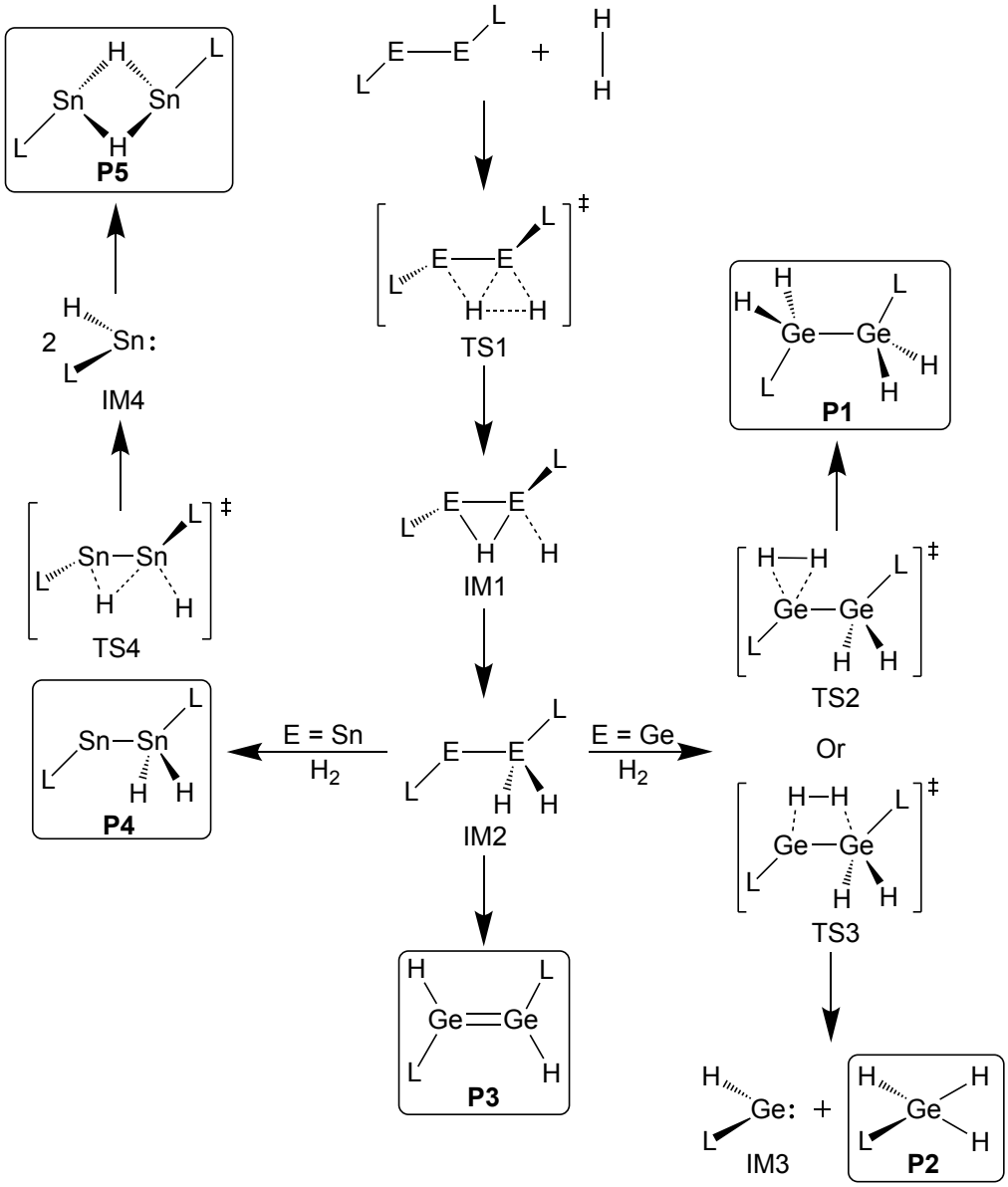

Figure 2.5. Mechanism of H_2 activation by ArEEAr (Ar = ^{Dip}Ar, ^{Trip}Ar^{iPr2}, E = Ge, Sn) dimers.

Later, amido digermynes were found to be highly reactive towards dihydrogen, however, they tend to show somewhat different reactivity than that of [{(^{Dip}Ar)Ge}$_2$]. The less bulkier amido digermyne [{(^{TMS}L*)Ge}$_2$] when reacted with dihydrogen forms a mixed-valent hydridogermane-germylene [(^{TMS}L*)GeGeH$_2$(L^{*TMS})] quantitatively, in solution and also in solid-state within 20 minutes at ambient temperature.[41] The ^{1}H NMR spectrum shows a very broad hydride resonance at δ 6.1 ppm, which sharpens at -50 °C. This gives evidence of an equilibrium between mixed-valent hydride and symmetrical [{(^{TMS}L*)GeH}$_2$] species in solution. Such isomerisation has been shown to be thermodynamically possible by the density functional theory (DFT) calculations.[54]

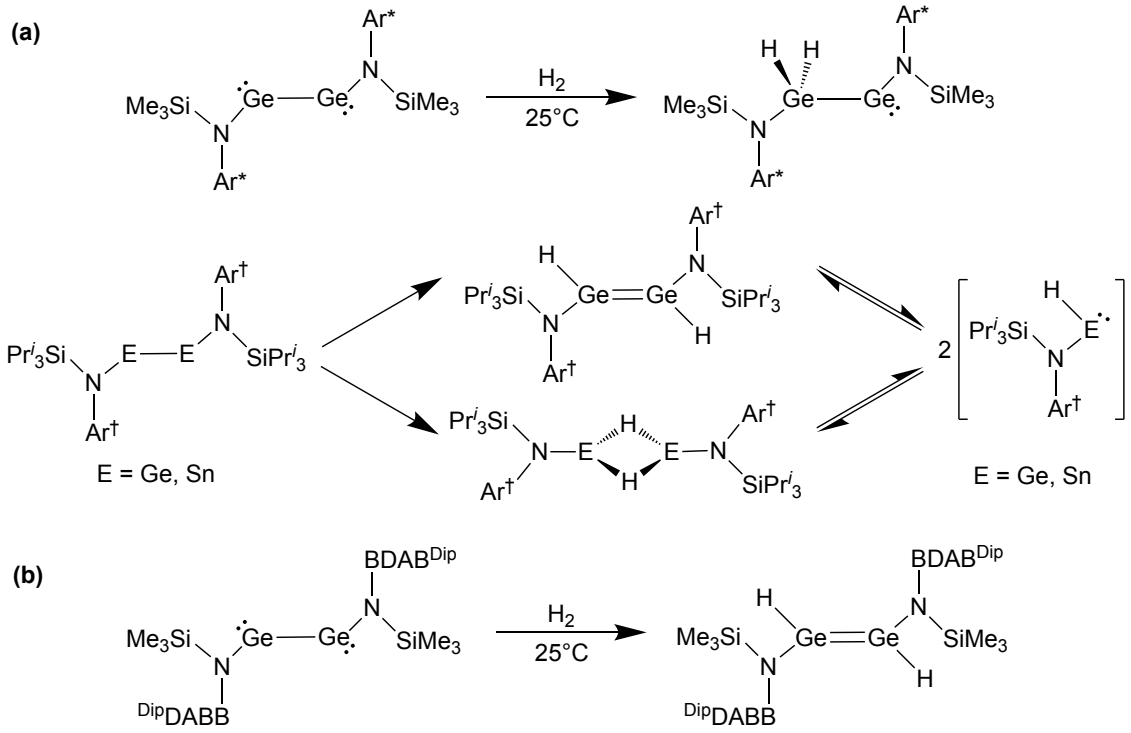

Scheme 2.15. H_2 activation by aryl-silyl amide stabilised digermynes and distannynes (**a**) and boryl-silyl amide stabilised digermyne (**b**).

In contrast, under similar conditions, the reaction of bulkier doubly bonded amido digermyne [{($^{i\text{Pr}}$L†)Ge}$_2$] with dihydrogen resulted in a hydrido digermene [{($^{i\text{Pr}}$L†)GeH}$_2$] (**Scheme 2.15**).[42] Attempts to isolate the di- or tri-hydrogenated products were not successful even at higher temperature and concentrations of dihydrogen. However, heating the reaction mixture to 100 °C shifts the ^{1}H NMR hydride resonance to δ 10.6 ppm from δ 8.21 ppm at room temperature. Additionally, a variable temperature UV-vis spectroscopic analysis revealed that an absorption band at a λ_{max} of 460 nm ($n_- \rightarrow n_+$ transition, 0 °C) disappears at 100 °C and an isosbestic point was observed at 420 nm. These observations gave strong evidence of an equilibrium between hydrido germylenes [{($^{i\text{Pr}}$L†)GeH}] and [{($^{i\text{Pr}}$L†)GeH}$_2$].

The treatment of a boryl-amido digermyne with dihydrogen gave hydrido digermene product [{($^{\text{TBo}}$L)GeH}$_2$] in 6 hours with no further evidence of an equilibrium.[35] Amido distannye [{($^{i\text{Pr}}$L†)Sn}$_2$] also activates dihydrogen albeit at a slower rate as compared to the amido digermyne reaction with dihydrogen.[46] The reaction showed 70 % conversion to amido hydride bridged complex [{($^{i\text{Pr}}$L†)Sn}$_2$(μ-H)] after 24 hours, with the formation of a small amount of free ligand and elemental tin. This amido tin hydride complex also

partially dissociates to [($^{i\text{Pr}}$L†)SnH] in aromatic solvents, which was evidenced by ^{1}H NMR spectroscopy.

2.1.4.2 Reactions with CO_2, CS_2, N_2O

Singly bonded amido digermynes reduce CO_2 to form bis(germylene) oxide at temperatures as low as -40 °C with the release of CO gas.[55] Theoretical calculations reveal that the reaction goes via a three step mechanism, in which first CO_2 connects to one or two germanium centres by a side-on approach. Next, the insertion of CO_2 into Ge-Ge bond, followed by a rearrangement step, and finally a -CO elimination to yield the final product as [{($^{\text{TMS}}$L*)Ge}$_2$(μ-O)]. An alternative pathway to synthesise this compound is the reaction of digermyne with N_2O. Bu^{t}NCO, isocyanate and CS_2 also react with this amido digermyne and get reduced to form either [{($^{\text{TMS}}$L*)Ge}$_2$(μ-O)] or [{($^{\text{TMS}}$L*)Ge}$_2$(μ-S)] (**Scheme 2.16**).[55] These reactions proceed with the oxygen/sulphur insertion into Ge-Ge bonds. The singly bonded amido distannyne also reacts with CO_2 and forms a tin(II) carbonate complex [{($^{i\text{Pr}}$L†)Sn}$_2$(μ-CO$_3$)].[37] The reaction likely starts via the formation of an [{($^{i\text{Pr}}$L†)Sn}$_2$(μ-O)] intermediate, which reacts with one more equivalent of CO_2, in a similar fashion to a previous magnesium compound,[56] to form the final tin(II) carbonate complex.

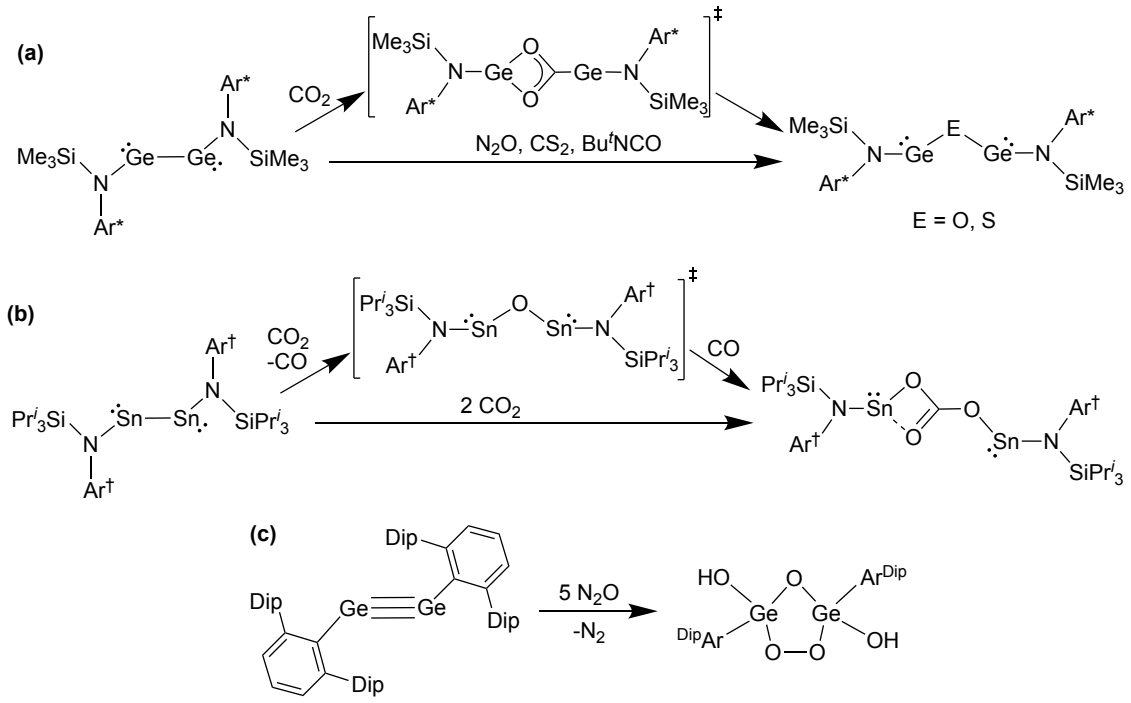

Scheme 2.16. Reactivity of amido digermyne with CO_2, N_2O, CS_2 and Bu^{t}NCO (**a**), amido distannyne with CO_2 (**b**) and terphenyl-stabilised digermyne with N_2O (**c**).

In contrast to this, Power's digermyne [{(^{Dip}Ar)Ge}$_2$] on reacting with N_2O yields a peroxide product which consists a Ge_2O_5 ring with cyclic germanium(IV) centres. The reaction progresses through formation of a peroxide species via a radical mechanism. The intermediate species further reacts with N_2O and finally abstracts the protons from solvent to result in the oxy, peroxy and terminal hydroxy complex [{(^{Dip}Ar)Ge(OH)}$_2$(μ-O)Ge(μ$_2$:η$_2$-O$_2$)].[57]

2.1.5 Monomeric two-Coordinate Hydride Complexes

2.1.5.1 Synthesis of Group 14 Element(II) Hydride Complexes

Since the first report on the isolation of divalent hydride complex in 2000, numerous group 14 element hydride complexes in the +2 oxidation state have been developed.[58] Typical routes for synthesis of group 14 element hydride complexes are[59] **i**) salt metathesis reaction between LEX (X = halide, E = Si-Pb, L = ligand) species and hydride sources (BH_4Li, BBu^s_3H), **ii**) σ-metathesis reaction of LEX complex (X = electronegative group, e.g. alkoxide) with a hydride source (preferred for selective hydride complex generation), **iii**) oxidative route which utilises the activation of dihydrogen by ditetrelynes (LEEL) and **iv**) reduction of LEX_2 species with reducing agents.

The first hydride species was [{(^{Trip}Ar)Sn(μ-H)}$_2$] synthesised by the addition of DIBAL-H solution to [(^{Trip}Ar)SnCl] in diethyl ether. Later on, the germanium(II) hydride complex [{(^{Dip}Ar)Ge(μ-H)}$_2$] was synthesised using L-selectride [(Bu^s_3)(H)BLi] with [(^{Dip}Ar)SnCl], and the lead(II) hydride complex [{(^{Trip}Ar)Pb(μ-H)}$_2$] via the addition of HBcat (cat = catecholato) to the [(^{Trip}Ar)(PPh_2PhCH)Pb] (**Scheme 2.17**).[48,60] All of these hydride complexes are dimeric in solid-state and have the hydride ligand either on each element centre or bridged between two element centres.

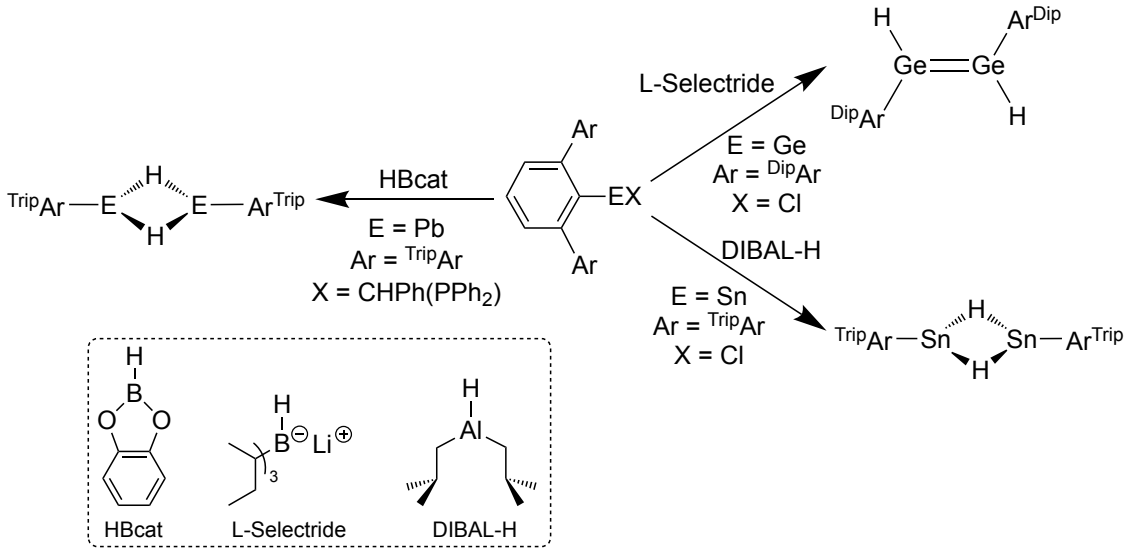

Scheme 2.17. Synthesis of terphenyl stabilised group 14 element(II) hydride complexes.

That being said, synthesis of the first monomeric 'pseudo' two-coordinate hydride complexes [($^{i\text{Pr}}$L†)EH] (E = Ge, Sn) was carried out in our group by treating the [($^{i\text{Pr}}$L†)ECl] complexes with L-Selectride or by the reaction of [($^{i\text{Pr}}$L†)GeOBu^{t}] complexes with HBpin/HBcat (pin = pinacolato).[42] These hydrides were originally isolated as dimers in solid-state, however, a dynamic conformational change to monomers was observed in solution due to the steric and electronic properties of the ligand employed. The evidence for the presence of monomeric complex was also confirmed by Lewis-base coordination of these hydride species with DMAP (DMAP = 4-Me$_2$NPy) (**Scheme 2.18**).

Later on, in 2015, increasing the ligand bulk to $^{t\text{BuO}}$L* and $^{t\text{BuO}}$L† allowed the isolation of first and only examples of 'true' two-coordinate germanium(II) hydride complexes.[61] These complexes were synthesised by a σ-metathesis route in two steps. The initial step involved the synthesis of [($^{t\text{BuO}}$L)GeOBu^{t}] species by the reaction of [($^{t\text{BuO}}$L)GeCl] with KOBu^{t} in toluene. Next, [($^{t\text{BuO}}$L)GeOBu^{t}] were reacted with catechol borane, resulting in monomeric two-coordinate hydride complexes [($^{t\text{BuO}}$L)GeH] (L = L*, L†). Both of these complexes are thermally stable and displayed the ^{1}H NMR hydride resonance at δ 10.02 ppm and δ 10.00 ppm, similar to the 'pseudo' two-coordinate hydride complex [($^{i\text{Pr}}$L†)GeH]. Additionally, the monomeric structures of these complexes were also confirmed by X-ray crystallography which did not show any Ge-O interaction(s). The SiCNGeH units of these compounds ([($^{t\text{BuO}}$L*)GeH] and [($^{t\text{BuO}}$L†)GeH]) were found to be planar with Ge-N bond distances of 1.877(4) Å and 1.886(3) Å, which also indicate possible N to Ge π-interactions.

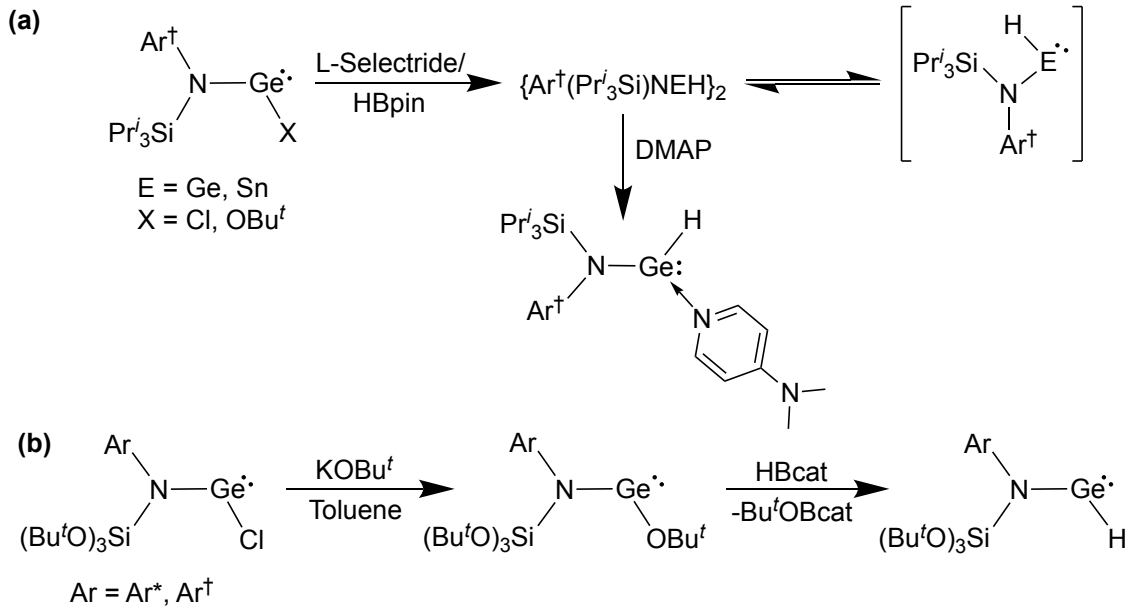

Scheme 2.18. Synthesis of monomeric 'pseudo' two-coordinate group 14 element(II) hydride complexes and DMAP coordination (**a**) and monomeric two-coordinate germanium(II) hydride complexes (**b**).

2.1.5.2 Reactivity of two-Coordinate Group 14 Element(II) Hydride Complexes

It was proposed in our group that the reactivity of two-coordinate hydride group 14 complexes towards catalysis could be considerably more than higher-coordinate group 14 element(II) hydride complexes. They possess a vacant valence p-orbital on the group 14 element centre that could pre-coordinate a substrate prior to bond activation.

The first examples of hydroelementation of unsaturated substrates by two-coordinate group 14 element hydride complexes were reported in 2014.[62] The pseudo hydride complexes [($^{i\text{Pr}}$L†)EH] were shown to effectively hydroborate various aldehydes and ketones to yield tetrel alkoxide complexes (**Scheme 2.19**). The treatment of these compounds with HBpin/HBcat gave boryl esters and hydride complexes [($^{i\text{Pr}}$L†)EH] (**Scheme 2.20**). These reactions occurred rapidly at ambient temperature compared to three-coordinate [($^{\text{Dip}}$Nacnac)EH] ($^{\text{Dip}}$Nacnac = [HC{N(Dip)C(Me)}$_2$]$^-$) (E = Ge, Sn) hydride complexes, which could only react with activated substrates under such conditions.[63–65] It should be noted that on reacting the borane and ketone in 1:1 a stoichiometric ratio in presence of 5.00-0.05 mol % of 'pseudo' monomeric hydride complex (depending on the substrate), generated the respective boryl esters in high yields.

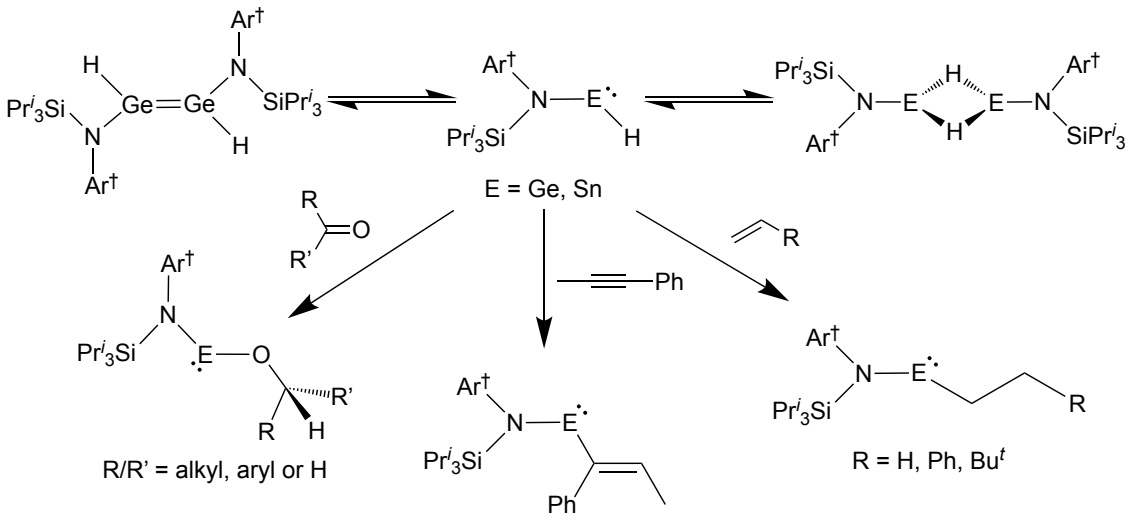

Scheme 2.19. Hydroelementation reactions of two-coordinate group 14 element hydride complexes with unsaturated substrates (alkenes, alkynes, aldehydes and ketones).

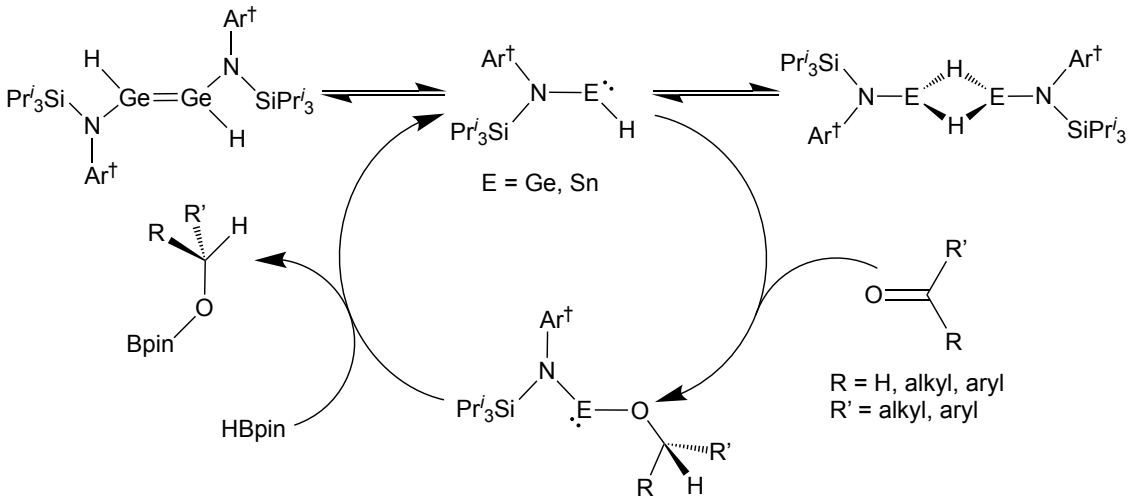

Scheme 2.20. Catalytic cycle for hydroboration of aldehydes and ketones using [($^{i\text{Pr}}$L†)EH] catalysts.

The 'pseudo' two-coordinate hydride complexes [($^{i\text{Pr}}$L†)EH] also undergo hydroelementation reactions with unsaturated C-C bonds (alkenes/alkynes) (**Scheme 2.20**).[66] The reaction of [($^{i\text{Pr}}$L†)EH] with alkenes or substituted alkenes yielded the corresponding alkyl or substituted alkyl tetrelenes. Further, the reactivity of [($^{i\text{Pr}}$L†)EH] with alkynes was also examined to assess if the double hydroelementation of the substrate was feasible. However, this did not occur, instead the formation of corresponding vinyl tetrelenes was observed.

2.2 Research Proposal

In the past, there have been several monodentate aryl-silyl amide ligands employed for the stabilisation of group 14 element complexes. However, slight modifications on ligand frameworks have led to substantial changes in the structure and reactivity of synthesised group 14 element(I) heavier alkyne analogues of type LEEL (L = bulky monodentate ligand, E = Si-Pb). Related studies regarding the effect of steric encumbrance of these ligands on synthesised complexes are still a surprising area for chemists' understanding. Therefore, widening the library of ligands to further explore group 14 element chemistry is an interesting domain of exploration. The steric and electronic properties of aryl-silyl amide ligands can be modified in a relatively simple manner as these ligands are easily accessible in a few steps and can be synthesised at very low cost. These versatile amide ligands give an opportunity of three possible modifications on the ligand framework **i**) flanking aryl groups, **ii**) central phenyl ring and **iii**) silyl side chain (**Figure 2.6**).

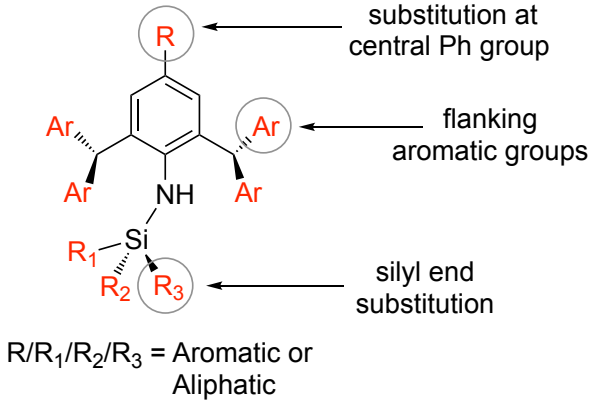

Figure 2.6. General structure and possible modification sites on aryl-silyl amine pro-ligand framework.

Hence, our goal was to synthesise novel bulky monodentate aryl-silyl amide ligands and utilise these ligands in synthesis of low-coordinate group 14 element(II) halide complexes. Moreover, we wished to shed light on steric encumbrance of these ligands and draw a comparison of steric encumbrance with previously reported monodentate aryl-silyl amide ligands. Finally, we also aimed to use the synthesised group 14 element(II) halide complexes in isolation of heavier alkyne LEEL analogues and two-coordinate monomeric hydride complexes.

2.3 Results and Discussion

2.3.1 Synthesis of Bulky Aryl-Silyl Amine Pro-Ligands

With the knowledge of previously reported bulky amide ligands, we sought to expand the range of this ligand class. We chose to explore all three modification centres in order to fully understand the properties of these ligands. That is why we decided to initially synthesise the reported bulky anilines **1-4** (**Scheme 2.21**). The general synthetic procedure for bulky anilines involves formation of an aryl Grignard reagent which is quenched with ethyl formate and water to result in respective di(aryl)methanol compounds, followed by further condensation with para-substituted anilines. Using this strategy, overall four anilines [2,6-$(Ph_2CH)_2$-4-Me-$PhNH_2$] (Ar^*NH_2) **1**,[15] [2,6-$(Ph_2CH)_2$-4-Pr^i-$PhNH_2$] ($Ar^\dagger NH_2$) **2**,[16] [2,6-{$(3,5\text{-}Bu^t{}_2Ph)_2CH$}$_2$-4-Me-$PhNH_2$] ($Ar^{***}NH_2$) **3**[67] and [2,6-{$(2\text{-}Nap)_2CH$}$_2$-4-Me-$PhNH_2$] ($Ar^NNH_2$) **4**[68] were synthesised. Aniline **3** could not be isolated in a good yield even after multiple attempts. Further, an attempt to synthesise [2,6-{$(2\text{-}Nap)_2CH$}$_2$-4-$Pr^i$$PhNH_2$] was not successful and a mixture of several species were seen in ^1H NMR spectrum, and the compound could not be purified by crystallisation and/or column chromatography.

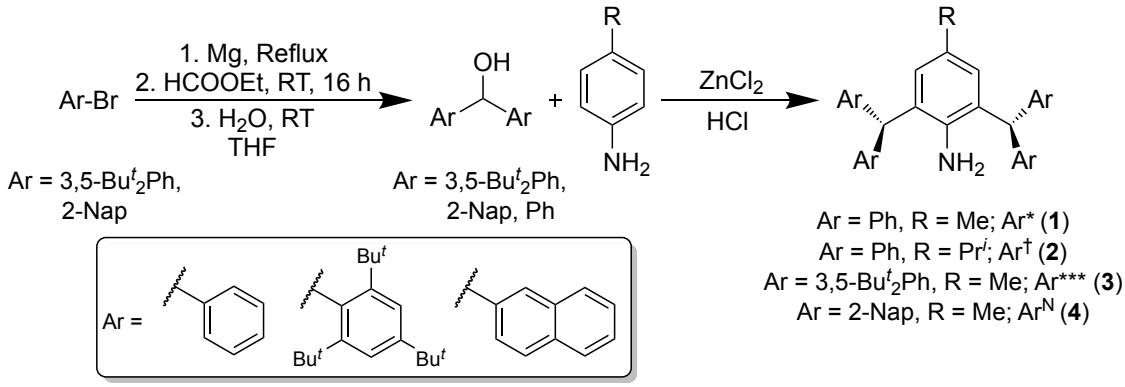

Scheme 2.21. Synthesis of bulky anilines **1-4**.

With several bulky anilines in hand, bulky aryl-silyl amine pro-ligands were targeted. For that purpose, a series of trisubstituted chlorosilanes Me_3SiCl **5**, $Pr^i{}_3SiCl$ **6,** 4-Bu^tPh_3SiCl **7**, and Cy_3SiCl **8** were chosen. The former two were commercially available and the rest were easily synthesised following literature procedures.[69,70] For pro-ligand synthesis, the anilines **1-4** were deprotonated using $LiBu^n$ in THF. The resulting lithium salts of anilines (ArNHLi) were added to respective THF solution of chlorosilanes (**5-8**), which was followed by 12-24 hours stirring. The reactions of **1.Li** and **2.Li** with **8** and

3.Li with **6** were carried out between -80 °C to ambient temperature for 12 hours. However, the reactions of **1.Li** and **2.Li** with **7** and **4.Li** with **5-8** did not show full conversion until being heated at 60 °C for 12 hours and 24 hours, respectively. The synthesis of pro-ligands **9-17** is outlined in **Scheme 2.22**. The amines **9-12** and **14-17** were isolated in 40-80 % yields while **13** could only be isolated in ~30 % yield even after multiple attempts. The ^{1}H NMR NH resonance for all ligands falls in the range of δ 1.90-3.00 ppm. The ligands **9-17** are air and moisture stable and show a characteristic NH stretch peak at ~3350 cm^{-1} in their IR spectra.

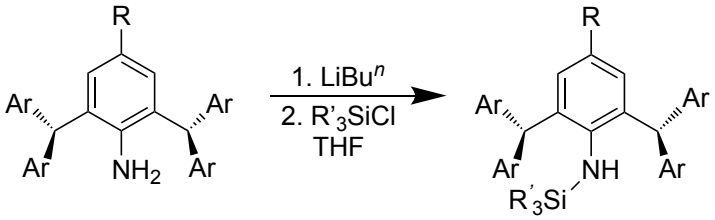

R = Me, R' = 4-Bu^{t}Ph, Ar = Ph, $^{t\text{BuPh}}$L*H (**9**)
R = Pr^{i}, R' = 4-Bu^{t}Ph, Ar = Ph, $^{t\text{BuPh}}$L†H (**10**)
R = Me, R' = Cy, Ar = Ph, $^{\text{Cy}}$L*H (**11**)
R = Pr^{i}, R' = Cy, Ar = Ph, $^{\text{Cy}}$L†H (**12**)
R = Me, R' = Me, Ar = 3,5-Bu$^{t}_{2}$Ph, $^{\text{TMS}}$L***H (**13**)
R = Me, R' = Me, Ar = 2-Nap, $^{\text{TMS}}$L$^{\text{N}}$H (**14**)
R = Me, R' = Pr^{i}, Ar = 2-Nap, $^{i\text{Pr}}$L$^{\text{N}}$H (**15**)
R = Me, R' = 4-Bu^{t}Ph, Ar = 2-Nap, $^{t\text{BuPh}}$L$^{\text{N}}$H (**16**)
R = Me, R' = Cy, Ar = 2-Nap, $^{\text{Cy}}$L$^{\text{N}}$H (**17**)

Scheme 2.22. Synthesis of bulky aryl-silyl amine pro-ligands.

The amine pro-ligands **10-12** and **16** were crystallised from minimum amounts of hexane, toluene or mixtures of toluene/hexane. The crystal structures of these pro-ligands are depicted in **Figure 2.7** and **Figure 2.8**. All of the compounds are monomeric in solid-state. They are similar to already reported aryl-silyl amine pro-ligands and will not be emphasised here.[17,22] For an insight into the steric bulk of the ligand a space-filling diagram of **10** is also given in **Figure 2.7**. Further, detailed bulk studies of these ligands have been performed using the software SambVca 2.1, which is discussed in section **2.3.3**.

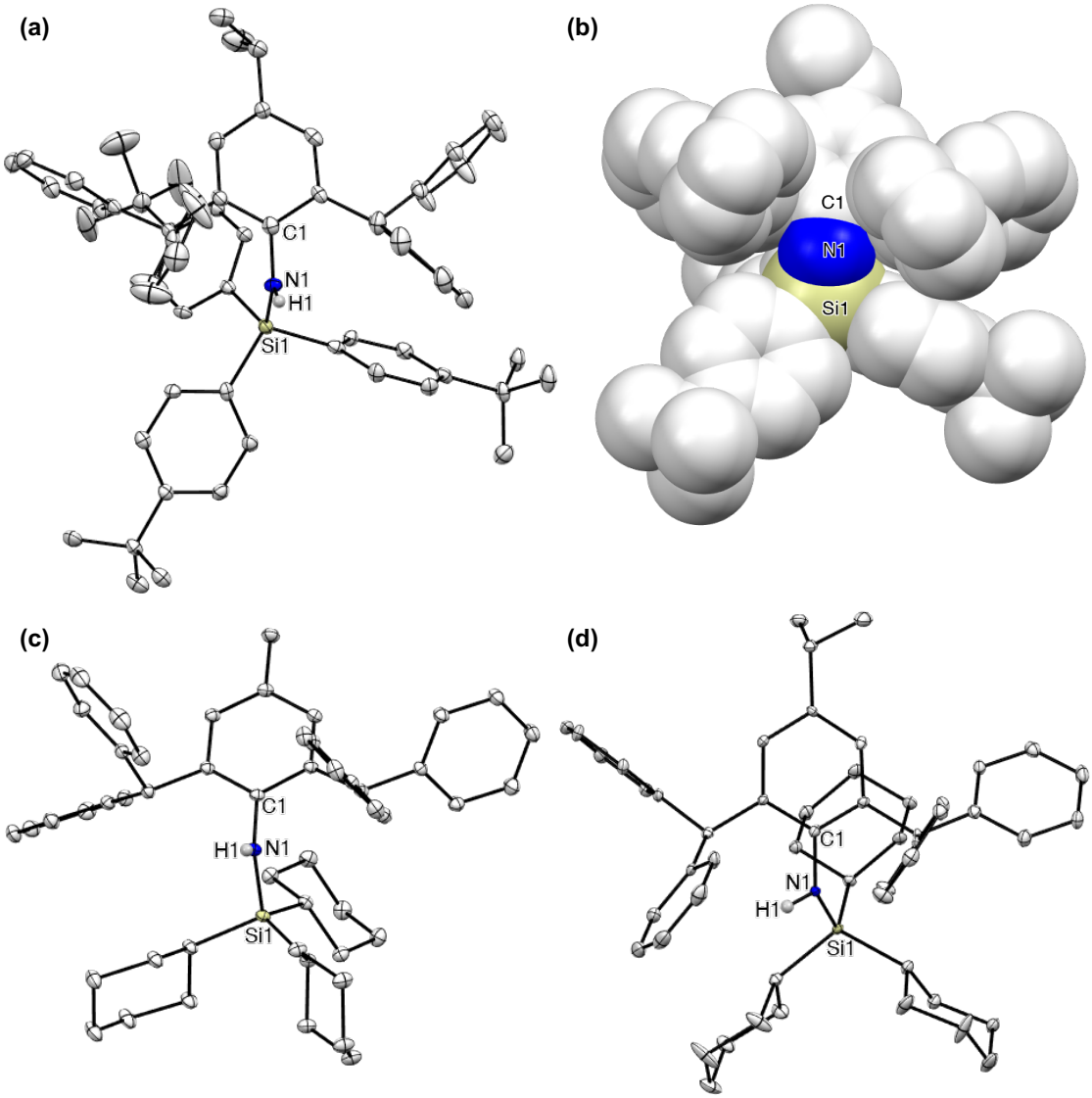

Figure 2.7. Molecular structures of [$^{t\text{Bu}}$L†H] (**10**) (**a**), [$^{\text{Cy}}$L*H] (**11**) (**c**) and [$^{\text{Cy}}$L†H] (**12**) (**d**) (thermal ellipsoids shown at 30 % probability). Hydrogen atoms except amine protons omitted for clarity. Selected bond lengths (Å) and angles (°) for **10**: N1-C1 1.435(8), N1-Si1 1.740(5), C1-N1-Si1 123.3(4); **11**: N1-C1 1.4297(13), N1-Si1 1.7572(10), C1-N1-Si1 124.15(7); **12**: N1-C1 1.427(5), N1-Si1 1.748(4), C1-N1-Si1 129.9(3); space-filling diagram of **10** (**b**).

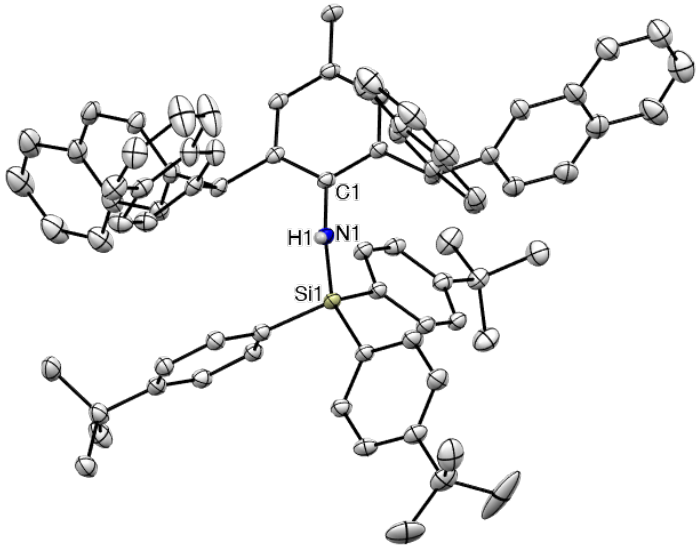

Figure 2.8. Molecular structure of [$^{t\text{Bu}}$L$^{\text{N}}$H] (**16**) (thermal ellipsoids shown at 20 % probability). Hydrogen atoms except H1 omitted for clarity. Selected bond lengths (Å) and angles (°): N1-C1 1.431(3), N1-Si1 1.725(2), C1-N1-Si1 125.50(17).

2.3.2 Synthesis of Aryl-Silyl Amido Group 14 Element(II) Halide Complexes

Having synthesised the monodentate aryl-silyl amine pro-ligands **9**-**17**, we attempted to deprotonate them using various alkali metal reagents, e.g. LiBu^n, KH (with a catalytic amount of HMDS (5 mol %), HMDS = HN(SiMe$_3$)$_2$) and KN(SiMe$_3$)$_2$ in THF. Only pro-ligands **9** and **10** could be successfully deprotonated using KH and KHMDS (5 mol %) in THF at RT overnight, affording the compounds **9.K** and **10.K** as light yellow colour free-flowing solids (**Scheme 2.23**). The formation of these was confirmed by various spectroscopic techniques. Both of the compounds showed an absence of NH proton in their ^{1}H NMR spectra.

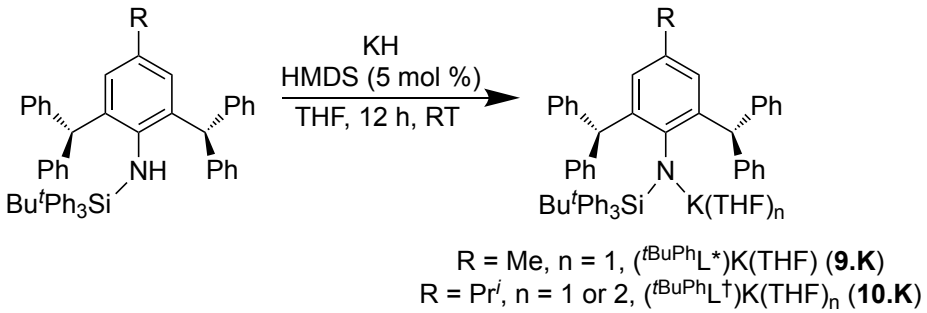

Scheme 2.23. Synthesis of aryl-silyl potassium amides **9.K** and **10.K**.

10.K was crystallised from THF and the molecular structure is depicted in **Figure 2.9**. It exists as a monomer in the solid-state with the potassium centre having *N*,arene-

interaction with one of the flanking phenyl groups and the nitrogen of central phenyl ring. K1 is further solvated by two THF molecules while ^{1}H NMR spectroscopic data shows the presence of only one THF molecule. This inconsistency may have arisen due to loss of one THF while pumping down the isolated material under vacuum. The coordination mode in **9.K** is similar to an earlier reported potassium amide [(^{TMS}L$^{\#}$)K(THF)$_2$] (^{TMS}L$^{\#}$ = (TMS)Ar$^{\#}$N; Ar$^{\#}$ = 2,6-(Ph$_2$CH)$_2$-4-Bu^{t}Ph).[71]

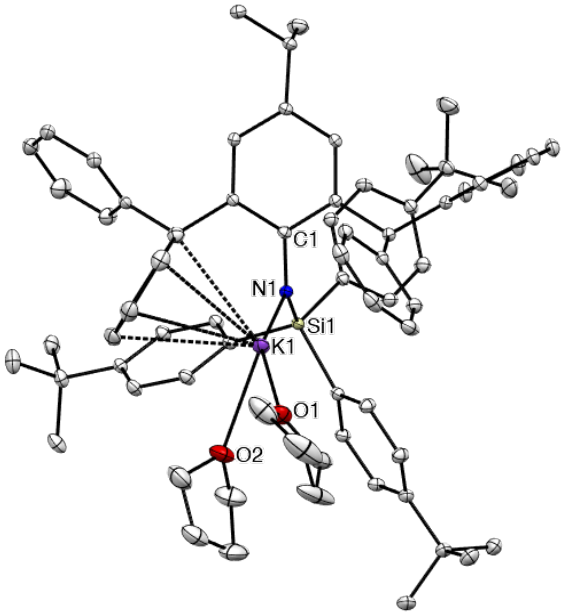

Figure 2.9. Molecular structure of [($^{t\text{Bu}}$L†)K(THF)$_2$] (**10.K**) (thermal ellipsoids shown at 20 % probability). Hydrogen atoms omitted for clarity. Selected bond lengths (Å) and angles (°): N1-C1 1.390(4), N1-Si1 1.671(3), N1-K1 2.683(3), K1-O1 2.691(3), K1-O2 2.734(3) C1-N1-K1 112.61(19), C1-N1-Si1 121.6(2), K1-N1-Si1 125.68(13), N1-K1-O1 156.16(10), N1-K1-O2 107.31(10).

In case of ligands **9-17**, the use of a slight excess of LiBu^{n} was found to be the most efficient way for *in situ* deprotonation of the ligands that generated the respective amido-lithium salts (**9.Li-17.Li**), which could be used for later salt elimination reactions.

Addition of a THF solution of potassium salts or *in situ* generated lithium salts of ligands to GeCl$_2$.dioxane in THF led to promising results, and the synthetic methods are outlined in **Scheme 2.24**. These reactions afforded germanium(II) chloride complexes **18-22** in moderate to good yields. All of the synthesised amido germanium(II) chloride complexes are stable at room temperature and ^{1}H NMR spectra suggested a single ligand environment. It was also observed that on changing the substituent on the silyl group from Bu^{t}Ph$_3$Si to Cy$_3$Si, the ^{29}Si{^{1}H} NMR resonance shifted downfield due to the

decrease in aromatic groups, which is similar to the trend seen in reported amido germanium(II) chlorides [$(R_3Si)Ar^*NGeCl$] (R = Ph, Ph_2Me, Me_3).[17]

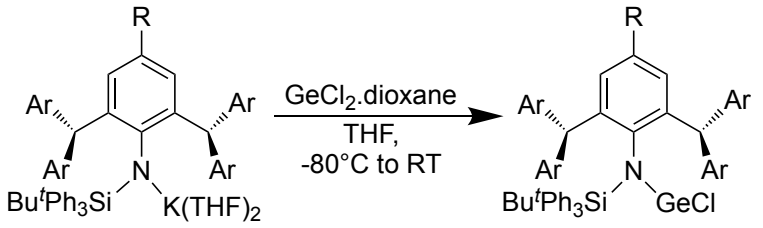

R = Me, R' = 4-Bu^{t}Ph, Ar = Ph, ($^{t\text{BuPh}}$L*)GeCl (**18**)
R = Pr^i, R' = 4-Bu^{t}Ph, Ar = Ph, ($^{t\text{BuPh}}$L†)GeCl (**19**)

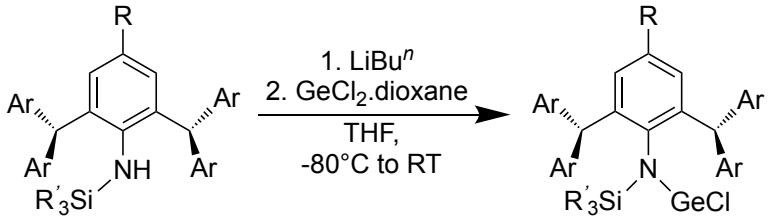

R = Me, R' = 4-Bu^{t}Ph, Ar = Ph, ($^{t\text{BuPh}}$L*)GeCl (**18**)
R = Pr^i, R' = 4-Bu^{t}Ph, Ar = Ph, ($^{t\text{BuPh}}$L†)GeCl (**19**)
R = Me, R' = Cy, Ar = Ph, ($^{\text{Cy}}$L*)GeCl (**20**)
R = Pr^i, R' = Cy, Ar = Ph, ($^{\text{Cy}}$L†)GeCl (**21**)
R = Me, R' = Me, Ar = 3,5-Bu$^t_2$Ph, ($^{\text{TMS}}$L***)GeCl (**22**)

Scheme 2.24. Synthesis of aryl-silyl amido germanium(II) chloride complexes **18**-**22**.

For the reactions of **14.Li**-**17.Li** with germanium(II) chloride, 50:50 mixtures of new species and protonated ligands were observed in ^{1}H NMR spectra, and clean germanium(II) chloride complexes could not be obtained. Further, efforts to synthesise any of the amido lead(II) halide complexes were unsuccessful. An instantaneous lead element deposition was seen in all cases on addition of lead(II) halides ($PbCl_2$ and $PbBr_2$) to the *in situ* generated lithium salts of the ligands.

The amido germanium(II) chloride complexes **18**-**22** were structurally characterised and their molecular structures are shown in **Figure 2.10** and **Figure 2.11**. All of the LGeCl complexes are monomeric in the solid-state, which confirms the substantial steric bulk of the amide ligands. The Ge-N and Ge-Cl bond lengths are within the expected range of similar reported bulky amido germanium(II) chloride complexes.[17,18] The N-Ge-Cl bond angles are in the range 98.6-100.5°, which are indicative of the presence of a stereochemically active lone pair at each germanium(II) centre. Additionally, the planar Si-N-Ge-Cl fragment suggests some overlapping of nitrogen's p-orbital lone pair with the empty p-orbital at germanium centre.

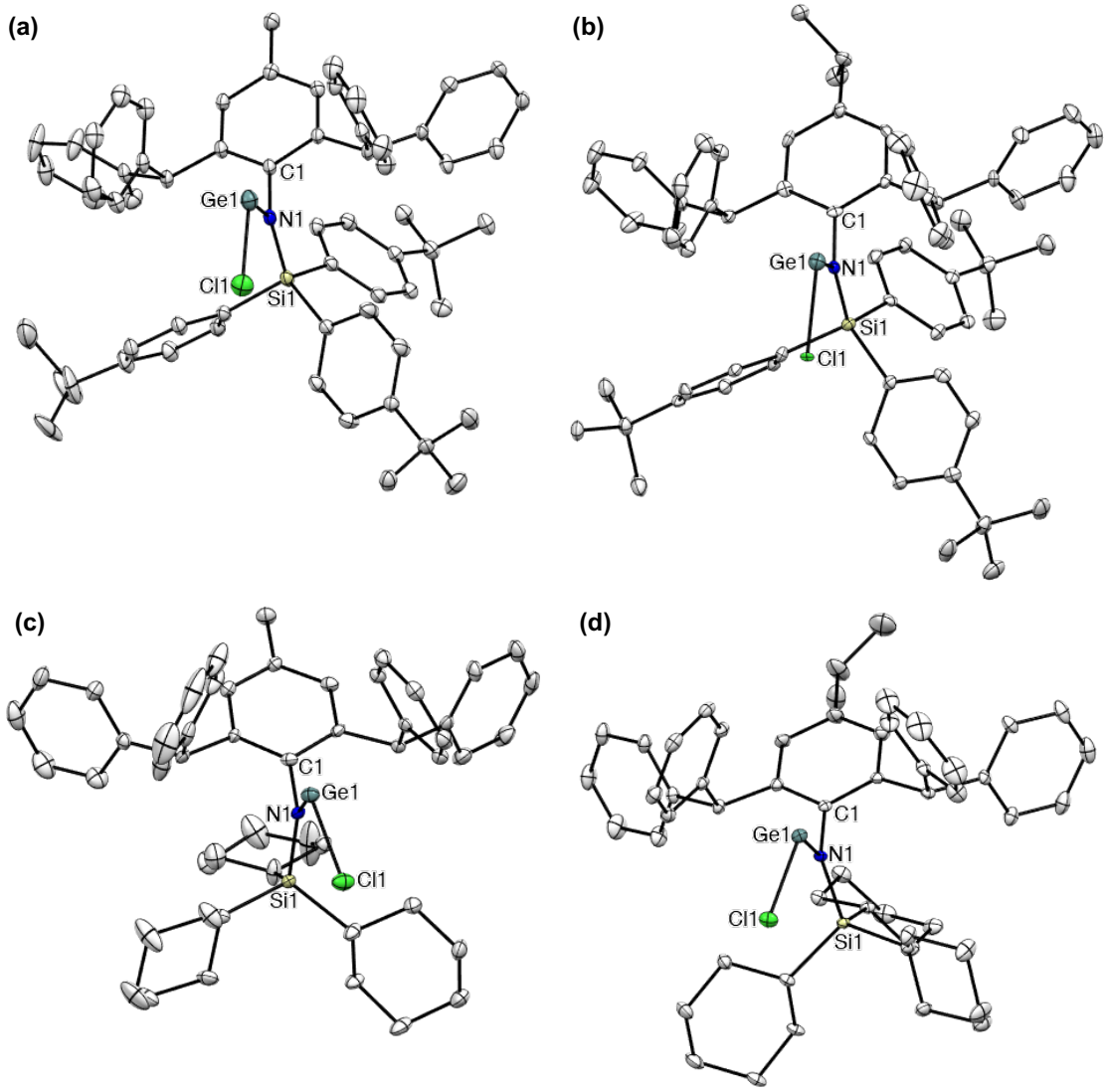

Figure 2.10. Molecular structures of [($^{t\text{BuPh}}$L*)GeCl] (**18**) (**a**), [($^{t\text{BuPh}}$L†)GeCl] (**19**) (**b**), [($^{\text{Cy}}$L*)GeCl] (**20**) (**c**) and [($^{\text{Cy}}$L†)GeCl] (**21**) (**d**) (thermal ellipsoids shown at 30 % probability). Hydrogen atoms omitted for clarity. Selected bond lengths (Å) and angles (°) for **18**: Ge1-Cl1 2.2415(15) , Ge1-N1 1.882(4), N1-C1 1.449(5), N1-Si1 1.754(4), N1-Ge1-Cl1 100.09(12), Si1-N1-Ge1 134.9(2), C1-N1-Ge1 108.1(3), C1-N1-Si1 117.0(3); **19**: Ge1-Cl1 2.3131(18), Ge1-N1 1.872(5), N1-C1 1.459(8), N1-Si1 1.758(5), N1-Ge1-Cl1 100.20(17), Si1-N1-Ge1 134.7(3), C1-N1-Ge1 110.5(4), C1-N1-Si1 114.7(4); **20**: Ge1-Cl1 2.2587(15), Ge1-N1 1.895(4), N1-C1 1.458(6), N1-Si1 1.780(4) N1-Ge1-Cl1 100.45(12), Si1-N1-Ge1 130.4(2), C1-N1-Ge1 110.4(3), C1-N1-Si1 118.8(3); **21**: Ge1-Cl1 2.263(2), Ge1-N1 1.886(5), N1-C1 1.450(7), N1-Si1 1.806(5), N1-Ge1-Cl1 99.64(15), Si1-N1-Ge1 131.7(3), C1-N1-Ge1 109.4(4), C1-N1-Si1 118.9(4).

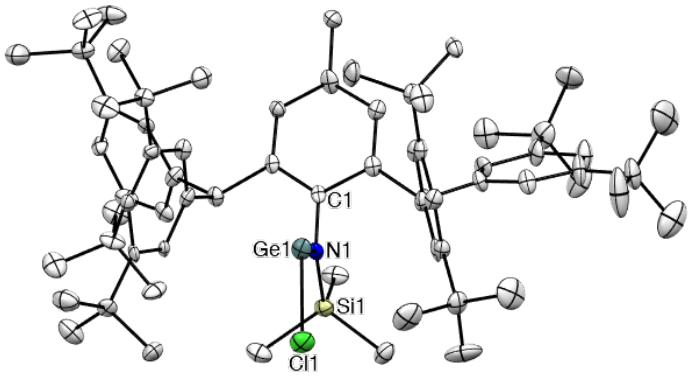

Figure 2.11. Molecular structure of [(^{TMS}L***)GeCl] (**22**) (thermal ellipsoids shown at 30 % probability). Hydrogen atoms omitted for clarity. Selected bond lengths (Å) and angles (°): Ge1-Cl1 2.261(3), Ge1-N1 1.877(10), N1-C1 1.435(14), N1-Si1 1.768(11), N1-Ge1-Cl1 98.6(3), Si1-N1-Ge1 132.2(5), C1-N1-Ge1 106.1(7), C1-N1-Si1 121.7(8).

2.3.3 Steric Profile

To survey the steric encumbrance offered by the ligands, a volume percentage of sphere around each germanium centre was calculated for two different sphere sizes. This percentage of volume is also called as percentage buried volume (% bV) and it represents the volume occupied by sterically demanding substituents around the element centre. The % bV of a ligand may depend on three factors: **1**) bulkiness of the ligand, **2**) steric arrangement of the ligand around the element centre and **3**) other unknown factors.[72]

A chlorogermylene family was used as a model system to compare the bulk of the newly synthesised ligands with earlier reports. For this purpose, the reported germanium(II) chloride complexes [($^{i\text{Pr}}$L*)GeCl] **27**, [($^{i\text{Pr}}$L†)GeCl] **28**, [(^{TMS}L$^{\#}$)GeCl] **29**, [(^{TMS}L*)GeCl] **30**, [(^{Ph}L*)GeCl] **31**, [(^{Ph2Me}L*)GeCl] **32**, [($^{t\text{BuO}}$L*)GeCl] **33**, and [($^{t\text{BuO}}$L†)GeCl] **34** were chosen and the geometries of these germanium(II) chloride complexes were optimised using DFT calculations at the bvp86/def2svp theory level. The crystal structures of the novel germanium(II) chloride complexes **18**-**22** were used as obtained and for Ar^{N} based ligands geometry optimisations were performed on model germanium(II) chloride complexes **23**-**26**. Thereafter, for determining the optimised structures, DFT calculations at the bvp86/def2svp theory level were carried out.

The % bVs were calculated using the software SambVca 2.1[73] for two different sphere sizes and the values are given in **Table 2.1**. At first, the distance 1.91 Å, which is also equal to sum of covalent radii of nitrogen and germanium, was chosen. Later, for the sake of comparison, bulk at 3.5 Å sphere radius was also calculated.

Table 2.1. % bVs at 1.9 Å and 3.5 Å sphere size of novel complexes **18**-**26** and reported complexes **27**-**34**.

LGeCl complex	% $bv_{1.9}$	% $bv_{3.5}$
[($^{t\text{BuPh}}$L*)GeCl] (18)	41.0	60.6
[($^{t\text{BuPh}}$L†)GeCl] (19)	46.4	65.1
[($^{\text{Cy}}$L*)GeCl] (20)	46.3	67.8
[($^{\text{Cy}}$L†)GeCl] (21)	43.6	64.3
[($^{\text{TMS}}$L***)GeCl] (22)	40.3	60.4
[($^{\text{TMS}}$L$^{\text{N}}$)GeCl] (23)	36.9	55.0
[($^{i\text{Pr}}$L$^{\text{N}}$)GeCl] (24)	37.9	58.0
[($^{t\text{BuPh}}$L$^{\text{N}}$)GeCl] (25)	38.1	58.1
[($^{\text{Cy}}$L$^{\text{N}}$)GeCl] (26)	38.1	58.5
[($^{i\text{Pr}}$L*)GeCl] (27)	38.3	59.4
[($^{i\text{Pr}}$L†)GeCl] (28)	41.0	60.0
[($^{\text{TMS}}$L$^{\#}$)GeCl] (29)	41.8	58.9
[($^{\text{TMS}}$L*)GeCl] (30)	38.6	57.6
[($^{\text{Ph}}$L*)GeCl] (31)	39.0	59.4
[($^{\text{Ph2Me}}$L*)GeCl] (32)	39.9	59.2
[($^{t\text{BuO}}$L*)GeCl] (33)	37.1	55.2
[($^{t\text{BuO}}$L†)GeCl] (34)	39.4	60.8

Note: the % bV calculations are based on solid-state structures with restricted rotation. In solution, the compounds may lead to different values of % bV due to the rotation of substituents.

At sphere radius 1.9 Å, the newly synthesised $^{t\text{BuPh}}$L† and $^{\text{Cy}}$L* are the bulkiest ligands, exhibiting the highest percentage buried volumes at 46.3 % and 46.4 %, respectively. The % bVs for other ligands vary from 38-42 %, while the ligand $^{\text{TMS}}$L* which contains a TMS- group displays the least % bV as 36.9 %.

Next, accounting for bulk at 3.5 Å sphere radius, the development of long-distance bulk becomes obvious, although it follows an almost similar trend as the 1.9 Å sphere radius. The ligands of complexes **23**, **30**, and **33** demonstrate the least bulky nature. The lesser % bV of **23** and **30** can again be understood on the basis of the presence of the smaller

silicon side group TMS-, which explains why the ligands with bulky silicon side groups are anticipated to produce larger % bV. In contrast, the compounds **17** and **33** which also consist of smaller TMS- and bulkier Bu^{t}O- groups at silicon, display an exceptionally larger and smaller % bV, 60.4 % and 55.2 %, respectively. This unexpected increase in % bV of **17** might have arisen due to the 3,5-Bu$^t_2$- groups at meta position of flanking phenyl groups. In case of **33,** the bulk can be explained based on the presence of an unknown factor and limitation of the software (SambVca 2.1) to consider the solid-state structure in only one configuration, while in solution the substituents are always in constant rotation. These values also lead us to the idea that the bulk is not only the important factor in deciding the % bV of the ligand around an element centre, the steric and some unknown factors also play an important role in determining the overall bulk of the compounds. On comparing the overall bulk of the reported ligands with the newly synthesised ligands, the later $^{t\text{BuPh}}$L†, $^{\text{Cy}}$L*, and $^{\text{Cy}}$L† were found to be the bulkiest ligands at both 1.9 Å and 3.5 Å sphere radius. This also confirms the large steric encumbrance of these ligands.

SambVca 2.1 also generates a 3D view of the magnitude of steric bulk around the element centre, which is called as the 'steric map' of the ligand. The steric maps of compounds **18-34** are displayed in Error! Reference source not found. and **Figure 2.13**. All of these ligands provide a non-uniform steric encumbrance along X, Y and Z-directions. The orange colour area displays the region occupied by the flanking phenyl groups and blue colour area shows the part taken by the silyl group. These maps agree well with our observation about the importance of the silyl group in deciding the ligand bulk, as it is always closer to the element centre in the solid-state structures.

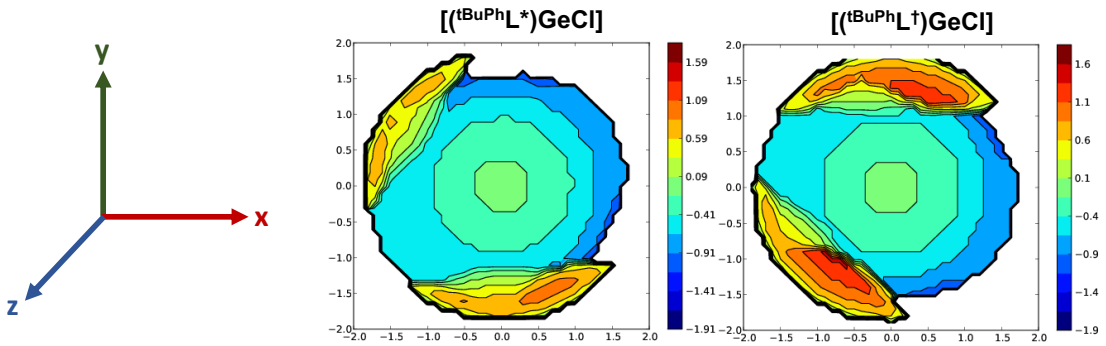

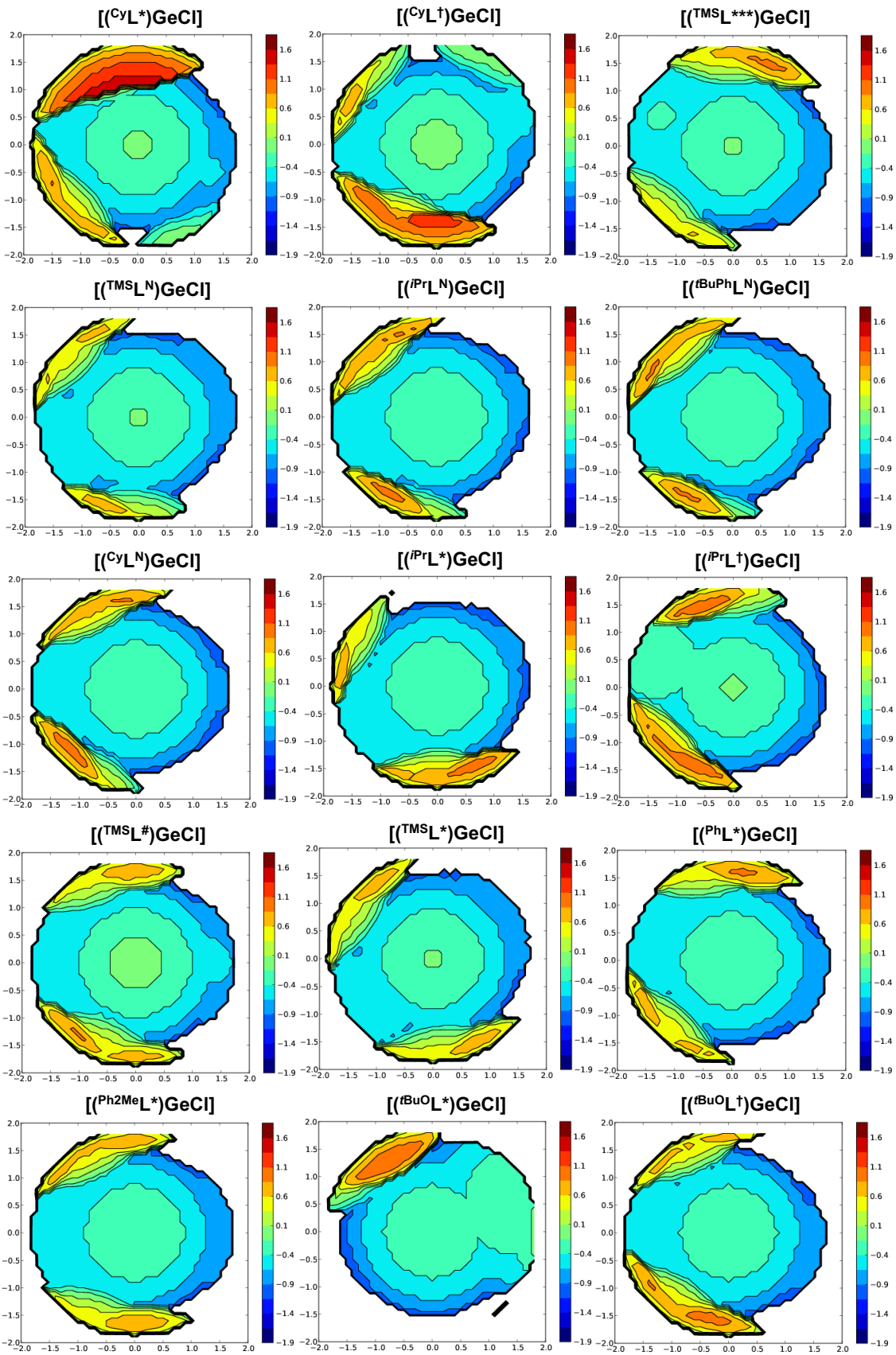

Figure 2.12. Steric maps at 1.9 Å sphere size for novel complexes **18-26** and previously reported complexes **27-34**.

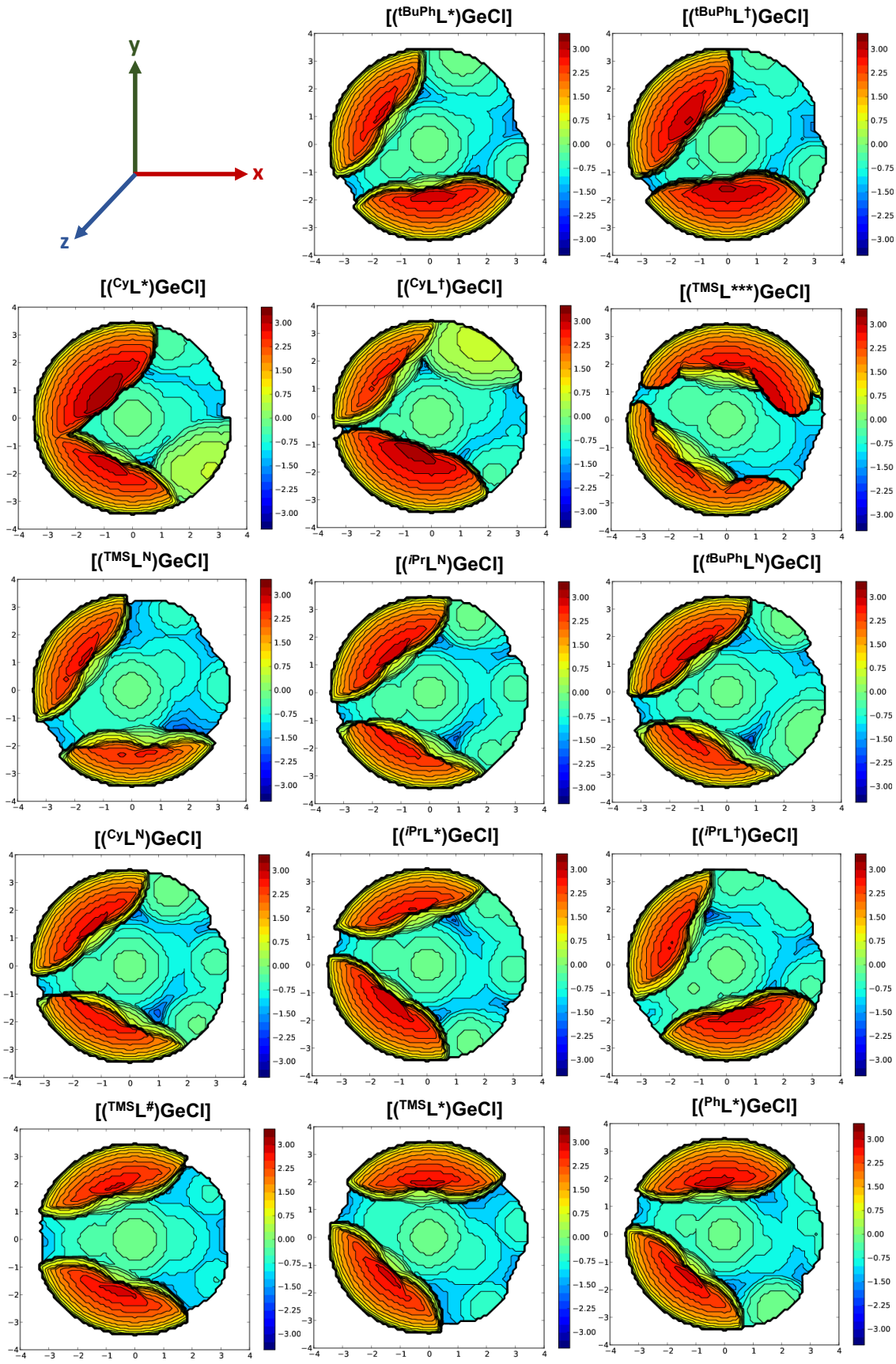
y
x
z
[(tBuPhL*)GeCl]
[(tBuPhL†)GeCl]
[(CyL*)GeCl]
[(CyL†)GeCl]
[(TMSL***)GeCl]
[(TMSLN)GeCl]
[(iPrLN)GeCl]
[(tBuPhLN)GeCl]
[(CyLN)GeCl]
[(iPrL*)GeCl]
[(iPrL†)GeCl]
[(TMSL#)GeCl]
[(TMSL*)GeCl]
[(PhL*)GeCl]

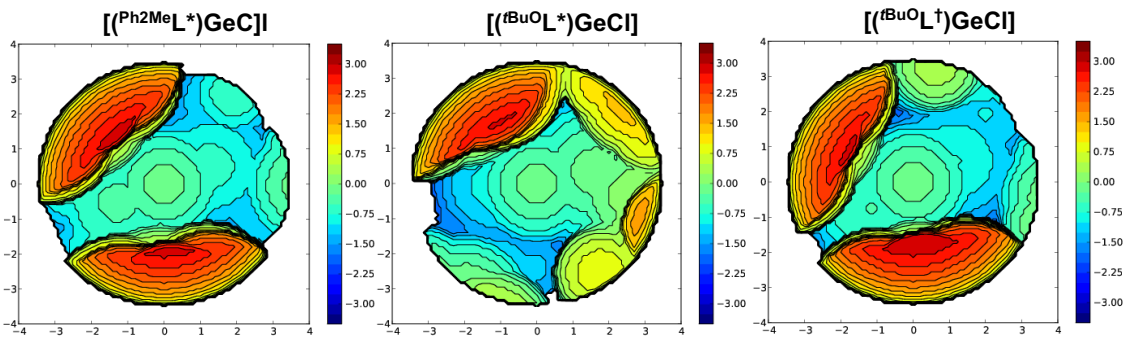

Figure 2.13. Steric maps at 3.5 Å sphere size for novel complexes **18**-**26** and previously reported complexes **27**-**34**.

2.3.4 Attempted Reductions of Amido Germanium(II) Chloride Complexes

With the synthesis of appropriate germanium(II) chloride precursors, the reduction of complexes **18**-**21** (**22** was not attempted due to low yield) was pursued with the hope of obtaining germanium(I) complexes. Due to previous success in reduction of amido group 14 element(II) halide complexes in our group, the magnesium(I) dimer, [{(^{Mes}Nacnac)Mg}$_2$] **35**,[74] which is a two-electron reductant, was chosen as the reducing agent (**Scheme 2.25**).

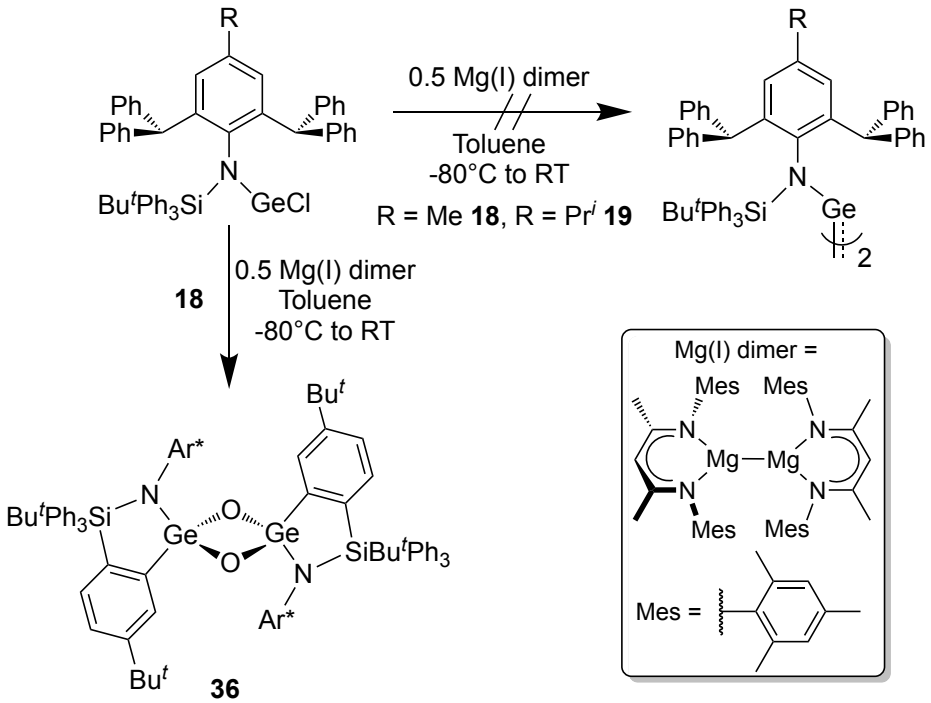

Scheme 2.25. Attempted reductions of amido germanium(II) chlorides **18** and **19**.

A dropwise addition of a toluene solution of **18** or **19** to a toluene solution of magnesium(I) dimer at -80 °C resulted in dark reddish-brown colored solutions (**Scheme 2.25**). ^{1}H NMR spectra of reaction solutions displayed the presence of new peaks. However, attempts to crystallise the products, even after multiple trials, resulted in either [{(^{Mes}Nacnac)MgCl}$_2$] or small brown coloured crystals, which were not suitable for X-ray diffraction. On one occasion, yellow coloured crystals of dimeric oxo bridged compound [{(^{tBuPh}L*)GeO}$_2$] **36** were isolated, but no spectroscopic data could be obtained due to low yield of the compound. Compound **36** seems likely to form due to advantageous oxygen in the solvent.

The molecular structure of **36** is shown in **Figure 2.14**. It contains a tetrahedral germanium (+4) element centre. The average Ge-N and Ge-O bond lengths in compound **36** are 1.83 Å and 1.80 Å. The four-membered Ge_2O_2 core is nearly planar, with average O-Ge-O and Ge-O-Ge bond angles of 87.29° and 93.15°, which are comparable to reported oxo bridged dimers.[66,75] One of the phenyl's -CH group of the silyl substituent Bu^{t}Ph$_3$Si- is activated by the germanium centre and forms a planar five-membered array, GeC_2SiN. The Ge_2O_2 core and five-membered GeC_2SiN ring are perpendicular to each other in order to minimise the steric repulsion in the whole system.

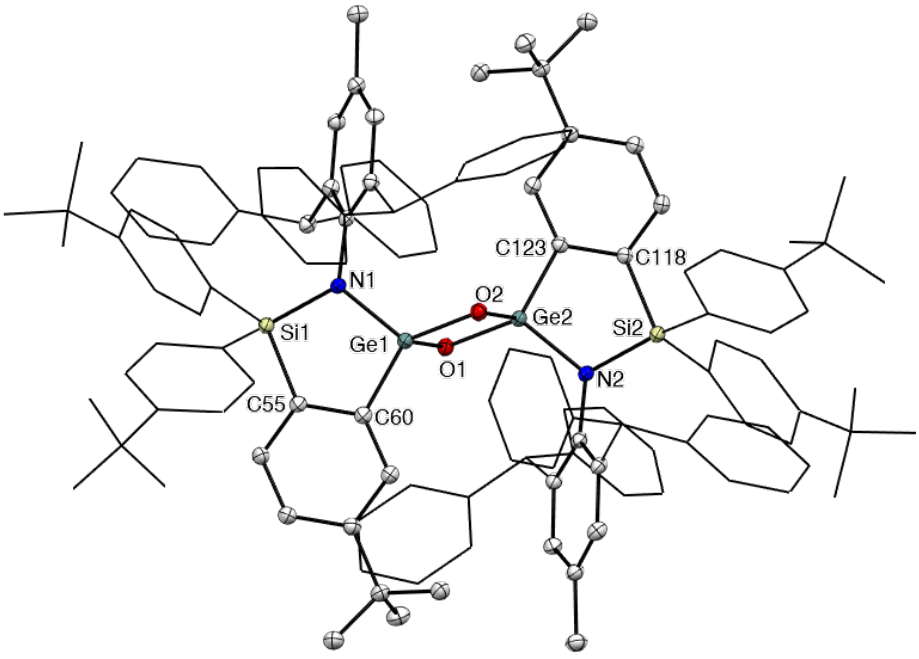

Figure 2.14. Molecular structure of [{(^{tBuPh}L*)GeO}$_2$] (**36**) (thermal ellipsoids shown at 30 % probability). Hydrogen atoms omitted for clarity; some Ph groups shown as wireframe for clarity. Selected bond lengths (Å) and angles (°): O1-Ge1 1.8102(19), O2-Ge1 1.7891(19), Ge1-C60 1.910(3), C60-C55 1.401(4), C55-Si1 1.869(3), Si1-N1 1.746(2), N1-Ge1 1.822(2), Ge1…Ge2

2.6044(9), O1…O2 2.476(3), N1-Ge1-C60 99.51(11), O1-Ge1-O2 86.91(9), Ge1-O1-Ge2 92.65(9), Ge1-C60-C55 110.80(19), C60-C55-Si1 117.50(19), Si1-N1-Ge1 111.45(11), N1-Ge1-O1 114.04(9), N1-Ge1-O2 116.89(9), C60-Ge1-O1 117.02(10), C60-Ge1-O2 123.47(10).

As compounds **18** and **19** did not seem suitable precursors for stabilising germanium(I) dimers, we moved our attention to the germanium(II) chlorides incorporating the Cy_3Si-group. Compounds **20** and **21** were successfully reduced using half an equivalent of [{(^{Mes}Nacnac)Mg}$_2$] in benzene and afforded a moderate isolated yield of amido digermynes **37** and **38**. The germanium(I) dimers **37** and **38** were obtained as extremely air and moisture sensitive orange colored crystals from a solution of benzene (**Scheme 2.26**). The solid-state structures of both the compounds are depicted in **Figure 2.15**.

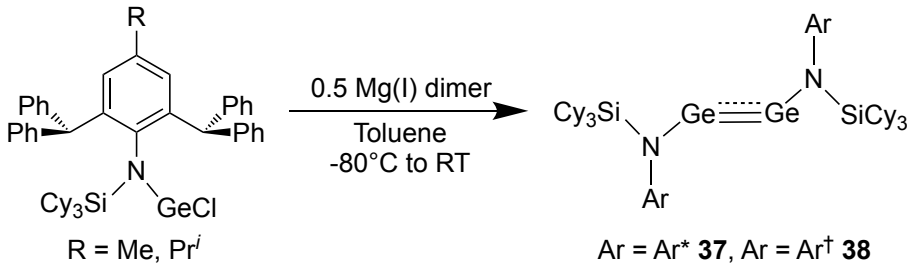

Scheme 2.26. Synthesis of aryl-silyl amido digermynes [{(^{Cy}L*)Ge}$_2$] **37** and [{(^{Cy}L†)Ge}$_2$] **38**.

Compounds **37** and **38** have a trans-bent geometries and are isostructural with earlier reported doubly bonded amido digermyne, i.e. [{(^{iPr}L†)Ge}$_2$] **39** (**Scheme 2.11**).[42] The Ge-Ge bond lengths in **37** and **38** are slightly smaller than in **39** (ca. 2.3668(3) Å) and also shorter than the sum of the average covalent bond radii of two germaniums (Ge-Ge single bond = 2.4 Å). The N-Ge-Ge bond angles (121.54° (**37**) and 121.92° (average in **38**)) are marginally more obtuse than **39** (ca. 119.61°). The digermynes **37** and **38** also have multiple Ge-Ge bond character, similar to **39**. This is attributed to the greater dihedral angles between the planes of Ge_2N_2 and GeNSiC species for the multiply bonded compounds. Therefore, Ge_2N_2 unit moves away from the planarity in bulkier amido digermynes. This prevents the planarisation of Ge_2NSiC unit thus disallows N-Ge π-bonding, unlike in the singly bonded digermyne [{(^{TMS}L*)Ge}$_2$]. Further, the Cy_3Si-groups take up the cis positions to minimise the steric repulsion in the synthesised compounds.

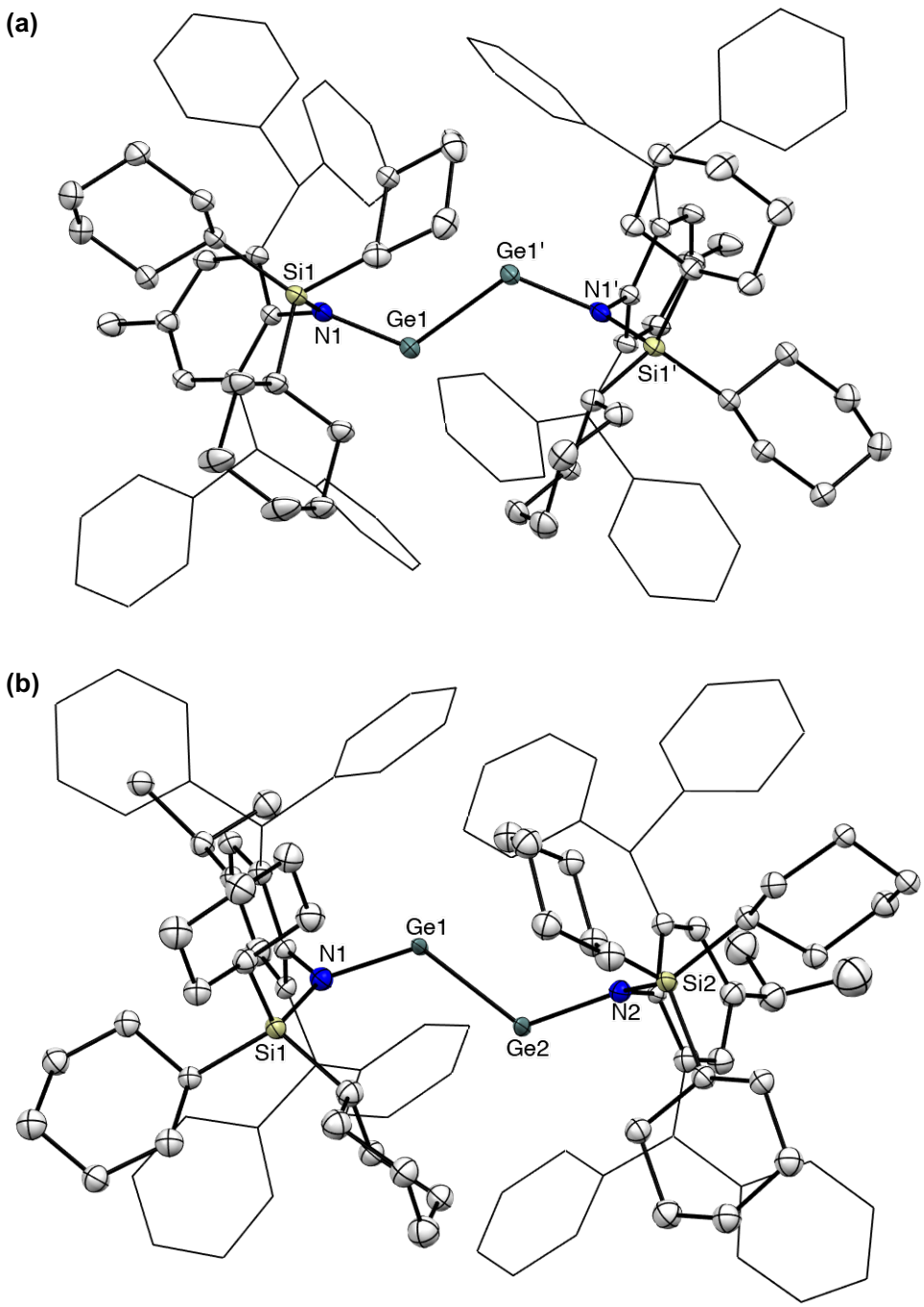

Figure 2.15. Molecular structures of [{(^{Cy}L*)Ge}$_2$] (**37**) (**a**) and [{(^{Cy}L*)Ge}$_2$] (**38**) (**b**) (thermal ellipsoids shown at 30 % probability). Hydrogen atoms omitted; some Ph groups shown as wireframe for clarity. Selected bond lengths (Å) and angles (°) for **37**: Ge1-Ge2 2.3574(9), Ge1-N1 1.867(4), N1-Si1 1.795(4), N1-C5 1.457(5), N1-Ge1-Ge2 121.54(11), C5-N1-Si1 122.0(3), C5-N1-Ge1 111.6(3), Si-N1-Ge1 124.89(18); **38**: Ge1-Ge2 2.362(3), Ge-N1 1.878(17), Ge2-N2 1.885(16), N1-Si1 1.791(18), N2-Si2 1.794(16), N1-C1 1.48(2), N2-C54 1.43(2), N1-Ge1-Ge2 123.2(5), N2-Ge2-Ge1 121.5(5), C1-N1-Si1 125.8(13), C54-N2-Si2 124.1(12), C1-N1-Ge1 110.7(12), C54-N2-Ge2 110.8(11), Si1-N1-Ge1 123.1(9), Si2-N2-Ge2 123.4(9).

2.3.5 Attempted Synthesis of Monomeric two-Coordinate Germanium(II) Hydride Complexes

As from the previous literature described in section **2.1.5**, the reactivity of 'true' two-coordinate monomeric amido germanium hydride complexes has not been well explored till date. The advantage of two-coordinate hydrides is the presence of coordinatively unsaturated germanium centre(s) (presence of empty p-orbital and a lone pair) which enhance their reactivity towards catalysis. Given the success of monomeric and pseudo monomeric two-coordinate amido germanium hydride complexes in the past, we sought to synthesise monomeric hydride complexes using the novel germanium(II) chloride complexes (**18**-**21**).

For the synthesis of hydride complexes we chose the standard route which involves salt metathesis of germanium(II) chloride complexes with a number of hydride sources (e.g. Li[BBu$^{s}_3$H], K[BBu$^{s}_3$H], $LiAlH_4$). In all cases, on addition of the hydride sources to toluene solutions of **18**-**21**, an initial colour change from colourless to pale yellow was observed. However, after stirring for an hour at room temperature yellow solids precipitated out and only the resonances for protonated ligands were observed in ^{1}H NMR spectra of the reaction mixtures (**Scheme 2.27**).

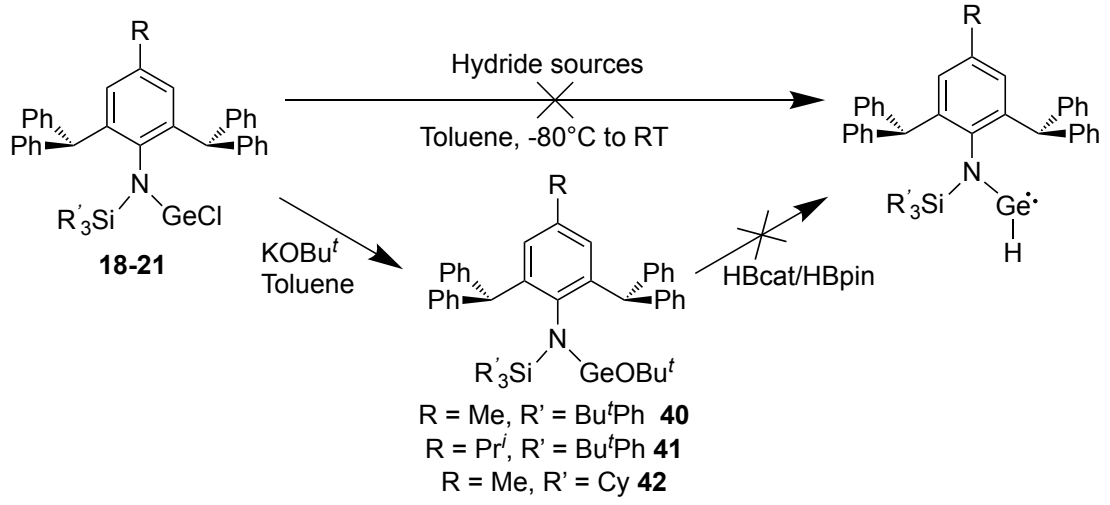

Scheme 2.27. Attempted synthesis of monomeric two-coordinate amido germanium(II) hydride complexes.

Due to the failure of the above method, we moved to another previously successful σ-metathesis route. We attempted to synthesise LGeOBu^t (L = ^{Cy}L*, ^{Cy}L† and ^{tBuPh}L* and ^{tBuPh}L†) species by reacting the germanium(II) chloride species with KOBu^t (**Scheme**

2.27). Using this procedure, the compounds [($^{t\text{BuPh}}$L*)GeOBu^{t}] (**40**), and [($^{t\text{BuPh}}$L†)GeOBu^{t}] (**41**) were isolated as white coloured solids and the compound [($^{\text{Cy}}$L*)GeOBu^{t}] (**42**) was isolated as colourless crystals. The formation of the respective germanium(II) butoxide species **40**-**42** were confirmed by ^{1}H NMR spectroscopy and new Bu^{t} resonances were observed between δ 0.83-1.15 ppm. The isolation of [($^{\text{Cy}}$L†)GeOBu^{t}] was unsuccessful as the reaction led to a large amount of protonated ligand and only 30 % conversion was seen in ^{1}H NMR spectrum of the mixture, which further decomposes to 100 % protonated ligand on working up the reaction mixture.

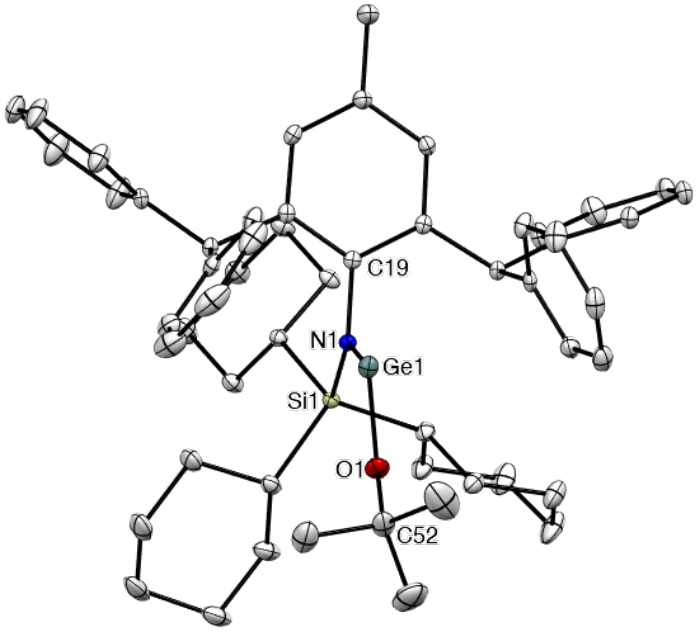

Figure 2.16. Molecular structure of [($^{\text{Cy}}$L*)GeOBu^{t}] (**42**) (thermal ellipsoids shown at 30 % probability). Hydrogen atoms omitted for clarity. Selected bond lengths (Å) and angles (°): Ge-N1 1.8875(12), N1-Si1 1.7870(13), Ge1-O1 1.7973(12), N1-C19 1.4534(18), Ge1-O1 1.7973(12), O1-C52 1.4401(19), O1-Ge1-N1 96.51(5), C19-N1-Si1 119.64(9), C19-N1-Ge1 107.88(9), Si1-N1-Ge1 132.34(7), Ge1-O1-C52 125.55(12).

Compound **42** was crystallised from a toluene/hexane mixture and its solid-state structure is given in **Figure 2.16**. Compound **42** is a monomer and features an N-Ge-O angle of 96.52° and a Ge-O-C angle of 125.58°, slightly more obtuse than in previously reported [($^{t\text{BuO}}$L*)GeOBu^{t}] (cf. N-Ge-O 97.24°, Ge-O-C 119.82° for [($^{t\text{BuO}}$L*)GeOBu^{t})].[61] The Ge1 centre possesses a lone pair of electrons which is also confirmed by a near right angle for N-Ge-O. The other metric parameters (Ge-O, Ge-N and N-Si bond distances) of compound **42** are comparable to those of [($^{t\text{BuO}}$L*)GeOBu^{t}] and not worthy of note here.

With the isolation of compounds **40**-**42**, the next step was to react them with a hydride source via σ-bond metathesis reaction. The treatment of toluene solutions of compounds **40**-**42** with one equivalent of HBcat/HBpin resulted in no reaction at room temperature. Heating the reaction mixtures involving **40** and **41** at 30 °C resulted in instantaneous metal precipitation, indicating decomposition, whereas, the reaction mixture involving compound **42** did not show any progress even after heating it to 60 °C.

2.4 Conclusion

In all, several new bulky aryl-silyl amide pro-ligands have been synthesised and successfully employed to stabilise various germanium(II) halide complexes of the type LGeCl (L = ligand employed). A comparative theoretical study of the extent of steric bulk of amide ligands concluded that the bulkiness is perhaps not the primary factor for steric protection offered by any ligand. There is always an additional unknown factor responsible for the ligand's overall steric bulk. The silyl side chain bulk was found to be more important in deciding the ligand's bulk. Further, two novel doubly bonded amido digermynes **37** and **38** were isolated and structurally characterised. Finally, attempts to isolate monomeric two-coordinate germanium(II) hydride complexes were unsuccessful at this stage. However, with the greater understanding of ligand bulk, synthesis of bulkier ligands could be carried out more efficiently in the future.

2.5 Experimental

[$^{t\mathrm{BuPh}}$L*H] (9). A solution of Ar*NH$_2$ (5.00 g, 11.38 mmol) in THF (50 mL) was cooled to -80 ºC and LiBu^{n} (7.8 mL, 12.52 mmol, 1.6 M solution in hexane) was added dropwise over 10 minutes. After the addition, the reaction mixture was warmed to room temperature, and stirred for 3 hours. To this reaction mixture, Bu^{t}Ph$_3$SiCl (5.71 g, 11.95 mmol) in THF (30 mL) was added at -80 ºC, the reaction was then heated to 55 ºC and stirred for 12 hours. Volatiles were subsequently removed *in vacuo*, and the residue extracted into toluene, and filtered. Removal of solvent under reduced pressure and washing of the residue with ca. 10 mL of cold hexane yielded **9** as pale-yellow powder (7.70 g, 78.2 %). M.p. > 260 °C; ^{1}H NMR (400 MHz, C$_6$D$_6$, 298 K) δ = 1.21 (s, 27H, C(C*H*$_3$)$_3$), 1.86 (s, 3H, C*H*$_3$), 2.71 (s, 1H, N*H*), 6.14 (s, 2H, Ph$_2$C*H*), 6.86 (d, $^{3}J_{HH}$ = 7.2 Hz, 6H, Ar-*H*), 7.02 (t, $^{3}J_{HH}$ = 7.2 Hz, 6H, Ar-*H*), 7.11 (d, $^{3}J_{HH}$ = 7.4 Hz, 8H, Ar-*H*), 7.24 (d, $^{3}J_{HH}$ = 8.1 Hz, 6H, Ar-*H*), 7.60 (d, $^{3}J_{HH}$ = 8 Hz, 6H, Ar-*H*); ^{13}C{^{1}H} NMR (101 MHz,

C_6D_6, 298 K) δ = 21.4 (*C*H_3), 31.4 (C(*C*H_3)$_3$), 34.8 (*C*(CH$_3$)$_3$), 52.8 (Ph$_2$*C*H), 125.2, 125.3, 125.7, 126.4, 128.4, 128.6, 128.7, 128.8, 129.3, 130.0, 130.1, 130.2, 132.7, 134.0, 136.1, 136.6, 139.5, 142.9, 145.0, 152.9 (Ar-*C*); ^{29}Si{^{1}H} NMR (80 MHz, C_6D_6, 298 K) δ = -18.9; IR ν/cm^{-1} (ATR): 3356 (br w, NH), 3058 (w), 3023 (w), 2960 (s), 2904 (w), 2869 (w), 1597 (s), 1494 (s), 1445 (s), 1387 (vs), 1362 (m), 1325 (w), 1265 (s), 1206 (w), 1135 (s), 1085 (vs), 1031 (m), 917 (w), 883 (m), 842 (w), 823 (s), 802 (w), 748 (m), 699 (vs); acc. mass calc. for $C_{63}H_{68}NSi$ (MH^+): 866.5043; found: 866.5126.

[$^{t\text{BuPh}}$L†H] (10). A solution of Ar†NH$_2$ (5.00 g, 10.70 mmol) in THF (50 mL) was cooled to -80 ºC and LiBu^n (7.4 mL, 11.77 mmol, 1.6 M solution in hexane) was added dropwise over 10 minutes. After the addition, the reaction mixture was warmed to room temperature, and stirred for 3 hours. To this reaction mixture Bu^{t}Ph$_3$SiCl (5.37 g, 11.24 mmol) in THF (30 mL) was added at -80 ºC, and the reaction was then stirred at room temperature for 12 hours. Volatiles were subsequently removed *in vacuo*, and the residue extracted into toluene (80 mL). The extract was filtered, concentrated to ca. 15 mL and stored at -30 ºC overnight to yield pale-yellow crystals of **10** (7.60 g, 79.50 %). M.p. 195 °C; ^{1}H NMR (400 MHz, C_6D_6, 298 K) δ = 0.95 (d, $^3J_{HH}$ = 6.9 Hz, 6H, CH(C*H*$_3$)$_2$), 1.22 (s, 27H, C(C*H*$_3$)$_3$), 2.49 (sept, $^3J_{HH}$ = 6.9 Hz, 1H, C*H*(CH$_3$)$_2$), 2.74 (s, 1H, N*H*), 6.12 (s, 2H, Ph$_2$C*H*), 6.89-7.12 (t, $^3J_{HH}$ = 8 Hz, 20H, Ar-*H*), 7.24 (d, $^3J_{HH}$ = 8.2 Hz, 6H, Ar-*H*), 7.58 (d, $^3J_{HH}$ = 8.2 Hz, 6H, Ar-*H*); ^{13}C{^{1}H} NMR (101 MHz, C_6D_6, 298 K) δ = 24.1 (CH(*C*H$_3$)$_2$), 31.4 (C(*C*H$_3$)$_3$), 33.9 (*C*H(CH$_3$)$_2$), 34.8 (*C*(CH$_3$)$_3$), 52.9 (Ph$_2$*C*H), 2×125.2, 125.3, 126.4, 127.2, 128.4, 2×128.7, 130.0, 130.2, 132.7, 136.0, 136.1, 136.6, 139.8, 142.8, 144.9, 145.0, 145.1, 152.9 (Ar-*C*); ^{29}Si{^{1}H} NMR (80 MHz, C_6D_6, 298 K) δ = -18.7; IR ν/cm^{-1} (Nujol): 3338 (br w, NH), 3060 (w), 3025 (w), 2956 (s), 2867 (w), 1597 (s), 1545 (w), 1493 (s), 1444 (s), 1386 (s), 1361 (s), 1319 (w), 1266 (s), 1202 (w), 1162 (w), 1135 (w), 1086 (vs), 1031 (m), 966 (w), 893 (s), 824 (vs), 748 (s), 698 (vs); acc. mass calc. for $C_{65}H_{72}NSi$ (MH^+): 894.5423; found: 894.5356.

[$^{\text{Cy}}$L*H] (11). This compound was prepared following a similar method to that for [$^{t\text{BuPh}}$L*H], but using Ar*NH$_2$ (5.00 g, 11.38 mmol) in THF (50 mL), LiBu^n (7.8 mL, 12.52 mmol, 1.6 M solution in hexane), and Cy$_3$SiCl (4.26 g,13.66 mmol) in THF (30 mL). Storage of the reaction mixture at -30 °C for 1 day resulted in deposition of **11** as colourless crystals (5.75 g, 70.6 %). M.p. 253 °C; ^{1}H NMR (400 MHz, C_6D_6, 298 K) δ = 1.19-1.40 (m, 19H, Cy-*H*), 1.70 (d, $^3J_{HH}$ = 8.1 Hz, 8H, Cy-*H*), 1.83-1.85 (m, 6H, Cy-

H), 1.85 (s, 3H, C*H*$_3$) (signal at 1.84 and 1.85 overlap), 2.04 (s, 1H, NH), 6.30 (s, 2H, Ph$_2$CH), 6.93 (s, 2H, Ar-H), 7.06 (t, $^3J_{HH}$ = 7.3 Hz, 4H, Ar-*H*), 7.18-7.29 (m, 14H, Ar-*H*); ^{13}C{^{1}H} NMR (101 MHz, C$_6$D$_6$, 298 K) δ = 21.2 (Cy-*C*), 27.5 (*C*H$_3$), 27.9, 29.0, 29.1 (Cy-*C*), 52.7 (Ph$_2$*C*H), 126.7, 127.9, 128.6, 130.2, 132.4, 141.0, 141.3, 145.2 (Ar-*C*); ^{29}Si{^{1}H} NMR (80 MHz, C$_6$D$_6$, 298 K) δ = -4.7; IR ν/cm^{-1} (ATR): 3369 (br w, NH), 3062 (w), 3022 (w), 2916 (vs), 2844 (s), 1598 (m), 1492 (vs), 1444 (vs), 1323 (w), 1264 (m), 1248 (w), 1167 (w), 1127 (w), 1107 (w), 1079 (m), 1029 (s), 999 (s), 912 (s), 890 (s), 871 (s), 844 (s), 821 (w), 797 (w), 761 (m), 738 (s), 699 (vs); acc. mass calc. for C$_{51}$H$_{62}$NSi (MH$^+$): 716.4573; found: 716.4636.

[^{Cy}L†H] (12). This compound was prepared following a similar method to that for [$^{t\text{BuPh}}$L†H], but using Ar†NH$_2$ (5.00 g, 10.70 mmol) in THF (50 mL), LiBu^n (7.4 mL, 11.77 mmol, 1.6 M solution in hexane), and Cy$_3$SiCl (4.01 g, 12.84 mmol) in THF (30 mL). Storage of the reaction mixture at -30 °C for 1 day resulted in deposition of **12** as colourless crystals (6.60 g, 82.9%). M.p. 235 °C; ^{1}H NMR (400 MHz, C$_6$D$_6$, 298 K) δ = 0.94 (d, $^3J_{HH}$ = 6.8 Hz, 6H, CH(C*H*$_3$)$_2$), 1.19-1.36 (m, 18H, Cy-*H*), 1.69-1.85 (m, 14H, Cy-*H*), 2.06 (s, 1H, N*H*), 2.49 (m, $^3J_{HH}$ = 6.8 Hz, 1H, C*H*(CH$_3$)$_2$), 6.29 (s, 2H, Ph$_2$C*H*), 6.96 (s, 2H, Ar-*H*), 7.05 (t, $^3J_{HH}$ = 7.6 Hz, 4H, Ar-*H*), 7.18-7.29 (m, 16H, Ar-*H*); ^{13}C{^{1}H} NMR (101 MHz, C$_6$D$_6$, 298 K) δ = 24.1 (CH(*C*H$_3$)$_2$), 27.6, 27.9, 2×29.0 (Cy-*H*), 33.8 (*C*H(CH$_3$)$_2$), 52.9 (Ph$_2$C*H*), 126.7, 127.3, 128.6, 130.1, 140.9, 141.5, 143.3, 145.2 (Ar-*C*); ^{29}Si{^{1}H} NMR (80 MHz, C$_6$D$_6$, 298 K) δ = -4.6; IR ν/cm^{-1} (ATR): 3340 (w, NH), 3024 (w, NH), 2917 (vs), 2845 (s), 1599 (m), 1492 (vs), 1445 (vs), 1360 (m), 1320 (w), 1291(w), 1258 (s), 1166 (w), 1110 (m), 1074 (m), 1029 (s), 998 (s), 910 (m), 890 (s), 842 (s), 819 (m), 799 (w), 759 (m), 736 (m), 724 (s), 696 (vs); acc. mass calc. for C$_{53}$H$_{66}$NSi (MH$^+$): 744.4886; found: 744.4956.

[^{TMS}L***H] (13). A solution of Ar***NH$_2$ (1.00 g, 1.13 mmol) in THF (20 mL) was cooled to -80 ºC and LiBu^n (0.77 mL, 1.24 mmol, 1.6 M solution in hexane) was added dropwise over 10 minutes. After the addition, the reaction mixture was warmed to room temperature, and stirred for 3 hours. To this reaction mixture TMSCl (0.15 mL, 1.18 mmol) in THF (10 mL) was then added at -80 ºC, and the reaction was stirred at room temperature for 12 hours. Volatiles were subsequently removed *in vacuo*, and the residue extracted into hexane (20 mL) and filtered. Removal of volatiles under reduced pressure yielded **13** as an analytically pure white powder (0.50 g, 46.2 %). M.p. 230 °C; ^{1}H NMR

(400 MHz, C_6D_6, 298 K) δ = 0.22 (s, 9H, Si(C*H*$_3$)$_3$), 1.29 (s, 45H, C(*CH*$_3$)$_3$), 1.32 (s, 27H, C(*CH*$_3$)$_3$), 1.84 (s, 3H, *CH*$_3$), 2.21 (s, 1H, N*H*), 6.39 (s, 1H, Ph$_2$C*H*), 6.49 (s, 1H, Ph$_2$C*H*), 7.08-7.33 (m, 10H, Ar-*H*), 7.41 (d, $^3J_{HH}$ = 4 Hz, 4H, Ar-*H*); $^{13}C\{^1H\}$ NMR (101 MHz, C_6D_6, 298 K) δ = 3.9 (Si*C*H$_3$), 20.6 (*C*H$_3$), 31.6 (br, C(*C*H$_3$)$_3$), 34.9, 35.0 (*C*(CH$_3$)$_3$), 52.3, 53.4 (Ph$_2$*C*H), 119.7, 119.8, 124.7, 125.2, 130.0, 131.9, 142.1, 142.6, 144.4, 144.6, 150.3, 150.5 (Ar-*C*); $^{29}Si\{^1H\}$ NMR (80 MHz, C_6D_6, 298 K) δ = 5.2; IR ν/cm^{-1} (ATR): 3400 (br w, NH), 3066 (w), 2954 (vs), 2903 (m), 2866 (m), 1595 (s), 1523 (w), 1476 (m), 1433 (m), 1393 (m), 1362 (s), 1296 (w), 1250 (vs), 1203 (s), 1123 (m), 1094 (w), 1024 (m), 918 (s), 904 (vs), 876 (s), 835 (vs), 758 (w), 745 (w), 715 (s); acc. mass calc. for $C_{68}H_{102}NSi$ (MH^+): 960.7782; found: 960.7761.

[^{TMS}L^{N}H] (14). A solution of Ar*NH$_2$ (1.00 g, 1.56 mmol) in THF (20 mL) was cooled to -80 ºC and LiBu^n (1.1 mL, 1.72 mmol, 1.6 M solution in hexane) was added dropwise over 10 minutes. After the addition, the reaction mixture was warmed to room temperature, and stirred for 3 hours. To this reaction mixture TMSCl (0.21 mL, 1.64 mmol) in THF (10 mL) was then added at -80 ºC. The reaction mixture was heated to 60 ºC and stirred for 2 days. Volatiles were subsequently removed *in vacuo*, and the residue was extracted into toluene, and filtered. Removal of solvent under reduced pressure and washing of the residue with ca. 2×5 mL of pentane yielded the **14** as a pink colored powder (0.49 g, 44.0 %). M.p. 163 °C; ^1H NMR (400 MHz, C_6D_6, 298 K) δ = 0.19 (s, 9H, Si(*CH*$_3$)$_3$), 1.82 (s, 3H, *CH*$_3$), 1.98 (s, 1H, N*H*), 6.55 (s, 2H, Nap$_2$C*H*), 7.07 (s, 2H, Ar-*H*), 7.19-7.70 (m, 28H, Ar-*H*); $^{13}C\{^1H\}$ NMR (101 MHz, C_6D_6, 298 K) δ = 4.1 (Si(*C*H$_3$)$_3$), 21.2 (*C*H$_3$), 53.4 (Nap$_2$*C*H), 126.0, 126.4, 128.0, 128.4, 128.5, 129.0, 130.5, 132.9, 134.2, 140.9, 141.8, 142.2 (Ar-*C*); $^{29}Si\{^1H\}$ NMR (80 MHz, C_6D_6, 298 K) δ = 3.5; IR ν/cm^{-1} (ATR): 3354 (w, NH), 3050 (w), 2952 (w), 1921 (w), 1631 (m), 1600 (s), 1506 (s), 1458 (s), 1357 (m), 1250 (vs), 1199 (w), 1125 (m), 1019 (w), 962 (m), 900 (vs), 857 (s), 836 (s), 818 (vs), 776 (s), 747 (vs), 747 (vs), 681 (s); acc. mass calc. for $C_{52}H_{46}NSi$ (MH^+): 712.3321; found: 712.3434.

[$^{i\text{Pr}}$L^{N}H] (15). This compound was prepared following a similar method to that for [^{TMS}L^{N}H] but using Ar^{N}NH$_2$ (1.00 g, 1.56 mmol) in THF (20 mL), LiBu^n (1.1 mL, 1.72 mmol, 1.6 M solution in hexane) and Pr$^i_3$SiCl (0.35 mL, 1.64 mmol) in THF (10 mL). The product was isolated as an off-white crystalline solid (0.98 g, 78.8 %). M.p. > 260 °C; ^1H NMR (400 MHz, C_6D_6, 298 K) δ = 1.06 (d, $^3J_{HH}$ = 4 Hz, 18H, SiCH(C*H*$_3$)$_2$), 1.40

(sept, $^{3}J_{HH}$ = 8 Hz, 3H, SiC*H*$(CH_3)_2$), 1.79 (s, 3H, *CH*$_3$), 2.42 (s, 1H, N*H*), 6.68 (s, 2H, nap$_2$C*H*), 7.11 (s, 2H, Ar-*H*), 7.20-7.52 (m, 16H, Ar-*H*), 7.61 (d, $^{3}J_{HH}$ = 7.6 Hz, 4H, Ar-*H*), 7.67 (d, $^{3}J_{HH}$ = 8.5 Hz, 4H, Ar-*H*), 7.75 (s, 4H, Ar-*H*); $^{13}C\{^{1}H\}$ NMR (101 MHz, C_6D_6, 298 K) δ = 14.9 (Si*C*H$(CH_3)_2$), 19.2 (SiCH(*C*H$_3)_2$), 21.2 (*C*H$_3$), 52.9 (Nap$_2$*C*H), 126.1, 126.4, 128.0, 128.4, 128.5, 129.0, 130.9, 132.9, 134.2, 140.8, 141.5, 142.3 (Ar-*C*); $^{29}Si\{^{1}H\}$ NMR (80 MHz, C_6D_6, 298 K) δ = 3.8; IR ν/cm^{-1} (ATR): 3350 (m, NH), 3053 (w), 2942 (m), 2865 (s), 1920 (w), 1632 (m), 1601 (s), 1506 (s), 1456 (vs), 1383 (w), 1241 (m), 1198 (w), 1068 (w), 1016 (w), 1003 (w), 961 (m), 920 (s), 881 (vs), 859 (s), 819 (vs), 777 (s), 761 (s), 745 (vs), 731 (s), 697 (w), 661 (m); acc. mass calc. for $C_{58}H_{58}NSi$ (MH^+): 796.4260; found: 796.4371.

[$^{t\mathrm{BuPh}}$L$^{\mathrm{N}}$H] (16). This compound was prepared following a similar method to that for [$^{\mathrm{TMS}}$L$^{\mathrm{N}}$H] but using Ar$^{\mathrm{N}}$NH$_2$ (1.00 g, 1.56 mmol) in THF (20 mL), LiBu^{n} (1.1 mL, 1.72 mmol, 1.6 M solution in hexane) and Bu^{t}Ph$_3$SiCl (0.79 g, 1.64 mmol) in THF (10 mL). Storage of the reaction mixture at -30 °C for 1 day resulted in deposition of **16** as colourless crystals (1.11 g, 66.6 %). M.p. > 260 °C; ^{1}H NMR (400 MHz, C_6D_6, 298 K) δ = 1.20 (s, 27H, C(C*H*$_3)_3$), 1.81 (s, 3H, C*H*$_3$), 2.99 (s, 1H, N*H*), 6.64 (s, 2H, Nap$_2$C*H*), 7.09 (m, 2H, Ar-*H*), 7.12-7.69 (m, 40H, Ar-*H*); $^{13}C\{^{1}H\}$ NMR (101 MHz, C_6D_6, 298 K) δ = 21.4 (*C*H$_3$), 31.4 (C(*C*H$_3)_3$), 34.8 (*C*(CH$_3)_3$), 53.1 (Nap$_2$*C*H), 125.3, 125.9, 126.1, 127.9, 128.1, 128.5, 128.6, 129.2, 130.6, 132.8, 132.9, 134.1, 134.5, 136.7, 140.1, 142.4, 142.7, 153.0 (Ar-*C*); $^{29}Si\{^{1}H\}$ NMR (80 MHz, C_6D_6, 298 K) δ = -18.5; IR ν/cm^{-1} (ATR): 3350 (w, NH), 3504 (m), 3019 (w), 2961 (s), 2905 (w), 2868 (w), 2370 (w), 1921 (w), 1631 (m), 1599 (s), 1545 (m), 1507 (s), 1459 (vs), 1388 (s), 1362 (s), 1316 (w), 1268 (vs), 1203 (m), 1137 (m), 1086 (vs), 1019 (m), 964 (w), 949 (w), 900 (m), 885 (m), 858 (s), 823 (vs), 778 (s), 748 (vs), 684 (w); acc. mass calc. for $C_{79}H_{76}NSi$ (MH^+): 1066.5747; found: 1066.5848.

[$^{\mathrm{Cy}}$L$^{\mathrm{N}}$H] (17). This compound was prepared following a similar method to that for [$^{\mathrm{TMS}}$L$^{\mathrm{N}}$H] but using Ar$^{\mathrm{N}}$NH$_2$ (1.00 g, 1.56 mmol) in THF (20 mL), LiBu^{n} (1.1 mL, 1.72 mmol, 1.6 M solution in hexane) and Cy$_3$SiCl (0.51 g, 1.64 mmol) in THF (10 mL). The product was isolated as an off-white crystalline solid (0.60 g, 41.9 %). M.p. 110 °C; ^{1}H NMR (400 MHz, C_6D_6, 298 K) δ = 1.21-1.36 (m, 17H, Cy-*H*), 1.69-1.77 (m, 10H, Cy-*H*), 1.81 (m, 3H, C*H*$_3$), 1.86 (br, 6H, Cy-*H*), 2.33 (s, 1H, N*H*), 6.71 (s, 2H, Nap$_2$C*H*), 7.20-7.72 (m, 28H, Ar-*H*), 7.82 (s, 2H, Ar-*H*);$^{13}C\{^{1}H\}$ NMR (101 MHz, C_6D_6, 298 K) δ

= 21.3 (*C*H$_3$), 25.2, 27.5, 27.9, 28.0, 28.4, 28.7, 29.0, 29.1 (Cy-*C*), 53.0 (Nap$_2$*C*H), 126.1, 126.4, 128.4, 2×128.5, 129.0, 130.7, 133.0, 134.2, 140.9, 141.6, 142.5 (Ar-*C*); ^{29}Si{^{1}H} NMR (80 MHz, C$_6$D$_6$, 298 K) δ = -4.3; IR ν/cm^{-1} (ATR): 3345 (w, NH), 3051 (w), 3019 (w), 2911 (s), 2842 (s), 1909 (w), 1629 (w), 1599 (m), 1505 (s), 1443 (vs), 1355 (m), 1262 (s), 1196 (w), 1168 (w), 1099 (m), 1071 (w), 1037 (w), 997 (m), 960 (w), 890 (vs), 854 (s), 816 (vs), 776 (m), 742 (vs), 679 (w); acc. mass calc. for C$_{67}$H$_{70}$NSi (MH$^+$): 916.5277; found: 916.5262.

[(*t*^{BuPh}L*)K(THF)] (9.K). A mixture of *t*^{BuPh}L*H (5.00 g, 5.78 mmol) and KH (0.28 g, 6.93 mmol) was dissolved in THF (50 mL) and a catalytic amount of hexamethyldisilazane (60 μL, ~5 mol %) was added to it. The reaction mixture was then stirred overnight at ambient temperature under a flow of N$_2$. The resultant solution was subsequently filtered, and the volatiles were removed *in vacuo*. The residue was washed with 2×10 mL hexane and dried under vacuum for 1 hour affording a free-flowing light-orange colored powder (4.61 g, 81.8 %). M.p. 117 °C; ^{1}H NMR (400 MHz, C$_6$D$_6$, 298 K) δ = 1.30 (s, 27H, C(C*H$_3$*)$_3$), 1.39 (m, 4H, OCH$_2$C*H$_2$*), 2.11 (s, 3H, C*H$_3$*), 3.39 (m, 4H, OC*H$_2$*CH$_2$), 6.50 (s, 2H, Ph$_2$C*H*), 6.77-7.14 (m, 20H, Ar-*H*), 7.31 (d, $^3J_{HH}$ = 8.2 Hz, 6H, Ar-*H*), 7.75 (d, $^3J_{HH}$ = 8.1 Hz, 6H, Ar-*H*); ^{13}C{^{1}H} NMR (101 MHz, C$_6$D$_6$, 298 K) δ = 21.6 (*C*H$_3$), 25.8 (OCH$_2$*C*H$_2$), 31.7 (C(*C*H$_3$)$_3$), 34.7 (*C*(CH$_3$)$_3$), 52.7 (Ph$_2$*C*H), 67.8 (O*C*H$_2$CH$_2$), 121.2, 124.6, 125.1, 125.2, 125.6, 126.7, 127.4, 128.7, 129.0, 130.0, 130.7, 130.8, 136.0, 136.3, 138.7, 141.0, 146.8, 150.5, 151.0, 155.1 (Ar-*C*); ^{29}Si{^{1}H} NMR (80 MHz, C$_6$D$_6$, 298 K) δ = -42.9; IR ν/cm^{-1} (Nujol): 1595 (m), 1541 (w), 1425 (m), 1384 (m), 1266 (m), 1236 (w), 1201 (w), 1167 (w), 1113 (m), 1066 (vs), 1035 (m), 996 (m), 951 (s), 908 (s), 878 (m), 822 (s), 767 (m), 742 (s), 704 (s); anal. calc. for C$_{67}$H$_{74}$SiNKO: C 82.41 %, H 7.64 %, N 1.64 %, found: C 83.07 %, H 7.52 %, N 1.63 %.

[(*t*^{BuPh}L†)K(THF)] (10.K). This compound was prepared following a method similar to that for [(*t*^{BuPh}L*)K(THF)], but using [*t*^{BuPh}L†H] (5.00 g, 5.60 mmol), KH (0.28 g, 6.71 mmol) and hexamethyldisilazane (58 μL, ~5 mol%) in THF (50 mL). The product was isolated as a free-flowing light-yellow colored solid (4.75 g, 84.6 %). X-ray quality crystals were grown by layering a THF solution of reaction mixture with hexane. M.p. 150 °C (decomp.); ^{1}H NMR (400 MHz, C$_6$D$_6$, 298 K) δ = 1.11 (d, $^3J_{HH}$ = 6.9 Hz, 6H, CH(C*H$_3$*)$_2$), 1.31 (s, 27H, C(C*H$_3$*)$_3$), 1.40 (m, 4H, OCH$_2$C*H$_2$*), 2.68 (m, $^3J_{HH}$ = 6.9 Hz, 1H, C*H*(CH$_3$)$_2$), 3.52 (m, 4H, OC*H$_2$*CH$_2$), 6.50 (s, 2H, Ph$_2$C*H*), 6.58 (t, $^3J_{HH}$ = 7.3 Hz,

2H, Ar-*H*), 6.76 (t, $^{3}J_{HH}$ = 7.5 Hz, 4H, Ar-*H*), 6.84-7.18 (m, 16H, Ar-*H*), 7.34 (d, $^{3}J_{HH}$ = 8.2 Hz, 6H, Ar-*H*), 7.76 (d, $^{3}J_{HH}$ = 8.3 Hz, 6H, Ar-*H*); $^{13}C\{^{1}H\}$ NMR (101 MHz, C_6D_6, 298 K) δ = 24.9 (CH(*C*H$_3$)$_2$), 25.8 (OCH$_2$*C*H$_2$), 31.7 (C(*C*H$_3$)$_3$), 33.8 (*C*H(CH$_3$)$_2$), 34.7 (*C*(CH$_3$)$_3$), 53.0 (Ph$_2$*C*H), 67.8 (O*C*H$_2$CH$_2$), 124.6, 124.9, 125.6, 126.1, 127.3, 127.9, 128.6, 2×128.7, 129.0, 130.7, 130.8, 132.9, 136.3, 138.5, 141.1, 146.7, 150.6, 151.4, 155.4 (Ar-*C*); $^{29}Si\{^{1}H\}$ NMR (80 MHz, C_6D_6, 298 K) δ = -42.7; IR ν/cm^{-1} (Nujol): 3059 (w), 1593 (s), 1545 (w), 1490 (m), 1422 (vs), 1382 (s), 1295 (s), 1265 (s), 1177 (w), 1130 (m), 1078 (vs), 1046 (m), 1026 (m), 969 (w), 950 (s), 918 (w), 886 (s), 824 (vs), 765 (m), 738 (s), 702 (vs), 674 (m); anal. calc. for $C_{65}H_{70}SiNK$: C 83.73 %, H 7.57 %, N 1.50 %, found: C 83.25 %, H 7.65 %, N 1.55 %.

[(*t*BuPhL*)GeCl] (18). [(*t*BuPhL*)K(THF)] (2.00 g, 2.05 mmol) was dissolved in THF (30 mL), and the solution was added dropwise to a solution of $GeCl_2$.dioxane (0.50 g, 2.15 mmol) in THF (10 mL) at -80 ºC. The reaction mixture was warmed to room temperature and stirred overnight. Volatiles were subsequently removed *in vacuo*, and the residue extracted into toluene (30 mL). The extract was filtered, concentrated to ca. 8 mL and stored at -30 ºC overnight to yield [(*t*BuPhL*)GeCl] as off-white crystals (1.40 g, 70.2 %). M.p. 245 °C (decomp.); ^{1}H NMR (400 MHz, C_6D_6, 298 K) δ = 1.20 (s, 27H, C(C*H*$_3$)$_3$), 1.89 (s, 3H, C*H*$_3$), 6.31 (s, 2H, Ph$_2$C*H*), 6.57 (d, 4H, $^{3}J_{HH}$ = 6.9 Hz, Ar-*H*), 6.82-7.40 (m, 27H, Ar-*H*), 8.26 (br, 3H, Ar-*H*); $^{13}C\{^{1}H\}$ NMR (101 MHz, C_6D_6, 298 K) δ = 21.3 (*C*H$_3$), 31.4 (C(*C*H$_3$)$_3$), 34.8 (*C*(CH$_3$)$_3$), 52.5 (Ph$_2$*C*H), 125.1, 125.2, 2×126.4, 128.5, 129.7, 2×130.2, 130.3, 131.3, 132.7, 135.1, 136.6, 140.7, 142.9, 143.8, 144.6, 145.0, 146.0, 152.9 (Ar-*C*); $^{29}Si\{^{1}H\}$ NMR (80 MHz, C_6D_6, 298 K) δ = -15.1; IR ν/cm^{-1} (Nujol): 3061 (w), 3026 (w), 2954 (s), 1597 (m), 1544 (m), 1495 (s), 1451 (vs), 1379 (s), 1267 (s), 1196 (m), 1180 (m), 1136 (w), 1120 (w), 1085 (vs), 1019 (m), 979 (w), 914 (w), 889 (s), 874 (vs), 847 (s), 764 (s), 750 (vs), 729 (m), 701 (vs); MS/EI *m/z* (%): 973.6 (M^{+}, 1), 865.7 (*t*BuPhAr*NH^{+}, 4), 439.3 (Ar*NH$_2^{+}$, 100); anal. calc. for $C_{63}H_{66}SiNGeCl$: C 77.74 %, H 6.83 %, N 1.44 %, found: C 77.45 %, H 6.93 %, N 1.42 %.

[(*t*BuPhL†)GeCl] (19). This compound was prepared following a similar method to that for [(*t*BuPhL*)GeCl] but using [(*t*BuPhL†)K(THF)] (2.00 g, 1.99 mmol) in THF (30 mL), $GeCl_2$.dioxane (0.48 g, 2.09 mmol) in THF (10 mL). Storage of the reaction mixture at -30 °C for 2 days resulted in deposition of [(*t*BuPhL†)GeCl] as pale-yellow crystals (1.70 g, 85.2 %). M.p. 185 °C; ^{1}H NMR (400 MHz, C_6D_6, 298 K) δ = 0.98 (d, $^{3}J_{HH}$ = 6.9 Hz, 6H,

CH(C*H*$_3$)$_2$), 1.22 (s, 27H, C(C*H*$_3$)$_3$), 2.51 (sept, $^3J_{HH}$ = 6.9 Hz, 1H, C*H*(CH$_3$)$_2$), 6.27 (s, 2H, Ph$_2$C*H*), 6.55 (d, 4H, $^3J_{HH}$ = 7.1 Hz, Ar-*H*), 6.79-7.37 (m, 27H, Ar-*H*), 8.26 (bs, 3H, Ar-*H*); ^{13}C{^{1}H} NMR (101 MHz, C$_6$D$_6$, 298 K) δ = 24.3 (CH(*C*H$_3$)$_2$), 31.4 (C(*C*H$_3$)$_3$), 34.1(*C*H(CH$_3$)$_2$), 34.8 (*C*(CH$_3$)$_3$), 52.7 (Ph$_2$*C*H), 125.2, 125.5, 126.5, 127.4, 128.4, 129.8, 2×130.2, 131.3, 132.7, 135.8, 136.6, 137.7, 141.2, 143.7, 145.0, 145.1, 146.0, 146.1, 152.9 (Ar-*C*); ^{29}Si{^{1}H} NMR (80 MHz, C$_6$D$_6$, 298 K) δ = -14.6; IR ν/cm^{-1} (Nujol): 3062 (w), 3027 (w), 2957 (s), 1598 (s), 1545 (w), 1494 (s), 1387 (s), 1266 (s), 1200 (m), 1161 (w),1136 (w), 1117 (w), 1084 (vs), 1033 (m), 919 (w), 884 (vs), 869 (m), 848 (s), 825 (s), 806 (w), 764 (m), 750 (s), 700 (vs); MS/EI *m/z* (%): 966.65 (M-Cl, 2), 760.65 (^{t}BuPh$_2$HSiArN^{*+}, 10), 427.25 (^{t}BuPh$_3$Si$^+$, 100); anal. calc. for C$_{65}$H$_{70}$SiNGeCl: C 77.96 %, H 7.05 %, N 1.40 %, found: C 77.39 %, H 7.18 %, N 1.57 %.

[(^{Cy}L*)GeCl] (20). A solution of [^{Cy}L*H] (2.00 g, 2.80 mmol) in THF (30 mL) was cooled to -80 ºC and LiBu^n (1.92 mL, 3.07 mmol, 1.6 M solution in hexane) was added dropwise over 10 minutes. After the addition, the reaction mixture was warmed to room temperature, and stirred for 3 hours. This reaction mixture was then added to GeCl$_2$.dioxane (0.68 g, 2.94 mmol) in THF (10 mL) at -80 ºC. The resultant solution was warmed to room temperature and stirred for 12 hours. Volatiles were subsequently removed *in vacuo*, and the residue extracted into hot hexane (50 mL). The extract was filtered, concentrated to ca. 15 mL and stored at -30 ºC overnight to yield pale-yellow crystals of [(^{Cy}L*)GeCl] (1.42, 61.7 %). M.p. 248 °C; ^{1}H NMR (400 MHz, C$_6$D$_6$, 298 K) δ = 1.26-1.38 (bs, 12H, Cy-*H*), 1.71-1.86 (m, 15H, Cy-*H*), 1.86 (s, 3H, C*H*$_3$) (signal at 1.86 and 1.87 overlaps), 2.31 (br, 6H, Cy-*H*), 6.26 (s, 2H, Ph$_2$C*H*), 6.83-7.21 (m, 18H, Ar-*H*), 7.45 (d, $^3J_{HH}$ = 7.8 Hz ,4H, Ar-*H*); ^{13}C{^{1}H} NMR (101 MHz, C$_6$D$_6$, 298 K) δ = 21.2 (Cy-*C*), 27.5(*C*H$_3$), 28.5, 29.1, 30.2 (Cy-*C*), 52.2 (Ph$_2$C*H*), 126.9, 128.0, 128.9, 129.6, 130.2, 130.3, 131.3, 134.8, 140.9, 144.0, 144.6, 145.9 (Ar-*C*); ^{29}Si{^{1}H} NMR (80 MHz, C$_6$D$_6$, 298 K) δ = 5.8; IR ν/cm^{-1} (Nujol): 3024 (w), 1597 (w), 1493 (s), 1444 (m), 1266 (w), 1191 (m), 1102 (m), 1078 (w), 1032 (m), 1001 (m), 910 (m), 868 (s), 737 (s), 826 (s), 764 (m), 737 (vs), 723 (s), 699 (vs); MS/EI *m/z* (%): 659.5 (Ar*N(GeCl)SiH$_2$Cy$^+$, 46), 467.4 (Ar*NH$_2$Si$^+$, 62), 167.1 (Ph$_2$C$^+$, 100); anal. calc. for C$_{51}$H$_{60}$SiNGeCl: C 74.41 %, H 7.35 %, N 1.70 %, found: C 74.23 %, H 6.75 %, N 1.85 %.

[(^{Cy}L†)GeCl] (21). This compound was prepared following a similar method to that for [(^{Cy}L*)GeCl] but using [^{Cy}L†H] (2.00 g, 2.69 mmol) in THF (30 mL), LiBu^n (1.8 mL,

2.96 mmol, 1.6 M solution in hexane) and $GeCl_2$.dioxane (0.65 g, 2.82 mmol) in THF (10 mL). Storage of the reaction mixture at -30 °C for 2 days resulted in deposition of [($^{Cy}L^{\dagger}$)GeCl] as colourless crystals (1.57 g, 68.6 %). M.p. 178-183 °C; ^{1}H NMR (400 MHz, C_6D_6, 298 K) δ = 0.96 (d, $^3J_{HH}$ = 6.9 Hz, 6H, CH(*CH*$_3$)$_2$), 1.23-1.84 (m, 28H, Cy-*H*), 2.28 (bs, 5H, Cy-*H*), 2.50 (sept, $^3J_{HH}$ = 6.9 Hz, 1H, C*H*(CH$_3$)$_2$), 6.26 (s, 2H, Ph$_2$C*H*), 6.84 (t, $^3J_{HH}$ = 7.4 Hz, 2H, Ar-*H*), 6.98-7.21 (m, 16H, Ar-*H*), 7.46 (d, $^3J_{HH}$ = 7.0 Hz, 4H, Ar-*H*); ^{13}C{^{1}H} NMR (101 MHz, C_6D_6, 298 K) δ = 24.2, 25.9, 27.1, 27.5, 27.9, 28.3 (Cy-*C*), 29.1 (CH(*C*H$_3$)$_2$), 30.0 (Cy-*C*), 34.0 (*C*H(CH$_3$)$_2$), 52.4 (Ph$_2$*C*H), 127.0, 127.5, 128.6, 128.8, 129.6, 130.1, 130.3, 131.3, 141.2, 144.0, 144.7, 145.9 (Ar-*C*); ^{29}Si{^{1}H} NMR (80 MHz, C_6D_6, 298 K) δ = 6.1; IR ν/cm^{-1} (Nujol): 3061 (w), 2956 (w), 1598 (m), 1493 (s), 1445 (s), 1195 (m), 1158 (w), 1110 (m), 1077 (w), 1031 (s), 1000 (m), 966 (w), 910 (w), 891 (s), 874 (s), 835 (s), 819 (s), 763 (s), 739 (s), 727 (s), 698 (vs); MS/EI *m/z* (%): 740.5 ($Ar^*NH_2Si^+$, 40), 700.3 (M-GeCl-Pr^{i+}, 6), 167.1 (Ph_2C^+, 100); anal. calc. for $C_{53}H_{64}SiNGeCl$: C 74 .78 %, H 7.58 %, N 1.65 %, found: C 74.64 %, H 7.58 %, N 1.74 %.

[(^{TMS}L***)GeCl] (22). This compound was prepared following a similar method to that for [($^{Cy}L^*$)GeCl] but using [$^{TMS}L^{***}H$] (0.50 g, 0.70 mmol) in THF (15 mL), LiBu^n (0.48 mL, 0.77 mmol, 1.6 M solution in hexane) and $GeCl_2$.dioxane (0.13 g, 0.55 mmol) in THF (5 mL). Storage of the reaction mixture at -30 °C for 2 days resulted in deposition of [($^{TMS}L^{***}$)GeCl] as colourless crystals (0.19 g, 34.2 %). M.P. 259 °C; ^{1}H NMR (400 MHz, C_6D_6, 298 K) δ = 0.36 (d, 9H, Si(C*H*$_3$)$_3$), 1.38 (s, 72H, C(*CH*$_3$)$_3$), 1.91 (s, 3H, *CH*$_3$), 6.55 (s, 2H, Ph$_2$C*H*), 7.23 (s, 3H, Ar-*H*), 7.26 (s, 2H, Ar-*H*), 7.40 (s, 6H, Ar-*H*), 7.48 (s, 3H, Ar-*H*); ^{13}C{^{1}H} NMR (101 MHz, C_6D_6, 298 K) δ = 4.0 (Si(C*H*$_3$)$_3$, 20.7 (*C*H$_3$), 31.7 (*C*(CH$_3$)$_3$), 35.1 (*C*(CH$_3$)$_3$), 52.4 (Ph$_2$C*H*), 119.8, 125.3, 131.9, 132.0, 142.7, 144.7, 145.0, 150.4 (Ar-*C*); ^{29}Si{^{1}H} NMR (80 MHz, C_6D_6, 298 K) δ = 11.32; IR ν/cm^{-1} (Nujol): 3027 (w), 2955 (s), 1597 (s), 1494 (s), 1387 (w), 1264 (s), 1201 (s), 1161 (w), 1118 (w), 1085 (vs), 1032 (w), 917 (w), 884 (vs), 848 (s), 825 (s), 764 (m), 750 (vs), 729 (w), 700 (vs); anal. calc. for $C_{68}H_{100}SiNGeCl$: C 76.49 %, H 9.44 %, N 1.31 %, found: C 76.54 %, H 9.58 %, N 1.38 %.

[{(^{Cy}L*)Ge}$_2$] (37). A solution of [{(^{Mes}Nacnac)Mg}$_2$] (434 mg, 0.61 mmol) in benzene (10 mL) was added to a solution of [($^{Cy}L^*$)GeCl] (1.0 g, 1.21 mmol) in benzene (30 mL) at -80 °C. The reaction mixture was warmed to room temperature over 5 hours. It was

then filtered and concentrated to ca. 15 mL. The next day the solution was filtered again and stored at room temperature to yield [{(^{Cy}L*)Ge}$_2$] as reddish-orange crystals (615 mg, 64.2 %). M.p. 170 °C; ^{1}H NMR (400 MHz, C_6D_6, 298 K) δ = 1.25 (br, 20H, Cy-*H*), 1.48-1.76 (br, 35H, Cy-H), 1.81 (s, 3H, C*H*$_3$) (signal at 1.75 and 1.80 overlaps), 2.02 (bs, 9H, Cy-*H*), 2.35 (s, 1H, Cy-*H*), 6.10 (s, 4H, Ph$_2$C*H*), 6.77-7.13 (s, 20H, Ar-*H*), 7.25 (t, $^3J_{HH}$ = 7.5 Hz, 8H, Ar-H), 7.35 (d, $^3J_{HH}$ = 7.2 Hz, 8H, Ar-H), 7.50 (d, $^3J_{HH}$ = 7.7 Hz, 8H, Ar-H); ^{13}C{^{1}H} NMR (101 MHz, C_6D_6, 298 K) δ = 18.4 (Cy-*C*), 20.9 (*C*H$_3$), 21.3, 23.2, 27.4, 28.4, 29.3 (Cy-*C*), 50.9 (Ph$_2$*C*H), 126.7, 128.5, 128.6, 129.6, 131.1, 131.6, 132.8, 133.1, 144.3, 169.5 (Ar-*C*); ^{29}Si{^{1}H} NMR (80 MHz, C_6D_6, 298 K) δ = -21.9; IR ν/cm^{-1} (Nujol): 3060 (w), 1598 (m), 1494 (s), 1445 (s), 1195 (s), 1116 (m), 1096 (m), 1033 (m), 995 (w), 910 (w), 886 (w), 862 (m), 843 (s), 795 (s), 758 (s), 732 (s), 699 (vs); anal. calc. for $C_{102}H_{120}Si_2N_2Ge_2$: C 77.76 %, H 7.68 %, N 1.78 %, found: C 77.68 %, H 7.61 %, N 1.71 %.

[{(^{Cy}L†)Ge}$_2$] (38). This compound was prepared following a similar method to that for [{(^{Cy}L*)Ge}$_2$] but using [(^{Cy}L†)GeCl] (1.00 g, 1.17 mmol) in benzene (20 mL) and [{(^{Mes}Nacnac)Mg}$_2$] (420 mg, 0.59 mmol) in benzene (10 mL). The product was isolated as colourless reddish-orange crystals (638 mg, 66.5 %). M.p. 185 °C; ^{1}H NMR (400 MHz, C_6D_6, 298 K) δ = 0.95 (d, $^3J_{HH}$ = 6.7 Hz, 12H, CH(*CH*$_3$)$_2$), 1.25-1.98 (br m, 64H, Cy-*H*), 2.16 (s, 1H, Cy-*H*), 2.19 (s, 1H, Cy-*H*), 2.47 (m, $^3J_{HH}$ = 6.8 Hz, 2H, C*H*(CH$_3$)$_2$), 6.11 (br s, 4H, Ph$_2$C*H*), 6.77-7.39 (m, 36H, Ar-H), 7.50 (d, $^3J_{HH}$ = 7.5 Hz, 8H, Ar-H);^{13}C{^{1}H} NMR (101 MHz, C_6D_6, 298 K) δ = 18.4 (Cy-*C*), 24.0 (CH(*C*H$_3$)$_2$), 27.4, 2×28.4 (Cy-*C*), 29.3 (Cy-*C*), 33.6 (*C*H(CH$_3$)$_2$), 51.1 (Ph$_2$C*H*), 126.6, 126.7, 128.4, 128.5, 129.6, 130.8, 130.9, 131.1, 131.6, 141.0, 143.9, 145.9 (Ar-*C*); ^{29}Si{^{1}H} NMR (80 MHz, C_6D_6, 298 K) δ = -21.8; IR ν/cm^{-1} (Nujol): 3057 (w), 3028 (w), 1599 (w), 1492 (w), 1445 (s), 1194 (w), 1158 (w), 1116 (m), 1077 (w), 1033 (m), 997 (w), 914 (w), 880 (w), 838 (m), 792 (s), 760 (m), 724 (s), 698 (vs); MS/EI *m/z* (%): 816.5 (^{Cy}L*Ge$^+$, 84), 743.6 (^{Cy}L*H$^+$, 15), 167.1 (Ph$_2$C$^+$, 1); anal. calc. for $C_{106}H_{128}Si_2N_2Ge_2$: C 78.03 %, H 7.91 %, N 1.72 %, found: C 77.93 %, H 7.68 %, N 1.86 %.

[($^{t\text{BuPh}}$L*)GeOBu^t] (40). A solution of [($^{t\text{BuPh}}$L*)GeCl] (1.0 g, 1.03 mmol) in toluene (20 mL) was added to a suspension of KOBu^t (138 mg, 1.23 mmol) in toluene (15 mL) at -80 ºC, the mixture was warmed to ambient temperature and then stirred for 3 hours. The mixture was filtered and concentrated to ca. 6 mL and layered with hexane, affording

[($^{t\text{BuPh}}$L*)GeOBu^{t}] as a pure-white powder (0.62 g, 59.7 %). M.p. > 260 °C; ^{1}H NMR (400 MHz, C_6D_6, 298 K) δ = 0.84 (s, 9H, OC(CH_3)$_3$), 1.25 (s, 27H, C(CH_3)$_3$), 1.92 (s, 3H, CH_3), 6.42 (s, 2H, Ph$_2$CH), 6.58 (d, 4H, $^{3}J_{HH}$ = 7.3 Hz, Ar-H), 6.95-7.37 (m, 26H, Ar-H), 8.13 (d, 4H, $^{3}J_{HH}$ = 8.3 Hz, Ar-H); ^{13}C{^{1}H} NMR (101 MHz, C_6D_6, 298 K) δ = 21.4 (CH_3), 31.5 (C(CH_3)$_3$), 33.6 (OC(CH_3)$_3$, 34.7 (C(CH$_3$)$_3$), 52.3 (Ph$_2$CH), 73.1 (OC(CH$_3$)$_3$), 124.7, 125.2, 125.7, 126.1, 127.2, 128.6, 129.0, 129.3, 130.4, 130.5, 131.4, 133.8, 136.6, 137.6, 137.9, 142.0, 144.7, 145.2, 145.4, 152.2 (Ar-C); ^{29}Si{^{1}H} NMR (80 MHz, C_6D_6, 298 K) δ = -17.0; IR ν/cm^{-1} (Nujol): 3062 (w), 3027 (w), 2956 (s), 1598 (m),1494 (s), 1387 (s), 1265 (s), 1200(m), 1161 (w), 1117(w), 1085 (s), 1032 (m), 939 (w), 919 (w), 884 (vs), 848 (s), 825 (vs), 805 (w), 765 (m), 750 (s), 700 (vs); anal. calc. for $C_{67}H_{75}SiNGeO$: C 79.59 %, H 7.48 %, N 1.39 %, found: C 79.11 %, H 7.09 %, N 1.31 %.

[($^{t\text{BuPh}}$L†)GeOBu^{t}] (41). This compound was prepared following a similar method to that for [($^{t\text{BuPh}}$L*)GeOBu^{t}] but using [($^{t\text{BuPh}}$L†)GeCl] (1.00 g, 1.00 mmol) in toluene (20 mL) and KOBu^{t} (134 mg, 1.20 mmol) in toluene (15 mL). The product was isolated as off-white powder (0.55 g, 53.0 %). M.p. 256 °C; ^{1}H NMR (400 MHz, C_6D_6, 298 K) δ = 0.86 (s, 9H, OC(CH_3)$_3$), 1.00 (d, 6H, $^{3}J_{HH}$ = 6.9 Hz, CH(CH_3)$_2$), 1.24, 1.25 (two s, 27H, C(CH_3)$_3$), 2.54 (m, 1H, $^{3}J_{HH}$ = 6.9 Hz, CH(CH$_3$)$_2$), 6.38 (s, 2H, Ph$_2$CH), 6.57 (d, 4H, $^{3}J_{HH}$ = 7.2 Hz, Ar-H), 6.94-7.39 (m, 26H, Ar-H), 8.14 (d, 4H, $^{3}J_{HH}$ = 8.3 Hz, Ar-H), ^{13}C{^{1}H} NMR (101 MHz, C_6D_6, 298 K) δ = 24.3 (CH(CH_3)$_2$), 31.5, 31.6 (C(CH_3)$_3$), 33.6 (CH(CH$_3$)$_2$), 34.7 (C(CH$_3$)$_3$), 52.6 (Ph$_2$CH), 73.1 (OC(CH$_3$)$_3$), 124.6, 124.7, 125.7, 126.1, 127.2, 127.6, 128.6, 129.1, 129.3, 130.4, 131.3, 2×136.6, 137.6, 137.8, 144.7, 144.8, 145.2, 145.6, 152.2 (Ar-C); ^{29}Si{^{1}H} NMR (80 MHz, C_6D_6, 298 K) δ = -16.5; IR ν/cm^{-1} (Nujol): 1599 (w), 1491 (m), 1260 (s), 1165 (w), 1103 (m), 1075 (m), 1030 (s), 889 (s), 845 (m), 799 (s), 764 (w), 726 (s), 701 (vs); anal. calc. for $C_{69}H_{79}SiNGeO$: C 79.76 %, H 7.66 %, N 1.35 %, found: C 71.19 %, H 7.53 %, N 1.11 %. % C does not match due to incomplete combustion of carbon.

[(^{Cy}L*)GeOBu^{t}] (42). This compound was prepared following a similar method to that for [($^{t\text{BuPh}}$L*)GeOBu^{t}] but using [(^{Cy}L*)GeCl] (1.00 g, 1.2 mmol) in toluene (20 mL) and KOBu^{t} (164 mg, 1.46 mmol) in toluene (15 mL). The product was isolated as colourless crystals (0.48 g, 45.9 %). M.p. 220 °C; ^{1}H NMR (400 MHz, C_6D_6, 298 K) δ = 1.14 (s, 9H, OC(CH_3)$_3$), 1.26-1.94 (m, 27H, Cy-H), 1.91 (s, 3H, CH_3), 2.30 (br s, 2H, Cy-H),

2.52 (br s, 4H, Cy-*H*), 6.40 (s, 2H, Ph_2CH), 6.90-7.22 (m, 18H, Ar-*H*), 7.52 (d, $^3J_{HH}$ = 7.4 Hz ,4H, Ar-*H*); $^{13}C\{^1H\}$ NMR (101 MHz, C_6D_6, 298 K) δ = 21.2 (CH_3), 27.5, 27.7, 27.9, 2×29.0, 29.2, 29.7, 30.1 (br s, Cy-*C*), 34.3 ($OC(CH_3)_3$), 51.9 (Ph_2CH), 73.1 ($OC(CH_3)_3$), 126.7, 127.2, 128.7, 129.0, 130.4, 130.6, 131.2, 133.4, 143.0, 144.8, 145.2, 145.4 (Ar-*C*); $^{29}Si\{^1H\}$ NMR (80 MHz, C_6D_6, 298 K) δ = -21.8; IR ν/cm^{-1} (Nujol): 3060 (w), 3026 (w), 1599 (w), 1492 (m), 1263 (w), 1234 (w), 1188 (s), 1117 (w), 1098 (m), 1032 (m), 998 (w), 939 (s), 873 (s), 839 (vs), 761 (w), 740 (s), 725 (s), 697 (vs); anal. calc. for $C_{55}H_{69}SiNGeO$: C 76.74 %, H 8.08 %, N 1.63 %, found: C 76.39 %, H 8.37 %, N 1.59 %.

2.6 References

1 C. F. H. Allen and F. P. Pingert, *J. Am. Chem. Soc.*, 1942, **64**, 1365–1371.

2 C.-J. F. Du, H. Hart and K. K. D. Ng, *J. Org. Chem.*, 1986, **51**, 3162–3165.

3 B. Schiemenz and P. P. Power, *Organometallics*, 1996, **15**, 958–964.

4 R. J. Wright, J. Steiner, S. Beaini and P. P. Power, *Inorg. Chim. Acta*, 2006, **359**, 1939–1946.

5 R. Wolf, C. Ni, T. Nguyen, M. Brynda, G. J. Long, A. D. Sutton, R. C. Fischer, J. C. Fettinger, M. Hellman, L. Pu and P. P. Power, *Inorg. Chem.*, 2007, **46**, 11277–11290.

6 C. Stanciu, A. F. Richards, J. C. Fettinger, M. Brynda and P. P. Power, *J. Organomet. Chem.*, 2006, **691**, 2540–2545.

7 R. Okazaki, M. Unno and N. Inamoto, *Chem. Lett.*, 1987, **16**, 2293–2294.

8 T. Sasamori, K. Hironaka, Y. Sugiyama, N. Takagi, S. Nagase, Y. Hosoi, Y. Furukawa and N. Tokitoh, *J. Am. Chem. Soc.*, 2008, **130**, 13856–13857.

9 T. Agou, Y. Sugiyama, T. Sasamori, H. Sakai, Y. Furukawa, N. Takagi, J. D. Guo, S. Nagase, D. Hashizume and N. Tokitoh, *J. Am. Chem. Soc.*, 2012, **134**, 4120–4123.

10 K. Nagata, T. Agou and N. Tokitoh, *Angew. Chem., Int. Ed.*, 2014, **53**, 3881–3884.

11 T. Matsuo, K. Suzuki, T. Fukawa, B. Li, M. Ito, Y. Shoji, T. Otani, L. Li, M. Kobayashi, M. Hachiya, Y. Tahara, D. Hashizume, T. Fukunaga, A. Fukazawa, Y. Li, H. Tsuji and K. Tamao, *Bull. Chem. Soc. Jpn.*, 2011, **84**, 1178–1191.

12 D. H. Harris and M. F. Lappert, *J. Chem. Soc., Chem. Commun.*, 1974, 895–896.

13 M. P. Coles, *Coord. Chem. Rev.*, 2015, **297**–**298**, 24–39.

14 P. A. T. W. Porskamp and B. Zwanenburg, *Synthesis*, 1981, 368–369.

15 G. Berthon-Gelloz, M. A. Siegler, A. L. Spek, B. Tinant, J. N. H. Reek and I. E. Markó, *Dalton Trans.*, 2010, **39**, 1444–1446.

16 E. W. Y. Wong, D. Dange, L. Fohlmeister, T. J. Hadlington and C. Jones, *Aust. J. Chem.*, 2013, **66**, 1144–1154.

17 J. Li, A. Stasch, C. Schenk and C. Jones, *Dalton Trans.*, 2011, **40**, 10448–10456.

18 T. J. Hadlington, J. Li and C. Jones, *Can. J. Chem.*, 2014, **92**, 427–433.

19 T. J. Hadlington, J. A. B. Abdalla, R. Tirfoin, S. Aldridge and C. Jones, *Chem. Commun.*, 2016, **52**, 1717–1720.

20 Y. Segawa, Y. Suzuki, M. Yamashita and K. Nozaki, *J. Am. Chem. Soc.*, 2008, **130**, 16069–16079.

21 C. N. de Bruin-Dickason, A. J. Boutland, D. Dange, G. B. Deacon and C. Jones, *Dalton Trans.*, 2018, **47**, 9512–9520.

22 E. W. Y. Wong, T. J. Hadlington and C. Jones, *Main Gr. Met. Chem.*, 2013, **36**, 133–136.

23 J. Hicks, T. J. Hadlington, C. Schenk, J. Li and C. Jones, *Organometallics*, 2013, **32**, 323–329.

24 J. Gavenonis and T. D. Tilley, *Organometallics*, 2002, **21**, 5549–5563.

25 L. Pu, M. M. Olmstead, P. P. Power and B. Schiemenz, *Organometallics*, 1998, **17**, 5602–5606.

26 R. S. Simons, L. Pu, M. M. Olmstead and P. P. Power, *Organometallics*, 1997, **16**, 1920–1925.

27 M. Stender, L. Pu and P. P. Power, *Organometallics*, 2001, **20**, 1820–1824.

28 B. E. Eichler, L. Pu, M. Stender and P. P. Power, *Polyhedron*, 2001, **20**, 551–556.

29 S. Hino, M. Olmstead, A. D. Phillips, R. J. Wright and P. P. Power, *Inorg. Chem.*, 2004, **43**, 7346–7352.

30 L. Pu, B. Twamley and P. P. Power, *Organometallics*, 2000, **19**, 2874–2881.

31 T. Sasamori, Y. Sugiyama, N. Takeda and N. Tokitoh, *Organometallics*, 2005, **24**, 3309–3314.

32 T. Sugahara, J. D. Guo, T. Sasamori, Y. Karatsu, Y. Furukawa, A. E. Ferao, S. Nagase and N. Tokitoh, *Bull. Chem. Soc. Jpn.*, 2016, **89**, 1375–1384.

33 K. Suzuki, Y. Numata, N. Fujita, N. Hayakawa, T. Tanikawa, D. Hashizume, K. Tamao, H. Fueno, K. Tanaka and T. Matsuo, *Chem. Commun.*, 2018, **54**, 2200–

2203.

34 N. Hayakawa, T. Sugahara, Y. Numata, H. Kawaai, K. Yamatani, S. Nishimura, S. Goda, Y. Suzuki, T. Tanikawa, H. Nakai, D. Hashizume, T. Sasamori, N. Tokitoh and T. Matsuo, *Dalton Trans.*, 2018, **47**, 814–822.

35 J. A. Kelly, M. Juckel, T. J. Hadlington, I. Fernández, G. Frenking and C. Jones, *Chem. - Eur. J.*, 2019, **25**, 2773–2785.

36 W. A. Merrill, R. J. Wright, C. S. Stanciu, M. M. Olmstead, J. C. Fettinger and P. P. Power, *Inorg. Chem.*, 2010, **49**, 7097–7105.

37 T. J. Hadlington, *On the Catalytic Efficacy of Low-Oxidation State Group 14 Complexes*, Springer Theses, 2017.

38 M. Stender, A. D. Phillips, R. J. Wright and P. P. Power, *Angew. Chem.*, 2002, **114**, 1863–1865.

39 Y. Peng, R. C. Fischer, W. A. Merrill, J. Fischer, L. Pu, B. D. Ellis, J. C. Fettinger, R. H. Herber and P. P. Power, *Chem. Sci.*, 2010, **1**, 461–468.

40 Y. Sugiyama, T. Sasamori, Y. Hosoi, Y. Furukawa, N. Takagi, S. Nagase and N. Tokitoh, *J. Am. Chem. Soc.*, 2006, **128**, 1023–1031.

41 J. Li, C. Schenk, C. Goedecke, G. Frenking and C. Jones, *J. Am. Chem. Soc.*, 2011, **133**, 18622–18625.

42 T. J. Hadlington, M. Hermann, J. Li, G. Frenking and C. Jones, *Angew. Chem., Int. Ed.*, 2013, **52**, 10199–10203.

43 A. D. Phillips, R. J. Wright, M. M. Olmstead and P. P. Power, *J. Am. Chem. Soc.*, 2002, **124**, 5930–5931.

44 L. Pu, A. D. Phillips, A. F. Richards, M. Stender, R. S. Simons, M. M. Olmstead and P. P. Power, *J. Am. Chem. Soc.*, 2003, **125**, 11626–11636.

45 R. C. Fischer, L. Pu, J. C. Fettinger, M. A. Brynda and P. P. Power, *J. Am. Chem. Soc.*, 2006, **128**, 11366–11367.

46 T. J. Hadlington and C. Jones, *Chem. Commun.*, 2014, **50**, 2321–2323.

47 L. Pu, B. Twamley and P. P. Power, *J. Am. Chem. Soc.*, 2000, **122**, 3524–3525.

48 J. Schneider, C. P. Sindlinger, K. Eichele, H. Schubert and L. Wesemann, *J. Am. Chem. Soc.*, 2017, **139**, 6542–6545.

49 J. D. Queen, M. Bursch, J. Seibert, L. R. Maurer, B. D. Ellis, J. C. Fettinger, S. Grimme and P. P. Power, *J. Am. Chem. Soc.*, 2019, **141**, 14370–14383.

50 G. H. Spikes, J. C. Fettinger and P. P. Power, *J. Am. Chem. Soc.*, 2005, **127**, 12232–12233.

51 L. Zhao, F. Huang, G. Lu, Z. X. Wang and P. V. R. Schleyer, *J. Am. Chem. Soc.*, 2012, **134**, 8856–8868.

52 Y. Peng, M. Brynda, B. D. Ellis, J. C. Fettinger, E. Rivard and P. P. Power, *Chem. Commun.*, 2008, 6042–6044.

53 S. Wang, T. J. Sherbow, L. A. Berben and P. P. Power, *J. Am. Chem. Soc.*, 2018, **140**, 590–593.

54 M. Hermann, C. Goedecke, C. Jones and G. Frenking, *Organometallics*, 2013, **32**, 6666–6673.

55 J. Li, M. Hermann, G. Frenking and C. Jones, *Angew. Chem., Int. Ed.*, 2012, **51**, 8611–8614.

56 R. Lalrempuia, A. Stasch, A. Stasch and C. Jones, *Chem. Sci.*, 2013, **4**, 4383–4388.

57 C. Cui, M. M. Olmstead, J. C. Fettinger, G. H. Spikes and P. P. Power, *J. Am. Chem. Soc.*, 2005, **127**, 17530–17541.

58 B. E. Eichler and P. P. Power, *J. Am. Chem. Soc.*, 2000, **122**, 8785–8786.

59 T. J. Hadlington, M. Driess and C. Jones, *Chem. Soc. Rev.*, 2018, **47**, 4176–4197.

60 A. F. Richards, A. D. Phillips, M. M. Olmstead and P. P. Power, *J. Am. Chem. Soc.*, 2003, **125**, 3204–3205.

61 T. J. Hadlington, B. Schwarze, E. I. Izgorodina and C. Jones, *Chem. Commun.*, 2015, **51**, 6854–6857.

62 T. J. Hadlington, M. Hermann, G. Frenking and C. Jones, *J. Am. Chem. Soc.*, 2014, **136**, 3028–3031.

63 A. Jana, H. W. Roesky, C. Schulzke and A. Döring, *Angew. Chem., Int. Ed.*, 2009, **48**, 1106–1109.

64 A. Jana, H. W. Roesky and C. Schulzke, *Inorg. Chem.*, 2009, **48**, 9543–9548.

65 A. Jana, H. W. Roesky and C. Schulzke, *Dalton Trans.*, 2010, **39**, 132–138.

66 T. J. Hadlington, M. Hermann, G. Frenking and C. Jones, *Chem. Sci.*, 2015, **6**, 7249–7257.

67 S. G. Weber, C. Loos, F. Rominger and B. F. Straub, *ARKIVOC*, 2012, **2012**, 226–242.

68 S. Dierick, D. F. Dewez and I. E. Markó, *Organometallics*, 2014, **33**, 677–683.

69 B. E. Lindfors, J. L. Male, D. R. Tyler and T. J. R. Weakley, *Acta Crystallogr. Sect. C: Cryst. Struct. Commun.*, 1998, **C54**, 694–695.

70 S. K. Liew, S. M. I. Al-Rafia, J. T. Goettel, P. A. Lummis, S. M. McDonald, L. J. Miedema, M. J. Ferguson, R. McDonald and E. Rivard, *Inorg. Chem.*, 2012, **51**, 5471–5480.

71 R. J. Schwamm, C. M. Fitchett and M. P. Coles, *Chem. - An Asian J.*, 2019, **14**, 1204–1211.

72 J. M. Smith, N. J. Coville, L. M. Cook and J. C. A. Boeyens, *Organometallics*, 2000, **19**, 5273–5280.

73 L. Falivene, Z. Cao, A. Petta, L. Serra, A. Poater, R. Oliva, V. Scarano and L. Cavallo, *Nat. Chem.*, 2019, **11**, 872–879.

74 S. P. Green, C. Jones and A. Stasch, *Science*, 2007, **318**, 1754–1758.

75 S. M. I. Al-Rafia, P. A. Lummis, M. J. Ferguson, R. McDonald and E. Rivard, *Inorg. Chem.*, 2010, **49**, 9709–9717.

Chapter 3
Utilisation of Bidentate Bis(amidinate) Ligands for Stabilisation of Dinuclear Main Group Element Complexes

3.1 Introduction

Despite the prevalence of main group element complexes stabilised using monodentate (discussed in chapter 2) and bidentate ligands, there are very few examples of low oxidation state main group element complexes stabilised by bis(bidentate) ligand systems. Herein, some examples of bidentate ligands and bis(bidentate) ligands will be discussed, as well as their use in the synthesis of main group element halide and element-element bonded complexes.

3.1.1 Bidentate Ligands

The term ligand was first introduced by Alfred Stock in 1916, and comes from the Latin word *ligare* which means 'to bind'.[1] Ligands can be classified into broad categories depending on the number of donor atoms that bind to a metal centre. Monodentate ligands which have one donor atom have been discussed in chapter 2. Similarly, multidentate ligands have two (bidentate) or more donor atoms to bind/donate to the central metal centre or ion. These ligands are also often referred to as chelating ligands, since they provide the 'chelate effect',[2] which increases their binding affinity towards a metal ion/centre as compared to monodentate ligands. The chelate effect can be explained by a large gain of entropy on using bidentate or multidentate ligands. From thermodynamics, the feasibility of a chemical process can be explained using $\Delta G = \Delta H - T\Delta S$, where ΔG, ΔH and ΔS are the change in Gibbs free energy, enthalpy and entropy, respectively. The use of chelating ligands renders a positive change in ΔS, thereby resulting in a favourable, more negative ΔG. Here is a classic example, when six monodentate NH_3 ligands are displaced with three bidentate en (en = ethylenediamine) ligands, the equilibrium constant increases 100,000 times in the second case (**Scheme 3.1**).[3]

$$[Co(H_2O)_6]^{2+} + 6\ NH_3 \rightleftharpoons [Co(NH_3)_6]^{2+} + 6\ H_2O \quad \textbf{(1)}$$

$$[Co(H_2O)_6]^{2+} + 3\ en \rightleftharpoons [Co(en)_3]^{2+} + 6\ H_2O \quad \textbf{(2)}$$

Scheme 3.1. Example of chelate effect on transition metal complexes.

The following section will discuss the bidentate *N,N'*-donor ligands (β-diketiminate, amidinate and guanidinate) and the stabilisation of main group element complexes particularly utilising amidinate ligands (**Figure 3.1**).

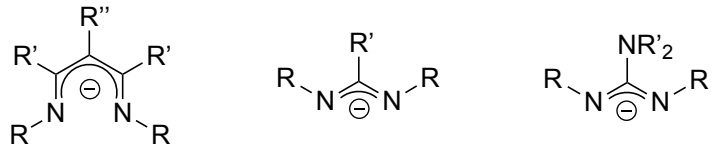

β-diketiminate
R = aryl or alkyl
R' = alkyl
R'' = H or alkyl

Amidinate
R = alkyl or aryl
R' = alkyl or aryl

Guanidinate
R = alkyl or aryl
R' = aryl

Figure 3.1. Bidentate nitrogen donor chelating ligands.

3.1.1.1 β-Diketiminate (Nacnac) Ligands

β-Diketiminates are isoelectronic to β-diketonato and β-enaminoketonato, also termed as 'Nacnac' ligands, which are bidentate, monoanionic [{(RNCR')$_2$CR"}$^-$] type ligands. These were first synthesised in 1968 by the reaction of an enamine ketone with triethoxy fluoroborate to form an imino ether, which further reacted with an amine to afford the tetrafluoroborate salt of the ligand. It could be further deprotonated by a methoxide base in anhydrous methanol to obtain the protonated ligand (**Scheme 3.2**).[4]

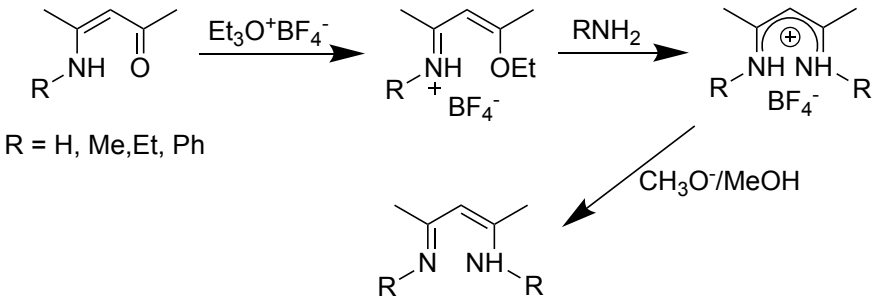

Scheme 3.2. First synthetic route to 'Nacnac' ligands.

A major development occurred in the 1990s with regards to the synthesis of Nacnac ligands, and it was recognised that these ligands could play a useful role as 'spectator ligands'.[5,6] Presently, there are various high yielding routes available for the synthesis of β-diketiminate ligands.[7] The most convenient route involves the condensation of β-

diketones with anilines in presence of acid, and trapping the water released during the reaction (e.g. using a Dean-Stark apparatus). While, this is easy and low cost, other routes are employed when this method is not effective e.g. in case of asymmetric Nacnacs, R' modification (**Figure 3.1**) or Nacnac synthesis with bulky aryl or alkyl substituents (**Scheme 3.3**).[8,9]

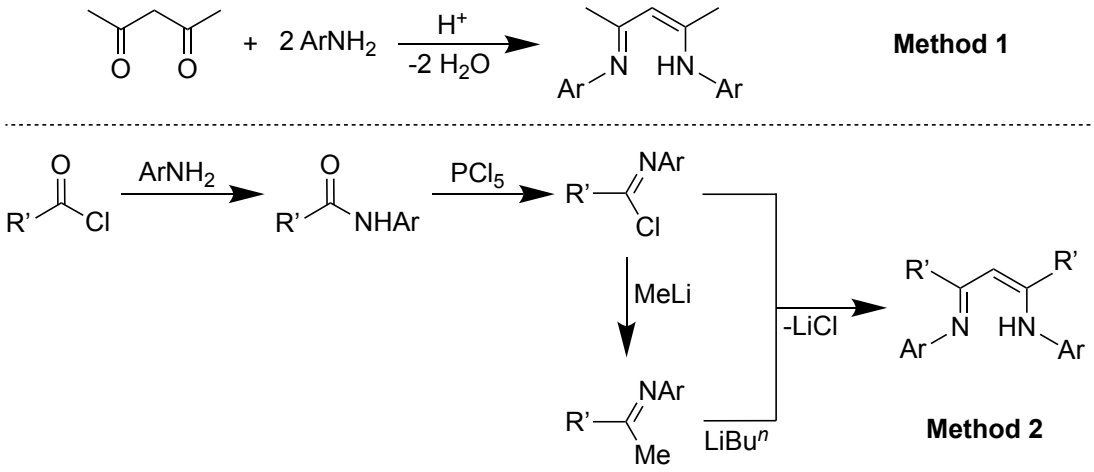

Scheme 3.3. Synthetic routes to general and R' substituted β-diketimine pro-ligands.

3.1.1.2 Amidinate and Guanidinate Ligands

Amidinates and guanidinates are bidentate, monoanionic [{R'C(NR)$_2$}$^-$] and [{R'$_2$NC(NR)$_2$}$^-$] ligands which are reminiscent of carboxylate anions. Similar to β-diketonates, amidinates are nitrogen donor bidentate ligands. The credit for amidinate ligands is given to Sanger and co-workers for the discovery of *N,N,N'*-tris(trimethylsilyl)benzamidine, [PhC(=NSiMe$_3$)N(SiMe$_3$)$_2$] in 1973, by the reaction of benzonitrile with [LiN(SiMe$_3$)$_2$].[10] The main advantage of these ligands is their easily accessible starting materials. There is a wide range of variation possible on carbon and nitrogen substituents (R' and R) which can tune the electronic and steric properties of the ligands. Moreover, increasing bulk at nitrogen and carbon atoms (R') decreases the NCN angle, inducing a convergent orientation of lone pairs which arises from the steric interactions of R and R' (**Figure 3.2**).[11]

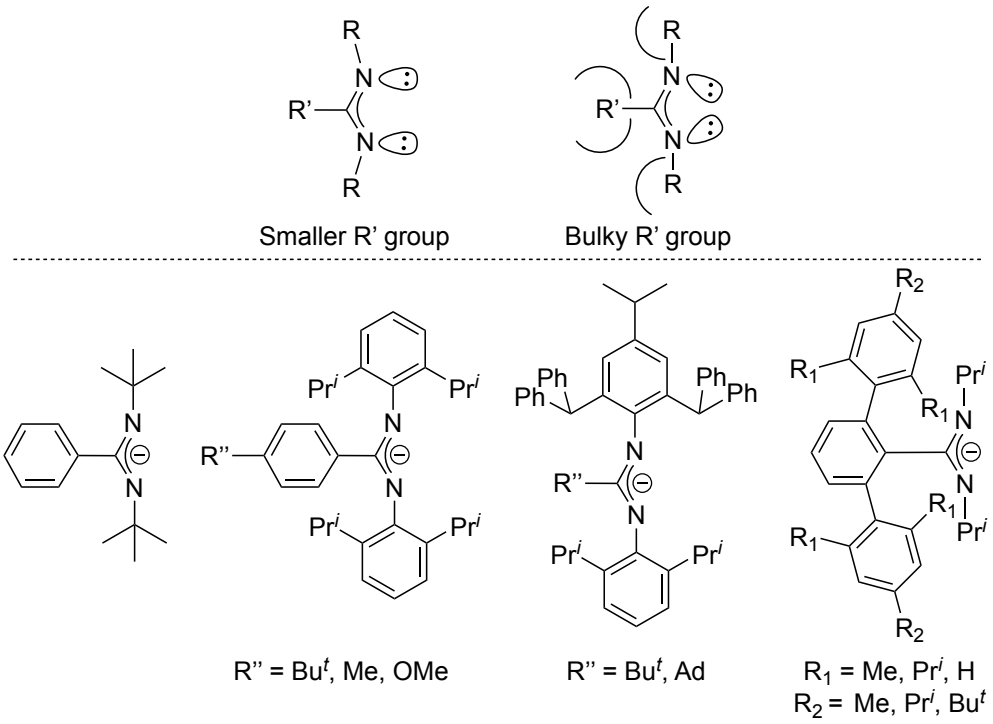

Figure 3.2. Effect of increasing bulk at the R' substituent and examples of some reported bulky amidinate ligands.

The general synthetic methods for amidinate ligands include- **1**) reaction of a carbodiimide with the lithium alkyl or aryl of choice, to afford the lithium amidinate, which can be hydrolysed to give the protonated ligand and, **2**) synthesis of an imidoyl chloride species with further addition of another alkyl or aryl amine in presence of a base (**Scheme 3.4**). Method **1** is limited by the carbodiimide sources while method **2** permits the synthesis of bulkier asymmetric amidinates.[12,13]

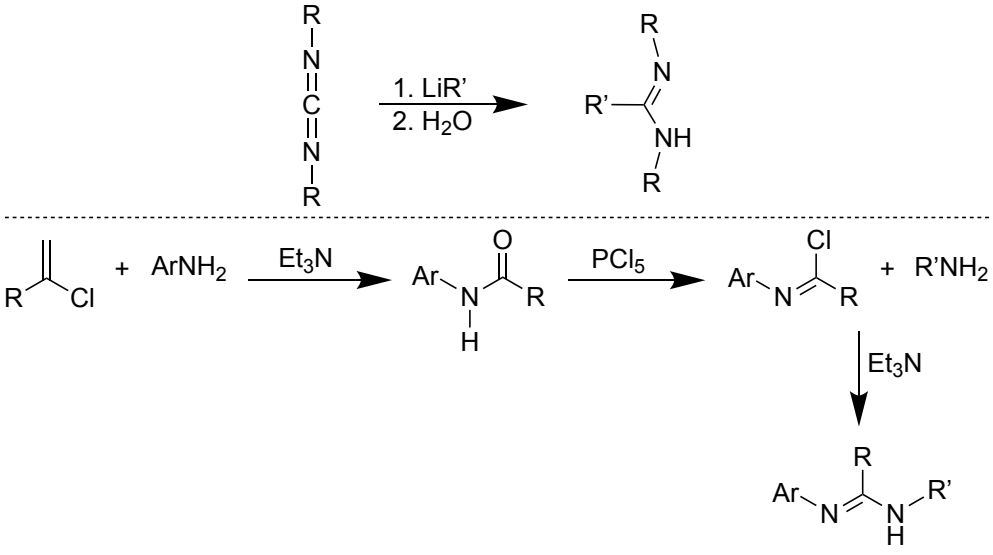

Scheme 3.4. General synthesis of amidine pro-ligands.

The closely related guanidinates and phosphaguanidinates, which contain a nitrogen or a phosphorus substituent at the central carbon of NCN fragment, can also be synthesised in similar ways as that shown in **Scheme 3.4**.[14] There are several other isoelectronic chelating ligands reported in the literature besides amidinates, guanidinates and phosphaguanidinates (**Figure 3.3**).

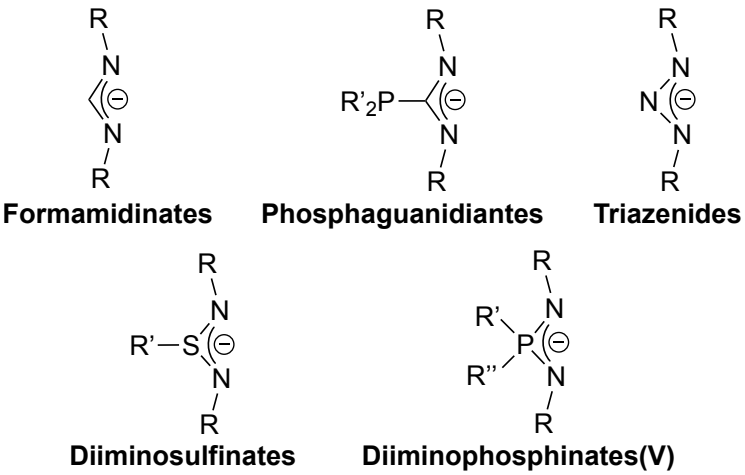

Figure 3.3. General structure of heteroallylic ligands.

3.1.2 Bis(bidentate) Ligands

Bifunctional ligands have gained massive attention in the last two decades due to the cooperative effect provided by these ligands upon complexation. These ligands contain two monoanionic bidentate units connected through a variety of linkers that are rigid or non-rigid. The bridging linkers not only tune the element-element distances in these ditopic ligand complexes but also decide the proximity and orientation of the two element fragments. Such ligands can be classified into two categories; homoditopic and heteroditopic depending on whether the connecting ligands are of same or different type (**Figure 3.4**).[15]

Figure 3.4. Schematic representation of homoditopic and heteroditopic ligands.

3.1.2.1 Bis(amidinate) Ligands

Binuclear amidinate ligands were developed two decades ago and since then a variety of bifunctional amidinates have been synthesised.[16,17] The bis(amidinate) ligands are divided into two classes based on their bridging linkers - nitrogen bridged amidinates and backbone bridged amidinates (**Figure 3.5**).

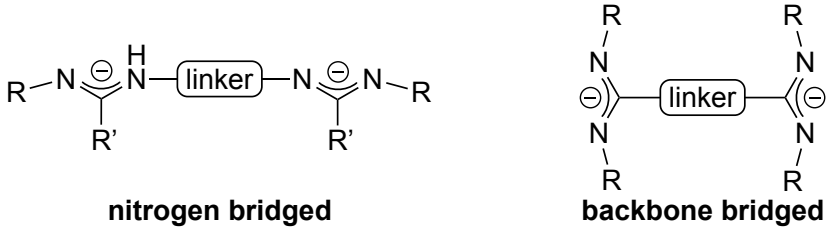

Figure 3.5. Types of binuclear amidinate ligands.

The synthesis and chemistry of nitrogen bridged bis(amidinates) will be discussed in chapter 4. The backbone bridged bis(amidinates) are generally synthesised by employing methods similar to the amidinates discussed in section **3.1.1.2** and involve the addition of the desired carbodiimide to *in situ* generated, doubly lithiated, linker molecule. Alternate routes are the reaction of two equivalents of the desired lithiated amine with dinitrile, or the addition of alkyl/aryl amine to bis(imidoylchloride) (**Scheme 3.5**).[18–21]

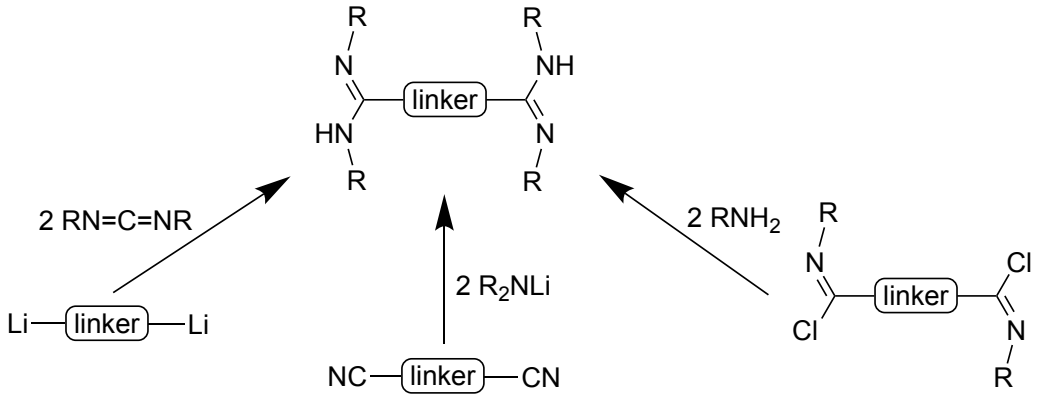

Scheme 3.5. Synthetic pathways for backbone bridged bis(amidine) pro-ligands.

There have been a variety of bis(amidinate) ligands synthesised using backbone bridging linkers like dibenzofuran, dimethylxanthine, -CH_2-, 1,2-disubstituted cyclohexane, 1,3- and 1,4- benzene, which have been accessed using suitable synthetic procedures (**Figure 3.6**).

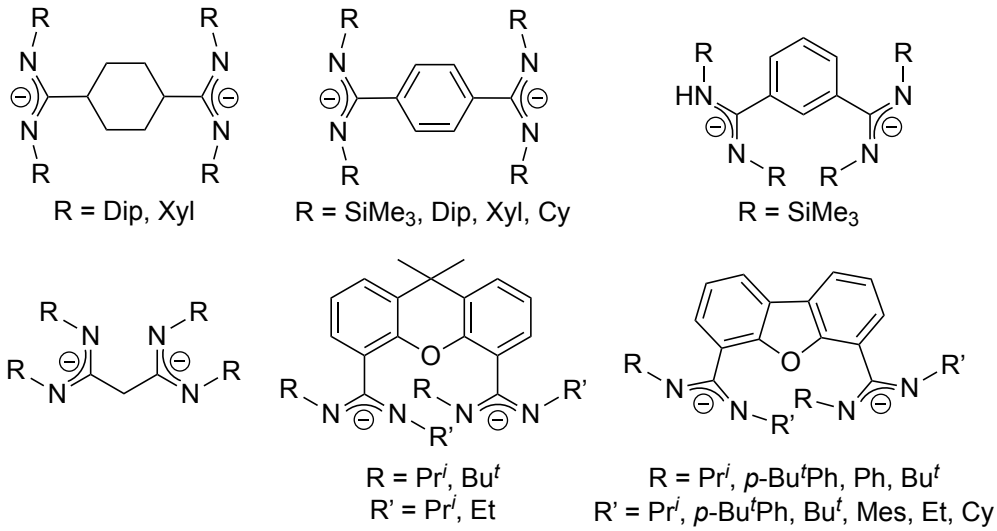

Figure 3.6. Types of literature reported binuclear amidinates.

3.1.3 Amidinate and Bis(amidinate) Ligands in Main Group Chemistry

Amidinate ligands have been extensively used to synthesise a range of main group element complexes. These ligands can provide various coordination modes when employed. The monodentate coordination mode **A**, which occurs in ligands containing bulky substituents, the most common bidentate *N,N'*-chelating mode **B** and the bridging coordination mode **C**. The group 11 elements gold, silver and copper tend to form dinuclear complexes containing two ligands. Another coordination mode is the *N*,aryl-chelating mode **D** which can be seen in the alkali metal and some of the group 13 element complexes (**Figure 3.7**).[22]

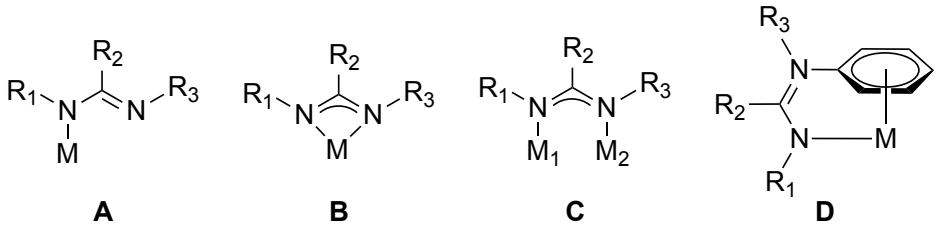

Figure 3.7. Common coordination modes of amidinates and guanidinates.

Metal amidinates can be accessed by several synthetic routes, however, the most common are-(**i**) insertion of a carbodiimide into metal alkyl or aryl bonds, (**ii**) protonlysis of amidines using metal alkyls as a base and (**iii**) salt metathesis reactions between alkali metal amidinates with metal halides.

3.1.3.1 Group 2 and 13 Element Complexes

The amidinate ligand chemistry of alkaline earth metals has significantly progressed in the last three decades with numerous amidinato magnesium halide complexes being prepared. The magnesium halide complexes bearing amidinate ligands have been synthesised most commonly by reacting *in situ* generated or commercially available Grignard reagents (RMgX, R=alkyl or aryl, X= Cl, Br, I) with an equivalent of carbodiimide or protonated ligands in coordinating solvents (THF, Et_2O) (**Scheme 3.6**). Most of the structurally characterised halide complexes are dimeric in the solid-state, where both nitrogens of each amidinate moiety are chelated to their respective magnesium centre. These complexes are bridged through two halogen atoms and the magnesium centres can be solvated by THF or Et_2O in the solid-state.[23,24] Complexes of amidinate ligands with highly sterically hindering terphenyl groups at the backbone carbon have been isolated as monomers in solid-state.[11]

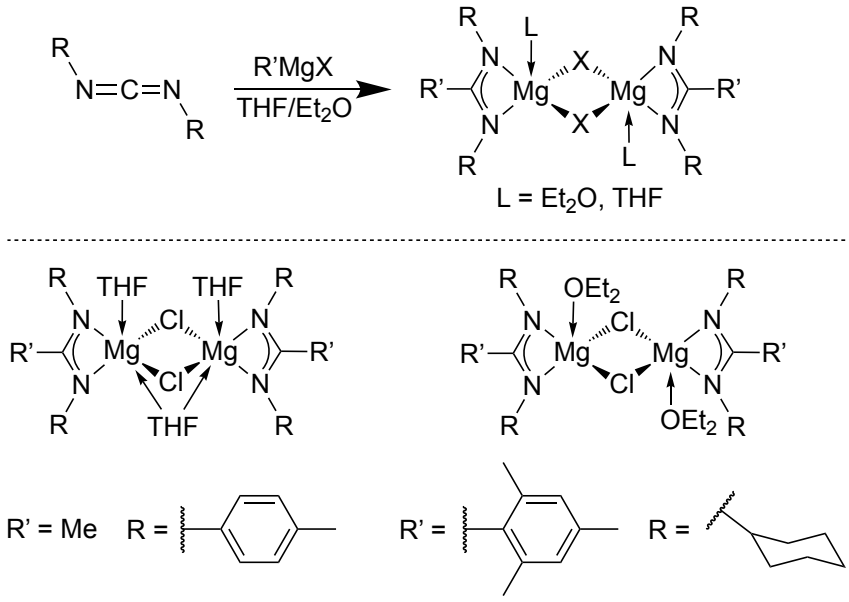

Scheme 3.6. Synthesis of magnesium(II) halide complexes and some known examples.

A particular guanidinate based complex of note was synthesised in 2007, with the first thermally stable dimeric magnesium(I) compound [{(Priso)Mg}$_2$] (Priso = [Pr$^i_2$NC(NDip)$_2$], Dip= 2,6-diisopropylphenyl) being isolated.[25] This used the closely related guanidinate ligand Priso. [{(Priso)Mg}$_2$] was synthesised by stirring the guanidinato magnesium(II) halide complex [(Priso)Mg(μ-I)$_2$Mg(OEt$_2$)(Priso)] over an excess of potassium metal in toluene for 24 hours leading to the formation of [{(Priso)Mg}$_2$] (**Scheme 3.7**). The three-coordinate magnesium centres adopt trigonal

planar geometries and the distance between the magnesium centres is 2.8508(12) Å. The complex was initially isolated as 30 % yield. Since then, the yield of other magnesium(I) complexes have been improved up to 70-80 % by using different reducing agents and synthetic strategies.[26]

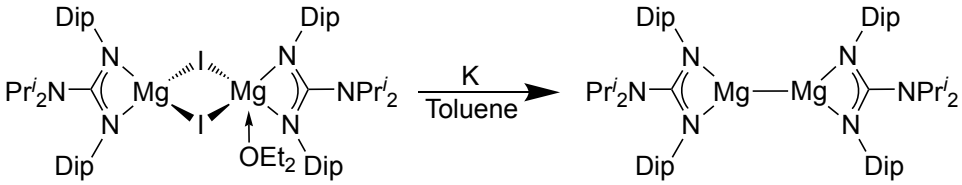

Scheme 3.7. Synthesis of the first magnesium(I) dimer [{(Priso)Mg}$_2$].

Neutral mononuclear aluminium compounds of the type AlX_3 (X = halide, alkyl) are of significant interest due to their numerous applications, e.g., as olefin polymerisation catalysts, and precursors for thin film deposition.[27,28] Amidinate supported aluminium halide complexes have been synthesised by reaction between alkali metal salts of the amidinate ligands and (alkyl) aluminium halides ($AlX_{2-n}R_n$), or by reacting the protonated ligands with aluminium alkyls followed by addition of iodine (**Scheme 3.8**). Few examples of amidinate supporting mononuclear aluminium complexes are [PhC(NPr^i)(NCy)AlMe$_2$], [PhC(NPr^i)(NCy)AlCl$_2$] (Cy = cyclohexyl), [Bu^{t}C(NDip)$_2$AlI$_2$] and [(Piso")AlMe$_2$] (Piso" = Bu^{t}C(NAr")$_2$, Ar'' = 2,6-Pr$^i_2$-4-(CPh$_3$)-Ph) and [(Piso") AlI$_2$].[29,30]

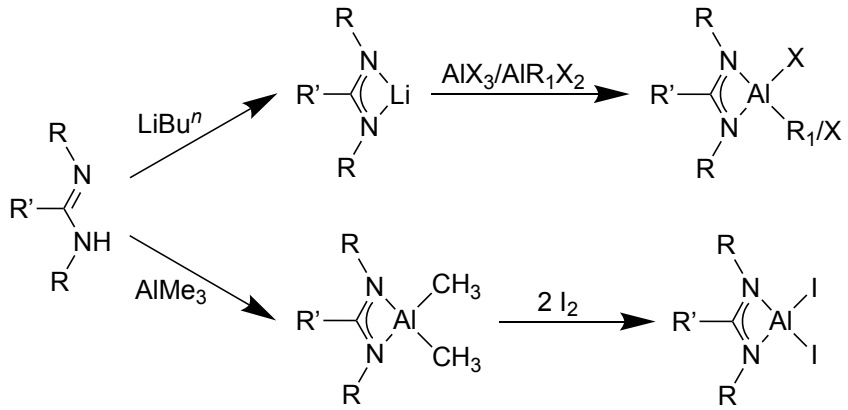

Scheme 3.8. Synthetic routes to mononuclear aluminium alkyl and aluminium halide complexes supported by amidinate ligands.

In recent years, various dinuclear aluminium(III) complexes have been explored as ring opening polymerisation catalysts for cyclic ethers, esters and propylene oxides.[31–34] The growing interest in these complexes is due to their access to cooperative bimetallic

mechanisms, in contrast to mononuclear aluminium complexes.[35,36] Normand et al. in 2013 proved that in terms of activation energy, dinuclear complexes give rise to a 5 to 10 fold increase towards ring opening polymerisation as compared to their mononuclear counterparts.[33] These dinuclear aluminium complexes [AlX_3(linker)AlX_3] can be synthesised along similar lines (**Scheme 3.8**) by using a stoichiometric amount of desired reagents. To date, there are several examples of dinuclear amidinate supported aluminium alkyls, while only a few examples of guanidinate bearing aluminium halide complexes are known (**Figure 3.8**).[37–40]

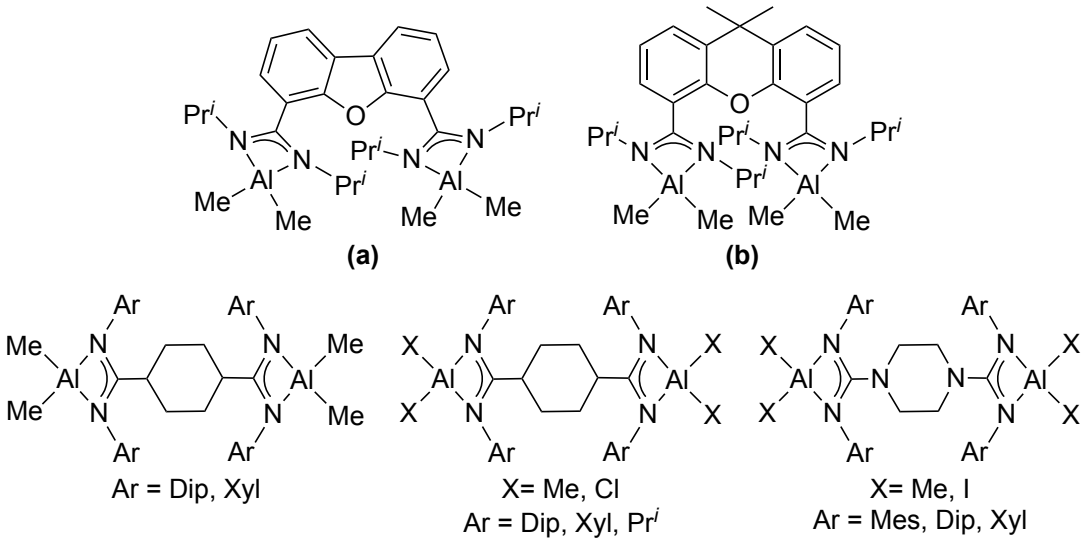

Figure 3.8. Dinuclear amidinate and guanidinate supported aluminium(III) complexes.

The geometry and metric parameters of these complexes are largely dependent on the bridging linkers. For example, the dibenzofuran and 9,9-dimethylxanthene linked aluminium methyl complexes (**a**) and (**b**) have different inter-aluminium distances (Al-Al) 6.5050(9) Å and 5.9303(9) Å, respectively. This difference in bond distances arises from the steric repulsion of the methyl groups' carbons which are attached to aluminium centres, thereby forcing the latter out of the amidinate NCN plane.[39] That being said, an amidinate supported aluminium(I) compound has not yet been isolated, although the first β-diketiminate supported aluminium(I) compound [{HC(CMeNDip)$_2$}Al] was reported in 2000.[41]

3.1.3.2 Group 14 Element Complexes

Amidinate ligands have also been extremely successful in stabilising novel and unusual group 14 element complexes.[42–44] In this context, the isolation of heavier tetrelenes and ditetrelenes have been of particular note. The general route for the synthesis of group 14

element(II) halides and silicon(IV) halide complexes is salt metathesis reactions of alkali metal salt of the corresponding ligand with an element(II) dihalide or element(IV) tetrahalide (in case of silicon). These halide complexes are further reduced to give low oxidation state complexes LEEL (L= ligand, E = Si, Ge, Sn) or LEX (in case of silicon, X = Cl, Br, I). With this in mind, Roesky and co-workers have isolated the bulky amidinate supported silicon(IV) complex, [{PhC(NBu^t)$_2$}SiCl$_3$]. Subsequently, this species was reduced with two equivalents of potassium metal in THF, leading to the isolation of the first amidinate complex incorporating a silicon(II) chloride fragment [{PhC(NBu^t)$_2$}SiCl] in 10 % yield.[45] A higher yielding route was developed, by which the lithium salt of the ligand [{PhC(NBu^t)$_2$}Li] was reacted with SiHCl$_3$ yielding [{PhC(NBu^t)$_2$}SiHCl$_2$].[46] Treating this complex with LiN(SiMe$_3$)$_2$ afforded [{PhC(NBu^t)$_2$}SiCl] in an improved yield of 90 % (**Scheme 3.9**).

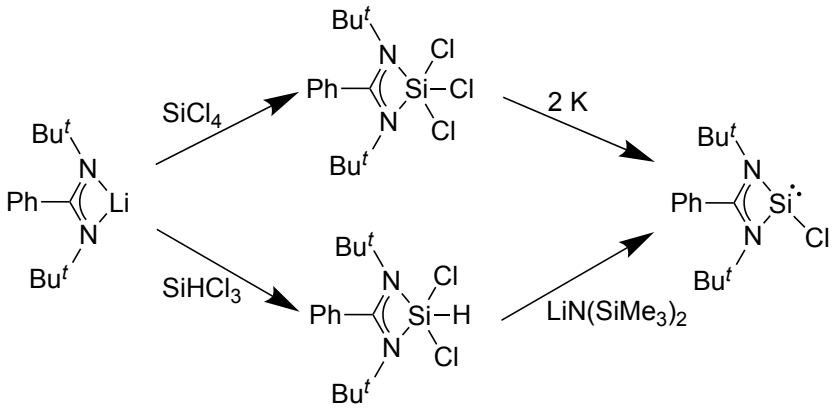

Scheme 3.9. Synthesis of the first amidinate stabilised chlorosilylene [{PhC(NBu^t)$_2$}SiCl].

When these silicon(IV) halides were reduced completely using three equivalents of KC$_8$, a base stabilised disilylene, [{PhC(NBu^t)$_2$Si}$_2$], was isolated in low yield (5 %).[47] Thereafter, in 2011 our group synthesised a high yielding Butiso (Butiso = [{4-Bu^{t}PhC(NDip)$_2$}$^-$]) ligand supported disilylene by reducing the corresponding trichloride [(Butiso)SiCl$_3$] with 1.5 equivalents of magnesium(I) dimer [{(^{Mes}Nacnac)Mg}$_2$] in almost quantitative yield (90 %) (**Scheme 3.10**).[48] Both of these disilylenes are thermally stable in the solid-state. Each silicon centre is three-coordinate and contains a lone pair of electrons. The Si-Si bond lengths in these singly bonded disilylenes are longer than the average covalent radii sum (2.20 Å). The ^{29}Si{^{1}H} NMR spectrum of [{(Butiso)Si}$_2$] shows a slightly downfield (δ = 96.9 ppm) chemical shift as compared to [{PhC(NBu^t)$_2$Si}$_2$] (δ = 75.7 ppm).

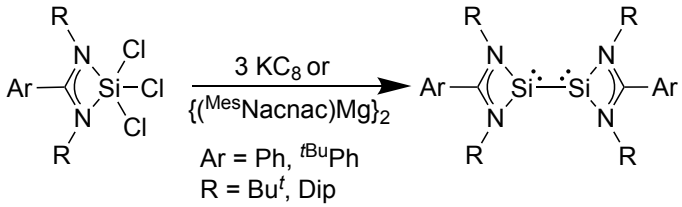

Scheme 3.10. Synthesis of the amidinate stabilised disilylene [{PhC(NBu^t)$_2$Si}$_2$] and [{(Butiso)Si}$_2$].

A noteworthy related class here is the bidentate amidinate based bis(silylene) species synthesised and developed by Driess and co-workers. In these bis(silylenes), the two amidinate ligands [PhC(NBu^t)$_2$Si] (NHSi) are connected via a bridging linker connecting the silicon centres. These complexes not only show silylene-like properties but also act as versatile three-coordinate bis(NHSi) ligands in the synthesis of coordination complexes.[49–51] The bridging linker groups can tune the distance between these two NHSi moieties. For example, a four-coordinate silicon(II) dimer was isolated in 75 % yield when the two NHSi units were brought closer using a smaller acenaphthene linker (**Scheme 3.11**). The Si-Si distance in this disilylene is 2.623(1) Å, which is much longer than in the earlier reported two coordinate disilylenes.[52] In contrast, the NHSi moieties, with larger linkers between the silicon atoms, are pointed towards each other with no bonding interactions, thereby forming a chelating "pocket" for metal coordination.[53] The general synthesis of these species involves the addition of the dilithiated linker to [{PhC(NBu^t)$_2$}SiCl], affording the chelating ligand of type [{PhC(NBu^t)$_2$Si}$_2$(linker)]. Examples of these types of ligands are shown in **Scheme 3.11**.

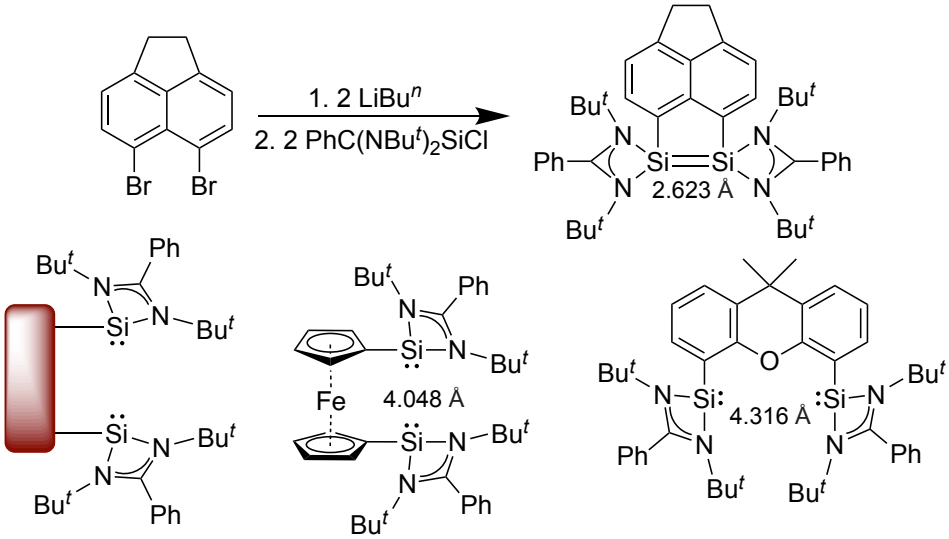

Scheme 3.11. Synthesis of silicon(II) dimer, general representation and examples of bis(NHSi) ligands.

Germanium(II) halide complexes bearing amidinate ligands are readily synthesised via the salt metathesis reactions between $GeCl_2$.dioxane and an alkali metal salt of the ligand (**Scheme 3.12**). The ligand bulk largely influences the synthesis of these complexes. In the case of less bulkier R and R' substituents (**Figure 3.1**), these ligands form L_2Ge species e.g. [{MeC(NPr^i)$_2$}$_2$Ge].[54] However, by increasing the bulk on the amidinate ligand, germanium(II) halide species are more favoured. These chlorogermylenes are monomeric in the solid-state and have bent N-Ge-Cl angles due to the presence of stereochemically active lone pair at the germanium centre. Several of these germanium(II) halide species have been reported to date.[55,56] The first amidinato germanium(I) dimer [{(Piso)Ge}$_2$] was synthesised in our group in 2006 by the reduction of [(Piso)GeCl] (Piso = [{Bu^{t}C(NDip)$_2$}$^-$]) over potassium metal in toluene.[57] This germanium(I) complex was isolated in 16 % yield and features a single bond between the two germanium centres (Ge-Ge = 2.6380(8) Å). Other germanium(I) dimers such as [{PhC(NBu^t)$_2$Ge}$_2$] and [{(Butiso)Ge}$_2$] have also been synthesised using bulky amidinate ligands and have Ge-Ge bond distances of 2.6136(9) Å and 2.569(5) Å, respectively.[58,48]

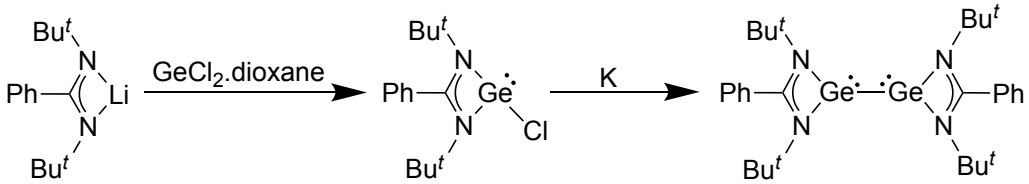

Scheme 3.12. Synthesis of first amidinate supported germanium(I) dimer.

Going down the group, there are also a number of reports detailing the synthesis of amidinato tin(II) halide complexes. These have been obtained by reacting the lithiated amidinate with $SnCl_2$ and can be isolated in moderate to good yields. The synthesised tin(II) halides with bulkier R and R' groups [{PhC(NBu^t)$_2$}SnCl], [(Butiso)SnCl], [{Bu^{t}C(NDip)$_2$}SnCl][48,59,60] are monomeric, while the complexes with Bu^n as the R' group at the backbone, [{Bu^{n}C(NDip)$_2$SnCl}$_2$] and [{Bu^{n}C(NCy)$_2$SnCl}$_2$] are asymmetric dimers in the solid-state.[60] The ^{119}Sn{^{1}H} NMR chemical shifts for the monomeric tin(II) halides were in the range of δ 28-30 ppm. To date only one amidinate stabilised low valent tin(I) dimer (36 % yield) has been reported, which was synthesised in 2011.[48] This singly bonded tin dimer [{(Butiso)Si}$_2$] was synthesised in a similar manner to the [{(Butiso)Si}$_2$] compound by reducing [(Butiso)SnCl] with 0.5 equivalents of [{(^{Mes}Nacnac)Mg}$_2$]. The ^{119}Sn{^{1}H} NMR shift was δ 777.7 ppm, which is

considerably downfield in comparison to the bidentate β-dikiteminate tin dimer [{(^{tBuMes}Nacnac)Sn}$_2$] (^{tBuMes}Nacnac = [HC{N(Mes)C(Bu^t)}$_2$]$^-$) (δ = 502.1 ppm).[61]

Meanwhile, only a few amidinato and guanidinato lead(II) chloride species have been isolated to date. They have been prepared in a similar manner as the germanium and tin halide species previously discussed. The known lead(II) halide complexes are [{(Piso)Pb(μ-Cl)}$_2$], [{(CyG)Pb(μ-Cl)}$_2$] (CyG = [Cy$_2$NC(NDip)$_2$]) and [{(HDG)Pb(μ-Cl)}$_2$] (HDG = [DipNC(NDip)$_2$]).[62] All of these crystallise as dimeric halide bridged species. The isolation of low-valent lead(I) dimer incorporating amidinate ligand is still unknown.

3.2 Research Proposal

As discussed from the literature presented in this chapter, bidentate ligands have stabilised a plethora of main group element complexes over recent years. However, the involvement of backbone bridged bulky bis(amidinates) for stabilisation of main group element complexes is comparatively limited. So far, only a few aluminium halide and alkyl complexes have been reported using bis(amidinate) ligands (Section **3.1**). Therefore expanding the chemistry of these ligands is a worthwhile goal.

The selection of bis(amidinate) ligands here is based on the accessible precursors and tuneable linkers which can provide a cooperating interaction. The amidinate fragments need to be sufficiently far from each other to avoid coordination to the same element centre. With this in mind, the synthesis of bulky bis(amidinate) ligands is expected to be accessible in a few steps and at low cost. Therefore, using rigid dibenzofurandiyl, phenylene and cyclohexylene groups as backbone bridged linkers will be attempted. The efficacy of these ligands for the stabilisation of low oxidation state group 2, 13 and 14 element halide complexes will be investigated. In the event of successful synthesis of these complexes, reduction of the LEX compounds with various reducing agents will be attempted in order to synthesise and isolate low-valent main group E-E bonded species or [{-ELE-}$_n$] type polymers.

3.3 Results and Discussion

3.3.1 Synthesis of Bulky Bidentate Bis(amidinate) Ligands

To expand the library of available dinuclear main group element complexes, two previously reported protonated ligands, namely [PhAmid$_2$H$_2$] (Ph = phenylene) (**1**) and CyAmid$_2$H$_2$ (Cy = cyclohexylene) (**2**) were chosen. These ligands were selected because **1** contains the rigid bridging linker Ph, while **2** contains the flexible linker Cy. In order to examine the effect of changing the bridging group, a new ligand system with a dibenzofurandiyl bridge and Dip substituents (on amidinate nitrogens) **3** was also proposed. The bidentate bis(amidinate) ligands **1**-**3** were synthesised from procedures in the literature (**Scheme 3.13**).[40,63,64]

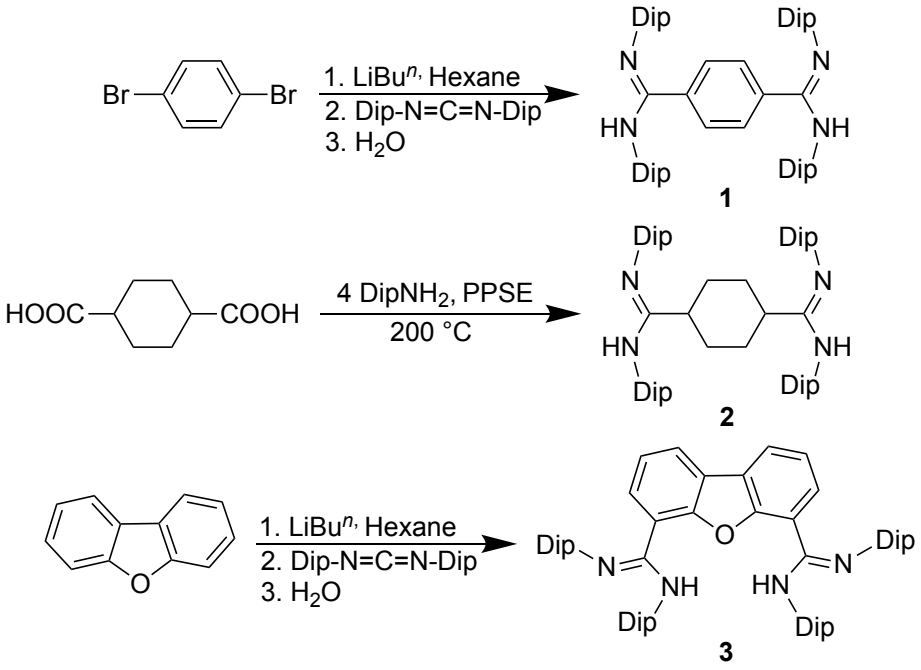

Scheme 3.13. Synthesis of pro-ligands CyAmid$_2$H$_2$ (**1**), CyAmid$_2$H$_2$ (**2**) and DBFAmid$_2$H$_2$ (**3**).

For **1** and **3**, the synthetic procedures involved the deprotonation of 1,4-dibromobenzene or dibenzofuran via addition of a slight excess of LiBu^n to give the respective 1,4-dilithiobenzene or 4,6-dilithiodibenzofuran salts followed by heating the mixtures to reflux for 12 hours in hexane. The dilithio salts were added directly to bis(2,6-diisopropylphenyl) carbodiimide to generate the corresponding lithium salts of the ligands, which were hydrolysed to afford the protonated ligands [PhAmid$_2$H$_2$] (**1**) and [DBFAmid$_2$H$_2$] (DBF = dibenzofurandiyl) (**3**). The formation of the novel pro-ligand **3** was confirmed by the ^{1}H NMR and ^{13}C{^{1}H} NMR spectroscopy. The ^{1}H NMR spectrum

exhibits two doublets for 24 isopropyl and two multiplets for 8 methine resonances. Further, NH peak appears a broad singlet at δ 7.28 ppm, which is much downfield compared to **1** and **2**. Compound **3** could be re-crystallised from toluene as yellow crystals. The molecular structure of **3** (**Figure 3.9**) shows all the bond lengths and bond angles are within the same range of previously reported amidine pro-ligands.[40,63,64]

The synthesis of **2** involved the reaction of 1,4-cyclohexanedicarboxylic acid with four equivalents of Dip aniline in the presence of *in situ* generated PPSE (polyphosphoric acid trimethylsilyl ester) at 200 °C. In this previously reported procedure, the oily reaction mixture was poured into a 1 M NaOH solution to produce a white solid. However, we slightly modified the work-up by sonicating the oily product for 2 hours with a 1 M NaOH solution, affording a white powder which was further washed with water. The solid was dissolved in hot toluene, filtered quickly, and the left-over solid residue was discarded. The pure ligand **2** was crystallised from the hot toluene filtrate in good isolated yield (81 %). These synthesised bis(amidine) pro-ligands **1**-**3** are air and moisture stable.

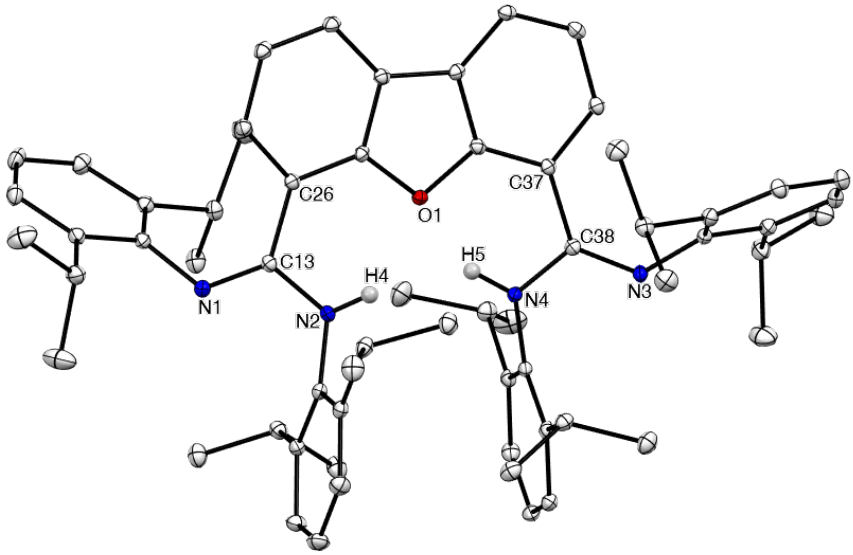

Figure 3.9. Molecular structure of [DBFAmid$_2$H$_2$] (**3**) (thermal ellipsoids shown at 20 % probability). Hydrogen atoms except H4 and H5 omitted for clarity. Selected bond lengths (Å) and angles (°): N1-C13 1.280(3) N2-C13 1.376(3) N3-C38 1.281(3) N4-C38 1.374(3) N1-C13-N2 120.1(2) N3-C38-N4 119.1(2)

3.3.2 Synthesis of Main Group Element Complexes

3.3.2.1 Bis(amidinato) Alkali Metal Salts

In order to synthesise the proposed main group element complexes, lithium, sodium and potassium bis(amidinato) salts of the ligands were prepared. All the ligands were

deprotonated via standard metalation procedures using either $LiBu^n$, NaH (with a catalytic amount of HMDS, HMDS = $HN(SiMe_3)_2$) or $KN(SiMe_3)_2$. Ligands **1**-**3** were readily deprotonated *in situ* using n-butyllithium leading to their respective dilithium bis(amidinato) salts [$PhAmid_2Li_2$] (**1.Li**), [$CyAmid_2Li_2$] (**2.Li**) and [$DBFAmid_2Li_2$] (**3.Li**), which could be subsequently used in salt elimination reactions with main group element halides. Colourless crystals of **1.Li** suitable for X-ray diffraction were grown from a 20:80 THF/hexane mixture. For comparison purposes, deprotonation of all ligands was attempted using NaH with catalytic HMDS and $KN(SiMe_3)_2$. Unfortunately, the synthesis of sodium bis(amidinato) salts were unsuccessful even after refluxing for 2 days in THF/toluene mixture. Ligands **1** and **3** were deprotonated using $KN(SiMe_3)_2$ in a THF/toluene mixture at 60 °C overnight, affording potassium bis(amidinato) salts as colourless solids, **1.K** and **3.K**. However, no NMR data for compounds **1.K** and **3.K** could be obtained, as both showed negligible solubility in typical deuterated solvents (C_6D_6 and $CDCl_3$), and thus were not used for the further salt elimination reactions (**Scheme 3.14**).

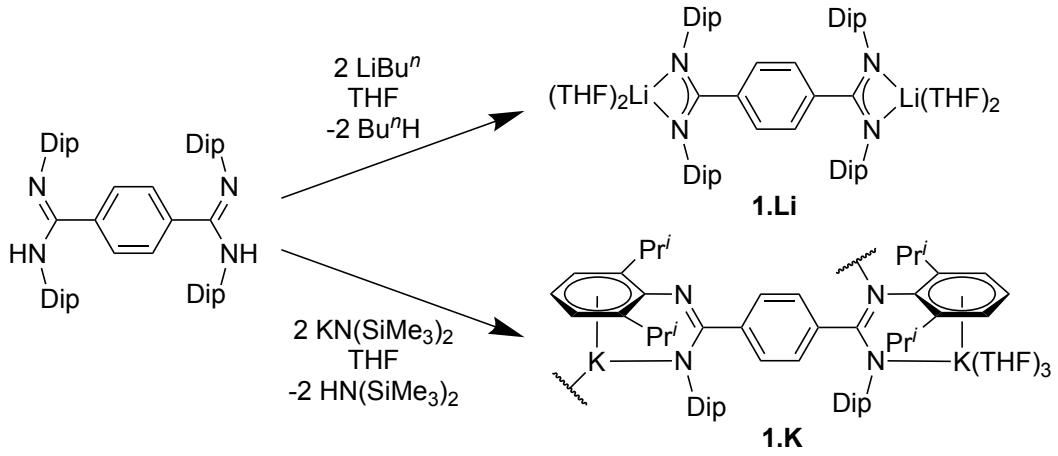

Scheme 3.14. Synthesis of bis(amidinato) alkali metal complexes **1.Li** and **1.K**.

The compounds **1.Li** and **1.K** were crystallographically characterised and the structures are depicted in **Figure 3.10**. **1.Li** is monomeric in the solid-state with both lithium centres having distorted tetrahedral geometries. Each lithium centre is *N,N'*-chelated by an amidinate fragment and coordinated by two molecules of THF, which is similar to previously reported mononuclear Dip substituted lithium(amidinate) complex.[19] In contrast, **1.K** has a polymeric structure with each potassium centre involving *N*,arene-chelation by an amidinate unit. One potassium centre K1 is further solvated by three THF molecules, while the other K2 has a dative interaction with the nitrogen centre on an

adjacent monomeric unit, thus generating a polymeric chain. (**Figure 3.11**) The different coordination modes for **1.Li** and **1.K** likely result from potassium having a greater degree of arenophilicity and a larger ionic radius, as compared to lithium. The coordination modes in **1.Li** and **1.K** are similar to earlier reported Dip substituted lithium(amidinato) and dinuclear bis(guanidinato) complexes, respectively.[65,66]

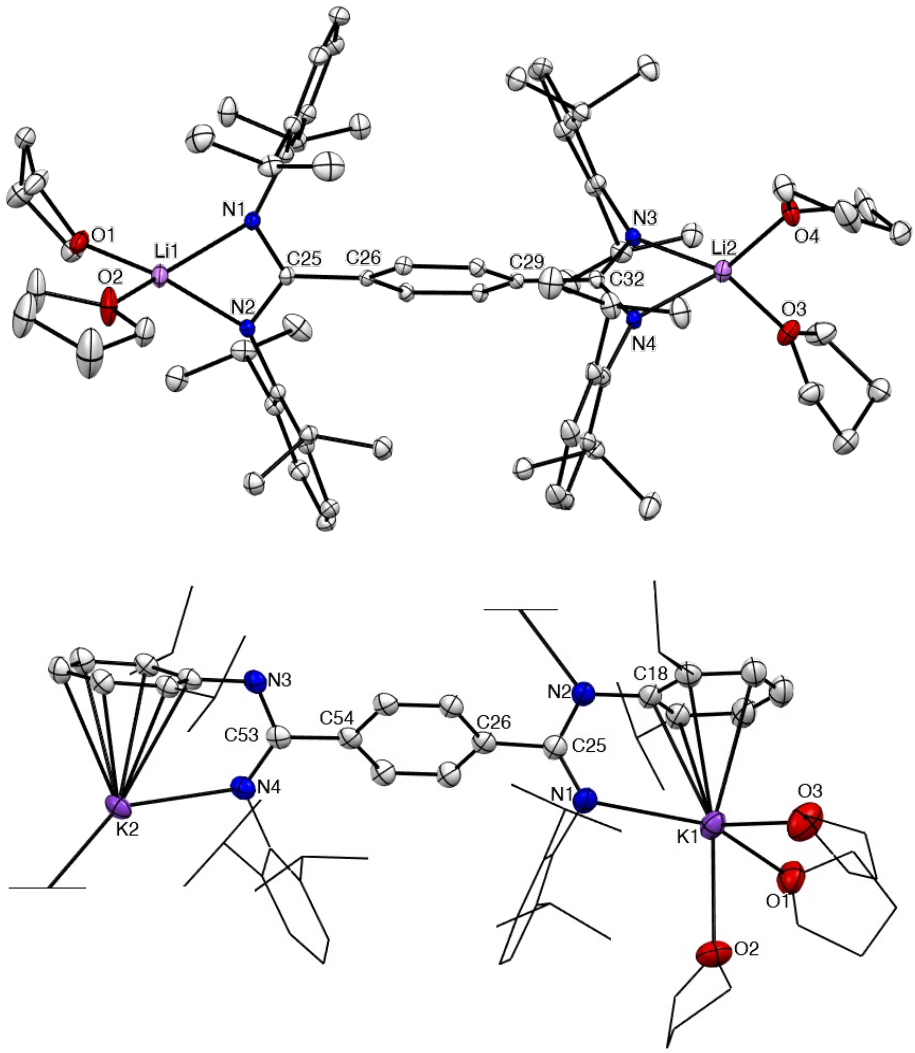

Figure 3.10. Molecular structures of [{$(THF)_2Li$}$_2$(μ-$PhAmid_2$)] (**1.Li**) and monomeric unit of [{$(THF)_3K$(μ-$PhAmid_2$)K}$_\infty$] (**1.K**) (thermal ellipsoids shown at 20 % probability). Hydrogen atoms omitted; some Dip groups and THF shown as wireframe for clarity. Selected bond lengths (Å) and angles (°) for **1.Li**: O1-Li1 1.961(5), N1-Li1 2.038(4), Li1-O2 1.970(5), Li1-N2 2.073(4), Li2-O3 1.931(4), Li2-O4 1.968(4), Li2-N3 1.995(4), Li2-N4 2.058(4), O1-Li1-O2 100.0(2), N1-Li1-N2 67.01(14), O3-Li2-O4 99.74(19), N3-Li2-N4 68.12(14). **1.K**: K1-O1 2.685(3), K1-N1 2.765(3), K1-O3 2.78(2), K1-O2 2.872(16), K2-N2 2.714(3), K2-N4 2.751(3), C25-N1-K1 130.5(2), C53-N4-K2 127.5(2), N2-K2-N4 132.78(9).

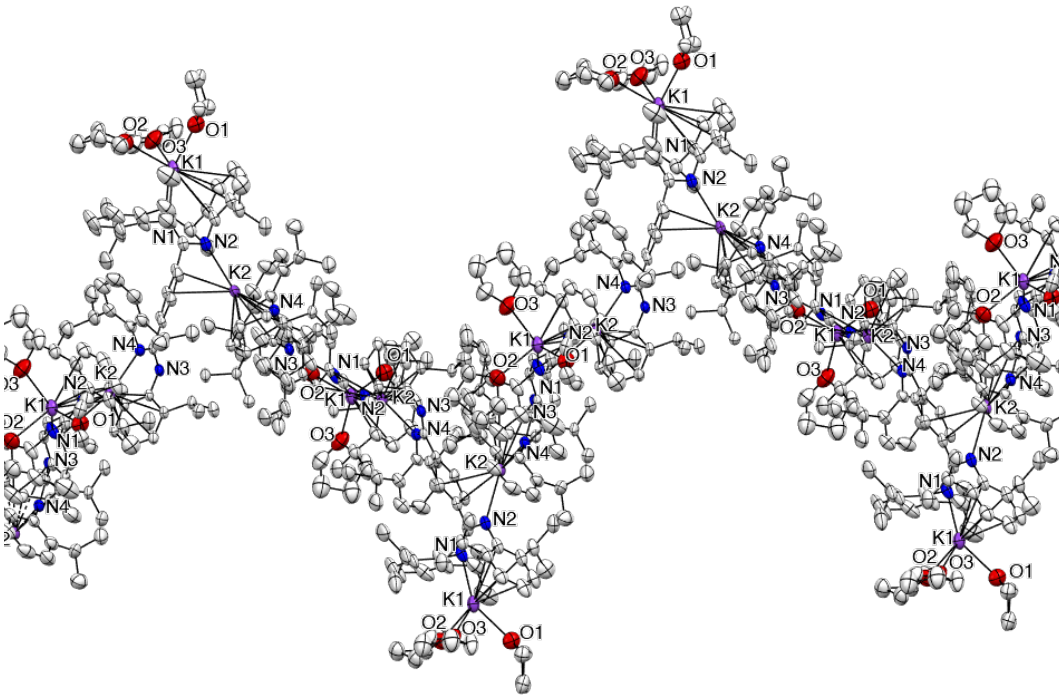

Figure 3.11. Polymeric expansion of [{(THF)$_3$K(μ-PhAmid$_2$)K}$_\infty$] (**1.K**).

3.3.2.2 Synthesis of Groups 2 and 13 Complexes

Binuclear magnesium(II) halide complexes can be synthesised via three pathways, **1**) salt metathesis reactions between alkali metal salt of the ligand and a magnesium dihalide, **2**) direct reaction of the protonated ligand with an alkyl Grignard reagent, or **3**) reaction of the protonated ligand with dialkyl magnesium reagent following the addition of iodine. In order to access bis(amidinato) magnesium(II) halide complexes, the second synthetic pathway was chosen since it had demonstrated high yields in previous reports.[67] The ligands **1**-**3** were reacted with two equivalents of a freshly prepared diethyl ether solution of the MeMgI Grignard reagent, affording the colourless complexes [(Et$_2$O)IMg(μ-PhAmid$_2$)MgI(OEt$_2$)$_2$] **4**, [{(Et$_2$O)$_2$IMg}$_2$(μ-CyAmid$_2$)] **5**, and [{(Et$_2$O)$_2$IMg}$_2$(μ-DBFAmid$_2$)] **6** in 55-70 % yields (**Scheme 3.15**). Compounds **4**-**6** are thermally stable in both the solid- and solution-states and they have been characterised by X-ray crystallography, ^{1}H and ^{13}C{^{1}H} NMR spectroscopy, elemental analysis, IR and mass spectrometry.

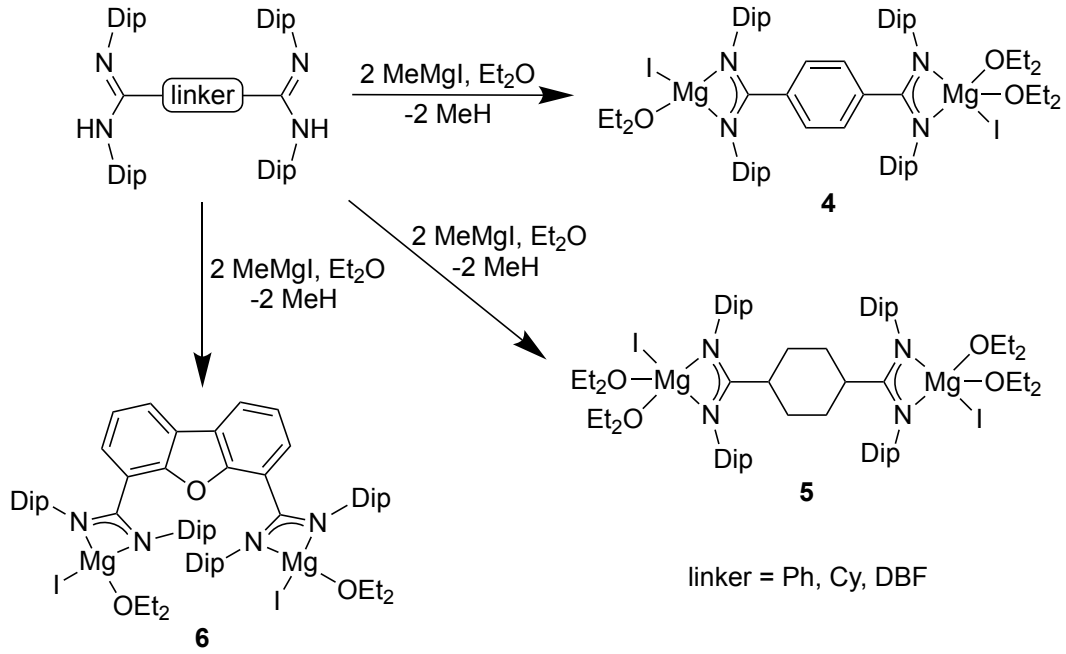

Scheme 3.15. Synthesis of bis(amidinato) magnesium complexes **4**-**6**.

Compounds **4**-**6** were crystallised from concentrated ether solutions and the crystal structures of **4**-**6** are depicted in **Figure 3.12** and **Figure 3.13**. All of the compounds are monomeric and each magnesium centre incorporates a terminal iodide ligand, as well as a *N,N'*-chelated amidinate moiety. Both magnesium centres of compound **6** are four-coordinate, display distorted tetrahedral geometries and are coordinated by one diethyl ether donor, whereas compound **5** has a five-coordinate, distorted trigonal bipyramidal geometry around the magnesium centres, encompassing two diethyl ether ligands. This difference in ether ligation is likely a result of proximal bulk around the magnesium centres due to the different bridging groups. In contrast, compound **4** has a typical four-coordinate magnesium centre Mg1 with a single diethyl ether coordination giving rise to a distorted tetrahedral geometry, and another five-coordinate Mg2 centre consisting of two diethyl ether donors, resulting in a distorted square pyramidal geometry.

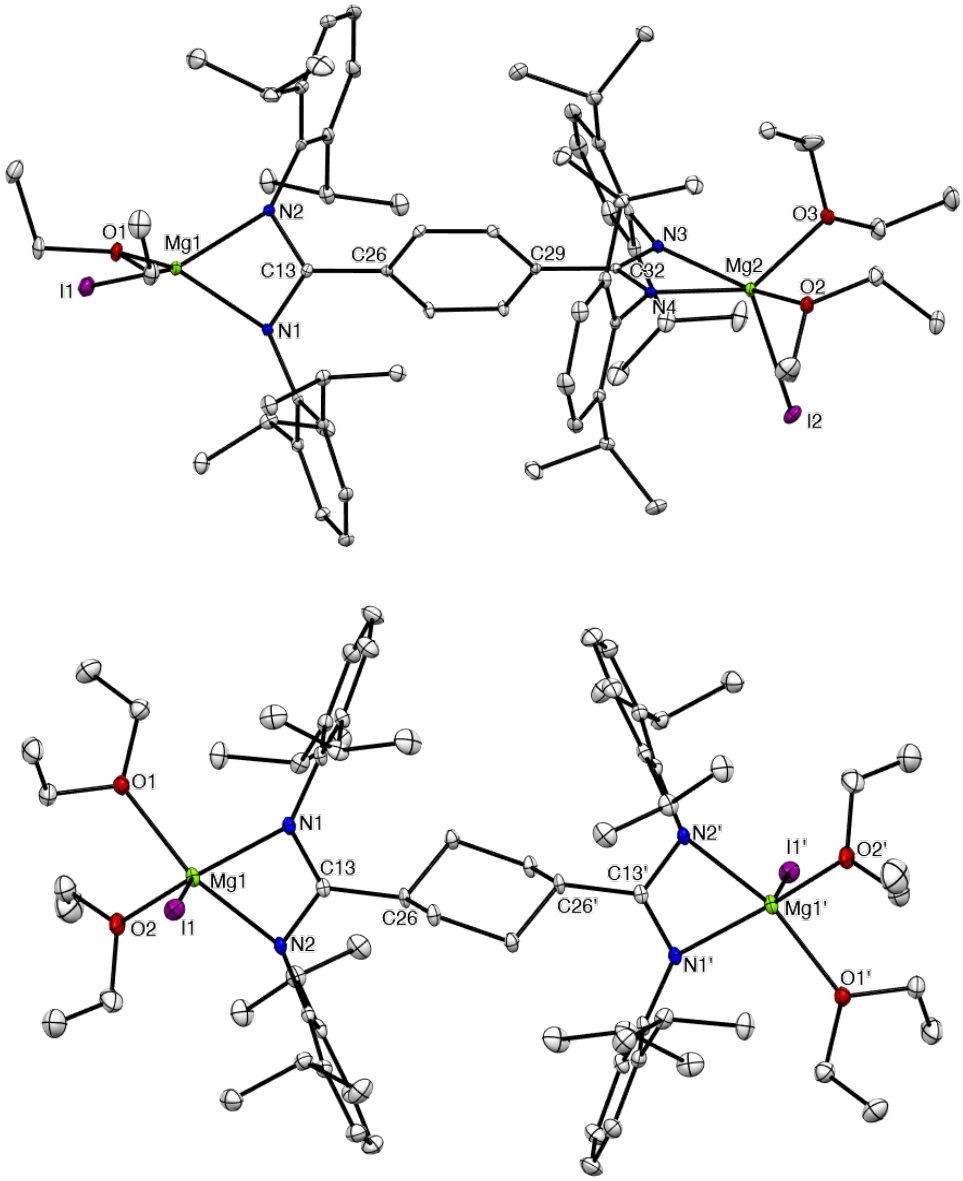

Figure 3.12. Molecular structures of [(Et_2O)IMg(μ-$PhAmid_2$)MgI(OEt_2)$_2$] (**4**) and [(Et_2O)$_2$IMg(μ-$CyAmid_2$)] (**5**) (thermal ellipsoids shown at 20 % probability). Hydrogen atoms omitted for clarity. Selected bond lengths (Å) and angles (°) for **4**: I1-Mg1 2.6441(12), Mg1-O1 2.011(2), Mg1-N2 2.063(3), Mg1-N1 2.088(3), I2-Mg2 2.7558(13), Mg2-O3 2.085(2), Mg2-N4 2.104(3), Mg2-O2 2.144(2), Mg2-N3 2.207(3), N2-Mg1-N1 65.70(10), O1-Mg1-I1 107.43(8), O3-Mg2-O2 90.01(10), N4-Mg2-N3 62.74(9), O3-Mg2-I2 103.35(8), O2-Mg2-I2 96.46(7); **5**: I1-Mg1 2.7586(12), Mg1-N1 2.076(3), Mg1-O2 2.089(3), Mg1-O1 2.156(3), Mg1-N2 2.190(3), N1-C13 1.332(5), N2-C13 1.339(5), O2-Mg1-O1 86.26(13), N1-Mg1-N2 63.29(12), O2-Mg1-I1 115.02(13), O1-Mg1-I1 93.95(9).

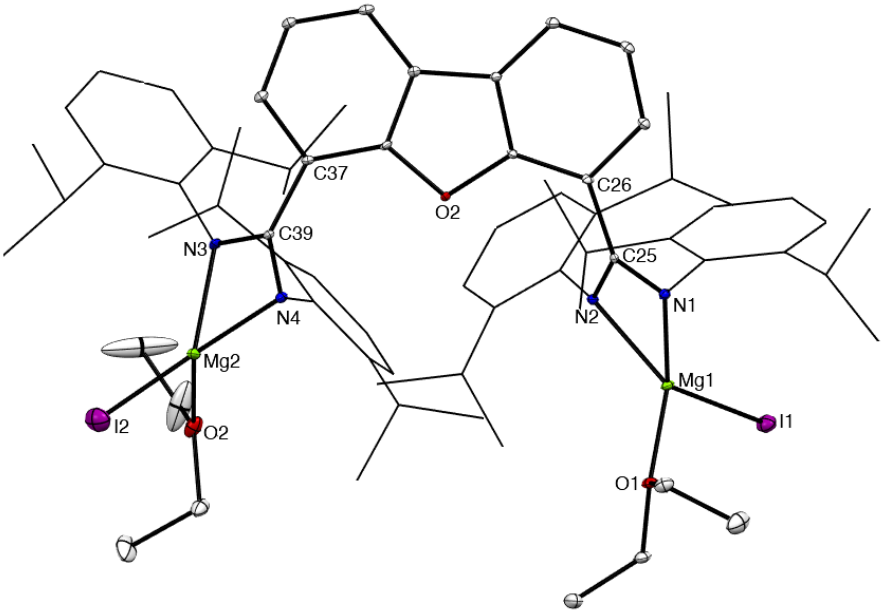

Figure 3.13. Molecular structure of [$(Et_2O)_2IMg(\mu\text{-}DBFAmid_2)$] (**6**) (thermal ellipsoids shown at 20 % probability). Hydrogen atoms omitted; Dip groups shown as wireframe for clarity. Selected bond lengths (Å) and angles (°): I1-Mg1 2.6402(16), Mg1-N1 2.079(4), Mg1-O1 2.012(4), Mg1-N2 2.076(4), N1-C25 1.345(6), N2-C25 1.337(6), N1-Mg1-N2 65.25(15), O1-Mg1-I1 103.56(11).

The bis(amidinato) aluminium iodide complex **7** was synthesised using *in situ* generated $PhAmid_2Li_2$ with AlI_3 (**Scheme 3.16**). This salt elimination reaction was carried out in toluene in order to avoid any coordination of the solvent to the aluminium centre. The molecular structure of the [$(I_2Al)_2(\mu\text{-}PhAmid_2)$] (**7**) is illustrated in **Figure 3.14**. Compound **7** is centrosymmetric and the aluminium centres are four-coordinate. Each aluminium centre possesses a distorted tetrahedral geometry with two iodide ligands and a *N,N'*-chelated amidinate unit. The ^{1}H and $^{13}C\{H\}$ NMR spectroscopic data were found to be in accordance with the solid-state structure and previously reported bis(guanidinato) aluminium complexes.[38] However, a $^{27}Al\{^{1}H\}$ NMR signal could not be observed possibly due to signal broadening caused by the quadrapolar nature of ^{27}Al (s=5/2).

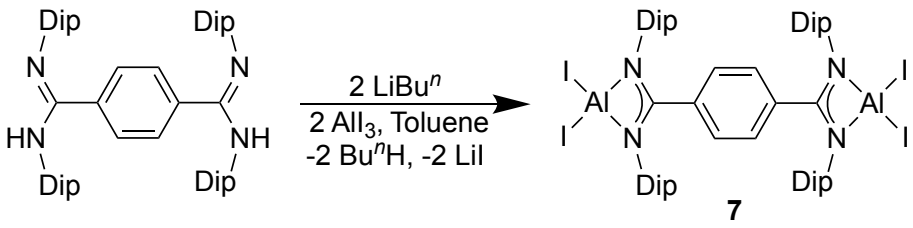

Scheme 3.16. Synthesis of bis(amidinato) aluminium complex **7**.

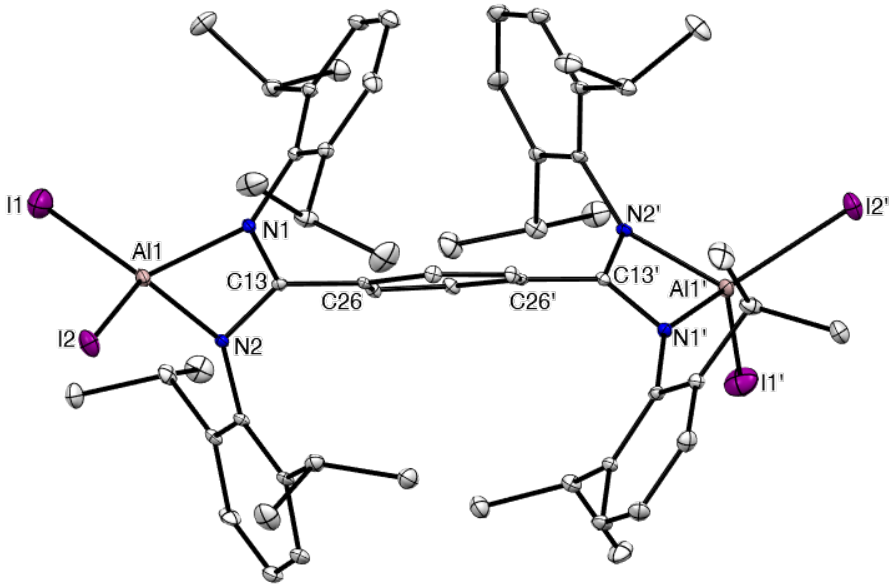

Figure 3.14. Molecular structure of [$(I_2Al)_2$(μ-$PhAmid_2$)] (**7**) (thermal ellipsoids shown at 20 % probability). Hydrogen atoms omitted for clarity. Selected bond lengths (Å) and angles (°): I1-Al1 2.433(2), Al1-N2 1.901(5), Al1-N1 1.913(5), Al1-I2 2.508(3), N2-Al1-N1 70.7(2), I1-Al1-I2 114.98(13).

3.3.2.3 Synthesis of Group 14 Element Complexes

A variety of dinuclear silicon(IV), germanium(II) and tin(II) halide compounds **8**-**14** were subsequently synthesised by salt elimination reactions. The treatment of the lithium salt of ligand **1** (**1.Li**) with two molar equivalents of appropriate silicon(IV) halides ($SiCl_4$, $SiBr_4$ and $SiHCl_3$) in diethyl ether gave complexes **8**-**10**, respectively (**Scheme 3.17**). All the compounds could be crystallised from DCM or toluene solutions upon storing at -30 °C. The $^{29}Si\{^1H\}$ NMR spectra of all compounds exihibit a strong singlet resonace in the range of five-coordinate silicon complexes.[68] In the case of compounds **8** and **10** a singlet resonance in $^{29}Si\{^1H\}$ NMR was observed at δ -70.9 and -71.3 ppm, while **9** showed an upfield signal at δ -117.4 ppm, due to presence of less electronegative bromine groups as compared to chlorine in **8** and **10**. The ^1H and $^{13}C\{^1H\}$ NMR spectra show two sets of isopropyl methyl signals and one equivalent set of methine proton resonances. This observation could be explained on the basis of the rapid interconversion of N and Cl/H/Br positions, due to fluxional behaviour involved between axial and equatorial sites.

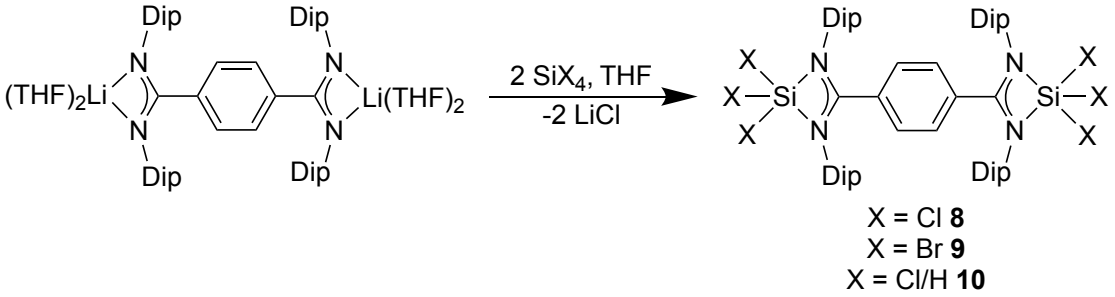

Scheme 3.17. Synthesis of bis(amidinato) silicon(IV) halide complexes **8**-**10**.

Compounds **8**-**10** were crystallographically characterised and their molecular structures are shown in **Figure 3.15** and **Figure 3.16**. Compounds **8**-**10** are monomeric and the bond angles around the silicon atoms indicate distorted trigonal pyramidal geometries. The atoms N1, Cl1/Br1 occupy axial positions, whereas N2, Cl2/Br2 and Cl3/Br3 are at equatorial positions in structures **8**-**10**, respectively. The amidinate ligand metrics indicate a partial delocalistion of the π-bond as evidenced by the backbone C-N bond lengths. Attempts to synthesise the silicon(IV) halide complexes of ligands **2** and **3** were unsuccessful, as although preliminary ^{1}H NMR spectra suggested a mixture of new species, none could be purified by crystallisation.

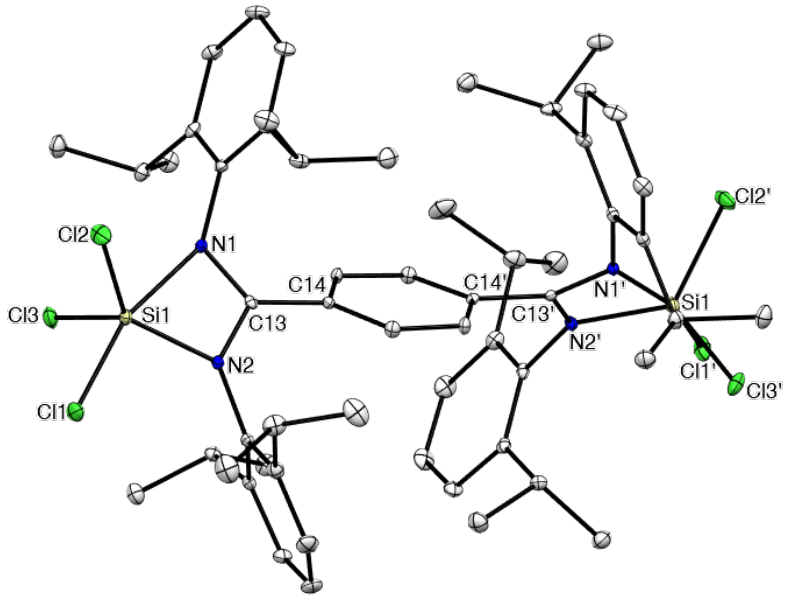

Figure 3.15. Molecular structure of [$(Cl_3Si)_2$(μ-$PhAmid_2$)] (**8**) (thermal ellipsoids shown at 20 % probability). Hydrogen atoms omitted for clarity. Selected bond lengths (Å) and angles (°): Cl1-Si1 2.1152(11), Cl2-Si1 2.0478(11), Cl3-Si1 2.0528(12), Si1-N2 1.797(2), Si1-N1 2.020(2), N2-Si1-N1 68.01(10), Cl2-Si1-Cl3 113.44(5), Cl2-Si1-Cl1 96.96(5), Cl3-Si1-Cl1 96.15(5).

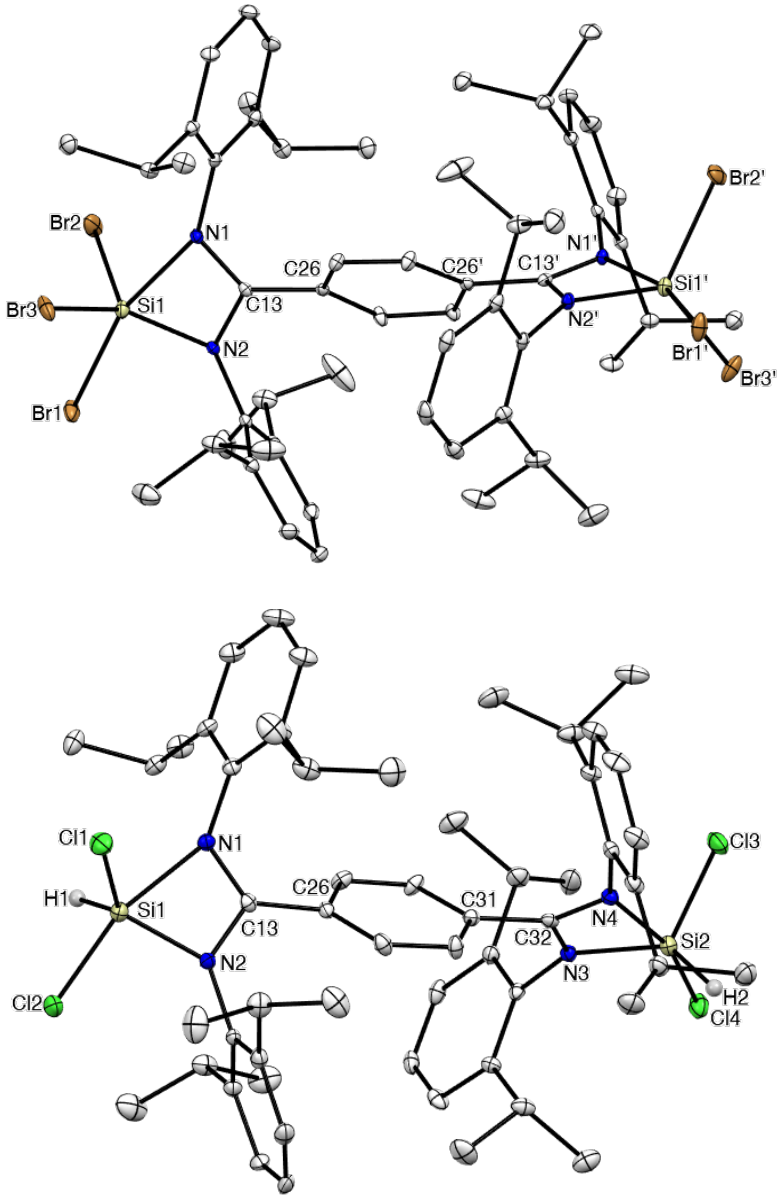

Figure 3.16. Molecular structures of [$(Br_3Si)_2$(μ-$PhAmid_2$)] (**9**) and [$(Cl_2HSi)_2$(μ-$PhAmid_2$)] (**10**) (thermal ellipsoids shown at 20 % probability). Hydrogen atoms except H1 and H2 are omitted for clarity. Selected bond lengths (Å) and angles (°) for **9**: Br1-Si1 2.2832(9), Si1-N2 1.782(3), Si1-N1 2.079(2), Si1-Br3 2.2208(9), Si1-Br2 2.223(2), N2-Si1-N1 67.66(11), Br3-Si1-Br2 113.01(9), Br3-Si1-Br1 96.28(4), Br2-Si1-Br1 98.08(6); **10**: Cl1-Si1 2.049(3), Si1-N2 1.791(7), Si1-N1 2.076(7), Si1-Cl2 2.114(3), Si1-H1 1.49(9), Si1-N3 1.784(7), Si1-Cl3 2.054(3), Si1-Cl4 2.117(3), Si1-N4 2.117(7), Si1-H2 1.42(8), N2-Si1-N1 67.1(3), N3-Si1-N4 66.7(3).

Having successfully synthesised the silicon(IV) halides, the related germanium(II), tin(II) and lead(II) complexes of the ligands **1-3** were targeted. The corresponding germanium(II) chlorides, [$(ClGe)_2$(μ-$PhAmid_2$)] **11,** [$(ClGe)_2$(μ-$CyAmid_2$)] **12**, and [$(ClGe)_2$(μ-$DBFAmid_2$)] **13**, were synthesised in fair to good isolated yields by treating **1.Li** and *in situ* generated **2.Li** and **3.Li**, with $GeCl_2$.dioxane in THF (**Scheme 3.18**). **1.Li**

and **3.Li** were also utilised in the synthesis of the [(ClSn)$_2$(μ-PhAmid$_2$)] **14,** and [(BrSn)$_2$(μ-DBFAmid$_2$)] **15** complexes. The isolation of any bis(amidinato) lead halide species were not successful, as in all the cases an insoluble product was formed upon addition of the alkali metal salts of the ligands to the lead(II) halides ($PbCl_2$ and $PbBr_2$), which could not be further identified.

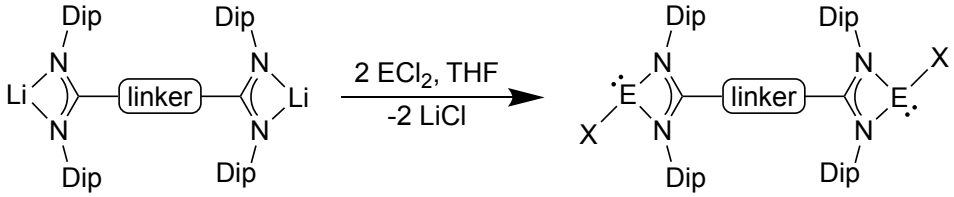

E = Ge, X = Cl, linker = Ph **11**
E = Ge, X = Cl, linker = Cy **12**
E = Ge, X = Cl, linker = DBF **13**
E = Sn, X = Cl, linker = Ph **14**
E = Sn, X = Br, linker = DBF **15**

Scheme 3.18. Synthesis of bis(amidinato) germanium(II) and tin(II) halide complexes **11**-**15**.

Complexes **11**-**15** were crystallised from concentrated toluene solutions and the molecular structures are given in **Figure 3.17** and **Figure 3.18**. The amidinate fragment is *N,N'*-chelated around the element centre and fully delocalised in **11**-**15**. These compounds are monomeric and possess a heavily distorted tetrahedral geometry around the germanium and tin centres. The amidinate moieties in compounds **11** and **14** are slightly out of the plane of their bridging phenylene group, possibily to minimise the steric strain in the systems. The central cyclohexylene group in compound **12** adopts a chair confirmation, while the dibenzofurandiyl bridge is planar in case of compounds **13** and **15**. The E-N (E = Ge, Sn) and E-Cl (Cl, Br) bond lengths are within the expected ranges and are similar to previously reported mononuclear Dip substituted group 14 amidinato germanium and tin halide complexes.[60,67] It is also worth noting that there is a decrease in the C-E-X angle from germanium to tin in these complexes, presumably due to an increase in the s-character of the lone pair on element centre, which is in agreement with the inert pair effect.

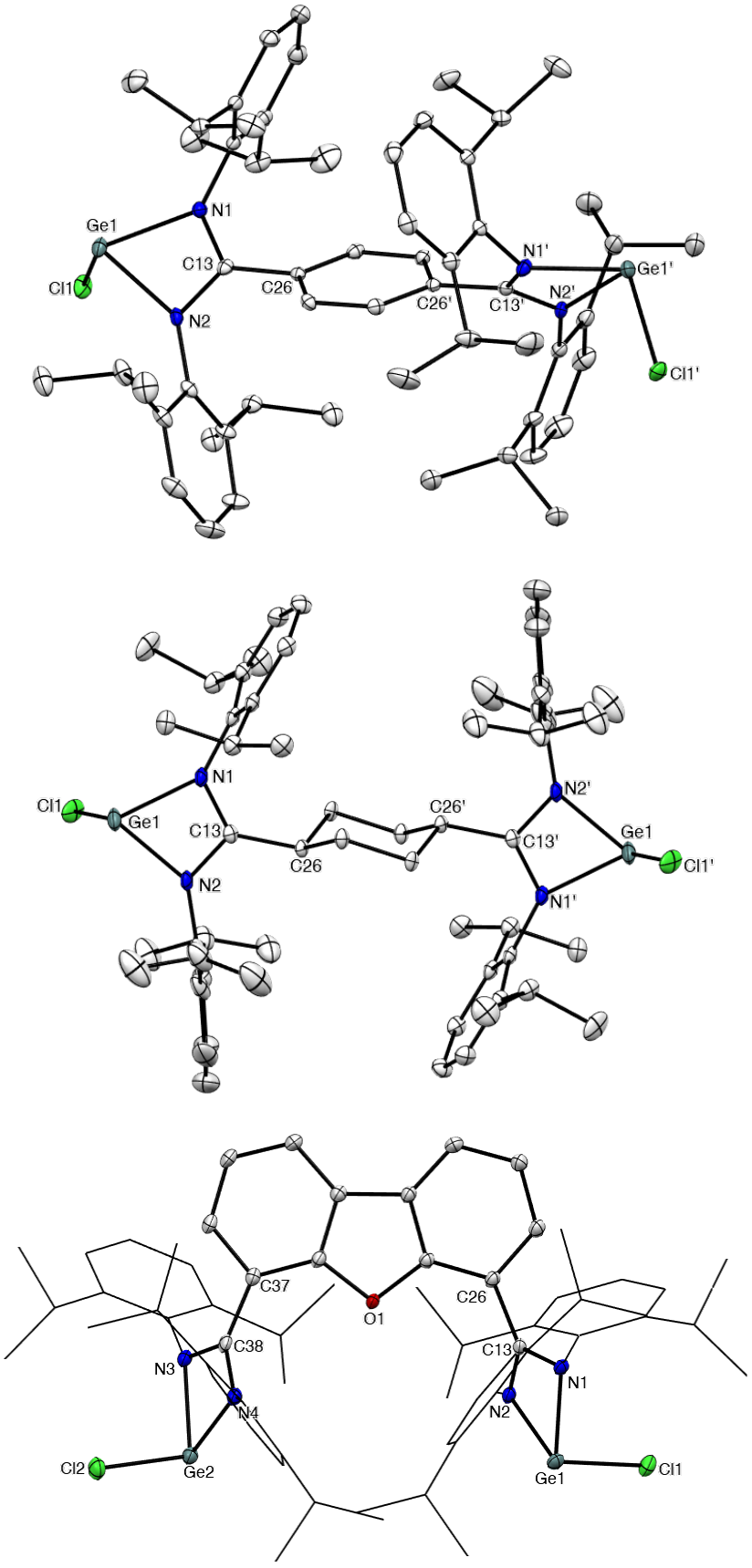

Figure 3.17. Molecular structures of [$(ClGe)_2$(μ-$PhAmid_2$)] (**11**) and [$(ClGe)_2$(μ-$CyAmid_2$)] (**12**) [$(ClGe)_2$(μ-$DBFAmid_2$)] (**13**) (thermal ellipsoids shown at 20 % probability). Hydrogen atoms

omitted; some Dip groups shown as wireframe for clarity. Selected bond lengths (Å) and angles (°) are given in **Table 3.1**.

Table 3.1. Bond distances (Å) and angles (°) for compounds **11**-**13**. The corresponding molecular structure for these compounds can be found in **Figure 3.17**.

	11	**12**	**13**
Ge1-N1	2.042(4)	2.042(4)	2.036(3)
Ge1-N2	2.032(4)	2.032(4)	2.028(3)
Ge1-Cl1	2.2151(16)	2.267(2)	2.2431(11)
N2-Ge1-N1	65.37(16)	64.65(16)	65.10(13)
N2-Ge1-Cl1	96.41(12)	96.34(13)	95.93(9)
N1-Ge1-Cl1	98.95(13)	98.76(13)	99.40(9)

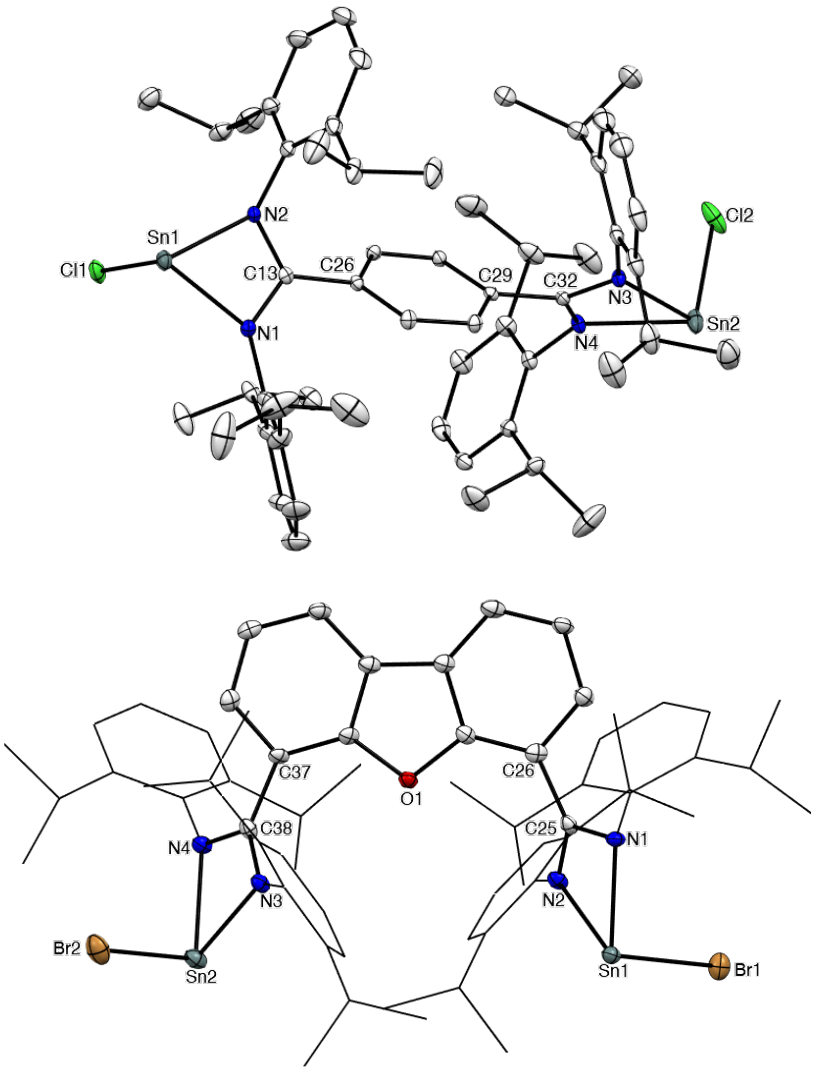

Figure 3.18. Molecular structures of $[(ClSn)_2(\mu\text{-}PhAmid_2)]$ (**14**) and $[(BrSn)_2(\mu\text{-}DBFAmid_2)]$ (**15**) (thermal ellipsoids shown at 20 % probability). Hydrogen atoms omitted; some Dip groups shown as wireframe for clarity. Selected bond lengths (Å) and angles (°) for **14**: Sn1-N1 2.219(3),

Sn1-N2 2.266(3), Sn1-Cl1 2.4578(18), N1-Sn1-N2 59.34(12), N1-Sn1-Cl1 91.84(10), N2-Sn1-Cl1 89.91(10); **15**: Sn1-N1 2.216(4), Sn1-N2 2.271(3), Sn1-Br1 2.6187(7), N1-Sn1-N2 59.27(17), N1-Sn1-Br1 97.84(12), N2-Sn1-Br1 90.30(12).

The spectroscopic data for these complexes is consistent with their solid-state structures. The ^{1}H NMR spectra of these complexes show four sets of doublets for isopropyl and two sets of septets for methine resonances. The ^{119}Sn{^{1}H} NMR spectra could not be obtained in case of **14** and **15** due to low solubility of these complexes in C_6D_6.

3.3.3 Reduction Attempts

3.3.3.1 Attempted Reductions of Group 2 and 13 Element Halide Complexes

Having synthesised a series of group 2 and 13 halide complexes (**4**-**7**), the reduction of these complexes was pursued to hopefully form low oxidation state Mg(I)-Mg(I) bonded polymers, or a dinuclear aluminium(I) compound. A number of different reducing agents were attempted for this purpose including Na metal, K metal, [{(^{Mes}Nacnac)Mg}$_2$], 5% w/w Na/NaCl and KC_8, but these were unsuccessful and in majority of the cases resulted in either free ligand or intractable product mixtures (**Scheme 3.19**).

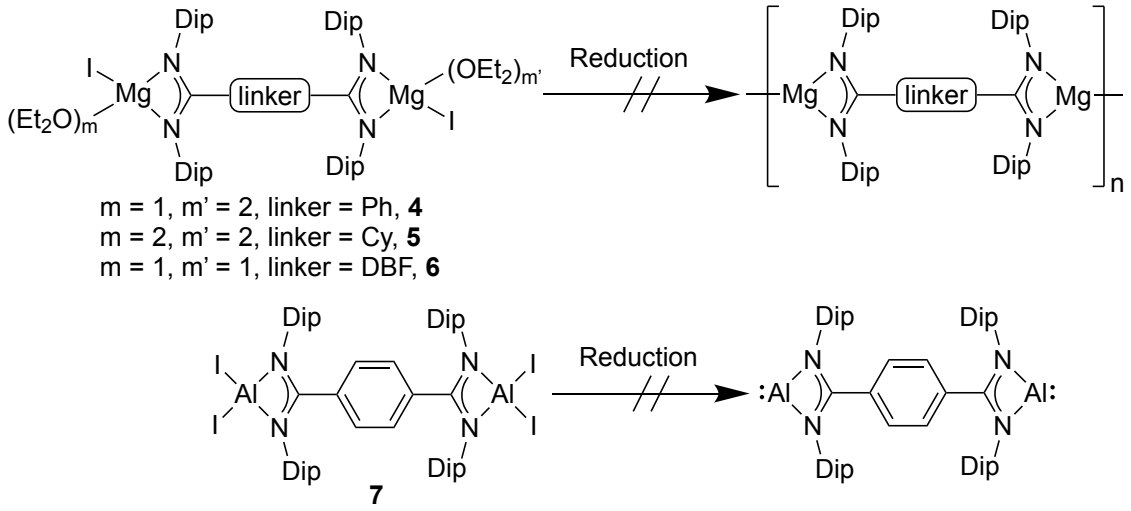

Scheme 3.19. Attempted reductions of bis(amidinato) magnesium and aluminium halides **4**-**7**.

Reactions of **4**-**7** with [{(^{Mes}Nacnac)Mg}$_2$] were the most promising, but X-ray quality crystals to ascertain the connectivity of the products could not be obtained, even after multiple attempts. The product of the reduction of compound **4** precipitated out as a yellow coloured solid, while reduction of compounds **5** and **6** gave off white, highly air sensitive products. No meaningful solution-state data could be obtained for these

compounds as they showed negligible solubility in organic solvents such as hexane, toluene and THF. The reduction of **7** led to a mixture of products of which none could be identified.

3.3.3.2 Reductions of Group 14 Element Halide Complexes

A key target of this study was the reduction of group 14 silicon(IV) halides such as compounds **8**-**10**, in order to generate the silicon(II) halosilylene analogues or low oxidation state silicon polymer species, e.g. [{-Si(NDip)$_2$C(C$_6$H$_4$)C(NDip)$_2$Si-}$_\infty$]. Attempts to reduce **8**-**10** using the reducing agents mentioned in section **3.3.3.1** resulted in green coloured solutions which later turned yellow upon attempted crystallisation. From these only crystals of the free ligands were isolated. The reduction of **8** with excess potassium in THF led to a darker green solution which changed to brown after 5 hours and only the polymeric potassium bis(amidinato) salt [{{(THF)K}$_2$(μ-PhAmid$_2$)}$_\infty$] **16** was recovered **(Scheme 3.20)**. Complex **16** was crystallised by slow vapour diffusion of hexane into a THF solution of the reaction mixture (**Figure 3.19)**. However, spectroscopic data for **16** could not be obtained due to its negligible solubility after crystallisation. Each potassium centre is coordinated by one THF and possesses a η^3-arene interaction with the amidinate moiety. The structure polymerises via this η^3-interaction of the Ar unit with other K1 metal centre (**Figure 3.20**).

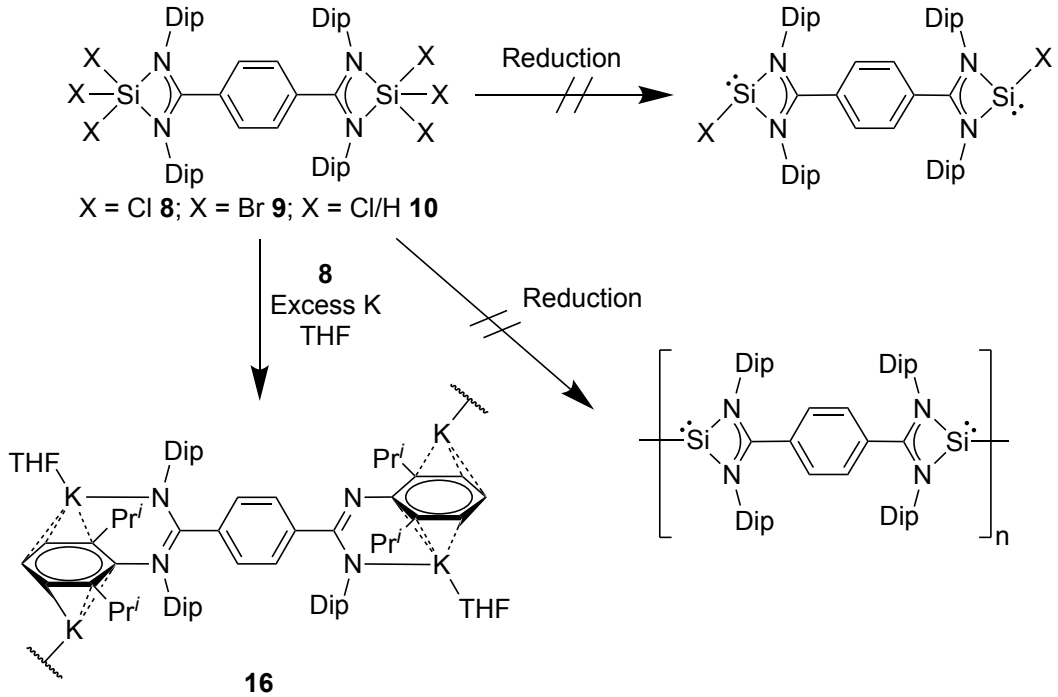

Scheme 3.20. Attempted reductions of silicon(IV) halides **8**-**10**.

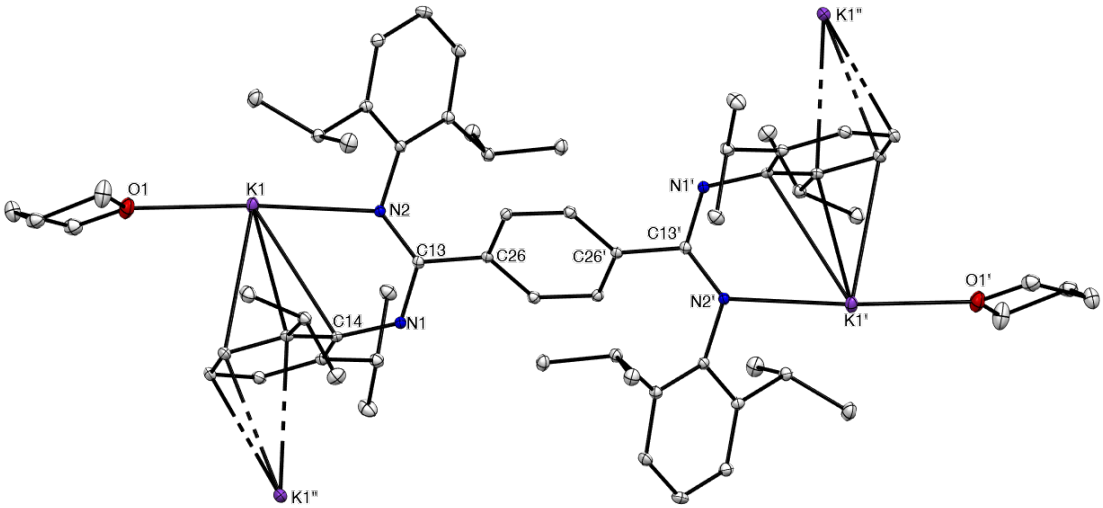

Figure 3.19. Molecular structure of monomeric unit of [{{(THF)K}$_2$(μ-PhAmid$_2$)}$_\infty$] (**16**) (thermal ellipsoids shown at 20 % probability). Hydrogen atoms omitted for clarity. Selected bond lengths (Å) and angles (°) for **16**: K1-O1 2.7270(15), K1-N2 2.8056(15), K1-C14 3.2860(17), N2-C13 1.334(2), N1-C13 1.322(2), O1-K1-N2 143.03(4), C13-N2-K1 129.97(10).

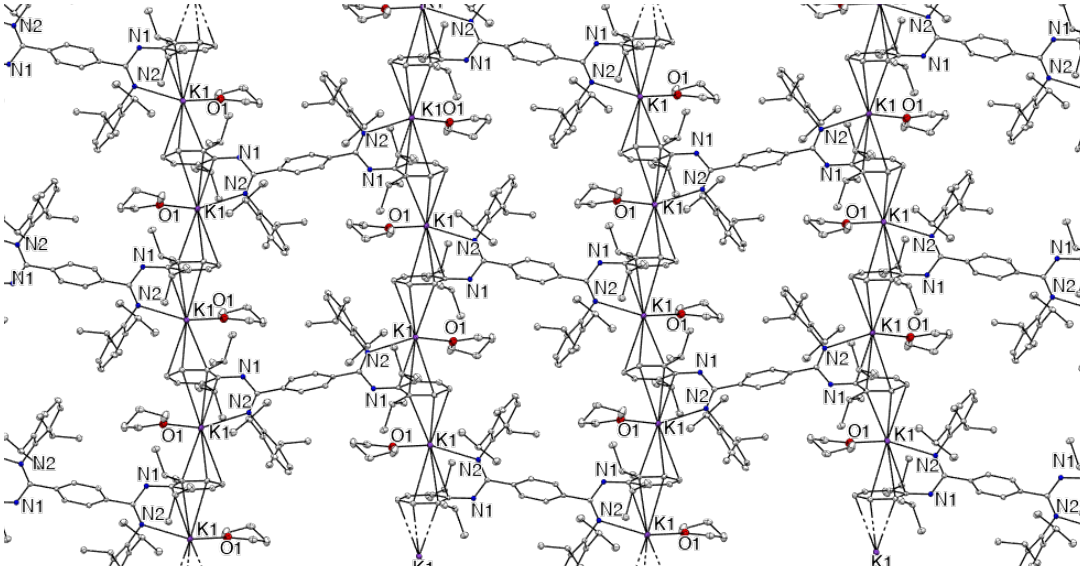

Figure 3.20. Polymeric expansion of [{{(THF)K}$_2$(μ-PhAmid$_2$)}$_\infty$] **16**.

In the past, bases such as LiN(SiMe$_3$)$_2$, KN(SiMe$_3$)$_2$ and N-hetrocyclic carbenes (NHCs) have been used for the reduction of mononuclear amidinato silicon hydride/chloride compounds which have led to amidinato silicon(I) and (II) species (section **3.1.3.2**). Using this approach, a toluene solution of **10** was reacted with LiN(SiMe$_3$)$_2$ or KN(SiMe$_3$)$_2$ which resulted in dark green coloured solutions. However, the isolation of any compound from these solutions could not be achieved. When a hot toluene solution of **9** was added to the respective toluene solution of NHCs [:C(RNCMe)] (R = Me (TMC) or Pr^i (IPrIMe)), an instantaneous colour change from a colorless solution to a green

solution was observed, which turned to dark red after stirring for 10 minutes (**Scheme 3.21**). The reaction mixtures were filtered and crystals of the single dehydrochlorinated, NHC coordinated, cyclohexa-2,5-diene-1,4-diylidene bridged, bis(diamido) silicon(IV) products **17** and **18** were unexpectedly isolated. Both compounds crystallised as deep red coloured solids from toluene in 20 % yields. Attempts to perform a double dehydrohalogenation of **10** did not occur even after using excess NHCs.

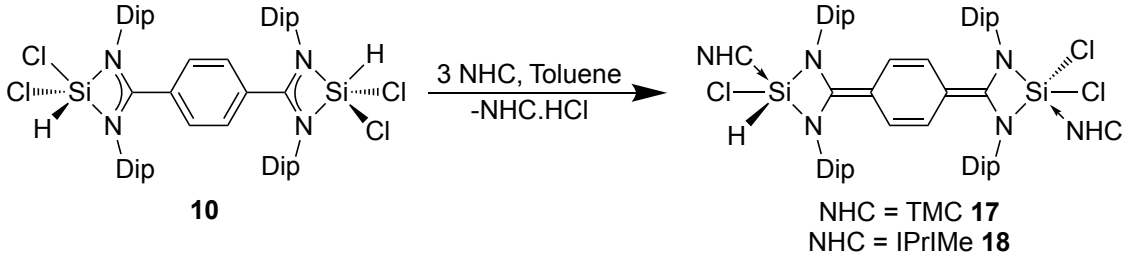

Scheme 3.21. Synthesis of bis(diamido) silicon(IV) complexes **17** and **18**.

The mechanism of the formation of **17** and **18** is not very clear, however, one can speculate that they involve an initial dehydrochlorination at one silicon centre, generating a chlorosilylene fragment. This could be followed by electronic rearrangement of the bridging phenylene ligand, intra- or intermolecular migration of a chloride or hydride ligand to the dehydrochlorinated silicon center, and finally NHC coordination of both bis(amido) silicon units. Whatever the case, we are unaware of any similar chemistry occurring for mononuclear amidinato silicon species. With that said, tetra-valent diamido silicon compounds have previously been generated via hydroelementation of amidinato silylenes.[46]

Only limited spectroscopic data could be obtained for compound **17** and **18**. Once they crystallised, **17** showed very low solubility in non-coordinating solvents such as benzene and toluene, while **18** is insoluble. Furthermore, the use of coordinating solvents such as THF led to decomposition of both the compounds to give protonated ligands. The ^{1}H NMR spectroscopic data for **17** in C_6D_6 were consistent with its solid-state structure. However, it exhibits three sets of non-overlapping and five sets of overlapping doublet resonances for the isopropyl methyl substituents and two overlapping and two non-overlapping multiplet methine resonances. A singlet signal for the hydride (Si-*H*) at δ 6.71 ppm was also observed, which is close to the reported silyl-silylene compound (cf. [PhC(NBu^t)Si-Si(H)(NBu^t)CPh], δ = 6.70 ppm).[69] The Si-H stretch of **17** and **18** was also confirmed by solid-state infrared spectra, which exhibit Si-H stretching bands at

wavenumbers (ν = 2105 cm^{-1} and 2118 cm^{-1} respectively) comparable to those recorded for related amidinato silicon(IV) hydride/chlorides (e.g. ν = 2160 cm^{-1} for [(Amid)SiHClMe];[70] 2190 cm^{-1} for **10**).

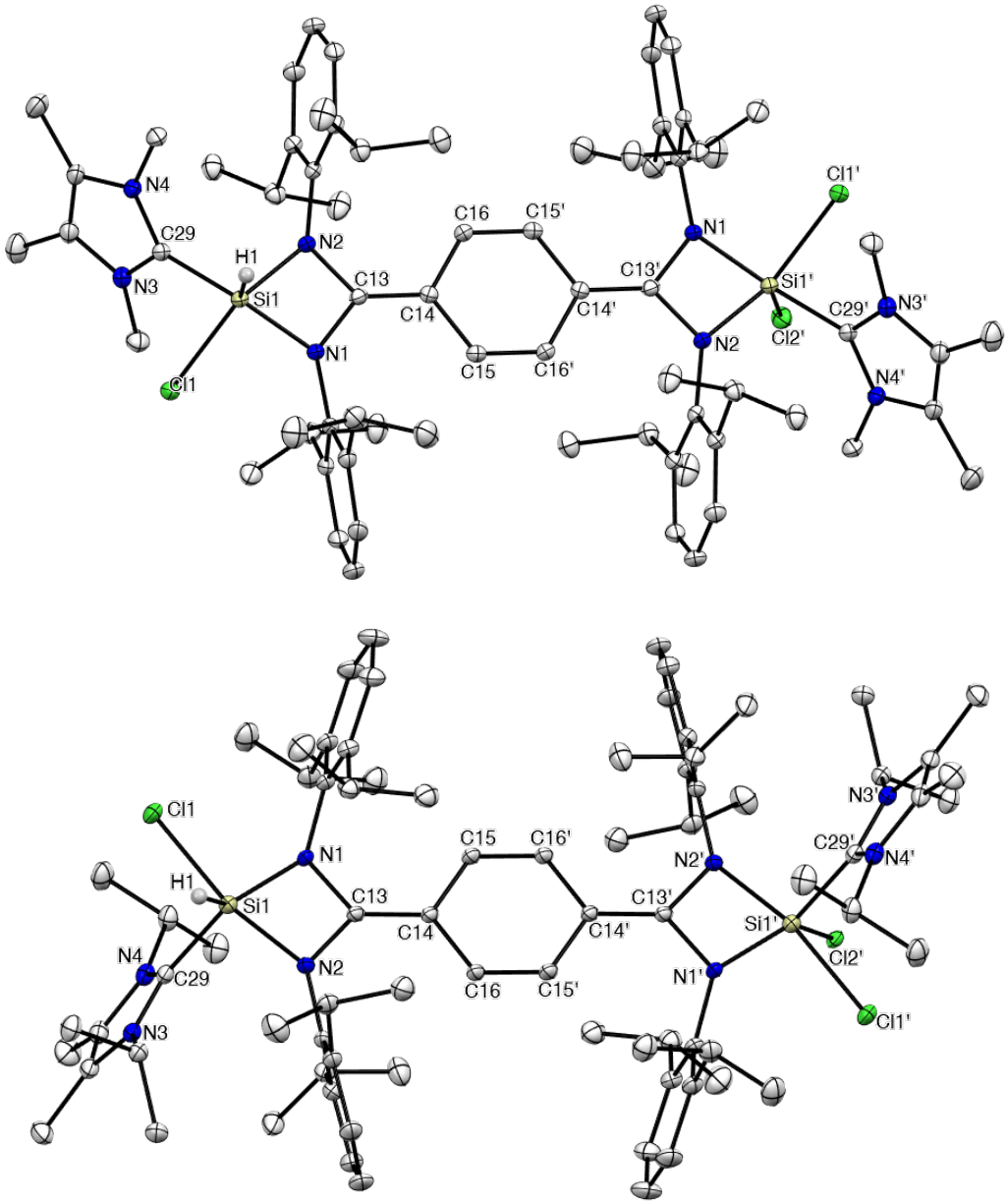

Figure 3.21. Molecular structures of **17** and **18** (thermal ellipsoids shown at 20 % probability). Hydrogen atoms except H1 omitted for clarity. Selected bond lengths (Å) and angles (°) for **17**: Cl1-Si1 2.2124(15), Si1-N1 1.772(3), Si1-N2 1.809(4), Si1-C29 1.970(4), Si1'-Cl2' 2.123(3), Si1-H1 1.476(8), N1-C13 1.410(5), N2-C13 1.399(5), C13-C14 1.370(6), C14-C16 1.452(6), C14-C15 1.458(6), C15-C16' 1.349(6), N1-Si1-N2 72.41(15), C29-Si1-Cl2 103.61(15), N1-Si1-H1 103(3), N2-Si1-H1 99(3); **18**: Cl1-Si1 2.2432(8), Si1-N1 1.7596(19), Si1-N2 1.8289(19), Si1-C29 1.954(2), Si1'-Cl2' 2.1369(11), Si1-H1 1.489(8), N1-Si1-N2 73.28(8), N1-Si1-C29 129.66(10), N2-Si1-C29 97.26(9), Cl2'-Si1'-Cl1' 83.84(4), C29-Si1-H1 107(3), Cl1-Si1-H1 86(3).

The molecular structures of compounds **17** and **18** are depicted in **Figure 3.21**. The crystal structures of compounds **17** and **18** are centrosymmetric, which requires the hydride ligand, H1, and the chloride, Cl2, to be disordered over one site with a 50 % occupancy of each. The silicon centres have a distorted square based pyramidal geometry, with H1 or Cl2 in the apical positions. All Si1 bonds lie in the normal ranges for similar, previously reported bonds.[71] The linker bridging both silicon centres give bond lengths which suggests the connectivity as two diamide moieties bridged by a cyclohexa-2,5-diene-1,4-diylidene unit. The C13-C14 and C15'/C15-C16/C16' distances in **17** and **18** are suggestive of double bonds, whilst the two C13-N bond lengths are closer to single bonding interactions. It should be noted however, that the tricyclic core of the molecule, viz. $[Si(DipN)_2C(C_6H_4)C(NDip)_2Si]$, is close to planar, and thus a degree of π-conjugation over this core can be expected.

The reduction of complexes **11-15** with a range of reducing agents mentioned in section **3.3.3.1** resulted in unidentifiable products. The reduction of **11** and **13** gave intense violet and dark pink coloured solutions, respectively, which were highly air and moisture sensitive. Multinuclear NMR studies did not show any peaks for the corresponding starting material, suggesting that all of the starting metal complexes **11-13** were consumed. Efforts to obtain crystals for X-ray diffraction were unsucessful as the compounds decompose after removal of the solvent under vacuum. Furthermore, it is worth mentioning that the reduction of compound **12** with $[\{(^{Mes}Nacnac)Mg\}_2]$ afforded a pink coloured solid that was insoluble and highly air and moisture sensitive. This compound was insoluble in all coordinating and non-coordinating solvents. A MALDI-TOF mass spectroscopic analysis of the material gave little evidence of a potential Ge-Ge bonded species as a small m/z peak at 1908.68 was observed (which is the equivalent to two monomeric units). However, no further evidence of Ge-Ge bonded germanium(I) polymers, $[\{\text{-}Ge(DipN)_2C(C_6H_{10})C(NDip)_2Ge\text{-}\}_\infty]$ could be obtained due to the negligible solubility of the pink species in the matrix and the air sensitive nature of the compound. With that said, when toluene suspensions of the pink coloured material were treated with the mild chlorinating agent, C_2Cl_6, the insoluble material was consumed, and compound **12** was regenerated with the complete consumption of the insoluble material. This does provide some evidence of amidinato germanium(I) products within the pink solid (**Scheme 3.22**).

E = Ge, X = Cl, linker = Ph **11**, DBF **13**
E = Sn, X = Cl, linker = Ph **14**
E = Sn, X = Br, linker = DBF **15**

Scheme 3.22. Attempted reductions of bis(amidinato) germanium(II) and tin(II) halides **11**-**15**.

3.4 Conclusion

To summarise, a novel bis(amidinato) ligand **3** was successfully synthesised to understand the effect of the bridging linker on the main group element complexes. The previously reported ligands **1** and **2** along with the novel ligand **3** were proposed to develop the coordination chemistry of bis(amidinato) main group systems and low oxidation state main group element polymers. The alkali metal salts of previously reported ligands were crystallographically characterised. Furthermore, the ligands and their alkali metal salts were successfully employed in the synthesis of novel bis(amidinato) magnesium(II), aluminum(III), silicon(IV), germanium(II) and tin(II) halide complexes (**4**-**15**). All of the bis(amidinato) element halide complexes have been treated with a range of s-block metal reducing agents or NHCs, in the hope of obtaining dinuclear or polymeric bis(amidinato) metal systems. Unfortunately, the reduction products using s-block metals could not be isolated. However, in case of NHCs, two cyclohexa-2,5-diene-1,4-diylidene bridged bis(diamido) silicon(IV) compounds could be obtained, the metalloid centres of which are coordinated by an NHC, a hydride and/or chloride ligands. From the reduction of compound **12** with [{(^{Mes}Nacnac)Mg}$_2$], some evidence for Ge^{I}-Ge^{I} bonded species was found, although the exact nature of the Ge^{I}-Ge^{I} bonded species could not be concluded. Furthermore, it might be possible for this compound to have some interesting reactivity towards small molecules which can prove the formation of Ge^{I}-Ge^{I} bonded species.

3.5 Experimental

[DBFAmid$_2$H$_2$] (3). LiBu^n (26.8 mL, 42.81 mmol, 1.6 M solution in hexane) was added to a solution of dibenzofuran (3.00 g, 17.84 mmol) in hexane (20 mL) and TMEDA (6.4 mL, 42.81 mmol). The suspension was stirred under reflux for 3 hours. Bis(2,6-

diisopropylphenyl) carbodiimide (13.90 g, 38.35 mmol) in hexane (20 mL) was added to the reaction mixture and stirred overnight at room temperature. The suspension was hydrolysed using water (40 mL) and stirred for 30 minutes at room temperature. The precipitate was filtered, washed with water and hexane, and dried under vacuum at 70 °C for 2 hours, giving pure $DBFAmid_2H_2$ as yellow powder. Single crystals suitable for X-ray diffraction were obtained from toluene at room temperature (8.20 g, 51.5 %). M.p. > 260 °C; ^{1}H NMR (400 MHz, C_6D_6, 298 K) δ = 0.80 (d, $^3J_{HH}$ = 6.8 Hz, 12H, CH(C*H*$_3$)$_2$), 0.90 (br, 12H, CH(C*H*$_3$)$_2$), 1.03 (d, $^3J_{HH}$ = 6.7 Hz, 12H, CH(C*H*$_3$)$_2$), 1.17 (br, 12H, CH(C*H*$_3$)$_2$), 3.12 (br, 4H, C*H*(CH$_3$)$_2$), 3.40 (br, 4H, C*H*(CH$_3$)$_2$), 6.59 (t, $^3J_{HH}$ = 7.7 Hz, 12H, Ar-*H*), 6.97-7.09 (m, 14H, Ar-*H*), 7.23 (d, $^3J_{HH}$ = 7.7 Hz, 2H, Ar-*H*), 7.39 (br, 2H, Ar-*H*); ^{13}C{^{1}H} NMR (101 MHz, C_6D_6, 298 K) δ = 22.9, 23.7, 24.2 (CH(*C*H$_3$)$_2$), 28.9, 29.7 (*C*H(CH$_3$)$_2$), 118.3, 122.3, 122.8, 123.6, 123.8, 123.9, 125.4, 127.7, 129.7, 135.3, 137.7, 145.3, 145.9, 147.7 (Ar-*C*), 152.8 (N*C*N); IR ν/cm^{-1} (ATR): 3458 (m, NH), 3057 (w), 2962 (m), 2967 (m), 1643 (vs), 1586 (s), 1502 (vs), 1468 (vs), 1422 (vs), 1401 (s), 1382 (m), 1359 (m), 1329 (m), 1229 (vs), 1254 (w), 1222 (m), 1202 (m), 1174 (vs), 1133 (m), 1101 (m), 1083 (m), 1059 (m), 935 (m), 852 (m), 791 (vs), 758 (vs), 684 (m); acc. mass calc. for $C_{62}H_{77}N_4O$ (MH^+): 893.6097; found: 893.6190.

[{(THF)$_2$Li}$_2$(μ-PhAmid$_2$)] (1.Li). LiBu^n (1.6 mL, 2.56 mmol, 1.6 M solution in hexane) was added to a solution of $PhAmid_2H_2$ (1.0 g, 1.25 mmol) in THF (30 mL) at -80 °C. The resultant solution was warmed to room temperature and stirred for 4 hours. All volatiles were removed *in vacuo* and the residue was washed with ca. 20 mL of hexane to yield **1.Li** as an off-white powder. X-ray quality crystals were grown by layering a THF solution of product with hexane (1.10 g, 80 %). M.p. 200-206 °C (decomp.); ^{1}H NMR (400 MHz, C_6D_6, 298 K) δ = 0.85-1.21 (br m, 48H, CH(C*H*$_3$)$_2$), 1.33 (br, 16H, OCH$_2$C*H*$_2$), 3.24-3.48 (br, 4H, 16H, C*H*(CH$_3$)$_2$, OCH$_2$C*H*$_2$), 3.70 (br, 4H, C*H*(CH$_3$)$_2$), 6.86-7.58 (br s, 16H, Ar-*H*); ^{13}C{^{1}H} NMR (101 MHz, C_6D_6, 298 K) δ = 23.2, 23.5, 25.5, 25.7 (CH(*C*H$_3$)$_2$), 25.9 (OCH$_2$*C*H$_2$), 28.1, 28.2 (*C*H(CH$_3$)$_2$), 67.9 (O*C*H$_2$CH$_2$), 120.9, 121.1, 122.9, 123.0, 141.0, 141.4 (Ar-*C*), 148.7 (N*C*N); ^{7}Li NMR (155 MHz, C_6D_6, 298 K) δ = 1.7; IR ν/cm^{-1} (Nujol): 1619 (vs), 1586 (s), 1563 (w), 1511 (w), 1048 (vs), 933 (w), 896 (s), 852 (s), 820 (w), 802 (s), 757 (vs), 680 (w); MS/EI *m/z* (%): 802.8 ($PhAmid_2H_3^+$, 11), 759.8 ($PhAmid_2H_3^+$-Pr^i, 16), 626.5 ($PhAmid_2H_3^+$-NDip, 72). A reproducible microanalysis could not be obtained for the compound as it consistently co-

crystallised with small amounts of the pro-ligand $PhAmid_2H_2$, which could not be separated after several recrystallisations.

[{(THF)$_3$K(μ-PhAmid$_2$)K}$_\infty$] (1.K). To a mixture of $PhAmid_2H_2$ (1.0 g, 1.25 mmol) and $KN(SiMe_3)_2$ (0.5 g, 2.5 mmol) was added THF/toluene (30 mL). The reaction mixture was then stirred at ambient temperature for 12 hours. The resultant suspension was subsequently filtered, volatiles were removed from the filtrate *in vacuo*, and the residue was washed with hexane (10 mL). The residue was dried under vacuum, affording **1.K** as an off-white powder (0.80 g, 60 %). A few X-ray quality crystals were grown by layering the initial reaction solution, prior to removal of volatiles, with hexane. M.p. 211-216 °C; compound **7** showed negligible solubility in normal deutrated solvents, therefore no useful solution-state spectroscopic data could be obtained; IR ν/cm^{-1} (Nujol): 1582 (w), 1560 (w), 1186 (s), 1083 (w), 1018 (m), 918 (s), 861 (m), 880 (s), 812 (vs), 766 (w), 731 (w); MS/EI *m/z* (%): 146.1 (DipNC$^+$-Pr^i, 100). A reproducible microanalysis could not be obtained for this compound as its negligible solubility in common organic solvents precluded it being purified by recrystallisation.

[(Et$_2$O)IMg(μ-PhAmid$_2$)MgI(OEt$_2$)$_2$] (4). A solution of $PhAmid_2H_2$ (1.0 g, 1.25 mmol) in diethyl ether (20 mL) was added to MeMgI (2.6 mL, 2.6 mmol, 1 M solution in diethyl ether) over 5 minutes at room temperature. The mixture was stirred for 3 hours and the solution then concentrated to ca. 15 mL under reduced pressure. Storage at -30 °C for 1 day resulted in the deposition of colourless crystals of **4** (1.10 g, 63 %). M.p. 200-210 °C (decomp.); ^{1}H NMR (400 MHz, C_6D_6, 298 K) δ = 0.85 (d, $^3J_{HH}$ = 6.9 Hz, 24H, CH(C*H*$_3$)$_2$), 0.97 (t, $^3J_{HH}$ = 7.0 Hz, 18H, OCH$_2$C*H*$_3$), 1.25 (d, $^3J_{HH}$ = 6.7 Hz, 24H, CH(C*H*$_3$)$_2$), 3.28 (q, $^3J_{HH}$ = 7.0 Hz, 4Hz, 12H, OC*H*$_2$CH$_3$), 3.50 (sept, $^3J_{HH}$ = 6.8 Hz, 8H, C*H*(CH$_3$)$_2$), 6.84 (s, 4H, Ar-*H*), 6.90-6.99 (m, 12H, Ar-*H*); ^{13}C{^{1}H} NMR (101 MHz, C_6D_6, 298 K) δ = 14.9 (OCH$_2$*C*H$_3$), 23.5, 26.9 (CH(*C*H$_3$)$_2$), 28.3 (*C*H(CH$_3$)$_2$), 66.5 (O*C*H$_2$CH$_3$), 123.8, 124.8, 128.5, 133.5, 141.7, 143.1, (Ar-*C*), 174.8 (N*C*N); IR ν/cm^{-1} (Nujol): 1099 (s), 1041 (vs), 957 (s), 934 (s), 898 (s), 854 (s), 825 (s), 802 (s), 773 (m), 759 (vs), 688 (m); MS/EI *m/z* (%): 802.7 (PhAmid$_2$H$_3^+$, 15), 759.6 (PhAmid$_2$H$_3^+$-Pr^i, 22), 626.5 (PhAmid$_2$H$_3^+$-NDip, 100); anal calc. for $C_{68}H_{102}I_2Mg_2N_4O_3$: C 61.59 %, H 7.75 %, N 4.23%; found: C 62.15 %, H 7.23 %, N 3.97 %.

[{(Et$_2$O)$_2$IMg}$_2$(μ-CyAmid$_2$)] (5). A solution of $CyAmid_2H_2$ (1.0 g, 1.24 mmol) in diethyl ether (20 mL) was added to MeMgI (2.6 mL, 2.6 mmol, 1 M solution in diethyl

ether) over 5 minutes. The resultant mixture was stirred for 3 hours and the solution was then concentrated to ca. 15 mL under reduced pressure. Storage at -30 °C for 1 day resulted in the deposition of colourless crystals of **5** (1.01 g, 58 %). M.p. 210-216 °C (decomp.); ^{1}H NMR (400 MHz, C_6D_6, 298 K) δ = 0.78 (m, 4H, Cy-*H*), 0.93 (t, $^{3}J_{HH}$ = 7.1 Hz, 24H, OCH_2CH_3), 1.16 (d, $^{3}J_{HH}$ = 6.8 Hz, 24H, $CH(CH_3)_2$), 1.24 (d, $^{3}J_{HH}$ = 6.7 Hz, 24H, $CH(CH_3)_2$), 1.53 (br d, $^{3}J_{HH}$ = 8.4 Hz, 4H, Cy-*H*), 2.12 (br s, 2H, Cy-*H*), 3.23 (q, $^{3}J_{HH}$ = 7.0 Hz, 4Hz, 16H, OCH_2CH_3), 3.49 (sept, $^{3}J_{HH}$ = 6.7 Hz, 8H, $CH(CH_3)_2$), 7.03-7.10 (m, 12H, Ar-*H*); ^{13}C{^{1}H} NMR (101 MHz, C_6D_6, 298 K) δ = 14.9 (OCH_2CH_3), 23.2 ($CH(CH_3)_2$), 27.3 (Cy-*C*), 28.3 ($CH(CH_3)_2$), 29.2 ($CH(CH_3)_2$), 42.2 (Cy-*C*), 66.5 (OCH_2CH_3), 123.6, 124.8, 128.6, 142.0, (Ar-*C*), 143.5 (N*C*N); IR ν/cm^{-1} (Nujol): 1096 (vs), 1042 (vs), 1001 (w), 957 (w), 934 (m), 890 (m), 856 (w), 832 (w), 802 (m), 769 (s), 751 (vs), 694 (w); MS/EI *m/z* (%): 808.9 ($PhAmid_2H_3^+$, 3), 765.8 ($PhAmid_2H_3^+$-Pr^{i}, 30), 632.5 ($PhAmid_2H_3^+$-NDip, 12); anal. calc. for $C_{72}H_{118}I_2Mg_2N_4O_4$: C 61.50 %, H 8.46 %, N 3.98 %; found: C 61.61 %, H 8.57 %, N 4.12 %.

[{(Et_2O)IMg}$_2$(μ-$DBFAmid_2$)] (6). A solution of $DBFAmid_2H_2$ (1.00 g, 1.12 mmol) in diethyl ether (20 mL) was added to MeMgI (2.5 mL, 2.46 mmol, 1 M solution in diethyl ether) over 5 minutes. The resultant mixture was stirred for 3 hours and the solution was then concentrated to ca. 12 mL under reduced pressure and 3 mL toluene was added to it. Storage at -30 °C for 1 day resulted in the deposition of colourless crystals of **6** (1.1 g, 73.2 %). M.p. 170 °C (decomp.); ^{1}H NMR (600 MHz, C_6D_6, 298 K) δ = -0.75 (d, $^{3}J_{HH}$ = 6.7 Hz, 6H, $CH(CH_3)_2$), 0.40 (d, $^{3}J_{HH}$ = 6.5 Hz, 6H, $CH(CH_3)_2$), 0.89 (br, 12H, OCH_2CH_3), 0.97 (d, $^{3}J_{HH}$ = 6.6 Hz, 6H, $CH(CH_3)_2$), 1.51 (d, $^{3}J_{HH}$ = 6.3 Hz, 6H, $CH(CH_3)_2$), 1.54 (d, $^{3}J_{HH}$ = 5.4 Hz, 6H, $CH(CH_3)_2$), 1.59 (d, $^{3}J_{HH}$ = 6.8 Hz, 6H, $CH(CH_3)_2$), 1.61 (d, $^{3}J_{HH}$ = 6.8 Hz, 6H, $CH(CH_3)_2$), 1.87 (d, $^{3}J_{HH}$ = 6.7 Hz, 6H, $CH(CH_3)_2$), 2.66 (m, 2H, $CH(CH_3)_2$), 3.46 (br, 8H, OCH_2CH_3), 3.96 (v br, 2H, $CH(CH_3)_2$), 4.08 (m, 2H, $CH(CH_3)_2$), 4.30 (m, 2H, $CH(CH_3)_2$), 6.58 (t, $^{3}J_{HH}$ = 7.7 Hz, 24H, Ar-*H*), 6.69 (d, $^{3}J_{HH}$ = 7.4 Hz, 24H, Ar-*H*), 6.91 (d, $^{3}J_{HH}$ = 7.7 Hz, 24H, Ar-*H*), 6.96 (t, $^{3}J_{HH}$ = 7.7 Hz, 24H, Ar-*H*), 7.01 (t, $^{3}J_{HH}$ = 7.6 Hz, 24H, Ar-*H*), 7.10-7.18 (m, 12H, Ar-*H*); ^{13}C{^{1}H} NMR (151 MHz, C_6D_6, 298 K) δ = 14.2 (OCH_2CH_3), 20.3, 23.7, 24.4, 25.5, 26.8, 27.1 ($CH(CH_3)_2$), 27.6, 28.6, 29.1, 29.2 2 ($CH(CH_3)_2$), 66.5 (OCH_2CH_3), 118.20, 120.7, 121.6, 123.5, 123.8, 124.4, 124.9, 125.0, 125.4, 129.3, 134.0, 140.8, 141.3, 141.7, 142.1, 143.9, 144.1, 153.2 (Ar-*C*), 171.3 (N*C*N); IR ν/cm^{-1} (Nujol): 3057 (w), 2960 (s), 1607 (w), 1582 (w), 1429 (s), 1386 (s), 1256 (m), 1191 (w), 1178 (w), 1150 (s), 1085 (s),

1030 (vs), 996 (s), 961 (w), 937 (w), 894 (s), 848 (m), 834 (w), 787 (s), 775 (s), 758 (s), 746 (s), 672 (w); anal. calc. for $C_{72}H_{118}I_2Mg_2N_4O_4$: C 62.65 %, H 7.06 %, N 4.18 %; found: C 62.66 %, H 6.94 %, N 4.10 %.

[(I$_2$Al)$_2$(μ-PhAmid$_2$)] (7). LiBu^n (1.6 mL of a 1.6 M solution in hexane) was added to a solution of PhAmid$_2$H$_2$ (1.0 g, 1.25 mmol) in toluene (30 mL) at -80 °C. The resultant solution was warmed to room temperature and stirred for 4 hours. This was then added to a suspension of AlI$_3$ (1.7 g, 2.6 mmol) in toluene (20 mL) at -80 °C and the reaction mixture slowly warmed to room temperature overnight. Volatiles were then removed *in vacuo* and the residue extracted with toluene (30 mL). The extract was filtered, and the solution concentrated to ca. 5 mL. Storage at -30 °C for 2 days resulted in deposition of **7** as colourless crystals (0.60 g, 35 %). M.p. 220-226 °C; ^{1}H NMR (400 MHz, C$_6$D$_6$, 298 K) δ = 0.66 (d, $^3J_{HH}$ = 6.9 Hz, 24H, CH(C*H*$_3$)$_2$), 1.25 (d, $^3J_{HH}$ = 6.6 Hz, 24H, CH(C*H*$_3$)$_2$), 3.45 (sept, $^3J_{HH}$ = 6.7 Hz, 8H, C*H*(CH$_3$)$_2$), 6.81(s, 4H, Ar-*H*), 6.82-6.96 (m, 12H, Ar-*H*); ^{13}C{^{1}H} NMR (101 MHz, C$_6$D$_6$, 298 K) δ = 23.2, 28.2 (CH(*C*H$_3$)$_2$), 28.8 (*C*H(CH$_3$)$_2$), 124.5, 127.9, 128.2, 129.4, 130.6, 134.5 (Ar-*C*), 144.8 (N*C*N); N.B. no signal was observed in the ^{27}Al NMR spectrum; IR ν/cm^{-1} (Nujol): 1099 (s), 1042 (w), 983 (s), 934 (s), 887 (w), 856 (s), 826 (w), 802 (vs), 761 (vs), 729 (w), 703 (s), 677 (s); MS/EI *m/z* (%): 803.0 (PhAmid$_2$H$_3^+$, 8), 759.8 (PhAmid$_2$H$_3^+$-Pr^i, 4), 626.7 (PhAmid$_2$H$_3^+$-NDip, 48); anal. calc. for $C_{56}H_{72}I_4Al_2N_4$: C 49.36 %, H 5.33 %, N 4.11 %; found: C 49.23 %, H 5.49 %, N 3.91 %.

[(Cl$_3$Si)$_2$(μ-PhAmid$_2$)] (8). A solution of SiCl$_4$ (0.40 mL, 3.6 mmol) in diethyl ether (20 mL) was added to a solution of **1.Li** (2.0 g, 1.8 mmol) in diethyl ether (30 mL) at -80 °C. The reaction mixture was slowly warmed to room temperature overnight. Volatiles were then removed *in vacuo* and the residue extracted with dichloromethane (30 mL). The extract was filtered, and the solution was concentrated to ca. 10 mL. Storage at -30 °C for 1 day resulted in deposition of **8** as colourless crystals (1.20 g, 62 %). M.p. > 260 °C; ^{1}H NMR (400 MHz, C$_6$D$_6$, 298 K) δ = 0.71 (d, $^3J_{HH}$ = 6.9 Hz, 24H, CH(C*H*$_3$)$_2$), 1.30 (d, $^3J_{HH}$ = 6.6 Hz, 24H, CH(C*H*$_3$)$_2$), 3.40 (sept, $^3J_{HH}$ = 6.8 Hz, 8H, C*H*(CH$_3$)$_2$), 6.81-6.95 (m, 16H, Ar-*H*); ^{13}C{^{1}H} NMR (101 MHz, C$_6$D$_6$, 298 K) δ = 23.5, 25.8 (CH(*C*H$_3$)$_2$), 29.1 (*C*H(CH$_3$)$_2$), 124.6, 128.7, 129.1, 129.8, 130.2, 135.2 (Ar-*C*), 145.3 (N*C*N); ^{29}Si{^{1}H} NMR (80 MHz, C$_6$D$_6$, 298 K) δ = -70.9; IR ν/cm^{-1} (Nujol): 1098 (s), 1053 (s), 987 (s), 933 (s), 861 (m), 838 (m), 805 (s), 791 (m), 771 (vs), 729 (s), 693 (s), 665 (w); MS/EI

m/z (%): 802.8 ($PhAmid_2H_3^+$, 10), 760.6 ($PhAmid_2H_3^+$-Pr^i, 33), 626.5 ($PhAmid_2H_3^+$-NDip, 66); anal. calc. for $C_{56}H_{72}Cl_6Si_2N_4$: C 62.86 %, H 6.78 %, N 5.24 %; found: C 62.63 %, H 6.87 %, N 5.35 %.

[(Br$_3$Si)$_2$(μ-PhAmid$_2$)] (9). This compound was prepared following a similar method to that for **8** but using **1.Li** (0.50 g, 0.45 mmol) in diethyl ether (20 mL) and $SiBr_4$ (0.12 mL, 0.95 mmol) in diethyl ether (20 mL). Storage of the reaction mixture at -30 °C for 1 day resulted in deposition of **9** as colourless crystals (0.50 g, 83 %). M.p. >260 °C; ^{1}H NMR (400 MHz, C_6D_6, 298 K) δ = 0.68 (d, $^3J_{HH}$ = 6.8 Hz, 24H, CH(C*H*$_3$)$_2$), 1.33 (d, $^3J_{HH}$ = 6.6 Hz, 24H, CH(C*H*$_3$)$_2$), 3.43 (sept, $^3J_{HH}$ = 6.7 Hz, 8H, C*H*(CH$_3$)$_2$), 6.82 (s, 4H, Ar-*H*), 6.84 (s, 4H, Ar-*H*), 6.93-6.99 (m, 8H, Ar-*H*); ^{13}C{^{1}H} NMR (101 MHz, C_6D_6, 298 K) δ = 23.8, 26.3, (CH(*C*H$_3$)$_2$), 29.2 (*C*H(CH$_3$)$_2$), 124.7, 127.4, 129.4, 130.3, 135.2, 145.6 (Ar-*C*), 166.1 (N*C*N); ^{29}Si{^{1}H} NMR (80 MHz, C_6D_6, 298 K) δ = -117.4; IR ν/cm^{-1} (Nujol): 1096 (vs), 1053 (w), 984 (s), 931 (s), 862 (w), 836 (w), 804 (s), 770 (vs), 729 (vs), 694 (s), 661 (s); MS/EI *m/z* (%): 802.6 ($PhAmid_2H_3^+$, 1), 626.5 ($PhAmid_2H_3^+$-NDip, 9); anal. calc. for $C_{56}H_{72}Br_6Si_2N_4$: C 50.31 %, H 5.43 %, N 4.19 %; found: C 50.17 %, H 5.52 %, N 4.85 %.

[(Cl$_2$HSi)$_2$(μ-PhAmid$_2$)] (10). This compound was prepared following a similar method to that for **8** but using **1.Li** (2.0 g, 1.80 mmol) in diethyl ether (30 mL) and $SiHCl_3$ (0.36 mL, 3.7 mmol) in diethyl ether (20 mL). Work-up in toluene, and storage of the toluene extract at -30 °C for 1 day resulted in deposition of **10** as colourless crystals (1.0 g, 55 %). M.p. 190-194 °C; ^{1}H NMR (400 MHz, C_6D_6, 298 K) δ = 0.71 (d, $^3J_{HH}$ = 6.9 Hz, 24H, CH(C*H*$_3$)$_2$), 1.26 (d, $^3J_{HH}$ = 6.7 Hz, 24H, CH(C*H*$_3$)$_2$), 3.27 (sept, $^3J_{HH}$ = 6.8 Hz, 8H, C*H*(CH$_3$)$_2$), 6.65 (s, 2H, Si-*H*), 6.82 (s, 4H, Ar-*H*), 6.84-6.96 (m, 12H, Ar-*H*); ^{13}C{^{1}H} NMR (101 MHz, C_6D_6, 298 K) δ = 23.9, 25.8 (CH(*C*H$_3$)$_2$), 29.2 (*C*H(CH$_3$)$_2$), 124.2, 124.5, 127.6, 128.7, 130.3, 135.0 (Ar-*C*), 144.9 (N*C*N); ^{29}Si{^{1}H} NMR (80 MHz, C_6D_6, 298 K) δ = -71.3; IR ν/cm^{-1} (Nujol): 2190 (Si-H str.), 1622 (vs), 1579 (s), 1056 (s), 988 (s), 934 (s), 827 (s), 802 (s), 767 (w), 756 (w), 731 (s), 679 (w); MS/EI *m/z* (%): 802.6 ($PhAmid_2H_3^+$, 8), 626.5 ($PhAmid_2H_3^+$-NDip, 54), 97 ($SiCl_2^+$, 91); anal. calc. for $C_{56}H_{74}Cl_4Si_2N_4$: C 67.18 %, H 7.45 %, N 5.60 %; found: C 67.20 %, H 7.71 %, N 5.39 %.

[(ClGe)$_2$(μ-PhAmid$_2$)] (11). A solution of **1.Li** (1.0 g, 0.91 mmol) in THF (20 mL) was added to a solution of $GeCl_2$.dioxane (0.42 g, 1.82 mmol) in THF (20 mL) at -80 °C. The

reaction mixture was slowly warmed to room temperature overnight then concentrated *in vacuo* to ca. 5 mL. Placing the solution at -30 °C for 2 days resulted in deposition of **11** as colourless crystals (0.50 g, 54 %). M.p. > 260 °C; ^{1}H NMR (400 MHz, C_6D_6, 298 K) δ = 0.71 (d, $^{3}J_{HH}$ = 6.9 Hz, 12H, CH(C*H*$_3$)$_2$), 0.77 (d, $^{3}J_{HH}$ = 7.2 Hz, 12H, CH(C*H*$_3$)$_2$), 1.06 (d, $^{3}J_{HH}$ = 6.8 Hz, 12H, CH(C*H*$_3$)$_2$), 1.34 (d, $^{3}J_{HH}$ = 6.6 Hz, 12H, CH(C*H*$_3$)$_2$), 3.32 (m, 4H, C*H*(CH$_3$)$_2$), 3.76 (m, 4H, C*H*(CH$_3$)$_2$), 6.82-6.96 (m, 16H, Ar-*H*); ^{13}C{^{1}H} NMR (101 MHz, C_6D_6, 298 K) δ = 22.4, 22.9, 26.7, 26.9 (CH(*C*H$_3$)$_2$), 28.8, 29.3, (*C*H(CH$_3$)$_2$), 124.4, 125.7, 127.1, 128.9, 132.0, 136.2, 143.8, 146.1 (Ar-*C*), 170.7 (N*C*N); IR ν/cm^{-1} (Nujol): 1613 (w), 1055 (w), 1035 (w), 973 (s), 933 (s), 864 (s), 829 (w), 799 (vs), 774 (s), 753 (vs), 683 (w); MS/EI *m/z* (%): 802.6 (PhAmid$_2$H$_3^+$, 1), 626.5 (PhAmid$_2$H$_3^+$-NDip, 9), 91.0 (PhCH$_2^+$, 100). A reproducible microanalysis could not be obtained for the compound as it consistently crystallised with a small amount of an unknown impurity which could not be separated by repeated recrystallisations.

[(ClGe)$_2$(μ-CyAmid$_2$)] (12). A solution of CyAmid$_2$H$_2$ (1.0 g, 1.24 mmol) in THF (50 mL) was cooled to -80 ºC and LiBu^n (1.7 mL, 2.72 mmol, 1.6 M solution in hexane) was added to this over 10 minutes. After the addition, the reaction mixture was warmed to room temperature, and stirred for 4 hours. This reaction mixture was then added to a solution of GeCl$_2$.dioxane (0.63 g, 2.7 mmol) in THF (20 mL) at -80 ºC. The reaction mixture was stirred for 12 hours at room temperature. Volatiles were subsequently removed *in vacuo*, and the residue extracted into hot toluene (50 mL). The extract was filtered, concentrated to ca. 20 mL and stored at -30 ºC overnight to yield colourless crystals of **12** (0.56 g, 44.2 %). M.p. > 260 °C; ^{1}H NMR (400 MHz, C_6D_6, 298 K) δ = 0.89 (m, 4H, Cy-*H*), 1.03-1.09 (m, 36H, CH(C*H*$_3$)$_2$), 1.33 (d, $^{3}J_{HH}$ = 6.6 Hz, 12H, CH(C*H*$_3$)$_2$), 1.67 (br, 4H, Cy-*H*), 1.86 (br, 2H, Cy-*H*), 3.25 (m, 4H, C*H*(CH$_3$)$_2$), 3.72 (m, 4H, C*H*(CH$_3$)$_2$), 6.89-7.04 (m, 12H, Ar-*H*); ^{13}C{^{1}H} NMR (101 MHz, C_6D_6, 298 K) δ = 22.4, 22.9, 27.3, 27.4 (CH(*C*H$_3$)$_2$), 27.6 (Cy-*C*), 28.7, 29.3 (*C*H(CH$_3$)$_2$), 41.3 (Cy-*C*), 123.4, 124.4, 127.3, 128.6, 129.3, 136.3, 144.2, 146.7 (Ar-*C*), 176.7 (N*C*N); IR ν/cm^{-1} (Nujol): 1102 (m), 1058 (s), 973 (w), 934 (w), 889 (w), 829 (w), 798 (s), 752 (s), 729 (m), 697 (s); MS/EI *m/z* (%): 808.8 (PhAmid$_2$H$_3^+$, 2), 765.8, (PhAmid$_2$H$_3^+$-Pr^i, 16), 632.6 (PhAmid$_2$H$_3^+$-NDip, 8), 57.1 (C(CH)$_3^+$, 100); anal. calc. for $C_{56}H_{78}Cl_2Ge_2N_4$: C 65.72 %, H 7.68 %, N 5.47 %; found: C 65.86 %, H 7.78 %, N 5.34 %.

[(ClGe)$_2$(μ-DBFAmid$_2$)] (13). A solution of DBFAmid$_2$H$_2$ (1.00 g, 1.12 mmol) in THF (50 mL) was cooled to -80 ºC and LiBu^n (1.5 mL, 2.46 mmol, 1.6 M solution in hexane) was added to this over 10 minutes. After the addition, the reaction mixture was warmed to room temperature, and stirred for 4 hours. This reaction mixture was then added to a solution of GeCl$_2$.dioxane (0.56 g, 2.41 mmol) in THF (20 mL) at -80 ºC. The reaction mixture was stirred for 12 hours at room temperature. Volatiles were subsequently removed *in vacuo*, and the residue extracted into hot toluene (30 mL). The extract was filtered and dried under vacuum. Addition of hexane (15 mL) to solid mixture and storage at -30 ºC overnight yield the colourless crystals of **13** (0.68 g, 54.8 %). M.p. > 260 °C; ^{1}H NMR (600 MHz, C$_6$D$_6$, 298 K) δ = -0.66 (br, 6H, CH(C*H*$_3$)$_2$), 0.38 (br, 6H, CH(C*H*$_3$)$_2$), 0.95 (br, 6H, CH(C*H*$_3$)$_2$), 1.45-1.55 (m, 24H, CH(C*H*$_3$)$_2$), 1.78 (br, 6H, CH(C*H*$_3$)$_2$), 2.82 (br, 2H, C*H*(CH$_3$)$_2$), 3.51 (br, 2H, C*H*(CH$_3$)$_2$), 4.24 (br, 2H, C*H*(CH$_3$)$_2$), 4.42 (br, 2H, C*H*(CH$_3$)$_2$), 6.57 (t, $^3J_{HH}$ = 7.7 Hz, 2H, Ar-*H*), 6.60 (br, 2H, Ar-*H*), 6.91-6.98 (m, 7H, Ar-*H*), 7.07 (d, $^3J_{HH}$ = 7.7 Hz, 2H, Ar-*H*), 7.11 (br, 2H, Ar-*H*), 7.29 (d, $^3J_{HH}$ = 6.7 Hz, 2H, Ar-*H*); ^{13}C{^{1}H} NMR (151 MHz, C$_6$D$_6$, 298 K) δ = 20.0, 24.3, 25.2, 27.3 (CH(*C*H$_3$)$_2$), 28.3, 29.0, 29.2, 29.4 (*C*H(CH$_3$)$_2$), 115.8, 122.5, 122.8, 123.8, 125.0, 125.1, 125.5, 126.0, 127.4, 127.6, 128.5, 134.7, 135.8, 142.3, 143.5, 144.7, 147.9, 152.8 (Ar-*C*), 168.4 (N*C*N); IR ν/cm^{-1} (Nujol): 3059 (w), 2958 (s), 1639 (w), 1611 (w),1586 (w), 1501 (w), 1442 (vs), 1424 (vs), 1404 (vs), 1384 (s), 1257 (s), 1178 (m), 1154 (s), 1100 (s), 1086 (vs), 1056 (m), 1020 (m), 990 (w), 968 (m), 936 (m), 915 (m), 884 (w), 852 (s), 799 (vs), 790 (vs), 765 (s), 756 (vs), 743 (vs), 743 (vs), 715 (w), 683 (w); anal. calc. for C$_{62}$H$_{74}$Cl$_2$Ge$_2$N$_4$O: C 67.24 %, H 6.74 %, N 5.06 %; found: C 67.35 %, H 6.89 %, N 4.92 %.

[(ClSn)$_2$(μ-PhAmid$_2$)] (14). This compound was prepared following a similar method to that for **11**, but using **1.Li** (1.0 g, 0.91 mmol) in THF (30 mL) and SnCl$_2$ (0.34 g, 1.80 mmol) in THF (20 mL). Storage of the concentrated reaction solution at -30 °C for 2 days resulted in deposition of colourless crystals of **14** (0.70 g, 69 %). M.p. 190-194 °C; ^{1}H NMR (400 MHz, C$_6$D$_6$, 298 K) δ = 0.72 (br, 12H, CH(C*H*$_3$)$_2$), 0.77 (br, 12H, CH(C*H*$_3$)$_2$), 0.98 (br s, 12H, CH(C*H*$_3$)$_2$), 1.37 (br, 12H, CH(C*H*$_3$)$_2$), 3.28 (br, 4H, C*H*(CH$_3$)$_2$), 3.79 (br, 4H, C*H*(CH$_3$)$_2$), 6.84 (br, 12H, Ar-*H*), 6.92 (br, 4H, Ar-*H*); ^{13}C{^{1}H} NMR (101 MHz, C$_6$D$_6$, 298 K) δ = 22.5, 23.1, 26.8, 27.2 (CH(*C*H$_3$)$_2$), 28.6, 28.9 (*C*H(CH$_3$)$_2$), 123.2, 124.3, 124.6, 126.4, 127.7, 134.3, 143.1, 145.5 (Ar-*C*), 173.3 (N*C*N); ^{119}Sn{^{1}H} NMR (149 MHz, C$_6$D$_6$, 298 K): no signal observed; IR ν/cm^{-1} (Nujol): 1020 (w), 959 (vs), 934 (s),

854 (s), 823 (s), 800 (s), 759 (vs), 683 (s); MS/EI *m/z* (%): 802.6 ($PhAmid_2H_3^+$, 14), 759.8 ($PhAmid_2H_3^+$-Pr^i, 14), 626.5 ($PhAmid_2H_3^+$-NDip, 100); anal. calc. for $C_{56}H_{72}Cl_2Sn_2N_4$: C 60.62 %, H 6.54 %, N 5.05 %; found: C 60.50 %, H 6.65 %, N 5.12 %.

[(BrSn)$_2$(μ-DBFAmid$_2$)] (15). This compound was prepared following a similar method to that for **13**, but using **3** (1.00 g, 1.12 mmol) in THF (30 mL), $LiBu^n$ (1.5 mL, 2.46 mmol, 1.6 M solution in hexane) and $SnBr_2$ (0.67 g, 2.41 mmol) in THF (20 mL). Storage of the concentrated reaction solution in toluene at -30 °C for 2 days resulted in deposition of colourless crystals of **15** (0.40 g, 27.7 %). M.p. 220 °C (decomp.); ^{1}H NMR (600 MHz, C_6D_6, 298 K) δ = -0.73 (d, $^3J_{HH}$ = 6.7 Hz, 6H, CH(CH_3)$_2$), 0.44 (d, $^3J_{HH}$ = 6.6 Hz, 6H, CH(CH_3)$_2$), 0.89 (d, $^3J_{HH}$ = 6.8 Hz, 6H, CH(CH_3)$_2$), 1.29 (br, 6H, CH(CH_3)$_2$), 1.46 (br, 6H, CH(CH_3)$_2$), 1.58 (br, 12H, CH(CH_3)$_2$), 1.70 (br, 6H, CH(CH_3)$_2$), 2.72 (br, 2H, CH(CH$_3$)$_2$), 3.56 (m, 2H, CH(CH$_3$)$_2$), 4.11 (br, 2H, CH(CH$_3$)$_2$), 4.41 (br, 2H, CH(CH$_3$)$_2$), 6.55-6.57 (m, 4H, Ar-*H*), 6.87 (t, $^3J_{HH}$ = 7.7 Hz, 2H, Ar-*H*), 6.94-7.09 (m, 10H, Ar-*H*), 7.25 (d, $^3J_{HH}$ = 7.8 Hz, 2H, Ar-*H*); ^{13}C{^{1}H} NMR (151 MHz, C_6D_6, 298 K) δ = 19.6, 22.9, 24.6, 25.9, 27.4, 28.1, 28.3, 28.8, 28.9, 2×29.1, (CH(*C*H$_3$)$_2$), 28.6, 28.9 (*C*H(CH$_3$)$_2$), 118.5, 122.1, 123.5, 123.9, 124.6, 125.0, 125.5, 126.7, 127.6, 128.4, 128.5, 134.8, 137.0, 137.3, 143.4, 144.4, 147.2, 152.7 (Ar-*C*), 169.8 (N*C*N); ^{119}Sn{^{1}H} NMR (149 MHz, C_6D_6, 298 K): no signal observed; IR ν/cm^{-1} (Nujol): 3058 (w), 1643 (w), 1608 (w), 1584 (w), 1497 (w), 1441 (vs), 1398 (s), 1270 (m), 1175 (w), 1154 (m), 1101 (m), 1083 (m), 1050 (w), 963 (w), 934 (w), 910 (w), 849 (m), 794 (s), 740 (m), 699 (w); A reproducible microanalysis could not be obtained for this compound.

[{(TMC)Cl$_2$Si}{μ-(DipN)$_2$C=(C$_6$H$_4$)=C(NDip)$_2$}{SiHCl(TMC)}] (17). A solution of **10** (0.20 g, 0.2 mmol) in toluene (20 mL) at 80 °C was added to a solution of TMC (0.075 g, 0.6 mmol) in toluene (10 mL) held at room temperature, resulting in dark red solution. The reaction mixture was stirred at room temperature for 2 hours. It was then filtered and concentrated to ca. 10 mL. Storage at -30 °C for 2 days resulted in the deposition of **17** as red crystals (0.050 g, 20 %). M.p. > 260 °C; ^{1}H NMR (400 MHz, C_6D_6, 298 K) δ = 0.98 (s, NCH$_3$CCH_3), 1.03 (d, $^3J_{HH}$ = 6.9 Hz, 6H, CH(CH_3)$_2$), 1.25 (d, $^3J_{HH}$ = 6.8 Hz, 6H, CH(CH_3)$_2$), 1.27 (d, $^3J_{HH}$ = 6.8 Hz, 6H, CH(CH_3)$_2$), 1.40 (d, $^3J_{HH}$ = 8 Hz, 6H, CH(CH_3)$_2$), 1.48 (3 x overlapping d, 18H, CH(CH_3)$_2$), 1.56 (d, $^3J_{HH}$ = 8 Hz, 6H, CH(CH_3)$_2$), 3.22 (s, NCH_3CCH$_3$), 3.55 (sept, $^3J_{HH}$ = 8Hz, 2H, CH(CH$_3$)$_2$), 3.93 (3 x overlapping sept, 6H,

C*H*(CH_3)$_2$), 4.91 (d, $^3J_{HH}$ = 8Hz, 2H, *H*C=C*H*), 5.05 (d, $^3J_{HH}$ = 8Hz, 2H, *H*C=C*H*), 6.71(s, 1H, Si-*H*), 6.94-7.11 (m, 12H, Ar-*H*); N.B. the solubility of the compound in non-coordinating deuterated solvents over extended periods was too low to obtain meaningful ^{13}C and ^{29}Si NMR data; IR ν/cm^{-1} (Nujol): 2105 (Si-H str.), 1623 (w), 1096 (m), 1020 (m), 863 (w), 801 (vs), 723 (m); MS/EI *m/z* (%): 802.7 (PhAmid$_2$H$_3^+$, 3), 626.5 (PhAmid$_2$H$_3^+$-NDip, 2). A reproducible microanalysis could not be obtained for the compound as it consistently crystallised with a small amount of an unknown impurity which could not be separated by recrystallisations.

[{(IPrIMe)Cl$_2$Si}{μ-(DipN)$_2$C=(C$_6$H$_4$)=C(NDip)$_2$}{SiHCl(IPrIMe)}] (18). This compound was prepared following a similar method to that employed for **17**, but using **10** (0.2 g, 0.2 mmol) in toluene (20 mL) and IPrIMe (0.11 g, 0.6 mmol) in toluene (10 mL). After work-up **18** was obtained as a dark red crystalline solid after storage at -30 °C for 2 days (0.060 g, 22 %). M.p. 222-226 °C; once crystallised, compound **18** showed negligible solubility in normal deuterated solvents. As a result, meaningful solution-state spectroscopic data could not be obtained for it. IR ν/cm^{-1} (Nujol): 2118 (Si-H str.) 1621 (s), 1552 (s), 1081 (m), 1043 (m), 933 (s), 802 (s), 776 (s), 727 (w), 697 (s); MS/EI *m/z* (%): 802.7 (PhAmid$_2$H$_3^+$, 2), 626.5 (PhAmid$_2$H$_3^+$-NDip, 16). A reproducible microanalysis could not be obtained for the compound as it consistently crystallised with a small amount of an unknown impurity which could not be separated.

3.6 References

1 W. H. Brock, K. A. Jensen, C. K. Jørgensen and G. B. Kauffman, *Polyhedron*, 1983, **2**, 1–7.

2 V. G. Schwarzenbach and A. Zobrist, *Helv. Chim. Acta*, 1952, **35**, 1291–1300.

3 G. A. Lawrance, *Introduction to Coordination Chemistry*, J. Wiley & Sons, West Sussex, 2010.

4 S. G. McGeachin, *Can. J. Chem.*, 1968, **46**, 1903–1912.

5 P. B. Hitchcock, M. F. Lappert and D.-S. Liu, *J. Chem. Soc., Chem. Commun.*, 1994, 1699–1700.

6 P. B. Hitchcock, M. F. Lappert and D.-S. Liu, *J. Chem. Soc., Chem. Commun.*, 1994, 2637–2638.

7 D. C. H. Do, A. Keyser, A. V. Protchenko, B. Maitland, I. Pernik, H. Niu, E. L.

Kolychev, A. Rit, D. Vidovic, A. Stasch, C. Jones and S. Aldridge, *Chem. - Eur. J.*, 2017, **23**, 5830–5841.

8 L. Bourget-Merle, M. F. Lappert and J. R. Severn, *Chem. Rev.*, 2002, **102**, 3031–3065.

9 P. H. M. Budzelaar, A. B. van Oort and A. G. Orpen, *Eur. J. Inorg. Chem.*, 1998, **1998**, 1485–1494.

10 A. R. Sanger, *Inorg. Nucl. Chem. Lett.*, 1973, **9**, 351–354.

11 J. A. R. Schmidt and J. Arnold, *J. Chem. Soc., Dalton Trans.*, 2002, 2890–2899.

12 M. P. Coles, *Dalton Trans.*, 2006, 985–1001.

13 J. Hong, L. Zhang, K. Wang, Z. Chen, L. Wu and X. Zhou, *Organometallics*, 2013, **32**, 7312–7322.

14 G. Jin, C. Jones, P. C. Junk, K. A. Lippert, R. P. Rose and A. Stasch, *New J. Chem.*, 2009, **33**, 64–75.

15 R. Kretschmer, *Chem. - Eur. J.*, 2020, **26**, 2099–2119.

16 N. H. Pilkington and R. Robson, *Aust. J. Chem.*, 1970, **23**, 2225–2236.

17 R. Robson, *Aust. J. Chem.*, 1970, **23**, 2217–2224.

18 H. A. Jenkins, D. Abeysekera, D. A. Dickie and J. A. C. Clyburne, *J. Chem. Soc., Dalton Trans.*, 2002, **20**, 3919–3922.

19 R. J. Baker and C. Jones, *J. Organomet. Chem.*, 2006, **691**, 65–71.

20 D. Lindauer, R. Beckert, M. Doring, P. Fehling and H. Gorls, *J. Prakt. Chem.*, 1995, **337**, 143–152.

21 C. T. Chen, L. H. Rees, A. R. Cowley and M. L. H. Green, *J. Chem. Soc., Dalton Trans.*, 2001, 1761–1767.

22 F. T. Edelmann, in *Advances in Organometallic Chemistry*, Elsevier Inc., 2008, Vol. 57, pp. 183–352.

23 T. Chlupatý, M. Bílek, J. Merna, J. Brus, Z. Růžičková, T. Strassner and A. Růžička, *Dalton Trans.*, 2019, **48**, 5335–5342.

24 B. M. Day, W. Knowelden and M. P. Coles, *Dalton Trans.*, 2012, **41**, 10930–10933.

25 S. P. Green, C. Jones and A. Stasch, *Science*, 2007, **318**, 1754–1758.

26 J. Hicks, M. Juckel, A. Paparo, D. Dange and C. Jones, *Organometallics*, 2018, **37**, 4810–4813.

27 S. Dagorne and D. A. Atwood, *Chem. Rev.*, 2008, **108**, 4037–4071.

28 L. S. Baugh and J. A. Sissano, *J. Polym. Sci., Part A: Polym. Chem.*, 2002, **40**, 1633–1651.

29 E. W. Y. Wong, D. Dange, L. Fohlmeister, T. J. Hadlington and C. Jones, *Aust. J. Chem.*, 2013, **66**, 1144–1154.

30 M. P. Coles, D. C. Swenson, R. F. Jordan and V. G. Young, *Organometallics*, 1997, **16**, 5183–5194.

31 L. Chen, W. Li, D. Yuan, Y. Zhang, Q. Shen and Y. Yao, *Inorg. Chem.*, 2015, **54**, 4699–4708.

32 W. Li, H. Ouyang, L. Chen, D. Yuan, Y. Zhang and Y. Yao, *Inorg. Chem.*, 2016, **55**, 6520–6524.

33 M. Normand, T. Roisnel, J. F. Carpentier and E. Kirillov, *Chem. Commun.*, 2013, **49**, 11692–11694.

34 F. Qian, K. Liu and H. Ma, *Dalton Trans.*, 2010, **39**, 8071–8083.

35 B. M. Trost and H. Ito, *J. Am. Chem. Soc.*, 2000, **122**, 12003–12004.

36 K. Maruoka, *Catalysis Today*, 2001, **66**, 33–45.

37 J. Grundy, M. P. Coles and P. B. Hitchcock, *J. Organomet. Chem.*, 2002, **662**, 178–187.

38 T. Peddarao, A. Baishya, S. K. Hota and S. Nembenna, *J. Chem. Sci.*, 2018, **130**, 1–7.

39 B. Clare, N. Sarker, R. Shoemaker and J. R. Hagadorn, *Inorg. Chem.*, 2004, **43**, 1159–1166.

40 Y. Lei, F. Chen, Y. Luo, P. Xu, Y. Wang and Y. Zhang, *Inorg. Chim. Acta*, 2011, **368**, 179–186.

41 C. Cui, H. W. Roesky, H. G. Schmidt, M. Noltemeyer, H. Hao and F. Cimpoesu, *Angew. Chem., Int. Ed.*, 2000, **39**, 4274–4276.

42 M. Asay, C. Jones and M. Driess, *Chem. Rev.*, 2011, **111**, 354–396.

43 F. T. Edelmann, *Coord. Chem. Rev.*, 1994, **137**, 403–481.

44 F. T. Edelmann, in *Advances in Organometallic Chemistry*, Elsevier Inc., 2013, Vol. 61, pp. 55–374.

45 C. W. So, H. W. Roesky, J. Magull and R. B. Oswald, *Angew. Chem., Int. Ed.*, 2006, **45**, 3948–3950.

46 S. S. Sen, H. W. Roesky, D. Stern, J. Henn and D. Stalke, *J. Am. Chem. Soc.*, 2010,

132, 1123–1126.

47 S. S. Sen, A. Jana, H. W. Roesky and C. Schulzke, *Angew. Chem., Int. Ed.*, 2009, **48**, 8536–8538.

48 C. Jones, S. J. Bonyhady, N. Holzmann, G. Frenking and A. Stasch, *Inorg. Chem.*, 2011, **50**, 12315–12325.

49 D. Gallego, S. Inoue, B. Blom and M. Driess, *Organometallics*, 2014, **33**, 6885–6897.

50 W. Wang, S. Inoue, E. Irran and M. Driess, *Angew. Chem., Int. Ed.*, 2012, **51**, 3691–3694.

51 A. Brück, D. Gallego, W. Wang, E. Irran, M. Driess and J. F. Hartwig, *Angew. Chem., Int. Ed.*, 2012, **51**, 11478–11482.

52 A. Kostenko and M. Driess, *J. Am. Chem. Soc.*, 2018, **140**, 16962–16966.

53 Y. P. Zhou, S. Raoufmoghaddam, T. Szilvási and M. Driess, *Angew. Chem., Int. Ed.*, 2016, **55**, 12868–12872.

54 H. H. Karsch, P. A. Schlüter and M. Reisky, *Eur. J. Inorg. Chem.*, 1998, 433–436.

55 M. El Ezzi, T. G. Kocsor, F. D'Accriscio, D. Madec, S. Mallet-Ladeira and A. Castel, *Organometallics*, 2015, **34**, 571–576.

56 C. Jones, R. P. Rose and A. Stasch, *Dalton Trans.*, 2008, 2871–2878.

57 S. P. Green, C. Jones, P. C. Junk, K. A. Lippert and A. Stasch, *Chem. Commun.*, 2006, **174**, 3978–3980.

58 S. Nagendran, S. S. Sen, H. W. Roesky, D. Koley, H. Grubmüller, A. Pal and R. Herbst-Irmer, *Organometallics*, 2008, **27**, 5459–5463.

59 S. S. Sen, M. P. Kritzler-Kosch, S. Nagendran, H. W. Roesky, T. Beck, A. Pal and R. Herbst-Irmer, *Eur. J. Inorg. Chem.*, 2010, 5304–5311.

60 T. Chlupatý, Z. Padělková, A. Lyka, J. Brus and A. Růika, *Dalton Trans.*, 2012, **41**, 5010–5019.

61 S. L. Choong, C. Schenk, A. Stasch, D. Dange and C. Jones, *Chem. Commun.*, 2012, **48**, 2504–2506.

62 A. Stasch, C. M. Forsyth, C. Jones and P. C. Junk, *New J. Chem.*, 2008, **32**, 829–834.

63 M. Li, J. Hong, Z. Chen, X. Zhou and L. Zhang, *Dalton Trans.*, 2013, **42**, 8288–

8297.

64 N. Kazeminejad, D. Munzel, M. T. Gamer and P. W. Roesky, *Chem. Commun.*, 2017, **53**, 1060–1063.

65 G. Jin, C. Jones, P. C. Junk, A. Stasch and W. D. Woodul, *New J. Chem.*, 2008, **32**, 835–842.

66 M. L. Cole, A. J. Davies, C. Jones and P. C. Junk, *J. Organomet. Chem.*, 2004, **689**, 3093–3107.

67 S. J. Bonyhady, C. Jones, S. Nembenna, A. Stasch, A. J. Edwards and G. J. McIntyre, *Chem. - Eur. J.*, 2010, **16**, 938–955.

68 R. Tacke and T. Ribbeck, *Dalton Trans.*, 2017, **46**, 13628–13659.

69 S. H. Zhang, H. X. Yeong, H. W. Xi, K. H. Lim and C. W. So, *Chem. - Eur. J.*, 2010, **16**, 10250–10254.

70 V. S. V. S. N. Swamy, M. K. Bisai, T. Das and S. S. Sen, *Chem. Commun.*, 2017, **53**, 6910–6913

71 *As determined from a survey of the Cambridge Crystallographic Database, January, 2021.*

Chapter 4
Use of Bis(amide) and (amidinate) Ligands to Stabilise Low Oxidation State Heavier N-donor Bis(tetrelenes)

4.1 Introduction

Since the isolation of the first heavier carbene analogues [{$(Me_3Si)_2CH$}$_2$E:] by Lappert,[1,2] the development of group 14 element complexes L_2E (E = Si-Pb) gained enormous research interest. The group 14 element centre exists in the +2 oxidation state in these compounds and they are often called tetrelenes or metallelenes. These tetrelenes have great importance in fundamental chemistry due to their similarities as well as differences when compared to carbenes.

To date, there have been several reports on the synthesis and reactivities of heavier tetrelenes.[3] These complexes have been shown to participate in small molecule activation and catalytic transformations.[4–8] In particular, the N-donor heavier carbene analogues gained significant attention due to their easy ligand access. The employed ligands also result in considerable differences in electronic properties and reactivities in these N-donor complexes in comparison to other heavier carbene analogues.

The introductory sections of this chapter details the synthesis of bulky bis(amide) and nitrogen bridged bis(amidinate) ligands. Further, the relevance of these nitrogen donor ligands towards the isolation of low oxidation state heavier group 14 element(II) tetrelenes and the reactivity of such carbene analogues will be discussed.

4.1.1 Bis(amide) Ligands

Amide ligands are closely related to the cyclopentadienyl anion. The electronic and steric properties of these ligands can be easily altered by small modifications on the nitrogen substituents. These modifications and development of mono amide ligands have largely been discussed in chapter 2 and bis(amide) ligands will be the major focus in this chapter. Bis(amides) are dianionic nitrogen donors of type [{NR(linker)NR'}$^{2-}$]. These ligands contain two monomeric amide fragments which are typically connected via organic

linker groups. The bridging linker group can enable cooperative effects upon complexation to main group element which, in turn, can directly influence the steric and electronic properties of the synthesised complex and reactivity of the resulting main group element centre towards various substrates.

The bis(amides) can be divided into two categories based on the linker groups- **a**) alkyl/aryl linker based ligands, and **b**) aryl-silyl ligands. The former were synthesised by reacting an alkyl/aryl amine with glyoxal solution, followed by reduction or 1,2-addition reaction, or by reacting the respective bridged dihalide species with lithiated amine (**Scheme 4.1**).[9–12]

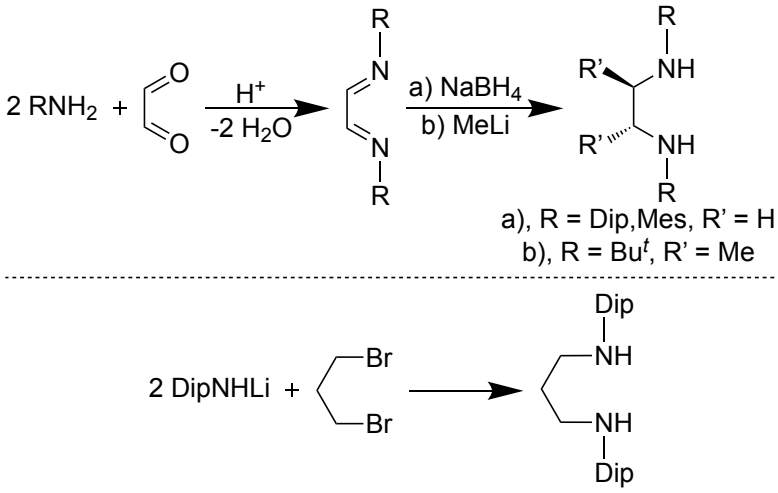

Scheme 4.1. Synthesis of aryl/alkyl bridged bis(amine) pro-ligands.

Aryl-silyl bis(amide) ligands are well known for their unique coordination properties in main group element chemistry and have been used for a number of low-coordinate main group element complexes. The synthesis of these ligands varies according to the bridging group and silyl substituents. The general synthetic routes are- **1**) the reaction of two equivalents of lithium amide R'NHLi with one equivalent of a bridged chlorosilane species [ClSi(R_2)-linker-Si(R_2)Cl], and **2**) treatment of trimethyl silyl chloride with dilithiated bis(amide) (**Scheme 4.2**).[13,14]

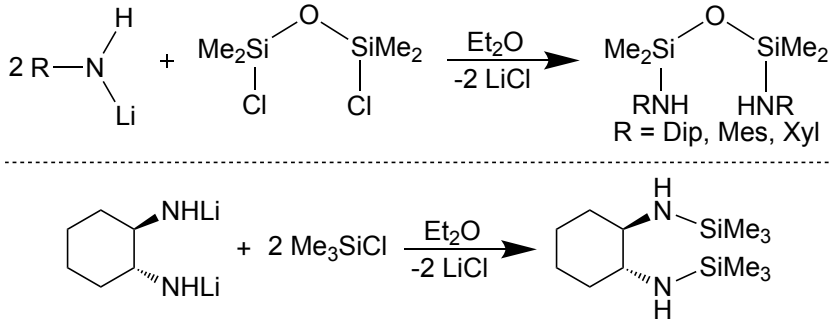

Scheme 4.2. Synthesis of aryl-silyl bis(amine) pro-ligands.

There have been a variety of bis(amide) ligands synthesised based on alkyl/aryl and aryl-silyl linkers such as ferrocenyl, -$(CH_2)_3$-, and phenyl to name a few (**Figure 4.1**).[15–22] The synthetic procedures for these ligands varies according to the linker groups. The incorporation of aryl groups into the backbone of these ligands increases the rigidity as well as the bulk of the ligands. Phenyl bridged bis(amide) ligands can exhibit ambidentate behaviour, similar to cyclopentadienyl bridged ligands. Furthermore, they can show metal coordination via their aromatic π-electron system or σ-coordination of amino group, or a combination of both with transition metals.[23,24] Contrary to that, for main group element complexes except alkali metals,[25,26] the isolated complexes are limited to utilisation of σ-coordination and there are no complexes known with a η^6 π-interaction so far.

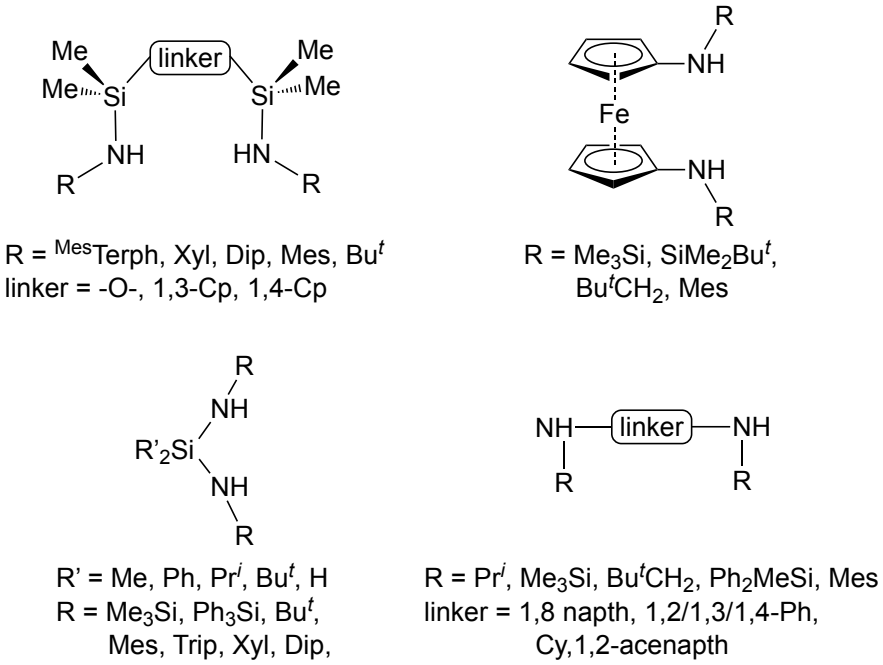

Figure 4.1. Reported bis(amine) pro-ligands in literature.

4.1.2 N-Bridged Bis(amidinate) Ligands

Two types of bis(amidinate) ligands, namely N-bridged and backbone bridged, have been used in main group element chemistry. The synthesis and chemistry of backbone bridged bis(amidinates) is discussed in chapter 3 while this section will only cover the N-bridged bis(amidinate) ligands. In general, N-bridged bis(amidinates) can be accessed by four routes[27]- (**i**) reaction of bis(carbodiimide) with R'EX_n (R = alkyl or aryl, E = main group element, X = halogen, n = 0, 1, 2) type organometallic compounds, followed by a hydrolysis step, (**ii**) treatment of imidoyl chloride with primary bis(alkyl) or bis(aryl) amines [H_2N-linker-NH_2], (**iii**) reacting bis(imidoylchloride) with two equivalents of primary alkyl or aryl amines [R'NH_2] in presence of a base, and lastly (**iv**) by addition of alkyl or aryl nitrile species to bis(secondary) metallated amines (**Scheme 4.3**).

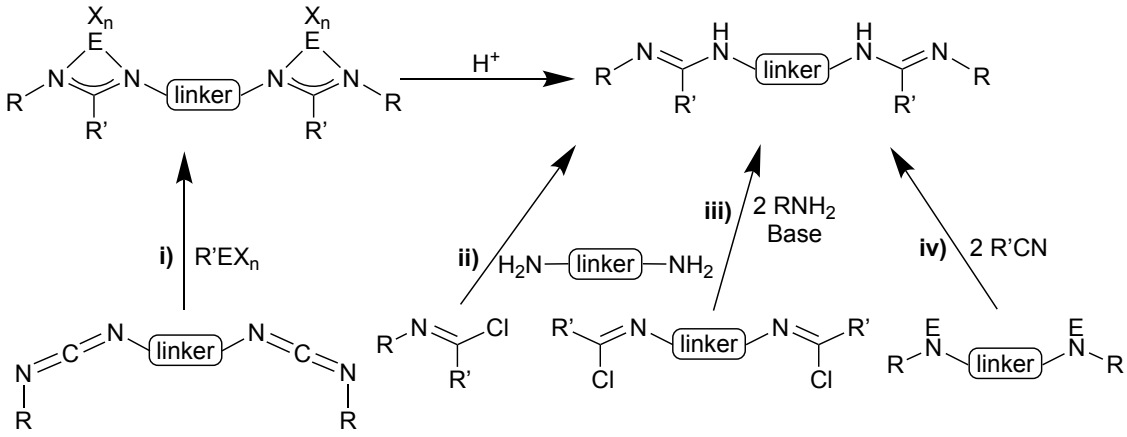

Scheme 4.3. Synthetic routes to N-bridged bis(amidine) pro-ligands.

The first route is restricted to only a few examples due to the synthetic limitations of bis(carbodiimides). However, it offers the direct formation of aluminium and zirconium complexes with more than 80 % isolated yields.[28,29] Route (**ii**) is beneficial for the synthesis of ligands with various linkers, but only few reports are available. The most convenient and widely used route is (**iii**), as it gives access to most of the ligands with varying backbone (R') and terminal (R) substituents. However, the least preferred route is (**iv**) which has not received much success in synthesising the bis(amidines), and only a few ligands have been accessed using this approach.[30]

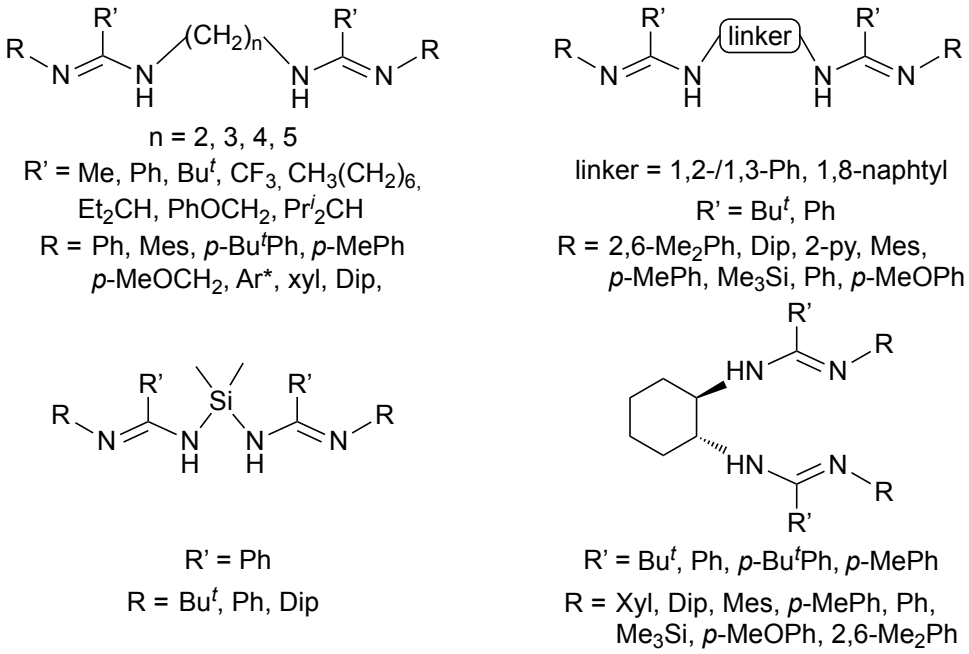

Figure 4.2. Reported N-bridged bis(amidine) pro-ligands.

Several bulky R and R' groups have been employed to change the electronic and steric properties of these ligands. Examples of N-bridged bis(amidine) pro-ligands with bridged linkers -C_2H_4-, -C_3H_6-, -C_5H_{10}-, -1,2-C_6H_{10}-, -$Si(CH_3)_2$-, 1,8-napthyl are given in **Figure 4.2**.[14,30–38]

4.1.3 Bis(amide) and Bis(amidinate) Coordinated Group 14 Element(II) Tetrelenes

The heavier carbene analogues are non-linear, divalent, singlet species of type R_2E (E = Si-Pb). The element centre E contains a lone pair of electrons and a vacant p-orbital. Bridged bis(amides) have been widely explored for the formation of heavier group 14 element(II) cyclic monomeric tetrelene complexes. These ligands provide various bidentate coordination modes upon complexation with group 14 element centres (**Figure 4.3**). The first mode **A** involves *N,N'*-chelation of the dianionic ligand to the element centre, and has been commonly seen for bis(amido) heavier tetrelenes.[15] Coordination mode **B** is similar to **A**, however, in this a central donating atom in bridging linker contributes to overall bonding to generate a κ-*N,X,N'*- (X = donating atom) tridentate mode. This mode has been observed for d-block elements with NON type ligands.[39] Lastly, the bridging mode **C**, in which the ligand can connect to two element centres, is common for group 1 and group 14 elements.[40,41] Similar coordination modes have also been seen for bis(amidinate) ligands and are well described in chapter 3.

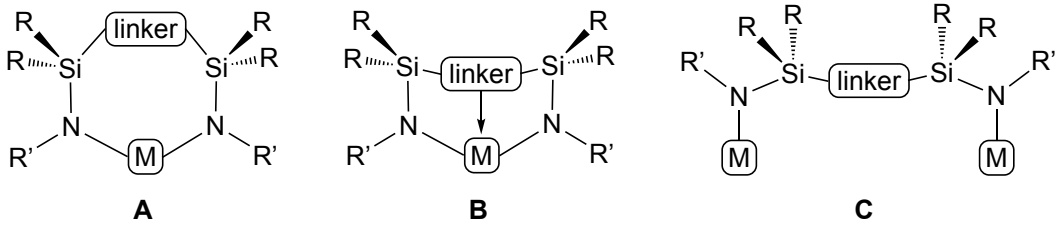

Figure 4.3. Common coordination modes of bis(amide) ligands.

The chemistry of cyclic tetrelenes, utilising bifunctional (diamino-substituted) ligands, has been an active area of research. These systems provide extra stability to the element centre as a result of cyclisation which gives rise to a chelating effect. The general synthesis of heavier tetrelenes involve the reduction of element(IV) complexes using reducing reagents such as KC_8, K/Na, naphthalenide, or treatment of EX_2 species with bifunctional alkali metal salts of the appropriate ligand (**Scheme 4.4**).

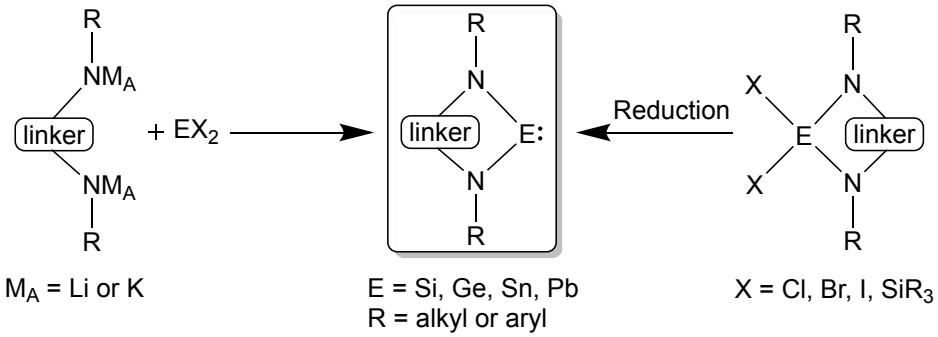

Scheme 4.4. General synthetic methods for heavier cyclic tetrelenes.

The first heavier N-donor cyclic tetrelene analogue was synthesised by Veith et al. in 1975. They synthesised a four-membered stannylene by reacting the lithiated ligand $Bu^tN(Li)SiMe_2N(Li)Bu^t$ with one equivalent of tin(II) chloride (**Scheme 4.5**).[42,43] Later in 1982, four-membered cyclic germylene and plumbylene were also isolated using similar synthetic procedure.[44] In addition to that, a corresponding silylene has been detected using a similar ligand system but was found to be stable only up to 77 K.[45]

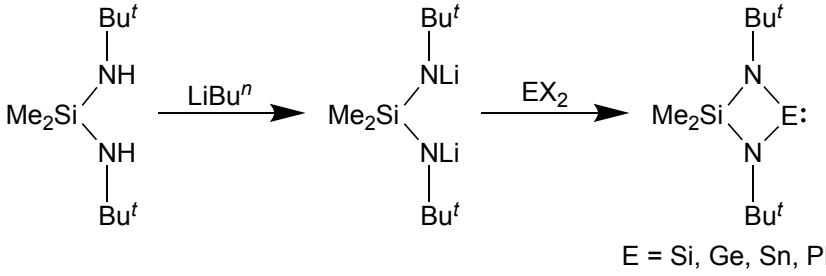

Scheme 4.5. Synthesis of cyclic tetrelenes (Si-Pb).

Since the isolation of the first cyclic tetrelene, a series of stable heavier main group element carbene analogues based on saturated and unsaturated backbones like -CH_2CH_2-, benzene, naphthalene, annulated derivatives have been developed (**Figure 4.4**).[3,46–48]

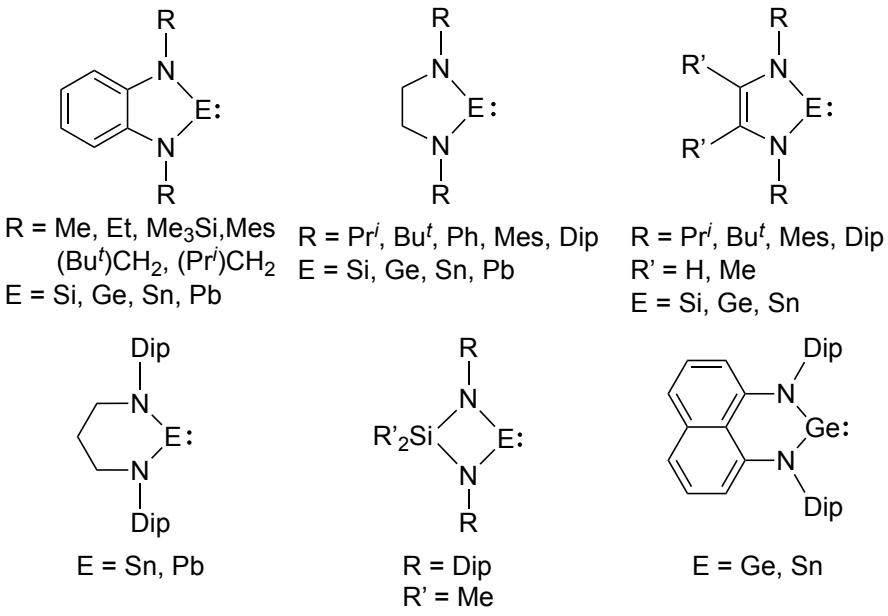

Figure 4.4. Examples of reported cyclic tetrelenes in literature.

Different from the previous tetrelenes, Lappert and co-workers isolated red coloured crystals of cyclic bis(stannylene) [1,3-Ph{$N(SiMe_3)$}$_2$Sn]$_2$ by reacting a phenyl bridged dilithium bis(amido) salt [1,3-Ph{$N(SiMe_3)$}$_2$Li]$_2$ with equimolar [{Sn(μ-Cl)$N(SiMe_3)_2$}$_2$] (**Scheme 4.6**).[40,41] This complex comprises two bis(amide) ligands bridged between two tin centres forming a meta-bis(stanylamino)cyclophane. It showed a singlet ^{119}Sn{^{1}H} NMR peak at δ 505 ppm which is upfield chemical shift compared to the heavier bis(stannylene) congener [1,4-Ph{$(SiMe_3)NSnN(SiMe_3)_2$}$_2$] (δ = 606 ppm).[49]

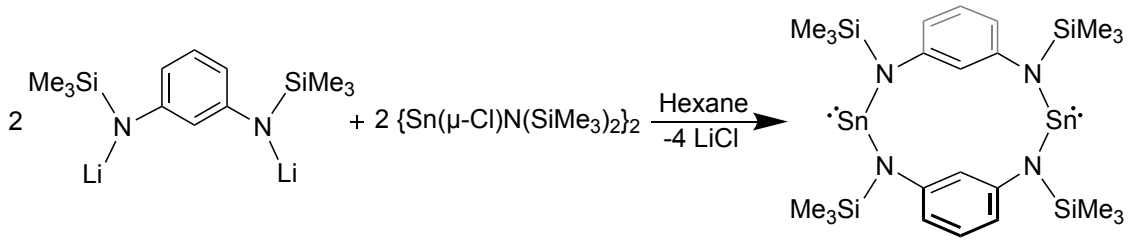

Scheme 4.6. Synthesis of a cyclic bis(stannylene).

Although the chemistry of heavier tetrelenes has attracted considerable attention, only limited examples of bis(tetrelenes) are known in literature. It is worth nothing that

another class of bis(tetrelenes) was also first introduced by Lappert and co-workers. They synthesised a bis(silylene) by dehalogenation of bis(dichlorosilane) precursor with KC_8 (**Scheme 4.7**).[50] In this bis(silylene) species two bis(amido) ligands stabilised silylene moieties were connected via a biphenyl linker group. The geometrical parameters of each silylene fragment in this compound were found to be close to those of the monomeric congeners.[51] However, the PhN_2Si fragments were not found to be in same plane, but twisted by 30.3(1)° angle.

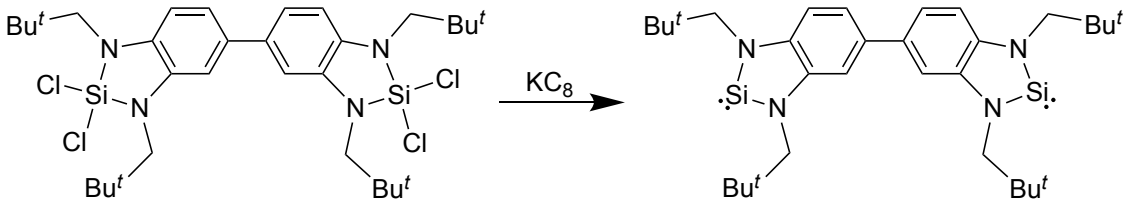

Scheme 4.7. Synthesis of the first tetra(amido) bis(silylene).

Further, such types of compounds have largely been developed in Hahn's group by utilising a series of alkyl or aryl bridging linkers based tetra(amide) ligands to synthesise several heavier bis(tetrelenes) by direct salt metathesis reactions. A few examples of these complexes are given **Figure 4.5**.[52–59]

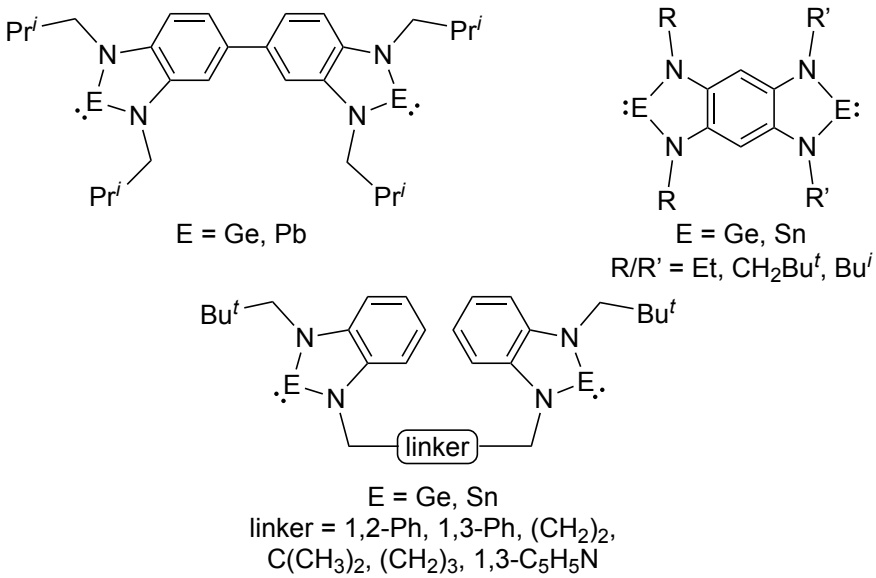

Figure 4.5. Examples of tetra(amido) bis(tetrelenes).

It was observed that the less bulkier nitrogen substituent and longer bridging group based bis(tetrelenes) exhibit a weak intermolecular E---E interaction ($(CH_2)_5$, bridging group based bis(germylene) Ge---Ge = 3.577(2) Å) which leads to a polymeric structure. In

contrast, the tetrelenes with shorter bridging groups show an intramolecular E---E interaction (e.g. 1,3-C_5H_5N bridging group based bis(germylene) Ge---Ge = 3.041(5) Å).

Amidinate ligands have been used to stabilise a series of mononuclear group 14 element(II) halide species and are discussed in detail in chapter 3. However, only few reports of germylene and silylene species, are available (**Scheme 4.8**). Interestingly, these species have been isolated in case of less bulky substituents on the nitrogen atom in the ligand framework. In this regard, silicon(II) species have been synthesised by the reductive HCl elimination reaction of silicon(IV) compound with $KN(SiMe_3)_2$.[60] In contrast, the synthesis of germanium(II) species proceeded via the reaction of two equivalents of respective amidinate lithium salt with one equivalent of germanium(II) chloride species.[61,62]

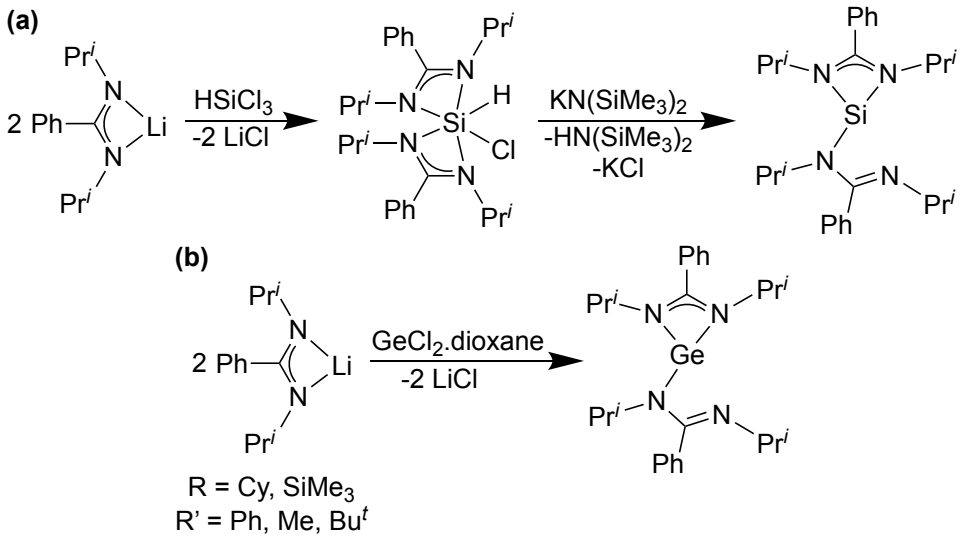

Scheme 4.8. Synthesis of silicon(II) (**a**) and germanium(II) (**b**) species.

Meanwhile, N-bridged amidinate coordinated group 14 element(II) species are still unknown. However, Kretschmer and co-workers have recently isolated N-bridged bis(amidinate) coordinated magnesium(II) complexes. They reacted various bis amidinate and guanidinate ligands with $MgBu^n_2$, $Mg(SiMe_3)_2$ and CH_3MgI affording several dinuclear magnesium species (**Scheme 4.9**).[63] All of these reactions (except CH_3MgI with $-(CH_2)_2-$ linker based ligand) formed either complex mixtures or homoleptic magnesium(II) complexes which illustrate the importance of electronic and steric features in the ligand framework. These complexes were isolated in more than 60 % yields. All of these complexes were dimeric (except the CH_3MgI reaction product) and

the bond lengths and bond angles were found to be similar to previously reported mononuclear magnesium species.[64,65]

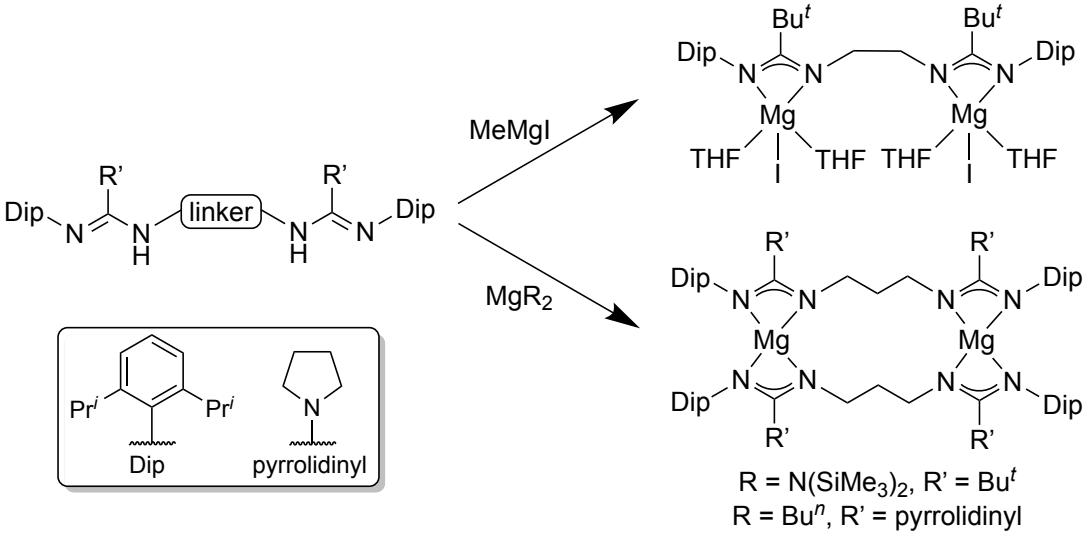

Scheme 4.9. Synthesis of nitrogen bridged bis(amidinato) magnesium compounds.

4.1.4 Reactivity of Heavier Tetrelenes and Bis(tetrelenes)

Based on their electronic structure, heavier tetrelenes are capable of both electrophilic and nucleophilic reactions due to their σ-donor and π-acceptor properties. The mechanism of σ- and π-bond activation by tetrelenes involves the filled n-orbital and empty p-orbital centres. The n-orbital centre can donate the electron pair (Lewis base) while the p-orbital can accept electrons (Lewis acid). This allows the initial electrophilic attack at the p-orbital, which is followed by nucleophilic attack from the n-orbital lone pair (**Figure 4.6**).[66]

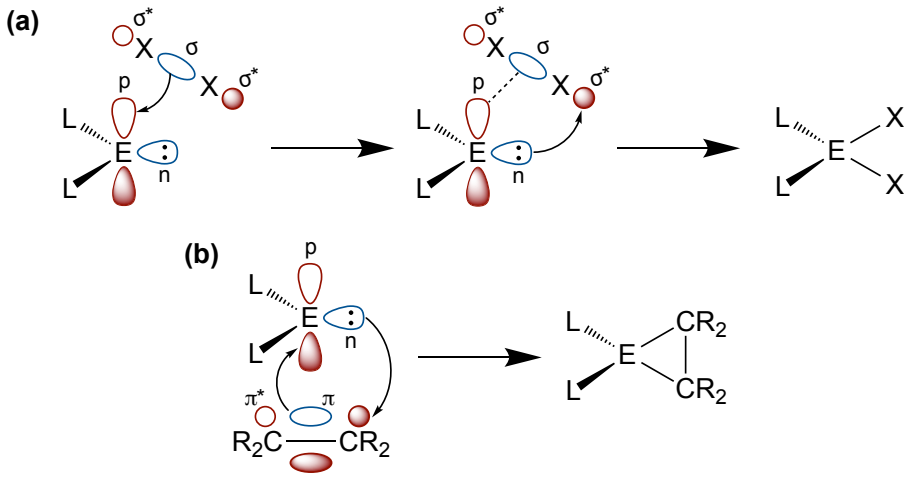

Figure 4.6. Mechanism for tetrelene activation of a σ-bond (**a**) and π-bond (**b**).

4.1.4.1 Reactions with σ-bonds

The evidence of initial reactivity of heavier amido tetrelenes(II) was reported by Lappert and co-workers in 1976. Various organic halide species, R-X, upon reaction with the tin(II) precursor [{$(Me_3Si)_2N$}$_2$Sn] under mild conditions in hexane gave oxidative addition products (**Scheme 4.10**).[67] The relative reactivities of the alkyl halides were found in the order RI > RBr > RCl. Moreover, the aryl halide ArI was found to be less reactive than the alkyl halide MeI due to the more stable Ar-X bonds.

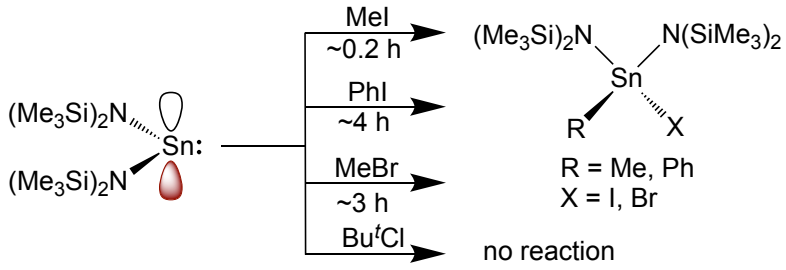

Scheme 4.10. Reactivity of an amido stannylene with various organic halides.

With the development of stable tetrelene chemistry, well-defined reactivity patterns started to emerge. Various stable cyclic tetrelenes were found to insert into σ-bonds to form terminal or bridged tetrelene(IV) products (**Scheme 4.11**).[46,47,68] Stable silylenes react with primary alcohols and water to afford alkoxysilane and disiloxane species, respectively. Similar to acyclic stannylenes the cyclic stannylenes also form oxidative addition products with MeI.

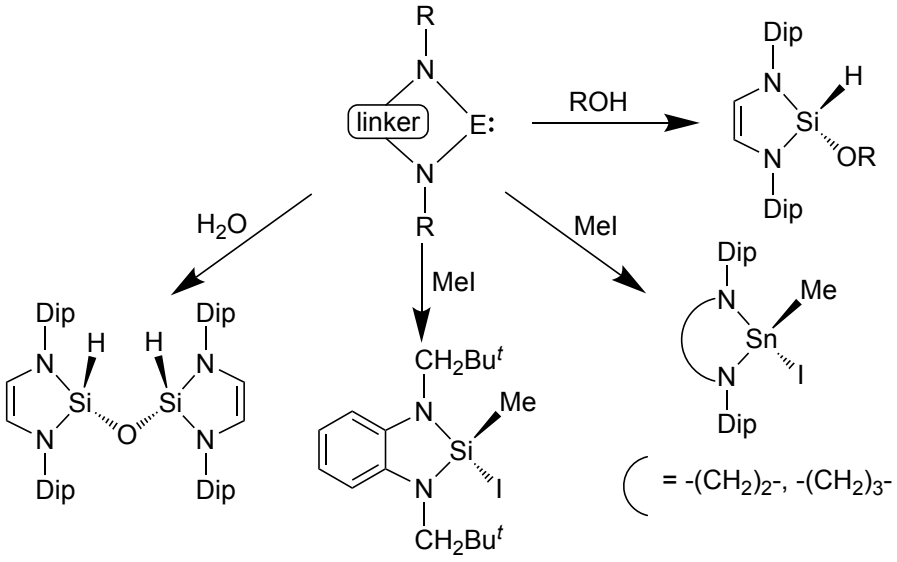

Scheme 4.11. Reactions of tetrelenes with σ-bonds.

4.1.4.2 Reactions with Chalcogens

In the following years, it was seen that heavier cyclic tetrelenes could react with elemental chalcogens to form bridged structures (**Scheme 4.12**). Interaction of a divalent cyclic germanium species [(Pr^i_2Si)(NDip)$_2$Ge] with chalcogen sources (Me_3NO and S_8) resulted in formation of oxo and sulphido bridged dimers. These complexes contain planar Ge_2X_2 (X = O, S) arrays.[15] In case of Veith's cyclic germylene, the reaction with Me_3NO forms a trimeric complex [{(Me_2Si)(NBu^t)$_2$Ge(μ-O)}$_3$] due to the reduced steric bulk at nitrogen and silicon centres.[69] Further, the reaction of the germylene [{(Me_2Si)(NDip)$_2$Ge}] with O_2 was expected to produce a germanone ($R_2Ge{=}O$), however due to the highly polar nature of Ge=O π-bond, a dimerization occurs to yield an oxo bridged complex which involves σ-linkages.[70] Silylenes and stannylenes reaction have also been reported to form similar bridged chalcogenides upon reacting with S_8, Se, Et_3PSe, Et_3Pte.[46,68]

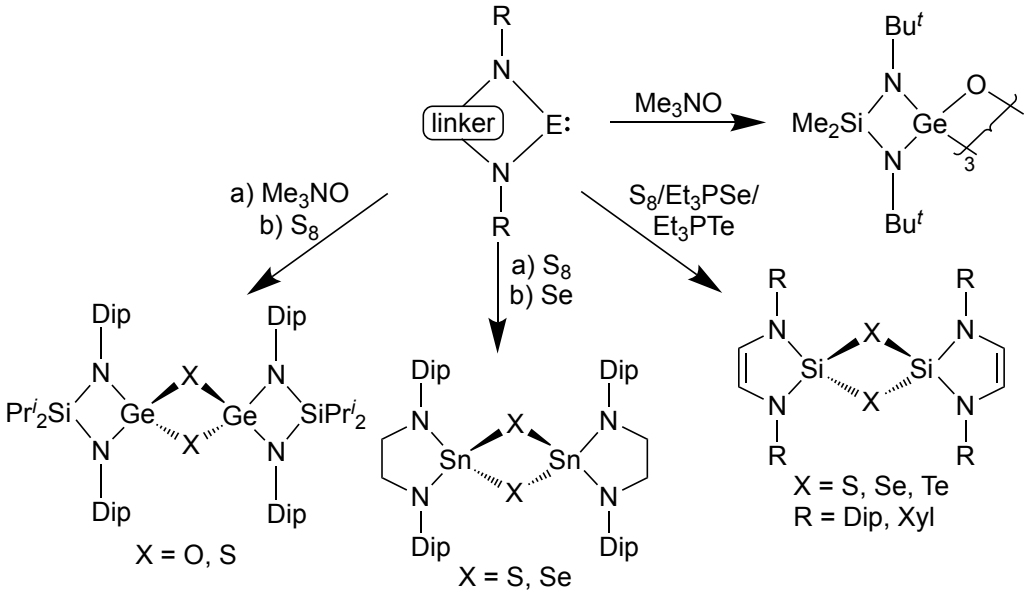

Scheme 4.12. Reactions of tetrelenes with chalcogens.

4.1.4.3 Reactions of Tetra(amido) Bis(teterelenes)

Tetra(amido) germylenes and stannylenes based on -$(CH_2)_5$- and -$CH_2C(CH_3)_2CH_2$- linkers were found to be capable of coordinating to transition metals. Upon reacting these complexes with [$Mo(CO)_4$(nbd)] (nbd = norbornadiene), the isolation of heteroleptic chelating complexes were observed, which were characterised by X-ray crystallography (**Scheme 4.13**).[71] These complexes contain a molybdenum atom coordinated by two tetrelene units and four CO ligands forming [Mo(η^2-bistetrelene)CO_4]. These complexes

formed due to the alkyl linker groups which make them flexible enough to coordinate to the molybdenum metal centre. All of these heavier carbene complexes not only act as σ-donors due to their Lewis basicity but also function as π-acceptors because of the Lewis acidity of empty p-orbital.

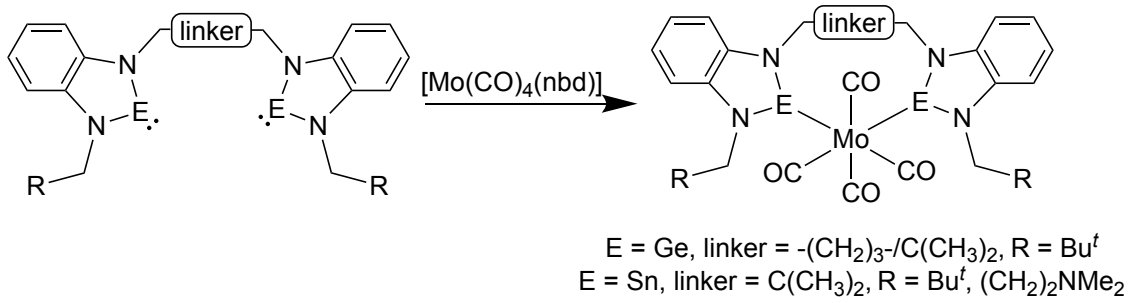

Scheme 4.13. Reactions of bis(tetrelenes) with $[Mo(CO)_4(nbd)]$.

4.2 Research Proposal

Given the literature precedent for low oxidation state tetrelene complexes, it seems plausible to suggest that these complexes can be stabilised by increasing the steric encumbrance of the ligands. In the past, a number of low oxidation state group 14 tetrelenes have been isolated, however, the area of heavier bis(tetrelenes) remains relatively unexplored. Thus, expanding this chemistry is a desirable goal.

In order to widen the ligand library, the starting point is the synthesis of various bulky bis(amide) and bis(amidinate) ligands with larger bridging groups. For comparison purposes, the bridging backbones with both alkyl and aryl groups were chosen so that the synthesised ligands, upon complexation with group 14 elements, will be more stable with minimum steric repulsion and optimum steric encumbrance. For bis(amide) ligands, di(aminodimethylsilyl)ethyl and diamino ethyl groups were selected as ligand skeletons to retain a similar electronic configuration as previously reported amido donor groups. Further, to increase the degree of structural rigidity and steric bulk on the silyl amide ligands, introduction of phenyl bridging and Pr^i_3Si- silyl end groups were proposed. The above-mentioned ligands will be utilised to synthesise heavier cyclophanes by reacting their lithium salts with equimolar EX_2 complexes (E = Ge, Sn, Pb, X = Cl, Br)(**Scheme 4.14**). Additionally, the use of N-bridged bis(amidinate) ligands for stabilising group 14 and group 2 element complexes will also be explored.

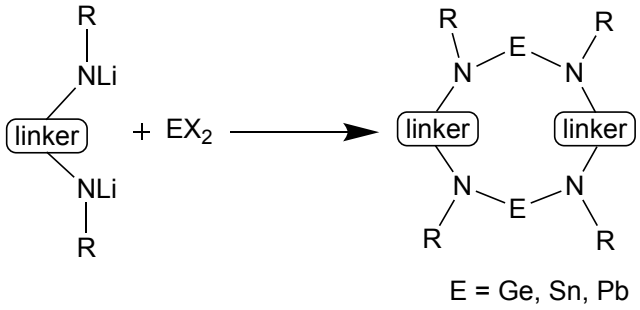

Scheme 4.14. Synthesis of group 14 element heavier cyclophanes.

4.3 Results and Discussion

4.3.1 Synthesis of Ligands

Given the knowledge of synthesis of binuclear ligands, we sought to expand the current range of available ligands of this class and to further use them in stabilising low oxidation state bis(tetrelenes). The following sections are segmented into alkyl bridged bis(amine), alkyl/aryl-silyl bridged bis(amine) and N-bridged bis(amidine) pro-ligands, where each section will dwell upon the particular type of ligand precursor. Each of these pro-ligands were spectroscopically characterised and further reacted with group 14 element halides.

To study the effect of bridging linkers on the overall bulk of the ligands and synthesised group 14 element complexes, earlier reported flexible bridging backbone linkers [-CH_2CH_2-] (**L1**), and [-$(Me_2)SiCH_2CH_2Si(Me_2)$-] (**L2**) as well as rigid bridging backbone linkers [-$(Me_2)Si(1,4\text{-}Ph)Si(Me_2)$-] (**L3**), [-NH(1,4-Ph)NH-] (**L4**) and [-NH(1,3-Ph)NH-] (**L5**) were chosen. Further, in order to synthesise the bis(amine) pro-ligands we chose to utilise the bulky anilines [$DipNH_2$] (Dip = 2,6-Pr^i_2Ph) (**1**), [Dip^YNH_2] (Dip^Y = 2,6-Pr^i_2-4-Pr^iPh) (**2**), [Dip^+NH_2] (Dip^+ = 2,6-Pr^i_2-4-Bu^tPh) (**3**), [Ar^*NH_2] (Ar^* = 2,6-$(Ph_2CH)_2$-4-MePh) (**4**), [$Ar^\dagger NH_2$] ($Ar^\dagger$ = 2,6-$(Ph_2CH)_2$-4-Pr^iPh) (**5**), diamines [1,4-$Ph(NH_2)_2$] (**6**), [1,3-$Ph(NH_2)_2$] (**7**), bis(chlorosilanes) [$Cl(Me_2)SiCH_2CH_2Si(Me_2)Cl$] (**8**), [$Cl(Me_2)Si(1,4\text{-}Ph)Si(Me_2)Cl$] (**9**) and chlorosilanes [$Me_2PhSiCl$] (**10**), [Ph_3SiCl] (**11**), [Pr^i_3SiCl] (**12**). These bulky anilines were chosen on the basis of their increasing bulk and were synthesised from literature procedures.[72–75] The bis(chlorosilanes) were considered because of the flexibility and rigidity of linker groups and were used as received from commercial sources.

4.3.1.1 Aryl Bridged Bis(amines)

For the synthesis of aryl bridged pro-ligands we sought to use the flexible linker [-CH_2CH_2-] (**L1**) due to the straightforward synthetic route to these linker based ligands reported in literature.[74,76] The initial step involved the synthesis of [^{Dip}DAB] and [^{Ar*}DAB] by treating glyoxal with two equivalents of the corresponding primary anilines [$DipNH_2$] (**1**) and [Ar^*NH_2] (**4**), generating the desired diazabutadienes **13** and **14**. These diazabutadienes were then reduced with $NaBH_4$ and $LiAlH_4$ to form [1,2-$(DipNH)_2$L1] (**15**) and [1,2-$(Ar^*NH)_2$L1] (**16**) pro-ligands, respectively (**Scheme 4.15**).[77]

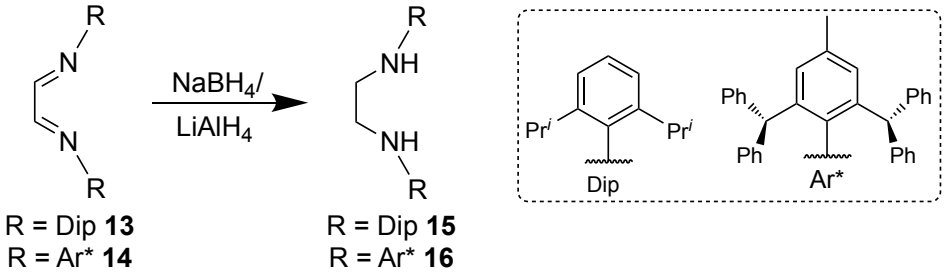

Scheme 4.15. Synthesis of bridging bis(amine) pro-ligands **15** and **16**.

The formation of these ligands was confirmed by ^{1}H NMR spectroscopy. Further, the pro-ligand **16** was crystallised from a toluene/pentane solution and the crystal structure is depicted in **Figure 4.7**.

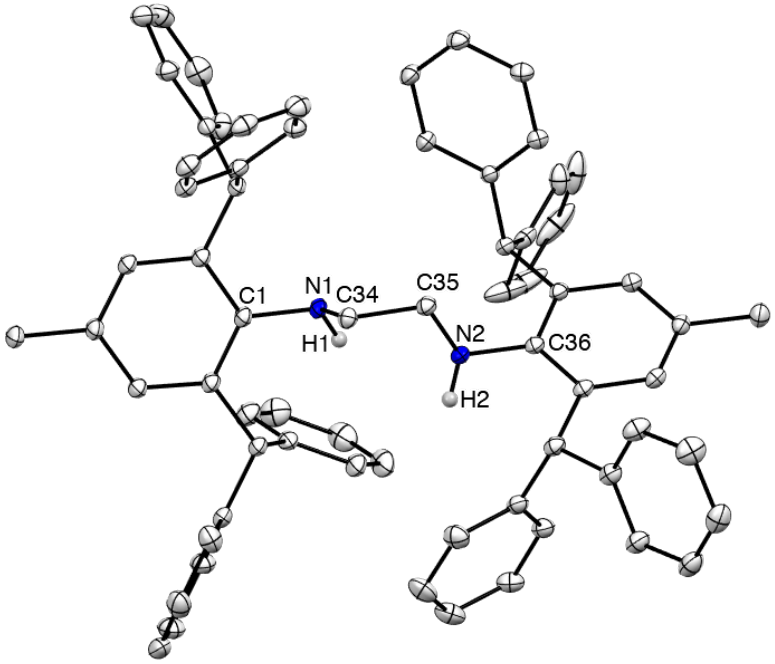

Figure 4.7. Molecular structure of [1,2-$(Ar^*NH)_2$L1] (**16**) (thermal ellipsoids shown at 20 % probability). Hydrogen atoms except H1 and H2 are omitted for clarity. Selected bond lengths

(Å) and angles (°): N1-C1 1.430(3), N2-C36 1.427(3), N1-C34 1.464(3), N2-C35 1.470(3), C34-C35 1.505(3), C1-N1-C34 111.90(18), C36-N2-C35 114.57(19).

4.3.1.2 Alkyl/Aryl-Silyl Bis(amines)

As discussed in chapter 2, silyl amide groups have proven to be excellent ligands for stabilising main group element centres due to the possibility of easy steric and electronic modifications. In the development of aryl/alkyl-silyl bis(amine) pro-ligands, three points of obvious modification are: bridging linkers, silyl groups and substituted anilines.

With several anilines and chlorosilanes at our disposal, the novel alkyl/aryl-silyl ligands were targeted. For the synthesis of **L2** and **L3** linkers based ligands, the literature reported procedures were adopted and the synthetic protocol is outlined in **Scheme 4.16**. The general synthesis started with the lithiation of desired aniline with $LiBu^n$ in diethyl ether, forming the lithium amide, which was further quenched with half an equivalent of corresponding bridged bis(chlorosilane) species Cl-linker-Cl (linker = **L2**, **L3**). This method allowed the isolation of clean pro-ligands [{(Dip)NH}$_2$L2] (**17**) (the ligand was not published prior to this work), [{(Dip^Y)NH}$_2$L2] (**18**), [{(Dip$^+$)NH}$_2$L2] (**19**) and [{(Ar†)NH}$_2$L3] (**20**) in yields of more than 60 %.

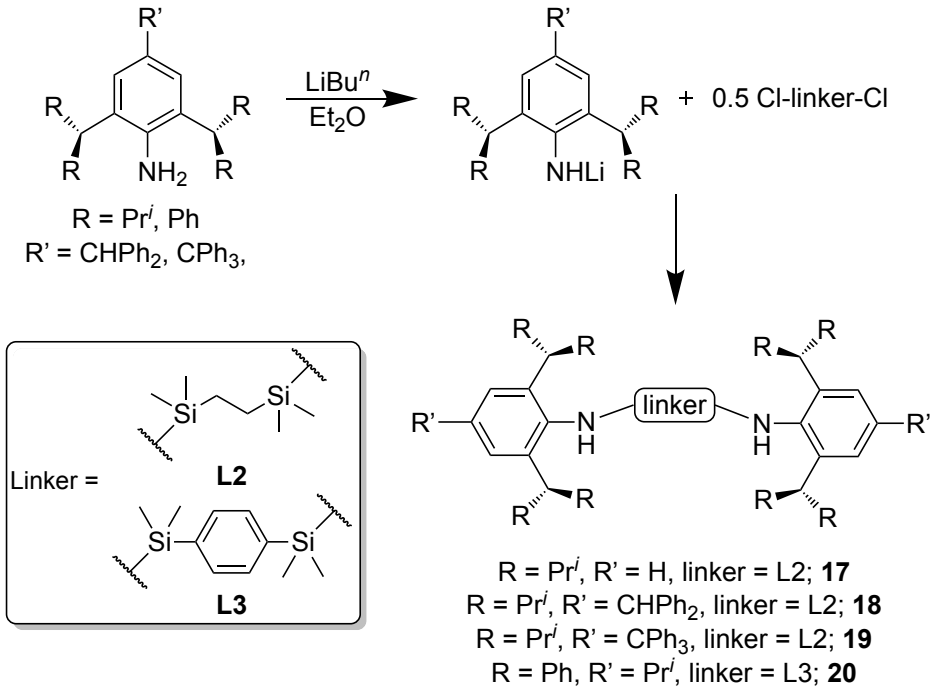

Scheme 4.16. Synthesis of pro-ligands **17**-**20**.

Crystals of pro-ligand **17** were grown from a pentane solution and the molecular structure is displayed in **Figure 4.8**. Ligand **17** has a centre of inversion and therefore possesses

single N-Si and N-H bond lengths. The two Dip groups are in a trans configuration to each other in order to minimise the steric repulsion arising from the Dip substituents.

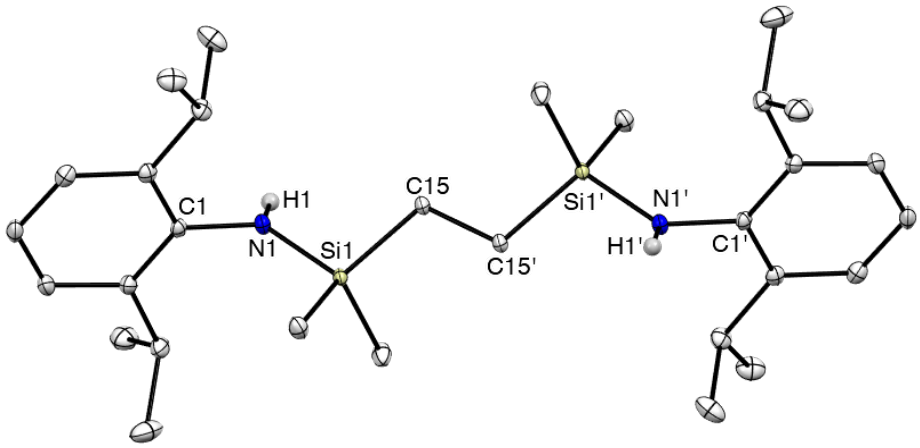

Figure 4.8 Molecular structure of [{(Dip)NH}$_2$L2] (**17**) (thermal ellipsoids shown at 30 % probability). Hydrogen atoms except H1s are omitted for clarity. Selected bond lengths (Å) and angles (°): C1-N1 1.4332(19), Si1-N1 1.7282(13), Si1-C15 1.8724(14), N1-Si1-C15 108.58(6).

In case of reactions of bis(chlorosilane) **8** with **4.Li** and **5.Li**, the reaction mixtures showed the absence of NH proton signals in ^{1}H NMR spectra (**Scheme 4.17**). Moreover, only half of the expected number of overall proton resonances for aniline groups were observed, which hint at the formation of single aniline substitution products. In fact, when the products of these reaction mixtures were crystallised, the cyclic products [(Ar*N)L2] **21** and [(Ar†N)L2] **22** were isolated (**Figure 4.9**).

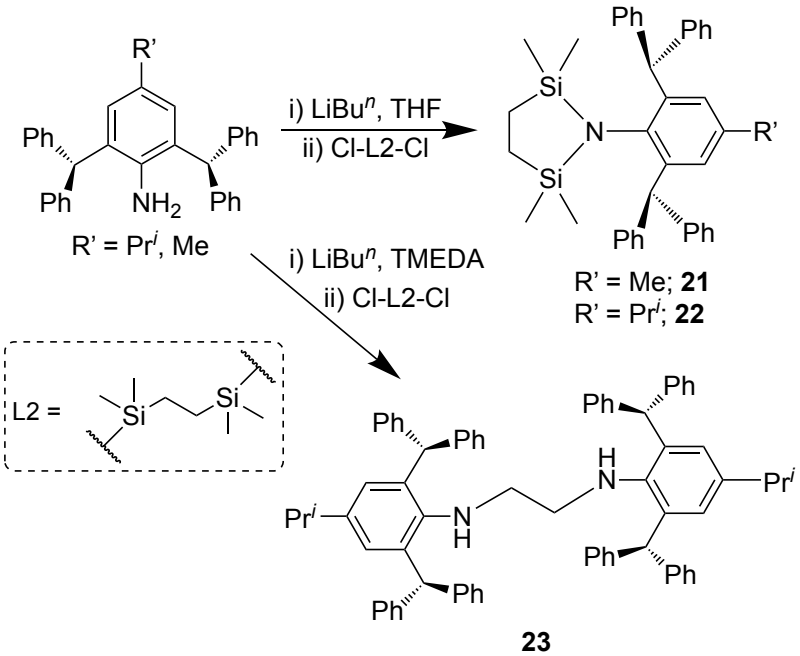

Scheme 4.17. Synthesis of cyclic products **21**, **22** and doubly substituted product **23**.

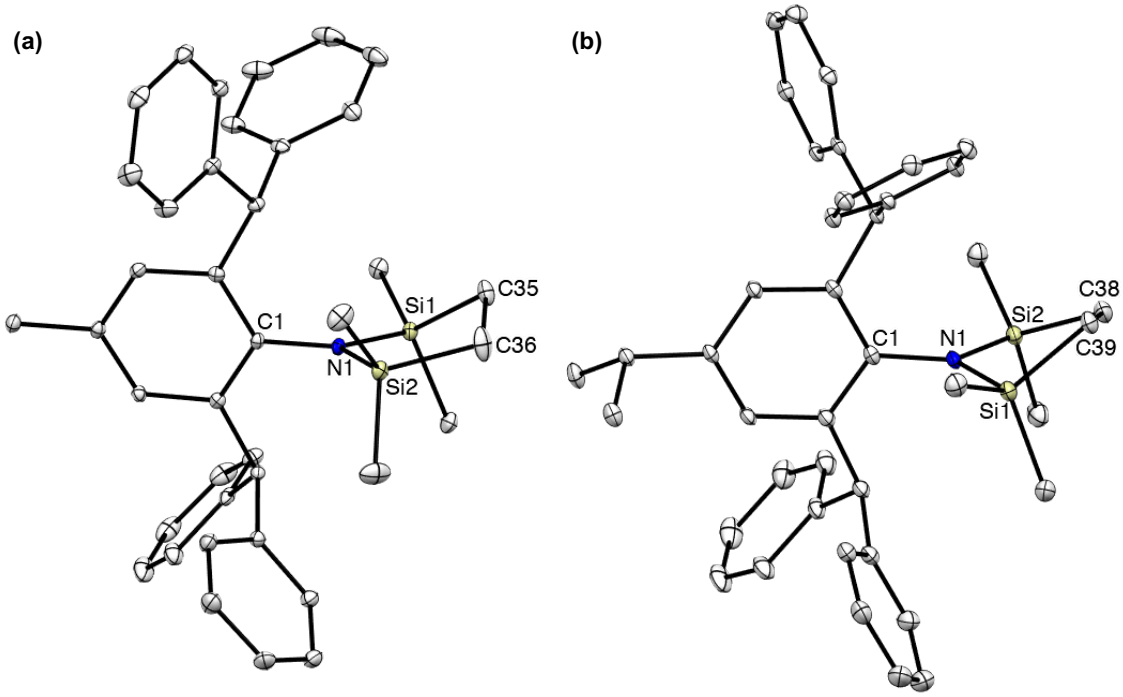

Figure 4.9. Molecular structures of [(Ar*N)L2] (**21**) (**a**) and [(Ar†N)L2] (**22**) (**b**) (thermal ellipsoids shown at 20 % probability). Hydrogen atoms omitted for clarity. Selected bond lengths (Å) and angles (°) for **21**: Si1-N1 1.7562(15), Si2-N1 1.7566(15), N1-C1 1.445(2), C35-C36 1.539(3), Si1-N1-Si2 110.03(8), N1-Si1-C35 98.81(8), N1-Si2-C36 99.15(8); **22**: Si1-N1 1.755(2), Si2-N1 1.740(2), N1-C1 1.434(3), C38-C39 1.526(5), Si1-N1-Si2 109.51(12), N1-Si1-C39 97.39(13), N1-Si2-C36 113.01(13).

These unexpected products **21** and **22** could have formed due to the deprotonation of the ArNH protons after the substitution of one aniline unit in **8**. This deprotonation resulted in more stable cyclised products to minimise the repulsion which could have been caused by bulkier ArNH (Ar = Ar* and Ar†) groups. To overcome this drawback, we proposed to use one equivalent of TMEDA (TMEDA = [{$(CH_3)_2NCH_2$}$_2$]) with LiBu^n for lithiation of anilines **4** and **5** (**Scheme 4.17**). This approach deoligomerises or deaggregates the hexameric LiBu^n and forms the more reactive monomer by coordinating to Li^+. Using this strategy, a disubstituted ligand **23** was crystallised from toluene which was further confirmed by the presence of one NH peak resonance integrating for two protons at δ 1.89 ppm in the ^{1}H NMR spectrum. It also showed a characteristic N-H stretch band at 3350 cm^{-1} in solid-state infrared spectrum. The crystal structure of **23** is displayed in **Figure 4.10**. Similar to **17**, the ligand **23** also possesses an inversion centre.

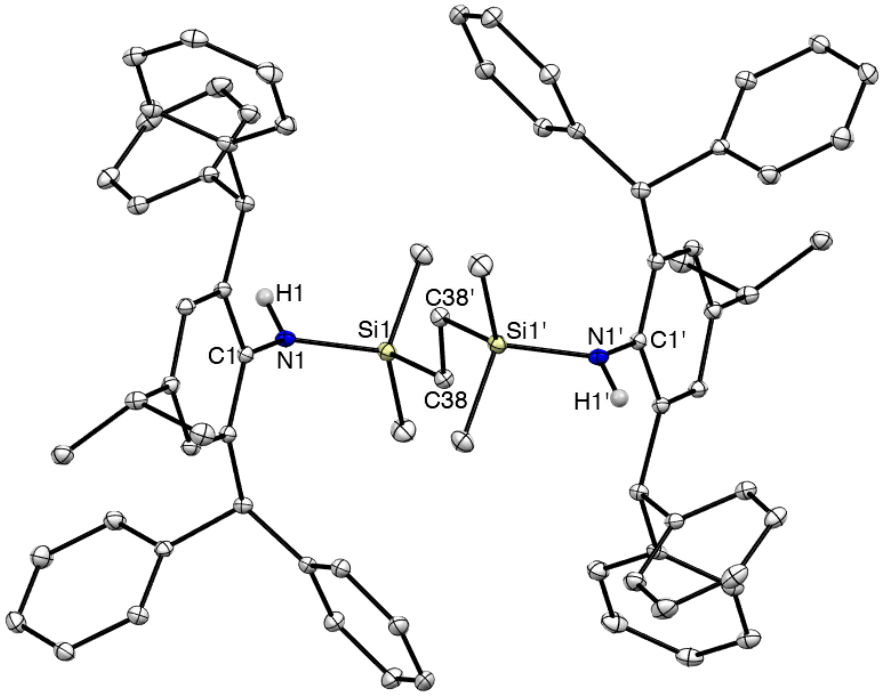

Figure 4.10. Molecular structure of [{(Ar†)NH}$_2$L2] (**23**) (thermal ellipsoids shown at 30 % probability). Hydrogen atoms except H1s are omitted for clarity. Selected bond lengths (Å) and angles (°): C1-N1 1.4208(16), Si1-N1 1.7411(11), Si1-C38 1.8675(14), N1-Si1-C38 110.03(6).

To avoid the above-mentioned single substitution problem, the use of a more rigid linker (phenylene) was also proposed. The synthesis of **L4** and **L5** linker based pro-ligands were slightly different compared to the **L3** based ligands. The diamines [1,4-Ph(NH$_2$)$_2$] (**6**) and [1,3-Ph(NH$_2$)$_2$] (**7**) were lithiated with two equivalents of LiBu^n, followed by reactions with bulkier chlorosilanes **10**-**12** (**Scheme 4.18**). The reactions of **6.Li** and **7.Li** with **10** and **12** resulted in doubly substituted ligands **24**-**27** in good isolated yields. The formation of ligands was also confirmed by the new resonances for silyl groups in ^{1}H NMR spectra. Reactions of **6.Li** and **7.Li** with **11** formed mixture of products which could not be separated by fractional crystallisation or by column chromatography.

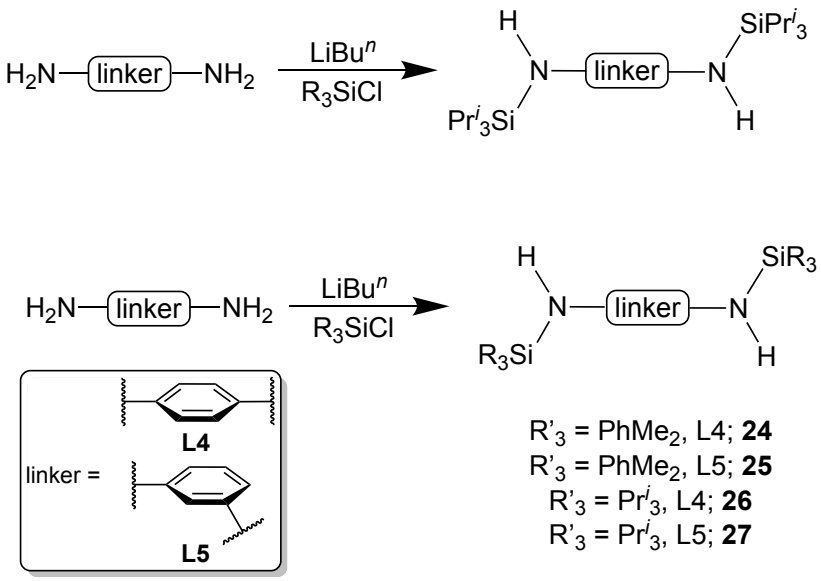

Scheme 4.18. Synthesis of pro-ligands **24-27**.

The ligand **25** was crystallised from a hexane solution (**Figure 4.11**) as a monomer in the solid-state with $PhMe_2Si$- groups situated trans to each other.

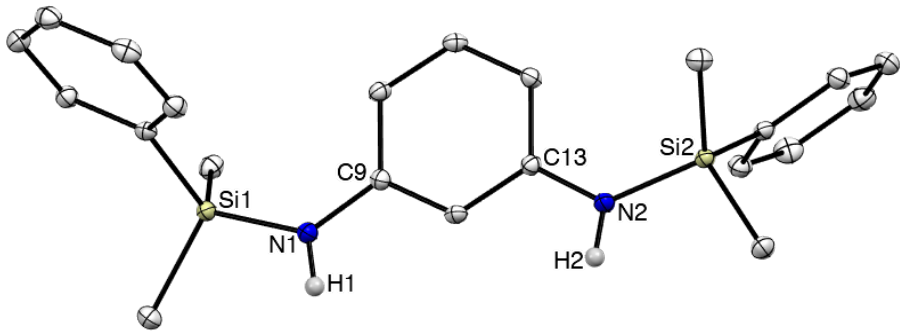

Figure 4.11. Molecular structure of [{$(Me_2PhSi)NH$}$_2$L5] (**25**) (thermal ellipsoids shown at 30 % probability). Hydrogen atoms except H1 and H2 are omitted for clarity. Selected bond lengths (Å) and angles (°): Si1-N1 1.7328(13), Si2-N2 1.7329(13), N1-C9 1.3988(19), N2-C13 1.3967(18), C9-N1-Si1 131.17(11), C13-N2-Si2 130.94(11).

4.3.1.3 N-Bridged Bis(amidines)

An N-bridged amidine pro-ligand was synthesised by the most versatile imidoylchloride method developed by Arnold.[38] The synthesis involved the initial reaction of two equivalents of Bu^tCOCl with [1,3-Ph$(NH_2)_2$] (**7**) in presence of Et_3N resulting in the formation of [(1,3-Ph)($Bu^tCONH)_2$] (**28**). This was further reacted with PCl_5 and the mixture was heated to reflux for one day to afford [(1,3-Ph)($NHC(O)Bu^t)_2$] (**29**). Finally, **29** was treated with two equivalents of $Ar^\dagger NH_2$ in the presence of Et_3N, and refluxed in toluene to give ligand [$(AmidAr^\dagger H)_2$L5] (**30**) in 80 % yield (**Scheme 4.19**). This ligand

was found to be insoluble in toluene or hexane and partially soluble in THF and chloroform, hence could not be further characterised by NMR spectroscopy. **30** was recrystallised as white coloured crystals from a THF/toluene mixture and the crystal structure shows all the bond lengths and bond angles within the same range of previous reported N-bridged amidine protonated ligands (**Figure 4.12**).[63]

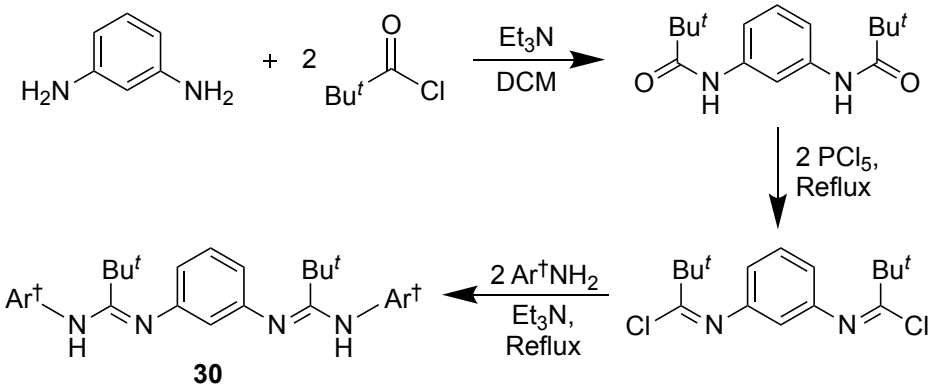

Scheme 4.19. Synthesis of nitrogen bridged bis(amidine) pro-ligand **30**.

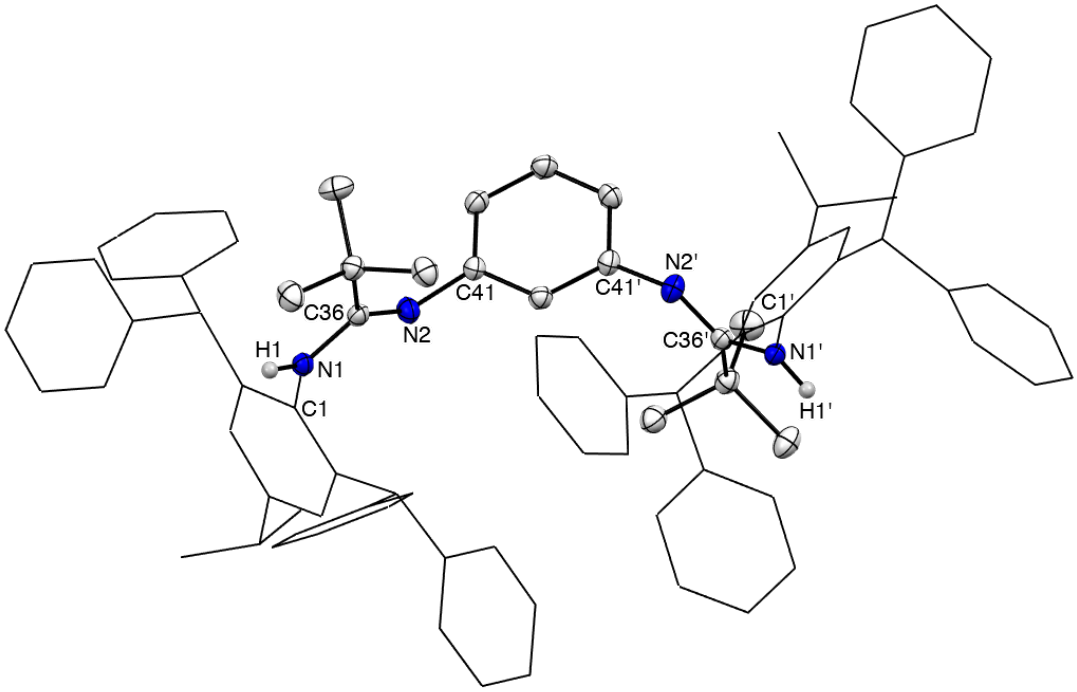

Figure 4.12. Molecular structure of [(AmidAr†H)$_2$L5] (**30**) (thermal ellipsoids shown at 20 % probability). Hydrogen atoms except H1s are omitted; Ar† groups shown as wireframe for clarity. Selected bond lengths (Å) and angles (°): N1-C1 1.422(3), N1-C36 1.345(3), N2-C36 1.301(3), N2-C41 1.408(3), N2-C361-N1 116.85(18), C36-N2-C41 131.35(19), C36-N1-C1 123.75(16).

4.3.2 Synthesis of Main Group Element Complexes

4.3.2.1 Lithiation of Synthesised Pro-Ligands

With several bis(amine) and the bis(amidine) pro-ligands in hand, we attempted to deprotonate these using two equivalents of LiBu^n or superbase (mixture of LiBu^n and KOBu^t) (**Scheme 4.20**). All of the pro-ligands, except **4**, were readily deprotonated *in situ* using an n-butyllithium solution in hexane, resulting in the corresponding bis(amido) dilithium salts **15.Li**, **(17-20).Li**, **(23-27).Li** and bis(amidinato) dilithium salt **30.Li**. Only ligand **4** could not be deprotonated even after multiple trials using superbase or KH/KHMDS. Further, it was possible to grow crystals of the THF adduct of **17.Li** from a 15:85 THF/hexane solution mixture.

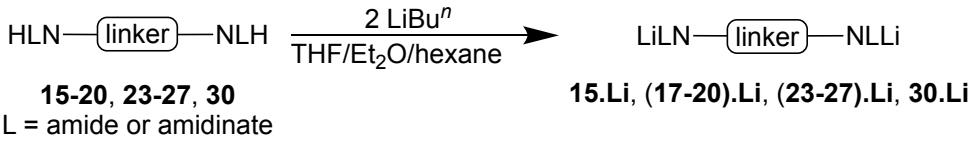

Scheme 4.20. Lithiation of pro-ligands **15-20, 23-27** and **30**.

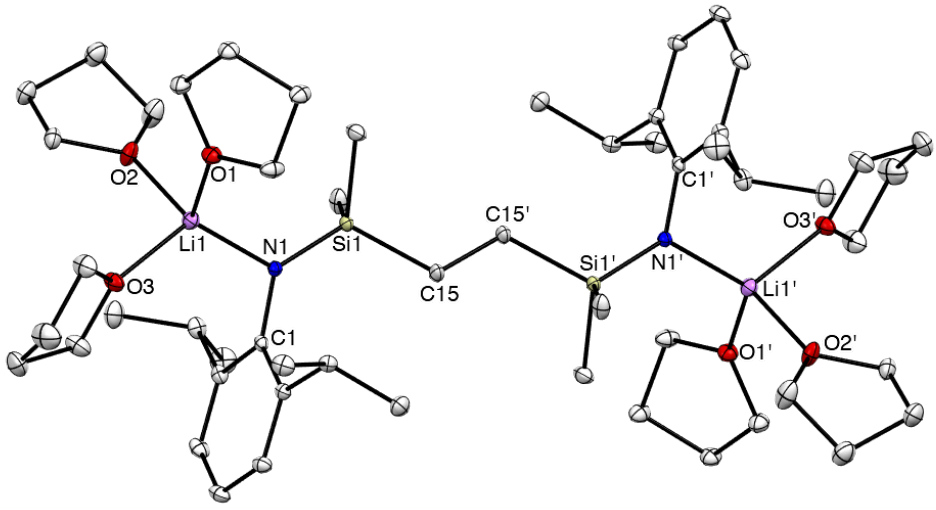

Figure 4.13. Molecular structure of [{(Dip)NLi}$_2$L2] (**17.Li**) (thermal ellipsoids shown at 30 % probability). Hydrogen atoms omitted for clarity. Selected bond lengths (Å) and angles (°): Si1-N1 1.6885(11), N1-C1 1.3907(17), Si1-C15 1.8880(15), N1-Li1 1.993(3), Li1-O1 1.997(3), Li1-O2 1.975(3), Li1-O3 2.031(3), Si1-N1-Li1 124.65(9), Si1-N1-C1 126.73(9).

The compound **17.Li** was characterised by single crystal X-ray crystallography and the molecular structure is displayed in **Figure 4.13**. **17.Li** is monomeric in the solid-state with both lithium centres exhibiting distorted tetrahedral geometries. The coordination sphere of each lithium centre is coordinatively saturated by three THF molecules and *N*-chelation by the amide fragment. The Li-N bond distances and Li-N-C bond angles in

17.Li are comparable to previously reported monomeric complexes [{Dip(SiMe$_3$)N}LiTHF$_3$] and [{Dip$^+$(SiMe$_3$)N}LiTHF$_3$].[78,79]

4.3.2.2 Synthesis of Amido Group 14 Element Complexes

The next step was to isolate cyclic low oxidation state group 14 element bis(tetrelenes) using the synthesised bulky ligands. For this purpose, *in situ* generated dilithium salts of the synthesised ligands were used subsequently in salt metathesis reactions with group 14 element halides.

The treatment of **15.Li**, **(17-20).Li** and **23.Li** with $GeCl_2$.dioxane did not result in desired low oxidation state cyclic main group element complexes (**Scheme 4.21**). In case of **15.Li**, a mixture of five-membered germylene and other unknown species were seen in the ^{1}H NMR spectrum, which could be due to the greater stability of the former cyclic system. In contrast, for lithium salts **(17-19).Li** and **23.Li**, the linker groups' resonances were not seen in the ^{1}H NMR spectra. On one of the crystallisation attempts, an unexpected product consisting of the bulky aniline coordinated to germanium(II) chloride [(Dip)N-$GeCl_2$] **30** was observed from the X-ray structure (**Figure 4.14**). This was later confirmed with ^{1}H NMR spectroscopy as well. Similar results were also seen in case of reaction mixtures of **18.Li**, **19.Li** and **23.Li** with germanium(II) chloride. This inability to form germylene complexes could be explained by the steric crowding caused by the bulky anilines, which leads to cleavage of Si-N bonds.

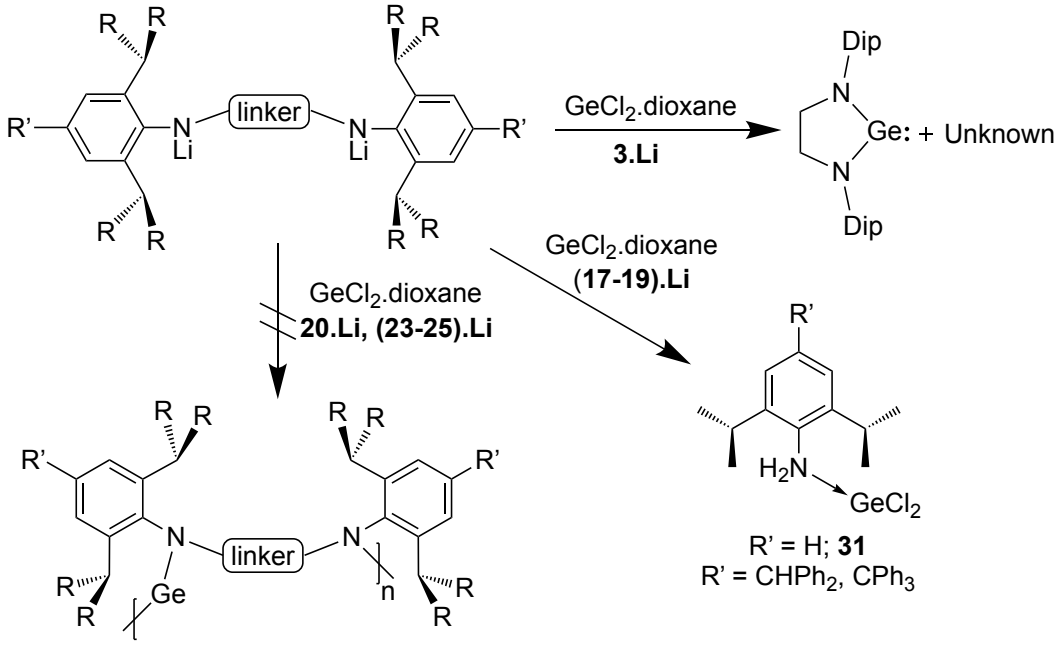

Scheme 4.21. Attempted synthesis of amido germanium(II) complexes.

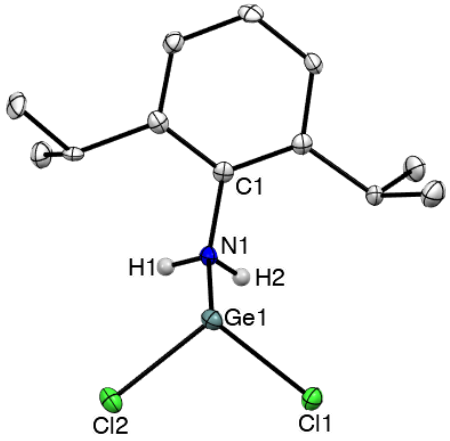

Figure 4.14. Molecular structure of [(Dip)N-$GeCl_2$] (**31**) (thermal ellipsoids shown at 30 % probability). Hydrogen atoms except H1 and H2 are omitted for clarity. Selected bond lengths (Å) and angles (°): Ge1-N1 2.186(4), Ge1-Cl1 2.2864(14), Ge1-Cl2 2.2869(13), Cl1-Ge1-Cl2 95.79(5), C1-N1-Ge1 110.0(3).

As the dilithium amides **3.Li**, **(17-20).Li**, **23.Li** did not seem suitable for stabilising germanium(II) species, we moved our attention to the rigid linker based aryl-silyl dilithium amides **20.Li** and **(24-27).Li**. However, **20.Li**, **23.Li** and **24.Li** did not show any promising results and in fact, unidentifiable mixtures of products were seen in ^{1}H NMR spectra, similar to the previous cases.

The addition of an equimolar amount of THF solutions of **24.Li** and **25.Li** to germanium(II) chloride solutions showed an instantaneous colour change to dark yellow. Both reaction mixtures formed new germanium(II) products **32** and **33** along with ca. 50 % protonated ligands. The reactions showed 90 % conversion when performed in hexane. The corresponding new germanium(II) complexes were found to be dimeric cyclic bis(germylenes) [{($Pr^i_3Si)_2$L4Ge}$_2$] **32** and [{($Pr^i_3Si)_2$L5Ge}$_2$] **33** (**Scheme 4.22**). On using two equivalents of germanium(II) chloride with **24.Li** and **25.Li**, the reactions did not form the monomeric bis(chlorogermylenes) [($Pr^i_3Si)_2$L($GeCl)_2$] (L = L4, L5) and only complexes **32** and **33** were obtained. The formation of these products is likely due to limited steric bulk of the ligand and the greater stability of cyclophanes. Compounds **32** and **33** are the first isolated examples of aryl-silyl amido germanium cyclophanes.

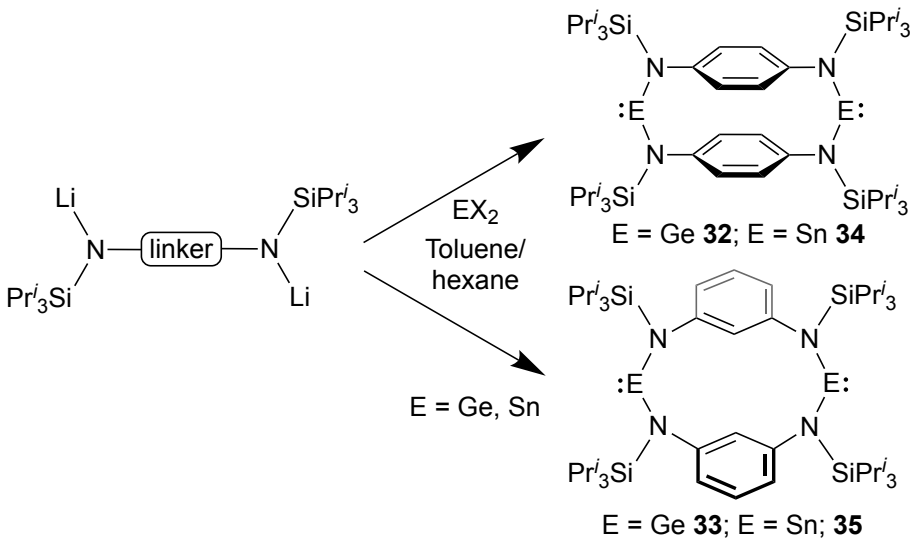

Scheme 4.22. Synthesis of germanium(II) and tin(II) cyclophanes **32**-**35**.

Complexes **32** and **33** were crystallised from concentrated hexane solutions and their molecular structures are given in **Figure 4.15**. **32** and **33** are centrosymmetric dimeric molecules with both the phenyl rings parallel to each other. All germanium centres are two-coordinate and exhibit a bent (V-shape) geometry around the germanium centre. The corresponding N-Ge-N bond angles in **32** and **33** are 109.81(15)° and 103.75(14)°, which indicate the presence of stereoactive lone pair of electrons at germanium centres. The average Ge-N bond lengths (1.874 Å, 1.873 Å) are as expected and consistent with those observed in analogous monomeric germylenes.[15,58] The planes of the phenylene rings in **32** and **33** are separated by 3.01 Å and 3.00 Å, respectively, with sideways displacement of 72.8°, 76.3° with N1-N2-N1'-N2' planes. This separation distances of the phenyl rings show a strong π-stacking interaction between them.[80]

The spectroscopic data for **32** and **33** are consistent with the solid-state structures. ^{1}H NMR spectra of these complexes showed one set of doublets for isopropyl methyl, and one set of septets for CH resonances. Furthermore, the analytical data for these complexes were also in accordance with the structures.

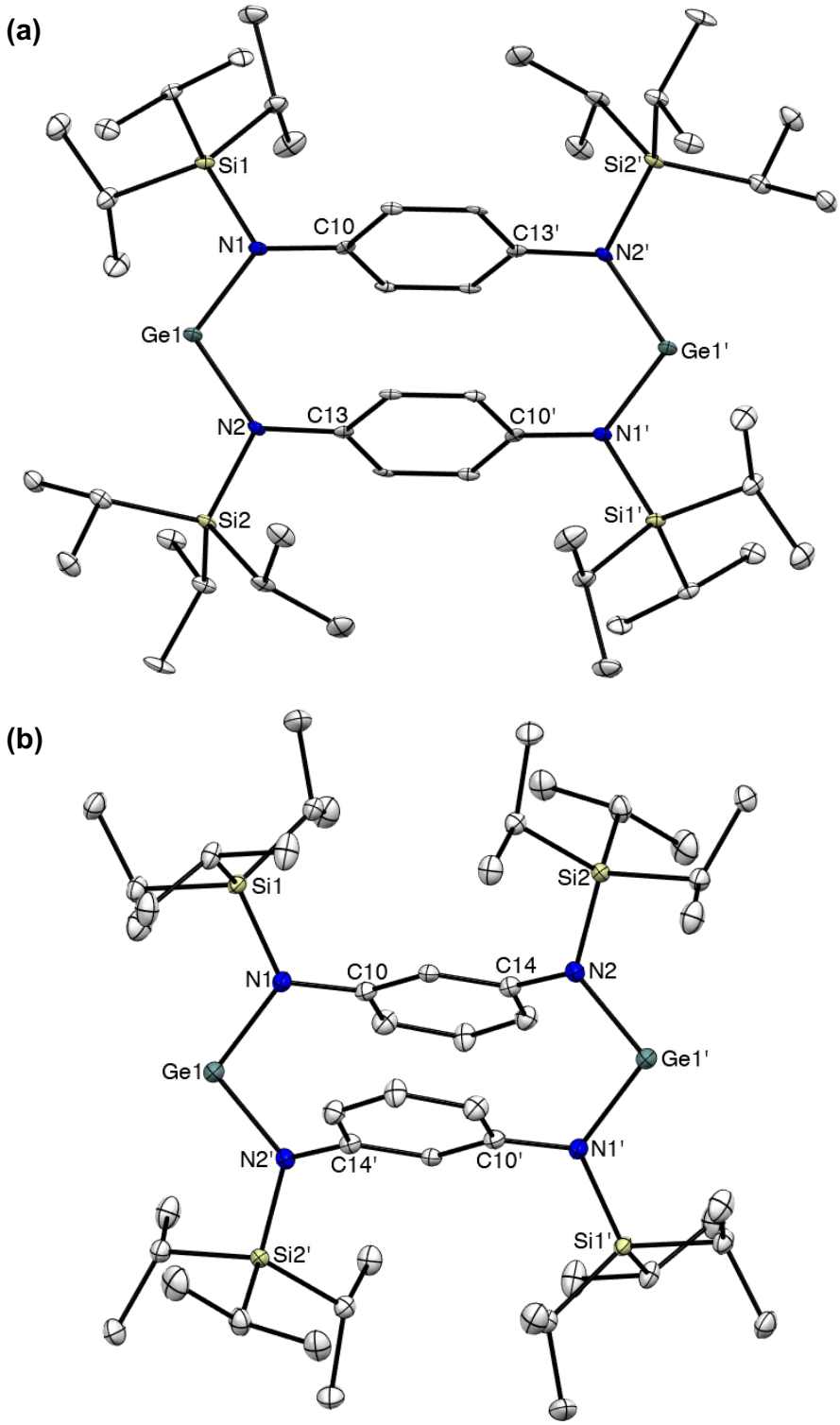

Figure 4.15. Molecular structures of [{($Pr^{i}_{3}Si$)$_2$L4Ge}$_2$] (**32**) (**a**) and [{($Pr^{i}_{3}Si$)$_2$L5Ge}$_2$] (**33**) (**b**) (thermal ellipsoids shown at 30 % probability). Hydrogen atoms omitted for clarity. Selected bond lengths (Å) and angles (°) for **32**: Ge1-N1 1.873(4), Ge1-N2 1.876(4), N1-Si1 1.770(4), N2-Si2 1.770(4), N1-Ge1-N2 109.81(16), Si1-N1-Ge1 118.4(2), Si2-N2-Ge1 115.4(2); **33**: Ge1-N1 1.867(3), Ge1-N2 1.880(3), N1-Si1 1.766(3), N2-Si2 1.755(3), N1-Ge1-N2 103.77(13), Si1-N1-Ge1 117.84(17), Si2-N2-Ge1 120.50(17).

The successful synthesis of germanium(II) cyclophanes prompted us to synthesise bis(stannynlenes) and bis(plumbylenes). To accomplish this, **24.Li** and **25.Li** were reacted with tin(II) bromide in toluene, which resulted in the formation of reddish-orange coloured [{(Pr$^i_3$Si)$_2$L4Sn}$_2$] **34** and [{(Pr$^i_3$Si)$_2$L5Sn}$_2$] **35** in 35 % and 40 % yields (**Scheme 4.22**). Due to the low solubility of these complexes in C_6D_6, ^{119}Sn NMR could not be obtained. The reactions of **24.Li** and **25.Li** with lead(II) bromide led to an instantaneous lead metal deposition.

The complexes **34** and **35** were crystallised from toluene solutions and the solid-state structures are displayed in **Figure 4.16** and **Figure 4.17**. Compounds **34** and **35** have similar structures as **32** and **33** with 3.09 Å and 3.13 Å parallel phenyl ring separations. The average Sn-N bond distance and N-Sn-N bond angles in **33** and **34** are 2.08 Å, 2.08 Å and 106.96(6)°, 99.4(2)°, which are close to previously reported compounds [{(Me$_3$Si)$_2$L5Sn}$_2$] (Sn-N = 2.068 Å, N-Sn-N = 98.3(3)°) and [{Mes(Me$_3$Si)N}$_2$Sn] (Sn-N = 2.059 Å, N-Sn-N = 105.8(1)°).[40,81]

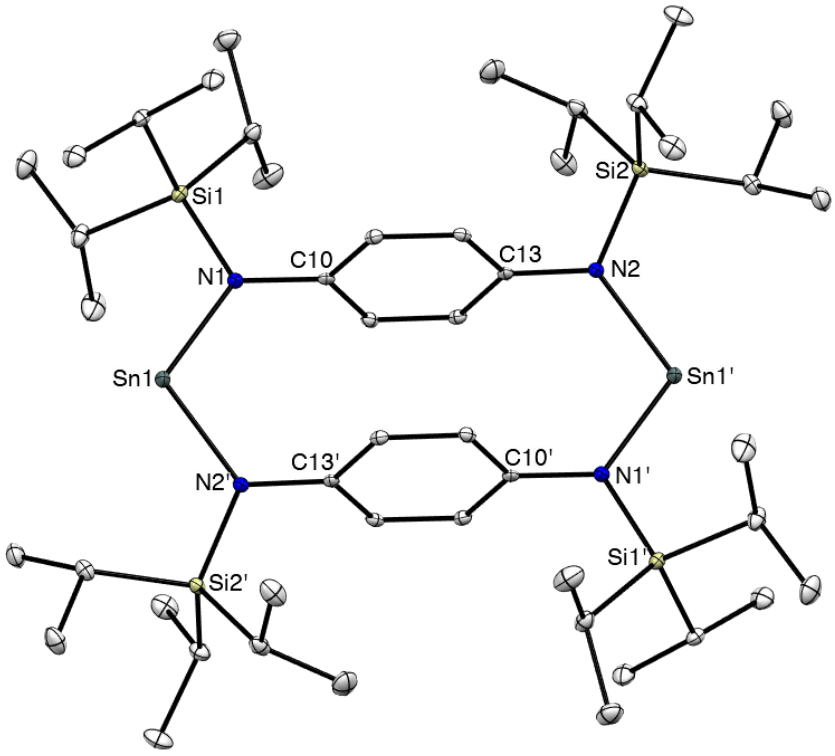

Figure 4.16. Molecular structure of [{(Pr$^i_3$Si)$_2$L4Sn}$_2$] (**34**) (thermal ellipsoids shown at 30 % probability). Hydrogen atoms omitted for clarity. Selected bond lengths (Å) and angles (°): Sn1-N1 2.0821(15), Sn1-N2 2.0753(14), N1-Si1 1.7588(15), N2-Si2 1.7617(15), N1-Sn1-N2 106.96(6), Si1-N1-Sn1 116.60(8), Si2-N2-Sn1 120.22(8);

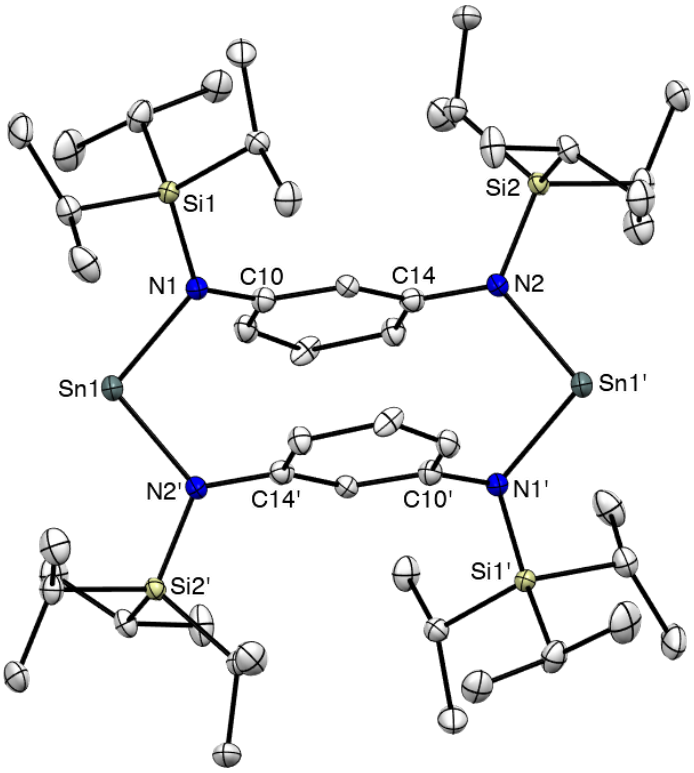

Figure 4.17 Molecular structure of [{($Pr^{i}_{3}Si)_2$L5Sn}$_2$] (**35**) (thermal ellipsoids shown at 30 % probability). Hydrogen atoms omitted for clarity. Selected bond lengths (Å) and angles (°): Sn1-N1 2.080(6), Sn1-N2 2.087(6), N1-Si1 1.733(6), N2-Si2 1.740(6), N1-Sn1-N2 99.4(2), Si1-N1-Sn1 120.8(3), Si2-N2-Sn1 117.3(3).

4.3.2.3 Synthesis of Amidinato Group 2 and Group 14 Element Complexes

Bis(amidinato) magnesium complexes can be accessed by treating protio-ligand **30** with two equivalents of magnesium reagents like methyl magnesium iodide MeMgI **36** and dibutyl magnesium Mg(Bu^{n})$_2$ **37** (**Scheme 4.23**). The reaction of **30** with **36** resulted in a good yield of the compound [L5(Amid$Ar^{\dagger}$)$_2${MgI(OEt_2)}$_2$] **38**. It is thermally stable in both solid- and solution-states and showed one diethyl ether ligand coordinated to each magnesium centre in the ^{1}H NMR spectrum. On the other hand, the reaction with **37** instantaneously afforded a white coloured compound **39** which was further verified by ^{1}H and ^{13}C NMR spectroscopic techniques. Despite multiple attempts, the crystallisation of **38** was not possible, while colourless crystals of **39** were obtained from toluene/hexane mixture (20:80).

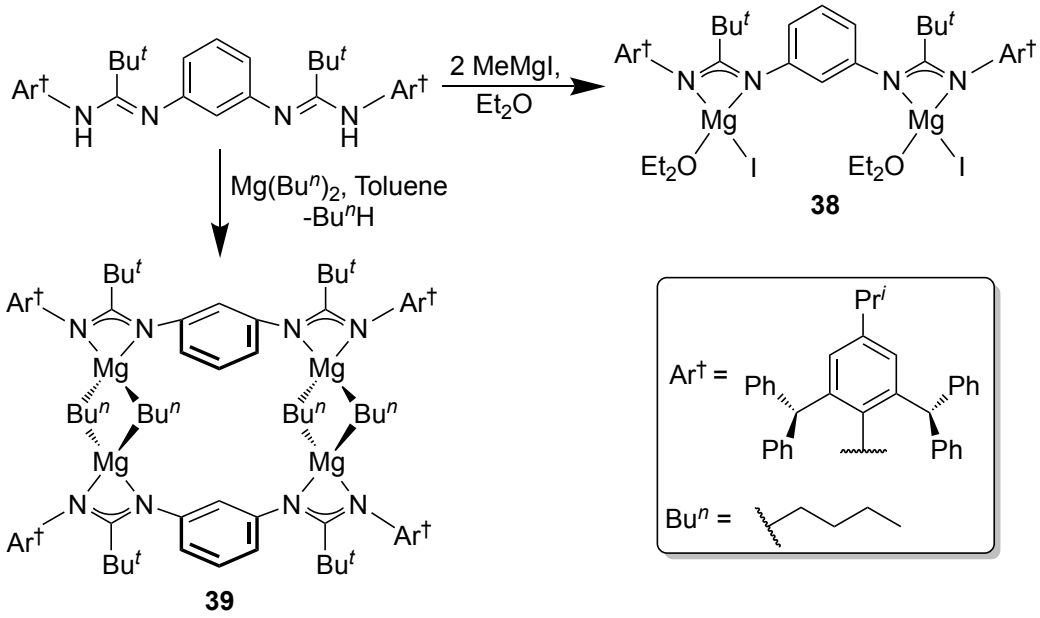

Scheme 4.23. Synthesis of bis(amidinato) magnesium(II) complexes **38** and **39**.

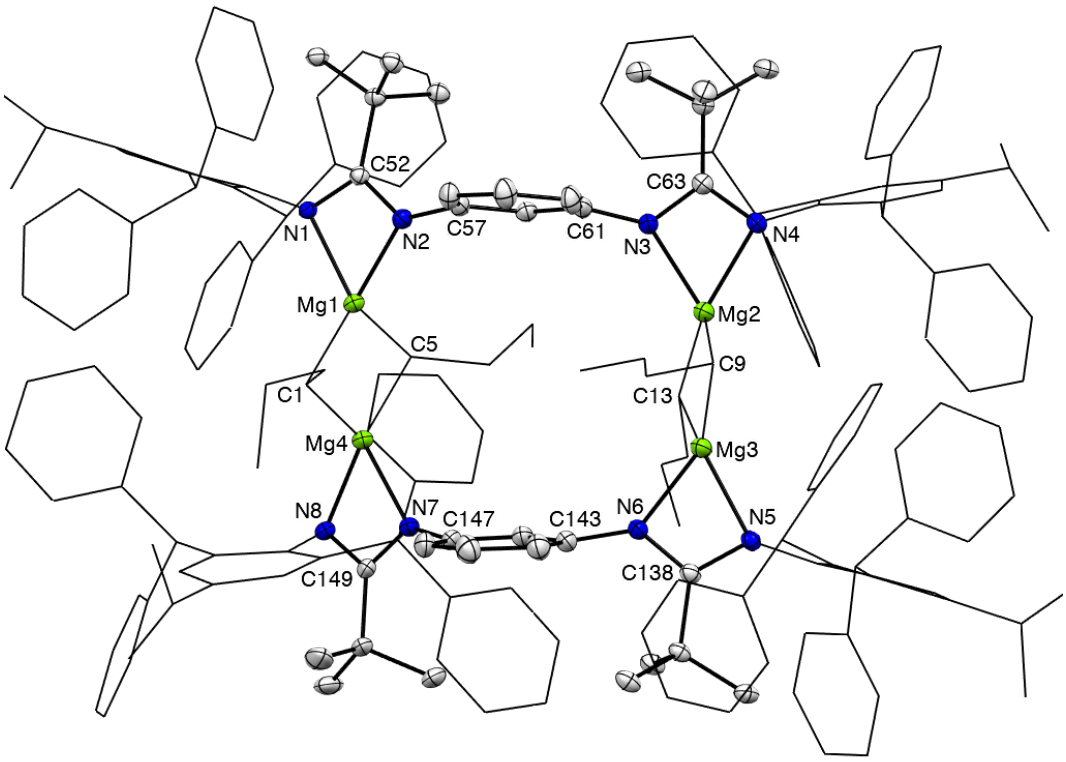

Figure 4.18. Molecular structure of [{L5(AmidAr†)$_2$(MgBu^n)$_2$}$_2$] (**39**). (thermal ellipsoids shown at 30 % probability). Hydrogen atoms omitted; Ar† and Bu^n groups shown as wireframe for clarity. Selected bond lengths (Å) and angles (°): Mg1-N1 2.072(2), Mg1-N2 2.036(3), N1-C52 1.343(4), N2-C52 1.331(4), N2-C57 1.425(4), Mg1-C1 2.168(13), Mg1-C5 2.258(5), Mg4-C1 2.242(15), Mg4-C5 2.223(4), N2-Mg1-N1 64.72(10), C1-Mg1-C5 105.8(4), N1-Mg1-C5 117.16(14), N2-Mg1-C5 114.57(14), N1-Mg1-C1 124.5(5), N2-Mg1-C1 126.1(5), Mg1-C1-Mg4 75.6(4), N2-C52-N1 110.6(3).

The dimeric complex **39** possesses four magnesium(II) centres that are each four-coordinate (**Figure 4.18**). Each magnesium centre incorporates one *N,N'*-chelating amidinate moiety and two n-butyl molecules bridged between two opposite magnesium amidinato units, thereby, forming two four-membered $Mg_2Bu^n_2$ rings. Unlike the previously discussed amido germanium(II) and tin(II) cyclophanes **33** and **35**, the central phenyl rings in **39** are non-planar with an angle of 13.15°. The Mg-N bond lengths and N-Mg-N bite angles are in range of 2.036(4) Å-2.069(3) Å and 64.38(15)°-65.25(14)°, respectively. The structure of **39** is reminiscent of Harders' β-diketiminate magnesium butyl complex [{NN-$(MgBu^n)_2$}$_2$] (NN = Dip(Nacnac)$_2$Dip; Nacnac$_2$ = [-NC(Me)CHC(Me)N-NC(Me)CHC(Me)N-]).[82]

Reaction of **30.Li** with $GeCl_2$.dioxane in a 1:2 stoichiometric ratio led to the formation of dinuclear monomeric germanium chloride complex [L5(AmidAr†)$_2$(GeCl)$_2$] **40** (**Scheme 4.24**) in 60 % yield. Compound **40** was fully characterised by ^{1}H, ^{13}C{^{1}H} NMR, IR spectroscopic techniques and elemental analysis.

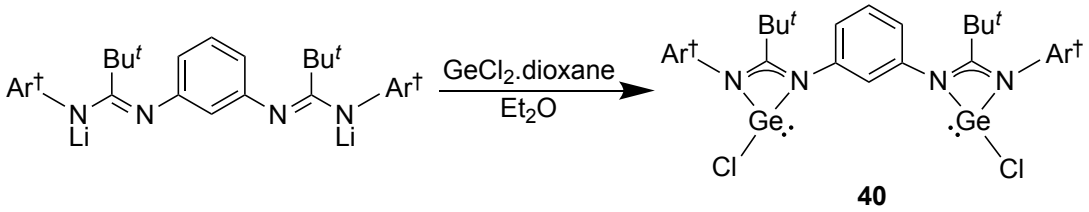

Scheme 4.24. Synthesis of bis(amidinato) germanium(II) chloride complex **40**.

Further, the reduction of complexes **38** and **40** was pursued using [{(^{Mes}Nacnac)Mg}$_2$] and KC_8 as reducing agents. In case of **38**, both of these reactions led to yellow coloured suspensions which could not be further purified (**Scheme 4.25**).

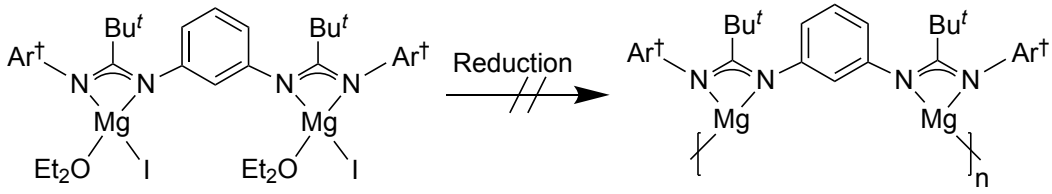

Scheme 4.25. Attempted reduction of bis(amidinato) magnesium iodide **38**.

The reaction of **40** with [{(^{Mes}Nacnac)Mg}$_2$] was unsuccessful and resulted in intractable product mixtures. However, reaction with KC_8 in toluene led to a yellow coloured solution from which a bis(cyclic) germanium(II) species [{L5(AmidAr†)$_2$Ge}$_2$] **41** was recovered (**Scheme 4.26**). Compound **41** was likely a product of disproportionation of

intermediate dimeric bis(amidinato) germanium(I) species. NMR spectroscopic analysis of **41** did not provide any useful information due to the negligible solubility in normal NMR solvent C_6D_6.

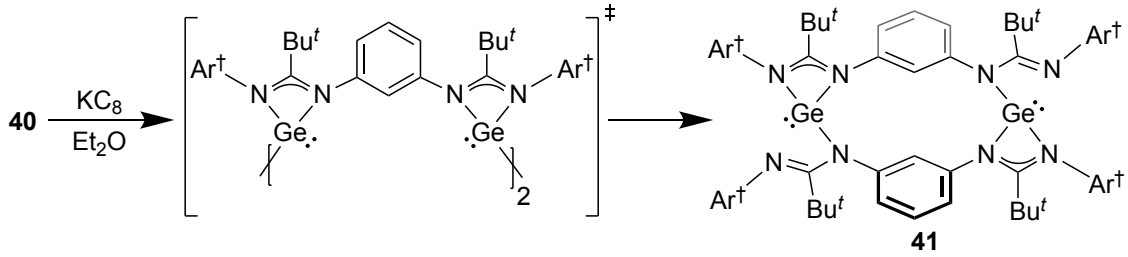

Scheme 4.26. Reduction of compound **41** with KC_8.

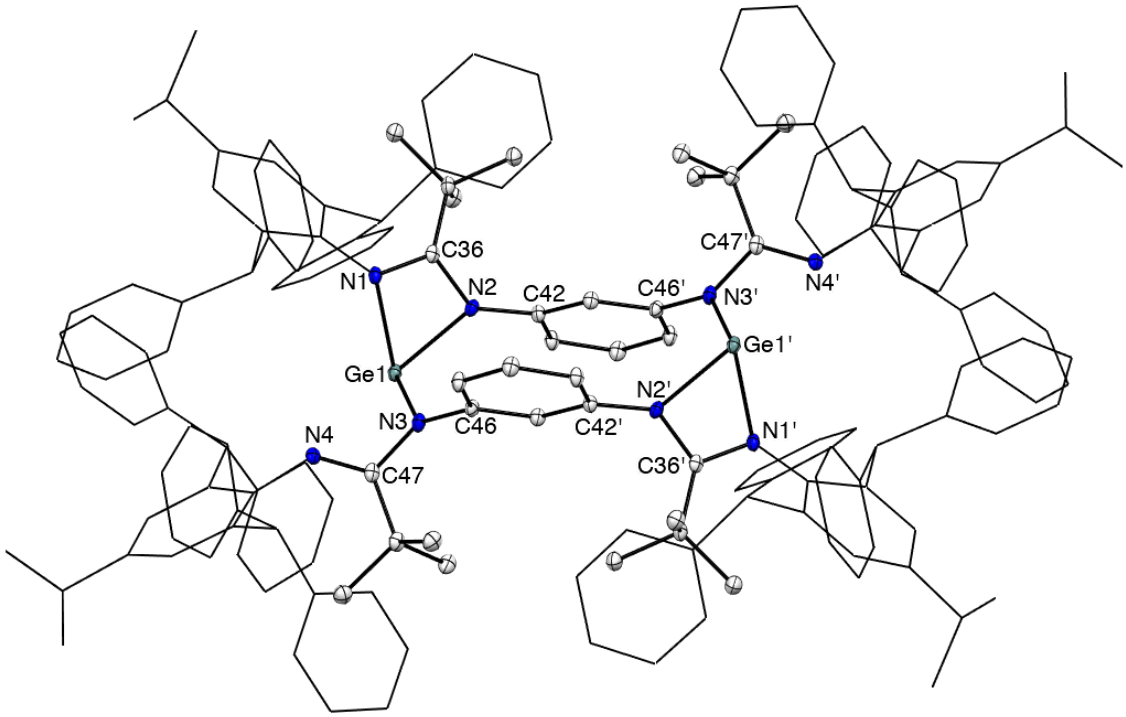

Figure 4.19. Molecular structure of [{L5(AmidAr†)$_2$Ge}$_2$] (**41**) (thermal ellipsoids shown at 30 % probability). Hydrogen atoms omitted; Ar† groups shown as wireframe for clarity. Selected bond lengths (Å) and angles (°): Ge1-N1 2.076(3), Ge1-N2 2.030(3), Ge1-N3 1.920(3), Ge1---N4 2.735, N1-C36 1.328(5), N2-C36 1.351(5), N3-C47 1.399(5), N4-C47 1.293(5), C42-N2 1.422(5), N3-C46 1.428(5), N2-Ge1-N1 62.92(12), N3-Ge1-N1 108.70(13), N3-Ge1-N2 99.34(13), N1-C36-N2 106.2(3), N4-C47-N3 112.3(3).

Complex **41** was crystallised from the toluene solution of the reaction mixture and the crystal structure is shown in **Figure 4.19**. Compound **41** is dimeric and possesses a distorted tetrahedral geometry around each germanium centre in which one vertex is occupied by a stereoactive lone pair of electrons. Each germanium centre exhibits bidentate *N,N'*-chelation by one side of the first bis(amidinate) unit and monodentate N-

donor by the same side of the other bis(amidinate) unit. The free imine nitrogens do not exhibit any other interactions. The central phenylene rings (Ph1, Ph2) maintain a similar π-stacking interaction as **33**, with 2.89 Å distance between them. Further, the Ge-N bond distances for the monodentate side (1.920(3) Å) are slightly shorter than the bidentate side (2.076(3) Å and 2.030(3) Å). All of the Ge-N (for monodentate and bidentate sides) bond lengths are in accordance with the reported monomeric germylene complex [{CyNC(Me)NCy}$_2$Ge].[62]

4.3.3 Reactivity of Synthesised Bis(tetrelenes)

Due to time constraints, only limited reactivity studies of bis(tetrelenes) **32-35** could be explored. Toluene solutions of complexes **32-35** were reacted with H_2, CO and NH_3. All of the reactions, except that of **32** with CO, resulted in formation of colourless species, that were confirmed as protonated ligands by ^{1}H NMR spectroscopy (**Scheme 4.27**). The reaction of **32** with CO gave a yellow colored solution, which consists of a new species (ca. 80 %) by NMR spectroscopy. However, efforts to obtain X-ray quality crystals were unsuccessful, as the compound decomposed to protonated ligand after 2-3 days.

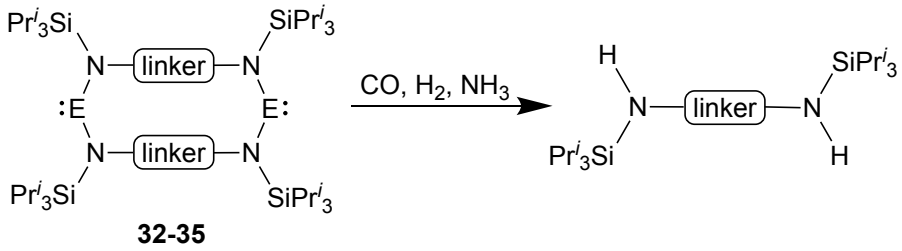

Scheme 4.27. Attempted small molecule activation using **32-35**.

4.4 Conclusion

This chapter has expanded on the synthesis of various novel bis(amine) and bis(amidine) pro-ligands based on different flexible and rigid linker groups. The rigid linker based amido ligands **26** and **27** were found effective for stabilisation of low oxidation state germanium(II) and tin(II) cyclophanes. Further, the N-bridged bis(amidinate) ligands were also employed in isolation of dinuclear magnesium(II) and germanium(II) halide complexes. The reduction of the later with KC_8 resulted in a cyclic germanium(II) product, possibly from the rearrangement of the germanium(I) species. In addition to that, only few reactivity studies of amido cyclophanes could be explored in detail. Currently the reactivity of synthesised cyclophanes with transition metals and Lewis

acids are underway. These results are an important step forward for the utilisation of dinuclear ligands for the isolation of bis(tetrelenes).

4.5 Experimental

[(Ar*N)L2] (16). A solution of [{Ar*NCH}$_2$] (4.00 g, 4.44 mmol) in THF (50 mL) was cooled to 0 ºC and $LiAlH_4$ (6.5 mL of 0.75 M solution in Et_2O, 4.88 mmol) was added dropwise over 5 minutes. After the addition, the reaction mixture was warmed to room temperature, and stirred for 6 hours. This reaction mixture was then cooled to 0 ºC and 0.5 mL water was slowly added, followed by 0.5 mL of 15 % aqueous sodium hydroxide and 1.5 mL of water. The resulting mixture was warmed to room temperature and stirred for 1 hour. The organic layer was extracted with dichloromethane (3×60 mL), dried using $MgSO_4$ and filtered. Solvents were removed under reduced pressure to afford an off-white solid. X-ray quality crystals were grown by layering toluene solution of the product with pentane (2.90 g, 72.2 %). M.p. 138-141 °C; ^{1}H NMR (400 MHz, C_6D_6, 298 K) δ = 1.89 (s, 6H, C*H*$_3$), 2.67 (s, 4H, C*H*$_2$), 3.36 (s, 2H, N*H*), 6.02 (s, 4H, C*H*Ph$_2$), 6.92 (s, 2H, Ar-*H*), 6.97-7.15 (m, 40H, Ar-*H*); ^{13}C{^{1}H} NMR (101 MHz, C_6D_6, 298 K) δ = 21.2 (*C*H$_3$), 50.9 (*C*H$_2$), 51.9 (*C*HPh$_2$), 126.6, 128.7, 130.1, 130.4, 132.9, 139.8, 143.5, 144.8 (Ar-*C*); IR ν/cm^{-1} (ATR): 3346 (br w, NH), 3059 (w), 3025 (m), 2915 (w), 2108 (w), 2082 (w), 1946 (w), 1877 (w), 1807 (w), 1598 (s), 1491 (s), 1447 (vs), 1324 (w), 1252 (m), 1132 (w), 1105 (w), 1077 (m), 1030 (m), 914 (w), 957 (w), 828 (w), 744 (s), 697 (vs); acc. mass calc. for $C_{68}H_{61}N_2$ (MH^+): 905.4834; found: 905.4909.

[{(Dip^Y)NH}$_2$L2] (18). A solution of Dip^{Y}NH$_2$ (3.20 g, 9.32 mmol) in Et_2O (50 mL) was cooled to -80 ºC and LiBu^n (6.4 mL of a 1.6 M solution in hexane, 10.26 mmol) was added dropwise over 10 minutes. After the addition, the reaction mixture was warmed to room temperature, and stirred for 3 hours. To this reaction mixture [Cl(Me$_2$)SiCH$_2$CH$_2$Si(Me$_2$)Cl] (1.00 g, 4.66 mmol) in Et_2O (20 mL) was then added at -80 ºC and the reaction was stirred for 12 hours. Volatiles were subsequently removed *in vacuo* and the residue was extracted into hexane (80 mL). The extract was filtered, concentrated to ca. 20 mL and stored at -30 ºC overnight to yield a light-orange colored powder (2.50 g, 65.8 %). M.p. 120 °C; ^{1}H NMR (400 MHz, C_6D_6, 298 K) δ = 0.12 (s, 12H, Si(C*H*$_3$)$_2$), 0.59 (s, 4H, SiC*H*$_2$), 1.16 (d, $^3J_{HH}$ = 6.9 Hz, 24H, CH(C*H*$_3$)$_2$), 2.13 (s, 2H, N*H*), 3.47 (sept, $^3J_{HH}$ = 6.9 Hz, 4H, C*H*(CH$_3$)$_2$), 5.54 (s, 2H, C*H*Ph$_2$), 7.01-7.21 (m, 24H, Ar-*H*); ^{13}C{^{1}H} NMR (101 MHz, C_6D_6, 298 K) δ = -1.4 (Si(*C*H$_3$)$_2$), 9.8 (Si*C*H$_2$),

23.9 (CH(CH$_3$)$_2$), 28.6 (CH(CH$_3$)$_2$), 57.4 (CPh$_3$), 124.7, 126.4, 128.5, 129.9, 138.2, 139.1, 144.2, 145.2 (Ar-C); ^{29}Si{^{1}H} NMR (80 MHz, C_6D_6, 298 K) δ = 5.0; IR ν/cm^{-1} (ATR): 3403 (m, NH), 3024(w), 2959 (s), 1869 (w), 1624 (s), 1597 (s), 1527 (w), 1492 (s), 1467 (s), 1446 (s), 1382 (m), 1358 (m), 1288 (w), 1252 (s), 1167 (w), 1133 (w), 1049 (s), 967 (w), 918 (w), 889 (w), 831 (s), 788 (s), 767 (s), 748 (s), 700 (vs); acc. mass calc. for $C_{56}H_{73}N_2Si_2$ (MH^+): 829.5312; found: 829.5113.

[{(Dip$^+$)NH}$_2$L2] (19). This compound was prepared following a similar method to that for [{(Dip^Y)NH}$_2$L2], but using Dip$^+$NH$_2$ (3.90 g, 9.30 mmol) in Et$_2$O (50 mL), LiBu^n (6.4 mL of a 1.6 M solution in hexane, 10.23 mmol), and [Cl(Me$_2$)SiCH$_2$CH$_2$Si(Me$_2$)Cl] (1.00 g, 4.65 mmol) in Et$_2$O (20 mL). Storage of the concentrated reaction solution in hexane at -30 °C for 1 day resulted in **19** as a white solid (4.60 g, 60.9 %). M.p. 190 °C; ^{1}H NMR (400 MHz, C_6D_6, 298 K) δ = 0.15 (s, 12H, Si(CH_3)$_2$), 0.61 (s, 4H, SiCH_2), 1.12 (d, $^3J_{HH}$ = 6.9 Hz, 24H, CH(CH_3)$_2$), 2.21 (s, 2H, NH), 3.45 (sept, $^3J_{HH}$ = 6.8 Hz, 4H, CH(CH$_3$)$_2$), 6.99-7.12 (m, 18H, Ar-H), 7.22 (s, 4H, Ar-H), 7.46 (m, 12H, Ar-H); ^{13}C{^{1}H} NMR (101 MHz, C_6D_6, 298 K) δ = -1.4 (Si(CH$_3$)$_2$), 9.8 (SiCH$_2$), 23.9 (CH(CH$_3$)$_2$), 28.9 (CH(CH$_3$)$_2$), 65.7 (CPh$_3$), 126.2, 127.0, 127.7, 131.8, 137.8, 141.8, 142.8, 147.9 (Ar-C); ^{29}Si{^{1}H} NMR (80 MHz, C_6D_6, 298 K) δ = 5.1; IR ν/cm^{-1} (ATR): 3382 (w, NH), 3052 (w), 2959 (s), 2870 (w), 1595 (m), 1492 (s), 1460 (s), 1442 (vs), 1362 (w), 1327 (vs), 1279 (s), 1249 (vs), 1214 (w), 1167 (m), 1124 (s), 1073 (m), 1036 (s), 895 (vs), 875 (m), 835 (s), 801 (s), 749 (s), 733 (vs), 698 (vs); acc. mass calc. for $C_{68}H_{81}N_2Si_2$ (MH^+): 981.5938; found: 981.5914.

[{(Ar†)NH}$_2$L3] (20). This compound was prepared following a similar method to that for [{(Dip^Y)NH}$_2$L2], but using Ar†NH$_2$ (1.00 g, 2.14 mmol) in Et$_2$O (30 mL), LiBu^n (1.5 mL of a 1.6 M solution in hexane, 2.35 mmol), and [Cl(Me$_2$)Si(1,4-Ph)Si(Me$_2$)Cl] (0.28 g, 1.07 mmol) in Et$_2$O (10 mL). Storage of the concentrated reaction solution in toluene at -30 °C for 2 days resulted in white coloured powder of **20** (0.80 g, 66.6 %). M.p. 191 °C; ^{1}H NMR (400 MHz, C_6D_6, 298 K) δ = 0.37 (s, 12H, Si(CH_3)$_2$), 0.93 (d, $^3J_{HH}$ = 6.9 Hz, 12H, CH(CH_3)$_2$), 2.15 (s, 2H, NH), 2.46 (m, 2H, $^3J_{HH}$ = 6.9 Hz, CH(CH$_3$)$_2$), 6.10 (s, 4H, Ph$_2$CH), 6.93 (s, 4H, Ar-H), 6.99-7.11 (m, 40H, Ar-H), 7.41 (s, 4H, Ar-H); ^{13}C{^{1}H} NMR (101 MHz, C_6D_6, 298 K) δ = -0.4 (Si(CH$_3$)$_2$), 24.1 (CH(CH$_3$)$_2$), 33.8 (CH(CH$_3$)$_2$), 53.1 (Ph$_2$$C$H) 126.5, 127.4, 128.6, 130.0, 133.2, 140.4, 140.9, 141.7, 143.9, 144.7 (Ar-C); ^{29}Si{^{1}H} NMR (80 MHz, C_6D_6, 298 K) δ = -4.7; IR ν/cm^{-1} (ATR): 3337

(w, NH), 3057 (w), 3025 (w), 2958 (m), 2867 (w), 1625 (w), 1599 (m), 1491 (m), 1447 (s),1225 (s), 1160 (w), 1131 (m), 1075 (m), 1030 (m), 970 (w), 894 (s), 860 (s), 813 (m), 793 (s), 761 (s), 744 (s), 699 (vs); acc. mass calc. for $C_{80}H_{81}N_2Si_2$ (MH^+): 1125.5938; found: 1125.5921.

[(Ar*N)L2] (21). Compound **21** was isolated in an attempt to synthesise the disubstituted ligand [{(Ar*)NH}$_2$L2], however the compound was also synthesised using equimolar quantities of Ar*NH$_2$ and [Cl(Me$_2$)SiCH$_2$CH$_2$Si(Me$_2$)Cl]. This compound was prepared following a similar method to that for [{(Dip^Y)NH}$_2$L2], but using Ar*NH$_2$ (1.00 g, 2.28 mmol) in THF (20 mL), LiBu^n (1.6 mL of a 1.6 M solution in hexane, 2.50 mmol), and [Cl(Me$_2$)SiCH$_2$CH$_2$Si(Me$_2$)Cl] (0.49 g, 2.28 mmol) in THF (10 mL). Storage of the concentrated reaction solution in toluene at -30 °C for overnight resulted in deposition of yellow coloured crystals of **21** (0.90 g, 66.3 %); M.p. 180 °C; ^{1}H NMR (400 MHz, C$_6$D$_6$, 298 K) δ = 0.10 (s, 12H, Si(C*H*$_3$)$_2$), 0.95 (s, 4H, SiC*H*$_2$), 1.88 (s, 3H, C*H*$_3$), 6.19 (s, 2H, C*H*Ph$_2$), 7.01-7.27 (m, 22H, Ar-*H*); ^{13}C{^{1}H} NMR (101 MHz, C$_6$D$_6$, 298 K) δ = 1.6 (Si(*C*H$_3$)$_2$), 8.9 (Si*C*H$_2$), 21.0 (*C*H$_3$), 28.9 (*C*HPh$_2$), 126.5, 128.5, 128.8, 130.0, 130.6, 132.2, 142.5, 145.5 (Ar-*C*); ^{29}Si{^{1}H} NMR (80 MHz, C$_6$D$_6$, 298 K) δ = 11.7; IR ν/cm^{-1} (ATR): 3026 (m), 2919 (m), 2094 (w), 1592 (s), 1484 (s), 1441 (vs), 1331 (w), 1246 (vs), 1127 (s), 1072 (w), 1028 (s), 916 (s), 885 (vs), 836 (m), 779 (vs), 691 (vs); acc. mass calc. for $C_{39}H_{44}NSi_2$ (MH^+): 582.3012; found: 582.3041.

[{(Ar†)NH}$_2$L2] (23). A solution of Ar†NH$_2$ (1.10 g, 2.35 mmol) and TMEDA (0.4 mL, 2.35 mmol) in Et$_2$O (30 mL) was cooled to -80 ºC and LiBu^n (1.6 mL of a 1.6 M solution in hexane, 2.59 mmol) was added dropwise over 10 minutes. After the addition, the reaction mixture was warmed to room temperature and stirred for 3 hours. To this reaction mixture [Cl(Me$_2$)SiCH$_2$CH$_2$Si(Me$_2$)Cl] (0.31 g, 1.18 mmol) in Et$_2$O (10 mL) was then added at -80 ºC and the reaction was stirred for 12 hours. Volatiles were subsequently removed *in vacuo* and the residue extracted into hot hexane (80 mL). The extract was filtered, concentrated to ca. 10 mL and stored at -30 ºC overnight to yield white coloured crystals (1.00 g, 64.1 %). M.p. 150 °C; ^{1}H NMR (400 MHz, C$_6$D$_6$, 298 K) δ = 0.15 (s, 12H, Si(C*H*$_3$)$_2$), 0.51 (s, 4H, SiC*H*$_2$), 0.95 (d, $^3J_{HH}$ = 6.9 Hz, 12H, CH(C*H*$_3$)$_2$), 1.89 (s, 2H, N*H*), 2.48 (sept, *J* = 6.9 Hz, 2H, C*H*(CH$_3$)$_2$), 6.20 (s, 4H, C*H*Ph$_2$), 6.95 (s, 4H, Ar-*H*), 7.00-7.22 (m, 40H, Ar-*H*); ^{13}C{^{1}H} NMR (101 MHz, C$_6$D$_6$, 298 K) δ = -0.9 (Si(*C*H$_3$)$_2$), 10.3 (Si*C*H$_2$), 24.1 (CH(*C*H$_3$)$_2$), 33.8 (*C*H(CH$_3$)$_2$), 53.1 (*C*HPh$_2$), 126.6, 127.3, 128.7, 130.0, 140.7, 141.5, 143.7, 144.9 (Ar-*C*); ^{29}Si{^{1}H} NMR

(80 MHz, C_6D_6, 298 K) δ = 5.1; IR ν/cm^{-1} (ATR): 3350 (m, NH), 3061 (w), 3024 (w), 2956 (m), 2869 (w), 1599 (w), 1493 (s), 1447 (vs), 1371 (w), 1320 (w), 1271 (m), 1249 (s), 1160 (w), 1134 (m), 1074 (w), 1031 (s), 900 (vs), 856 (s), 830 (vs), 782 (s), 764 (s), 745 (s), 721 (s), 699 (vs); acc. mass calc. for $C_{76}H_{81}N_2Si_2$ (MH^+): 1077.5938; found: 1077.5914.

[{(Me$_2$PhSi)NH}$_2$L4] (24). A solution of *p*-phenylenediamine (2.00 g, 18.51 mmol) in THF (50 mL) was cooled to -80 °C, and LiBu^n (24.3 mL of a 1.6 M solution in hexane, 38.86 mmol) was added to this over 10 minutes. After the addition, the reaction mixture was warmed to room temperature and stirred for 3 hours. To this reaction mixture a solution of $Me_2PhSiCl$ (6.2 mL, 37.01 mmol) in THF (20 mL) was then added at -80 ºC. The reaction mixture was stirred for 12 hours at room temperature. Volatiles were subsequently removed *in vacuo* and the residue extracted into hexane (30 mL). The extract was filtered, concentrated to ca. 20 mL and stored at -30 ºC overnight to yield very dark red colored powder (3.6 g, 51.7 %). M.p. 198 °C; ^{1}H NMR (400 MHz, C_6D_6, 298 K) δ = 0.31 (s, 12H, C*H*$_3$), 3.00 (s, 2H, N*H*), 6.45 (s, 4H, Ar-*H*), 7.18-7.20 (m, 6H, Ar-*H*), 7.56-7.59 (m, 4H, Ar-*H*); ^{13}C{^{1}H} NMR (101 MHz, C_6D_6, 298 K) δ = -1.2 (*C*H$_3$), 118.2, 129.6, 133.4, 134.1, 138.8, 139.2 (Ar-*C*); ^{29}Si{^{1}H} NMR (80 MHz, C_6D_6, 298 K) δ = -1.2; IR ν/cm^{-1} (ATR): 3305 (br w, NH), 3195 (w), 3005 (w), 2958 (m), 2112 (w), 1597 (m), 1499 (m), 1427(s), 1305 (w), 1253 (vs), 1161 (w), 1118 (s), 1044 (s), 826 (vs), 784 (vs), 723 (s), 696 (s); acc. mass calc. for $C_{22}H_{29}N_2Si_2$ (MH^+): 377.1869; found: 377.1873.

[{(Me$_2$PhSi)NH}$_2$L5] (25). This compound was prepared following a similar method to that for **24**, but using *m*-phenylenediamine (2.00 g, 18.51 mmol) in THF (50 mL), LiBu^n (24.3 mL of a 1.6 M solution in hexane, 38.86 mmol) and $Me_2PhSiCl$ (6.2 mL, 37.01 mmol) in THF (20 mL). Storage of the concentrated reaction solution in hexane at room temperature for 2 days resulted in deposition of **25** as red coloured crystals (3.20 g, 46.0 %). M.p. 75 °C; ^{1}H NMR (400 MHz, C_6D_6, 298 K) δ = 0.17 (s, 12H, C*H*$_3$), 3.22 (s, 2H, N*H*), 5.97 (s, 1H, Ar-*H*), 6.05 (d, $^3J_{HH}$ = 7.9 Hz, 2H, Ar-*H*), 6.90 (t, $^3J_{HH}$ = 7.9 Hz, 1H, Ar-*H*), 7.13-7.15 (m, 6H, Ar-*H*), 7.47-7.50 (m, 4H, Ar-*H*); ^{13}C{^{1}H} NMR (101 MHz, C_6D_6, 298 K) δ = 1.3 (*C*H$_3$), 104.9, 108.2, 127.9, 129.7, 130.2, 134.1, 138.6, 148.2 (Ar-*C*); ^{29}Si{^{1}H} NMR (80 MHz, C_6D_6, 298 K) δ = -5.9; IR ν/cm^{-1} (ATR): 3384 (m, NH), 3065 (w), 3017 (w), 2955 (w), 2893 (w), 1604 (s), 1585 (s), 1497 (vs), 1447 (w), 1425

(m), 1400 (vs), 1328 (s), 1265 (s), 1249 (vs), 1183 (m), 1165 (m), 1112 (vs), 1000 (vs), 890 (w), 827 (s), 814 (s), 785 (s), 751 (m), 727 (s), 698 (s), 682 (s); acc. mass calc. for $C_{22}H_{29}N_2Si_2$ (MH^+): 377.1869; found: 377.1986.

[{(Pr$^i_3$Si)NH}$_2$L4] (26). This compound was prepared following a similar method to that for **24**, but using *p*-phenylenediamine (2.00 g, 18.51 mmol) in THF (50 mL), LiBu^n (24.3 mL of a 1.6 M solution in hexane, 38.86 mmol) and Pr$^i_3$SiCl (7.9 mL, 37.01 mmol). Removal of the solvent *in vacuo* from the filtrate afforded a reddish-brown coloured powder (3.80 g, 48.8 %). M.p. 101 °C; ^{1}H NMR (400 MHz, C_6D_6, 298 K) δ = 1.10 (d, $^3J_{HH}$ = 6.4 Hz, 36H, CH(C*H*$_3$)$_2$), 1.13-1.19 (m, 6H, C*H*(CH$_3$)$_2$), 2.82 (s, 2H, N*H*), 6.61 (s, 4H, Ar-*H*); ^{13}C{^{1}H} NMR (101 MHz, C_6D_6, 298 K) δ = 12.9 (*C*H(CH$_3$)$_2$), 18.7 (CH(*C*H$_3$)$_2$), 118.9, 136.6 (Ar-*C*); ^{29}Si{^{1}H} NMR (80 MHz, C_6D_6, 298 K) δ = 4.6; IR ν/cm^{-1} (ATR): 3398 (m, NH), 3203 (br w), 3024 (w), 2941 (m), 2862 (vs), 2722 (w), 1832 (w), 1605 (w), 1506 (vs), 1464 (vs), 1362 (s), 1271 (vs), 1214 (w), 1163 (w), 1113 (m), 1073 (m), 1013 (s), 994 (s), 883 (vs), 813 (vs), 711 (vs), 657 (vs); acc. mass calc. for $C_{24}H_{49}N_2Si_2$ (MH^+): 421.3434; found: 421.3459.

[{(Pr$^i_3$Si)NH}$_2$L5] (27). This compound was prepared following a similar method to that for **24**, but using *m*-phenylenediamine (2.00 g, 18.51 mmol) in THF (50 mL), LiBu^n (24.3 mL of a 1.6 M solution in hexane, 38.86 mmol) and Pr$^i_3$SiCl (7.9 mL, 37.01 mmol). Removal of the solvent *in vacuo* from the filtrate afforded a brown coloured liquid (4.10 g, 52.7 %). M.p. liquid at R.T.; ^{1}H NMR (400 MHz, C_6D_6, 298 K) δ = 1.11 (d, $^3J_{HH}$ = 7.1 Hz, 36H, CH(C*H*$_3$)$_2$), 1.19-1.26 (m, 6H, C*H*(CH$_3$)$_2$), 3.01 (s, 2H, N*H*), 6.05 (s, 1H, Ar-*H*), 6.23 (d, $^3J_{HH}$ = 7.9 Hz, 2H, Ar-*H*), 7.02 (t, $^3J_{HH}$ = 7.9 Hz, 1H, Ar-*H*); ^{13}C{^{1}H} NMR (101 MHz, C_6D_6, 298 K) δ = 13.1 (*C*H(CH$_3$)$_2$), 18.7 (CH(*C*H$_3$)$_2$), 106.3, 108.0, 130.2, 149.1 (Ar-*C*); ^{29}Si{^{1}H} NMR (80 MHz, C_6D_6, 298 K) δ = 5.1; IR ν/cm^{-1} (ATR): 3402 (br w, NH), 2943 (s), 2892 (w), 2866 (vs), 1606 (vs), 1589 (m), 1496 (s), 1462 (s), 1400 (m), 1387 (m), 1367 (w), 1304 (m), 1263 (s), 1195 (vs), 1164 (m), 1072 (m), 993 (vs), 920 (m), 882 (vs), 826 (m), 758 (m), 732 (w), 709 (w), 677 (vs); acc. mass calc. for $C_{24}H_{49}N_2Si_2$ (MH^+): 421.3434; found: 421.3445

[(AmidAr†H)$_2$L5] (30). *m*-phenylendiamine (5.85 g, 54.13 mmol) and Bu^{t}C(O)Cl (13.3 mL, 108.26 mmol) were dissolved in dichloromethane (100 mL), and triethylamine (15.1 mL, 108.26 mmol) was added. The reaction mixture was stirred overnight and washed with 1 M $NaHCO_3$, followed by water (2×40 mL). The organic layer was separated and

dried over $MgSO_4$, then filtered. Volatiles were removed from the filtrate *in vacuo* to give [(1,3-Ph)(Bu^{t}CONH)$_2$] **28** as white powder (13.02 g, 87.1 %). **28** (4.00 g, 14.48 mmol) and PCl_5 (6.33 g, 30.41 mmol) were combined in a Schlenk flask. Toluene (50 mL) was added and the mixture was heated to reflux for 24 hours. The mixture was then evaporated to dryness and heated to 110 °C under vacuum for 1 hour to remove unreacted PCl_5. This yielded the moisture sensitive compound [(1,3-Ph)(NHC(O)Bu^t)$_2$] **29.** Compound **29** was redissolved in toluene (50 mL) and Ar†NH$_2$ (13.6 g, 29.11 mmol) and Et_3N (4.0 mL, 29.00 mmol) were added to it. This mixture was then refluxed at 110 °C for 3 days. The solvent was removed under reduced pressure, the solid residue was dissolved in Et_2O (100 mL) and a 1 M solution of Na_2CO_3 (30 mL) was added. The mixture was transferred to a separating funnel, the organic layer was washed with water (2×60 mL) and dried over $MgSO_4$. The organic layer was separated and volatiles were pumped down under vacuum to give a solid residue which was washed with toluene (3×30 mL), yielding the title compound **30** as white powder (14.10 g, 82.9 %). The X-ray quality crystals were grown by layering a THF solution of **30** with hexane. M.p. above 260 °C; compound **30** showed negligible solubility in normal deutrated solvents, therefore no useful solution-state spectroscopic data could be obtained; IR ν/cm^{-1} (ATR): 3461 (m), 3061 (w), 3022 (w), 2960 (m), 2869 (w), 1648 (vs), 1600 (m), 1578 (m), 1476 (vs), 1446 (s), 1397 (m), 1364 (m), 1320 (m), 1280 (m), 1258 (m), 1222 (w), 1165 (m), 1136 (m), 1116 (m), 1076 (s), 1030 (m), 1005 (w), 966 (w), 895 (m), 863 (m), 841 (w), 743 (s), 698 (vs); acc. mass calc. for $C_{86}H_{87}N_4$ (MH^+): 1175.6930; found: 1175.7098.

[{(Dip)NLi(THF)$_3$}$_2$L2] (17.Li). A solution of [{(Dip)NH}$_2$L2] (1.00 g, 2.01 mmol) in THF (30 mL) was cooled to -80 ºC and LiBu^n (2.6 mL of a 1.6 M solution in hexane, 4.23 mmol) was added dropwise over 10 minutes. After the addition, the reaction mixture was warmed to room temperature, and stirred for 3 hours. All volatiles were removed *in vacuo* and the residue was washed with ca. 20 mL of hexane to yield an off-white powder. X-ray quality crystals were grown by layering the THF solution of product with hexane (1.20 g, 63.3 %). M.p. 173 °C; ^{1}H NMR (400 MHz, C_6D_6, 298 K) δ = 0.41 (s, 12H, Si(C*H*$_3$)$_2$), 1.01 (s, 4H, SiC*H*$_2$), 1.33-1.38 (m, 48H, CH(C*H*$_3$)$_2$, OCH$_2$C*H*$_2$), 3.41 (t, $^3J_{HH}$ = 6.5 Hz, 24H, OC*H*$_2$CH$_2$), 4.15 (br s, 4H, C*H*(CH$_3$)$_2$), 6.90 (t, $^3J_{HH}$ = 7.5 Hz, 4H, Ar-*H*), 7.20 (d, $^3J_{HH}$ = 7.5 Hz, 4H, Ar-*H*); ^{13}C{^{1}H} NMR (101 MHz, C_6D_6, 298 K) δ = 2.0 (Si(*C*H$_3$)$_2$), 14.7 (Si*C*H$_2$), 25.0 (CH(*C*H$_3$)$_2$), 25.7 (OCH$_2$*C*H$_2$), 27.6 (*C*H(CH$_3$)$_2$), 68.0 (O*C*H$_2$CH$_2$), 122.8, 128.0, 128.2, 143.0 (Ar-*C*); ^{29}Si{^{1}H} NMR (80 MHz, C_6D_6, 298 K)

δ = -21.8; ^{7}Li NMR (156 MHz, C_6D_6, 298 K) δ = 0.69; IR ν/cm^{-1} (Nujol): 3025 (w), 1581 (s), 1412 (vs), 1258 (vs), 1227 (m), 1201 (w), 1141 (m), 1115 (s), 1102 (s), 1045 (vs), 952 (vs), 919 (w), 891 (s), 814 (s), 798 (vs), 757 (vs), 678 (m); anal. calc. for $C_{54}H_{98}Si_2N_2Li_2O_2$: C 68.89 %, H 10.49 %, N 2.98 %, found: C 68.69 %, H 10.44 %, N 3.47 %.

[{(Pr$^{i}_3$Si)$_2$L4Ge}$_2$] (32). A solution of **26** (1 g, 2.38 mmol) in hexane (30 mL) was cooled to -80 °C and LiBu^{n} (3.1 mL of a 1.6 M solution in hexane, 5.00 mmol) was added to this over 10 minutes. After the addition, the reaction mixture was warmed to room temperature and stirred for 3 hours. This reaction mixture was then added to a suspension of $GeCl_2$.dioxane (0.61 g, 2.61 mmol) in hexane (20 mL) at -80 ºC. The resultant solution was warmed to room temperature and stirred for 12 hours. The solution was filtered and concentrated to ca. 10 mL. Placing the solution at -30 °C for 2 days resulted in deposition of **32** as yellow coloured crystals (0.55 g, 46.9 %). M.p. 247 °C; ^{1}H NMR (400 MHz, C_6D_6, 298 K) δ = 1.16 (d, $^{3}J_{HH}$ = 7.4 Hz, 72H, CH(C*H*$_3$)$_2$), 1.37 (sept, $^{3}J_{HH}$ = 7.4 Hz, 12H, C*H*(CH$_3$)$_2$), 6.27 (s, 8H, Ar-*H*); ^{13}C{^{1}H} NMR (101 MHz, C_6D_6, 298 K) δ = 13.4 (*C*H(CH$_3$)$_2$), 19.2 (CH(*C*H$_3$)$_2$), 128.7, 141.3 (Ar-*C*); ^{29}Si{^{1}H} NMR (80 MHz, C_6D_6, 298 K) δ = 9.4; IR ν/cm^{-1} (Nujol): 3078 (w), 2961(s), 1489(s), 1382 (w), 1253 (m), 1212 (vs), 1099 (m), 1068 (m), 1012 (s), 1000 (m), 938 (s), 917 (m), 876 (s), 862 (vs), 824 (vs), 739 (vs), 717 (s), 677 (m), 664 (s); anal. calc. for $C_{48}H_{92}Ge_2N_4Si_4$: C 58.66 %, H 9.44 %, N 5.70 %, found: C 58.68 %, H 5.58 %, N 5.53 %.

[{(Pr$^{i}_3$Si)$_2$L5Ge}$_2$] (33). This compound was prepared following a similar method to that for **32**, but using **27** (1 g, 2.38 mmol) in hexane (30 mL), LiBu^{n} (3.1 mL of a 1.6 M solution in hexane, 5.00 mmol) and $GeCl_2$.dioxane (0.61 g, 2.61 mmol) in hexane (20 mL). Storage of the concentrated reaction solution at -30 °C for 2 days resulted in deposition of dark-yellow coloured crystals of **33** (0.49 g, 41.8 %). M.p. above 260 °C; ^{1}H NMR (400 MHz, C_6D_6, 298 K) δ = 1.19 (overlapping doublets, 72H, CH(C*H*$_3$)$_2$), 1.44 (sept, $^{3}J_{HH}$ = 7.4 Hz, 12H, C*H*(CH$_3$)$_2$), 6.29 (d, $^{3}J_{HH}$ = 7.8 Hz, 4H, Ar-*H*), 6.36 (s, 2H, Ar-*H*), 6.52 (t, $^{3}J_{HH}$ = 7.9 Hz, 2H, Ar-*H*); ^{13}C{^{1}H} NMR (101 MHz, C_6D_6, 298 K) δ = 13.1 (*C*H(CH$_3$)$_2$), 19.0, 19.1 (CH(*C*H$_3$)$_2$), 122.8, 128.5, 129.0, 146.7 (Ar-*C*); ^{29}Si{^{1}H} NMR (80 MHz, C_6D_6, 298 K) δ = 15.6; IR ν/cm^{-1} (Nujol): 1576 (vs), 1411 (w), 1383 (w), 1254 (s), 1162 (vs), 1076 (m), 1017 (m), 984 (vs), 917 (w), 880 (vs), 789 (vs), 728

(vs), 687 (vs); anal. calc. for $C_{48}H_{92}Ge_2N_4Si_4$: C 58.66 %, H 9.44 %, N 5.70 %, found: C 58.12 %, H 9.69 %, N 5.66 %.

[{(Pr$^i_3$Si)$_2$L4Sn}$_2$] (34). This compound was prepared following a similar method to that for **32**, but using **26** (1 g, 2.38 mmol) in toluene (30 mL), LiBu^n (3.1 mL of a 1.6 M solution in hexane, 5.00 mmol) and $SnBr_2$ (0.73 g, 2.61 mmol) in toluene (20 mL). Storage of the concentrated reaction solution at -30 °C for 2 days resulted in deposition of dark-red coloured crystals of **34** (0.38 g, 29.7 %). M.p. 180 °C; ^{1}H NMR (400 MHz, C_6D_6, 298 K) δ = 1.15 (d, $^3J_{HH}$ = 7.4 Hz, 72H, CH(C*H*$_3$)$_2$), 1.34 (sept, $^3J_{HH}$ = 7.3 Hz, 12H, *C*H(CH$_3$)$_2$), 6.27 (s, 8H, Ar-*H*); ^{13}C{^{1}H} NMR (101 MHz, C_6D_6, 298 K) δ = 13.4 (*C*H(CH$_3$)$_2$), 19.2 (CH(*C*H$_3$)$_2$), 127.4, 144.5 (Ar-*C*); ^{29}Si{^{1}H} NMR (80 MHz, C_6D_6, 298 K) δ = 8.6; IR ν/cm^{-1} (Nujol): 1459 (vs), 1281 (w), 1249 (w), 1210 (s), 1096 (w), 1068 (w), 1011 (m), 876 (s), 857 (s), 798 (w), 739 (vs), 660 (s); anal. calc. for $C_{48}H_{92}Sn_2N_4Si_4$: C 53.63 %, H 8.63 %, N 5.21 %, found: C 53.39 %, H 8.35 %, N 5.05 %.

[{(Pr$^i_3$Si)$_2$L5Sn}$_2$] (35). This compound was prepared following a similar method to that for **32**, but using **27** (1 g, 2.38 mmol) in toluene (30 mL), LiBu^n (3.1 mL of a 1.6 M solution in hexane, 5.00 mmol) and $SnBr_2$ (0.73 g, 2.61 mmol) in toluene (20 mL). Storage of the concentrated reaction solution at -30 °C for 2 days resulted in deposition of red coloured crystals of **35** (0.35 g, 27.3 %). M.p. 200 °C (decomp.); ^{1}H NMR (400 MHz, C_6D_6, 298 K) δ = 1.07 (d, $^3J_{HH}$ = 6.4 Hz, 36H, CH(C*H*$_3$)$_2$), 1.24 (m, 36H, 12H, C*H*(CH$_3$)$_2$, CH(C*H*$_3$)$_2$), 5.52 (s, 2H, Ar-*H*), 6.40 (d, $^3J_{HH}$ = 7.7 Hz, 4H, Ar-*H*), 6.86 (t, $^3J_{HH}$ = 7.7 Hz, 2H, Ar-*H*); ^{13}C{^{1}H} NMR (101 MHz, C_6D_6, 298 K) δ = 13.3 (*C*H(CH$_3$)$_2$), 19.0, 19.1 (CH(*C*H$_3$)$_2$), 107.9, 125.7, 128.4, 151.7 (Ar-*C*); ^{29}Si{^{1}H} NMR (80 MHz, C_6D_6, 298 K) δ = 6.7; ^{119}Sn{^{1}H} NMR (149 MHz, C_6D_6, 298 K): no signal observed; IR ν/cm^{-1} (Nujol): 3056 (w), 1586 (m), 1529 (s), 1491 (w), 1160 (s), 1076 (w), 1044 (s), 1019 (s), 933 (s), 845 (w), 764 (vs), 722 (s), 689 (vs), 664 (s); A reproducible microanalysis could not be obtained for the compound as it consistently co-crystallised with small amounts of the pro-ligand **25**, which could not be separated after several recrystallisations.

[L5(AmidAr†)$_2${MgI(OEt$_2$)}$_2$] (38). A solution of [(AmidAr†H)$_2$L5] (1.0 g, 0.85 mmol) in diethyl ether (30 mL) was added to MeMgI (1.8 mL, 1.79 mmol, 1 M solution in diethyl ether) over 5 minutes at room temperature. The mixture was stirred for 3 hours and the solution then concentrated to ca.15 mL under reduced pressure. Storage at -30

°C for 1 day resulted in white coloured powder of **38** (1.01 g, 73.2 %). M.P. 210 °C; ^{1}H NMR (400 MHz, C_6D_6, 298 K) δ = 0.88 (t, $^{3}J_{HH}$ = 7.1 Hz, 12H, OCH_2CH_3), 1.00-1.03 (m, 30H, $CH(CH_3)_2$, $C(CH_3)_3$), 2.57 (sept, $^{3}J_{HH}$ = 6.8 Hz, 2H, $CH(CH_3)_2$), 3.09 (br, 8H, OCH_2CH_3), 6.55 (s, 4H, Ph_2CH), 6.97-7.28 (m, 29H, Ar-*H*), 7.43 (d, $^{3}J_{HH}$ = 7.6 Hz, 7H, Ar-*H*), 7.71 (d, $^{3}J_{HH}$ = 7.7 Hz, 7H, Ar-*H*); ^{13}C{^{1}H} NMR (101 MHz, C_6D_6, 298 K) δ = 14.7 (OCH_2CH_3), 24.2 ($CH(CH_3)_2$), 31.2 ($C(CH_3)_3$), 33.7 ($CH(CH_3)_2$), 43.3 ($C(CH_3)_3$), 52.5 (Ph_2CH) 67.1 (OCH_2CH_3), 122.3, 126.3, 126.7, 128.6, 128.7, 130.3, 130.7, 137.6, 141.9, 144.1, 145.6, 149.2 (Ar-*C*), N*C*N resonance not observed; IR ν/cm^{-1} (Nujol): 3057 (w), 3023 (w), 2957 (w), 1582 (m), 1490 (m), 1448 (vs), 1215 (w), 1187 (m), 1149 (w), 1077 (w), 1033 (vs), 966 (w), 894 (w), 836 (w), 762 (m), 745 (m), 699 (vs); anal. calc. for $C_{94}H_{104}I_2Mg_2N_4O_3$: C 69.51 %, H 6.45 %, N 3.45 %; found: C 69.12 %, H 6.82 %, N 3.48 %.

[{L5(AmidAr†)$_2$(MgBu^{n})$_2$}$_2$] (39). $Mg(Bu^{n})_2$ (1.8 mL of a 1 M solution in heptane, 1.79 mmol) was added to a solution of [$(AmidAr^{\dagger}H)_2$L5] (1.0 g, 0.85 mmol) in toluene (30 mL) over 5 minutes at room temperature. The mixture was stirred for 3 hours and the solution then concentrated to ca.15 mL under reduced pressure and layered with hexane. Storage of reaction mixture at room temperature for 3 days resulted in deposition of **39** as white coloured crystals (0.80 g, 70.6 %). M.p. 215 °C (decomp.); ^{1}H NMR (600 MHz, C_6D_6, 298 K) δ = -0.76 (br s, 4H, $CH(CH_2)_2CH_3$), 0.67 (br s, 12 H, $CH(CH_3)_2$), 0.74 (br s, 6H, $CH(CH_3)_2$), 0.79 (br s, 6H, $CH(CH_3)_2$), 1.00 (s, 18H, $C(CH_3)_3$), 1.07 (s, 18H, $C(CH_3)_3$), 1.26-1.28 (m, 6H, $CH(CH_2)_2CH_3$), 1.31 (br, 16H, $CH(CH_2)_2CH_3$), 1.50 (br m, 6H, $CH(CH_2)_2CH_3$), 2.52 (br m, 2H, $CH(CH_3)_2$), 2.61 (br m, 2H, $CH(CH_3)_2$), 5.99 (s, 4H, 1.50 Ph_2CH), 6.40 (s, 4H, 1.50 Ph_2CH), 6.65-7.80 (m, 96H, Ar-*H*); ^{13}C{^{1}H} NMR (151 MHz, C_6D_6, 298 K) δ = 14.0, 14.7 ($CH(CH_3)_2$), 24.3, 25.2 ($C(CH_3)_3$), 31.0, 31.1, 31.3, 31.7 ($CH(CH_2)_2CH_3$), 33.9 ($CH(CH_3)_2$), 43.4 ($C(CH_3)_3$), 54.2 (Ph_2CH), 126.6, 126.9, 127.6, 2×128.6, 128.8, 129.8, 130.1, 138.2, 142.5, 143.7, 144.1, (Ar-*C*), N*C*N resonance not observed; IR ν/cm^{-1} (Nujol): 3061 (w), 3024 (w), 2955 (m), 1586 (m), 1493 (s), 1449 (vs), 1398 (vs), 1381 (vs), 1269 (w), 1215 (w), 1189 (m), 1123 (w), 1075 (m), 1031 (s), 1004 (w), 952 (w), 920 (w), 893 (w), 866 (w), 802 (w), 781 (m), 761 (w), 746 (s), 699 (vs); anal. calc. for $C_{188}H_{200}Mg_4N_8$: C 84.61 %, H 7.55 %, N 4.20 %; found: C 84.34 %, H 7.69 %, N 4.12 %.

[L5(AmidAr†)$_2$(GeCl)$_2$] (40). A solution of [(AmidAr†H)$_2$L5] (1.0 g, 0.85 mmol) in THF (50 mL) was cooled to -80 ºC and LiBu^n (1.1 mL, 1.79 mmol, 1.6 M solution in hexane) was added to this over 10 minutes. After the addition, the reaction mixture was warmed to room temperature, and stirred for 4 hours. This reaction mixture was then added to a solution of $GeCl_2$.dioxane (0.414 g, 1.79 mmol) in THF (20 mL) at -80 ºC. The resultant solution was warmed to room temperature and stirred for 12 hours. Volatiles were subsequently removed *in vacuo* and the residue extracted into hot toluene (50 mL). The extract was filtered, concentrated to ca. 20 mL and stored at -30 ºC overnight to yield white coloured powder of **40** (0.68 g, 57.5 %). M.p. 208 °C (decomp.); ^{1}H NMR (400 MHz, C_6D_6, 298 K) δ = 0.88 (s, 18H, C(C*H*$_3$)$_3$), 0.93 (d, 36H, $^3J_{HH}$ = 6.8 Hz, 12H, CH(C*H*$_3$)$_2$), 2.46 (sept, $^3J_{HH}$ = 6.9 Hz, 2H, C*H*(CH$_3$)$_2$), 5.96 (br s, 4H, Ph$_2$C*H*), 6.86-7.79 (m, 48 H, Ar-*H*); ^{13}C{^{1}H} NMR (101 MHz, C_6D_6, 298 K) δ = 23.9 (CH(*C*H$_3$)$_2$), 28.9 (C(C*H*$_3$)$_3$), 33.8 (*C*H(CH$_3$)$_2$), 42.3 (C(C*H*$_3$)$_3$), 51.3 (Ph$_2$*C*H), 127.1, 128.4, 128.7, 128.8, 128.9, 129.0, 129.5, 130.1, 131.0, 139.9, 143.4, 145.8 (Ar-*C*), N*C*N resonance not observed; IR ν/cm^{-1} (Nujol): 3057 (w), 3022 (w), 2953 (m), 1593 (vs), 1489 (s), 1448 (vs), 1412 (vs), 1263 (w), 1211 (w), 1182, 1151 (w), 1121 (w), 1075 (s), 1029 (s), 963 (w), 896 (w), 868 (w), 844 (w), 807 (w), 763 (w), 742 (w), 697 (vs); A reproducible microanalysis could not be obtained for the compound as it consistently crystallised with a small amount of an unknown impurity which could not be separated by repeated recrystallisations.

[{L5(AmidAr†)$_2$Ge}$_2$] (41). A solution of **40** (0.6 g, 0.43 mmol) in toluene (20 mL) was added to a slurry of KC_8 (0.13 g, 0.95 mmol) in toluene (10 mL) at -80 °C. The mixture was warmed to room temperature and stirred for 4 hours. Volatiles were then removed *in vacuo* and residue was extracted into toluene (20 mL). The extract was filtered, concentrated to ca. 10 mL and placed at room temperature overnight to yield yellow crystals of **41** (0.21 g, 39.2 %). M.p. 208 °C (decomp.); IR ν/cm^{-1} (Nujol): 3060 (w), 3024 (w), 2958 (w), 1647 (s), 1579 (m), 1493 (m), 1476 (s), 1447 (s), 1397 (w), 1260 (vs), 1136 (w), 1094 (m), 1076 (s), 1029 (s), 1016 (s), 895 (w), 864 (w), 798 (vs), 762 (w), 744 (w), 698 (vs); A reproducible microanalysis could not be obtained for this compound as its negligible solubility in common organic solvents precluded it being purified by recrystallisation.

4.6 References

1 M. J. S. Gynane, D. H. Harris, M. F. Lappert, P. P. Power and P. Rividre, *J. Chem. Soc., Dalton Trans.*, 1977, 2004–2009.

2 P. J. Davidson and M. F. Lappert, *J. Chem. Soc., Chem. Commun.*, 1973, 317.

3 Y. Mizuhata, T. Sasamori and N. Tokitoh, *Chem. Rev.*, 2009, **109**, 3479–3511.

4 X. Wang, Z. Zhu, Y. Peng, H. Lei, J. C. Fettinger and P. P. Power, *J. Am. Chem. Soc.*, 2009, **131**, 6912–6913.

5 Y. Peng, J. D. Guo, B. D. Ellis, Z. Zhu, J. C. Fettinger, S. Nagase and P. P. Power, *J. Am. Chem. Soc.*, 2009, **131**, 16272–16282.

6 C. Yan, Z. Xu, X. Q. Xiao, Z. Li, Q. Lu, G. Lai and M. Kira, *Organometallics*, 2016, **35**, 1323–1328.

7 Y. Wu, C. Shan, Y. Sun, P. Chen, J. Ying, J. Zhu, L. Liu and Y. Zhao, *Chem. Commun.*, 2016, **52**, 13799–13802.

8 Y. P. Zhou and M. Driess, *Angew. Chem., Int. Ed.*, 2019, **58**, 3715–3728.

9 J. D. Scollard, D. H. McConville and J. J. Vittal, *Organometallics*, 1995, **14**, 5478–5480.

10 A. J. Arduengo, R. Krafczyk, R. Schmutzler, H. A. Craig, J. R. Goerlich, W. J. Marshall and M. Unverzagt, *Tetrahedron*, 1999, **55**, 14523–14534.

11 M. G. Gardiner and C. L. Raston, *Inorg. Chem.*, 1995, **34**, 4206–4212.

12 J. M. Kliegman and R. K. Barnes, *Tetrahedron*, 1970, **26**, 2555–2560.

13 F. Haftbaradaran, A. M. Kuchison, M. J. Katz, G. Schatte and D. B. Leznoff, *Inorg. Chem.*, 2008, **47**, 812–822.

14 J. F. Li, L. H. Weng, X. H. Wei and D. S. Liu, *J. Chem. Soc., Dalton Trans.*, 2002, 1401–1405.

15 S. M. I. Al-Rafia, P. A. Lummis, M. J. Ferguson, R. McDonald and E. Rivard, *Inorg. Chem.*, 2010, **49**, 9709–9717.

16 H. L. Dong, H. B. Tong, X. H. Wei, S. P. Huang and D. S. Liu, *Acta Crystallogr., Sect. E*, 2005, **61**, 1354–1355.

17 H. Chen, R. A. Bartlett, V. R. Dias, M. M. Olmstead and P. P. Power, *Inorg. Chem.*, 1991, **30**, 2487–2494.

18 L. H. Gade, C. H. Galka, K. W. Hellmann, R. M. Williams, L. De Cola, I. J. Scowen and M. McPartlin, *Chem. - Eur. J.*, 2002, **8**, 3732–3746.

19 R. Murugavel, N. Palanisami and R. J. Butcher, *J. Organomet. Chem.*, 2003, **675**, 65–71.

20 J. Okuda, *Chem. Ber.*, 1990, **123**, 1649–1651.

21 A. Shafir and J. Arnold, *Inorg. Chim. Acta*, 2003, **345**, 216–220.

22 A. Shafir, M. P. Power, G. D. Whitener and J. Arnold, *Organometallics*, 2001, **20**, 1365–1369.

23 X. Dai, P. Kapoor and T. H. Warren, *J. Am. Chem. Soc.*, 2004, **126**, 4798–4799.

24 W. H. Miles, M. J. Robinson, S. G. Lessard and D. M. Thamattoor, *J. Org. Chem.*, 2016, **81**, 10791–10801.

25 R. J. Schwamm, M. P. Coles and C. M. Fitchett, *Organometallics*, 2015, **34**, 2500–2507.

26 B. E. Eichler, A. D. Phillips and P. P. Power, *Organometallics*, 2003, **22**, 5423–5426.

27 R. Kretschmer, *Chem. - Eur. J.*, 2020, **26**, 2099–2119.

28 M. Bayram, D. Bla, C. Wo and S. Schulz, *Organometallics*, 2014, **33**, 2080–2087.

29 W. Zhang and L. R. Sita, *Adv. Synth. Catal.*, 2008, **350**, 439–447.

30 S.-D. Bai, R.-Q. Liu, T. Wang, F. Guan, Y.-B. Wu, J.-B. Chao, H.-B. Tong and D.-S. Liu, *Polyhedron*, 2013, **65**, 161–169.

31 C. O'Dea, O. Ugarte Trejo, J. Arras, A. Ehnbom, N. Bhuvanesh and M. Stollenz, *J. Org. Chem.*, 2019, **84**, 14217–14226.

32 M. Stollenz, J. E. Raymond, L. M. Pérez, J. Wiederkehr and N. Bhuvanesh, *Chem. - Eur. J.*, 2016, **22**, 2396–2405.

33 A. O. Tolpygin, A. S. Shavyrin, A. V. Cherkasov, G. K. Fukin and A. A. Trifonov, *Organometallics*, 2012, **31**, 5405–5413.

34 M. V. Yakovenko, A. V. Cherkasov, G. K. Fukin, D. Cui and A. A. Trifonov, *Eur. J. Inorg. Chem.*, 2010, 3290–3298.

35 S.-D. Bai, J.-P. Guo and D.-S. Liu, *Dalton Trans.*, 2006, 2244–2250.

36 M. S. Hill, P. B. Hitchcock and S. M. Mansell, *Dalton Trans.*, 2006, **60**, 1544–1553.

37 A. J. Hill and J. V. Johnston, *J. Am. Chem. Soc.*, 1954, **76**, 920–922.

38 G. D. Whitener, J. R. Hagadorn and J. Arnold, *J. Chem. Soc., Dalton Trans.*, 1999, 1249–1255.

39 E. W. Y. Wong, A. K. Das, M. J. Katz, Y. Nishimura, R. J. Batchelor, M. Onishi and D. B. Leznoff, *Inorg. Chim. Acta*, 2006, **359**, 2826–2834.

40 H. Braunschweig, C. Drost, P. B. Hitchcock, M. F. Lappert and L. J.-M. Pierssens, *Angew. Chem., Int. Ed. Engl.*, 1997, **36**, 261–263.

41 H. Ikeda, T. Monoi, Y. Nakayama and H. Yasuda, *J. Organomet. Chem.*, 2002, **642**, 156–162.

42 M. Veith, *Angew. Chem., Int. Ed.*, 1975, **14**, 263–264.

43 M. Veith, *Z. Naturforsch.*, 1978, **33b**, 7–13.

44 M. Veith and M. Grosser, *Z. Naturforsch., B: J. Chem. Sci.*, 1982, **37**, 1375–1381.

45 M. Veith, E. Werle, R. Lisowsky, R. Köppe and H. Schnöckel, *Chem. Ber.*, 1992, **125**, 1375–1377.

46 S. M. Mansell, C. A. Russell and D. F. Wass, *Dalton Trans.*, 2015, **44**, 9756–9765.

47 M. Haaf, T. A. Schmedake and R. West, *acc. Chem. Res.*, 2000, **33**, 704–714.

48 R. Dasgupta and S. Khan, in *Advances in Organometallic Chemistry*, Elsevier Inc., 1st edn., 2020, Vol. 74, pp. 105–152.

49 H. Braunschweig, P. B. Hitchcock, M. F. Lappert and L. J.-M. Pierssens, *Angew. Chem.*, 1994, **106**, 1243–1245.

50 B. Gehrhus, P. B. Hitchcock and M. F. Lappert, *Z. Anorg. Allg. Chem*, 2005, **631**, 1383–1386.

51 B. Gehrhus, M. F. Lappert, J. Heinicke, R. Boese and D. Blaser, *J. Chem. Soc., Chem. Commun.*, 1995, 1931–1932.

52 A. V. Zabula, F. E. Hahn, T. Pape and A. Hepp, *Organometallics*, 2007, **26**, 1972–1980.

53 F. E. Hahn, A. V. Zabula, T. Pape and A. Hepp, *Eur. J. Inorg. Chem.*, 2007, 2405–2408.

54 A. V. Zabula, T. Pape, A. Hepp, F. M. Schappacher, U. C. Rodewald, R. Pöttgen and F. E. Hahn, *J. Am. Chem. Soc.*, 2008, **130**, 5648–5649.

55 A. V. Zabula, T. Pape, A. Hepp and F. Ekkehardt Hahn, *Organometallics*, 2008, **27**, 2756–2760.

56 J. V. Dickschat, D. Heitmann, T. Pape and F. E. Hahn, *J. Organomet. Chem.*, 2013, **744**, 160–164.

57 F. E. Hahn, A. V. Zabula, T. Pape and A. Hepp, *Z. Anorg. Allg. Chem.*, 2008, **634**, 2397–2401.

58 S. Krupski, J. V. Dickschat, A. Hepp, T. Pape and F. E. Hahn, *Organometallics*, 2012, **31**, 2078–2084.

59 F. E. Hahn, A. V. Zabula, T. Pape, A. Hepp, R. Tonner, R. Haunschild and G. Frenking, *Chem. - Eur. J.*, 2008, **14**, 10716–10721.

60 K. Junold, J. A. Baus, C. Burschka and R. Tacke, *Angew. Chem., Int. Ed.*, 2012, **51**, 7020–7023.

61 D. Matioszek, N. Katir, N. Saffon and A. Castel, *Organometallics*, 2010, **29**, 3039–3046.

62 S. R. Foley, C. Bensimon and D. S. Richeson, *J. Am. Chem. Soc.*, 1997, **119**, 10359–10363.

63 A. Rösch, S. H. F. Schreiner, P. Schüler, H. Görls and R. Kretschmer, *Dalton Trans.*, 2020, **49**, 13072–13082.

64 J. A. R. Schmidt and J. Arnold, *J. Chem. Soc., Dalton Trans.*, 2002, 2890–2899.

65 G. J. Moxey, F. Ortu, L. Goldney Sidley, H. N. Strandberg, A. J. Blake, W. Lewis and D. L. Kays, *Dalton Trans.*, 2014, **43**, 4838–4846.

66 V. Y. Lee and A. Sekiguchi, in *Organometallic Compounds of Low-Coordinate Si, Ge, Sn and Pb: From Phantom Species to Stable Compounds*, Wiley, New York, 2010, pp. 139–188.

67 M. J. S. Gynane, M. F. Lappert, S. J. Miles and P. P. Power, *J. Chem. Soc., Chem. Commun.*, 1976, 256–257.

68 P. Zark, A. Schäfer, A. Mitra, D. Haase, W. Saak, R. West and T. Müller, *J. Organomet. Chem.*, 2010, **695**, 398–408.

69 M. Veith, M. Notzel, L. Stahl and V. Huch, *Z. Anorg. Allg. Chem*, 1994, **620**, 1264–1270.

70 D. Yang, J. Guo, H. Wu, Y. Ding and W. Zheng, *Dalton Trans.*, 2012, **41**, 2187–2194.

71 A. V. Zabula and F. E. Hahn, *Eur. J. Inorg. Chem.*, 2008, 5165–5179.

72 K. Semba, M. Shinomiya, T. Fujihara, J. Terao and Y. Tsuji, *Chem. - Eur. J.*, 2013, **19**, 7125–7132.

73 E. W. Y. Wong, D. Dange, L. Fohlmeister, T. J. Hadlington and C. Jones, *Aust. J. Chem.*, 2013, **66**, 1144–1154.

74 G. Berthon-Gelloz, M. A. Siegler, A. L. Spek, B. Tinant, J. N. H. Reek and I. E. Markó, *Dalton Trans.*, 2010, **39**, 1444–1446.

75 L. Q. Hu, R. L. Deng, Y. F. Li, C. J. Zeng, D. S. Shen and F. S. Liu,

Organometallics, 2018, **37**, 214–226.

76 L. Hintermann, *Beilstein J. Org. Chem.*, 2007, **3**, 2–6.

77 C. Nolte, P. Mayer and B. F. Straub, *Angew. Chem., Int. Ed.*, 2007, **46**, 2101–2103.

78 T. J. Hadlington, J. Li and C. Jones, *Can. J. Chem.*, 2014, **92**, 427–433.

79 C. Schädle, C. Meermann, K. W. Törnroos and R. Anwander, *Eur. J. Inorg. Chem.*, 2010, 2841–2852.

80 C. Janiak, *J. Chem. Soc., Dalton Trans.*, 2000, 3885–3896.

81 Y. Tang, A. M. Felix, L. N. Zakharov, A. L. Rheingold and R. A. Kemp, *Inorg. Chem.*, 2004, **43**, 7239–7242.

82 J. Intemann, J. Spielmann, P. Sirsch and S. Harder, *Chem. - Eur. J.*, 2013, **19**, 8478–8489.

Chapter 5
Reactivity Studies of Amidinate Stabilised Singly Bonded Silicon(I) and Germanium(I) Dimers

5.1 Introduction

Over the last few decades, many low oxidation state group 14 element complexes have been isolated. Amongst them, some of the most significant discoveries are the stabilisation of low oxidation state heavier group 14 element(I) dimers LEEL (L = bulky ligands, E = Si-Pb), which can incorporate a number of bulky monodentate or bidentate ligands, as discussed in chapter 2-4.

Despite the growing library of group 14 element(I) dimers, there are only two reported examples of bidentate amidinate ligand stabilised silicon(I) dimers [{PhC(NBu^t)$_2$Si}$_2$] and [{Bu^{t}PhC(NDip)$_2$Si}$_2$].[1,2] The advantage of these monoanionic amidinate based dimers is the presence of a lone pair of electrons at each element centre which do not take part in any bonding. This makes them not only a Lewis base but also effective electrophiles for the activation of small molecules. Herein, the reactivity of amidinate ligand stabilised silicon(I) and germanium(I) compounds towards small molecules, unsaturated organic compounds and transition metal complexes will be discussed. Moreover, the reactivity studies of a few stable silicon(II) and germanium(II) systems will also be covered.

5.1.1 Reactivity of Silicon(I) and Germanium(I) Dimers

Since the isolation of amidinate ligand stabilised low oxidation state group 14 element(I) dimers (described in chapter 3), their chemistry has rapidly developed. The following section will discuss the reactivity of bidentate ligand stabilised singly bonded silicon(I) and germanium(I) dimers reported in literature so far.

5.1.1.1 Activation of Small Molecules

As discussed in the preceding chapters, low oxidation state dimers have been shown to activate various small molecules like H_2, CO_2 and N_2O. To date, several bond activations

have been achieved via insertion into the single bond, and their mechanism depends on the bonding between two element centres.

Singly bonded bidentate ligand stabilised silicon(I) dimers have been found to activate nitrous oxide and carbon dioxide. Being a major greenhouse gas, the activation of carbon dioxide has attracted significant attention. Alongside this, the activation of nitrous oxide, which is a mono oxygen transfer agent that only produces non-toxic dinitrogen as a by-product, has also seen interest.

The reaction of the amidinate stabilised singly bonded dimer [{PhC(NBu^t)Si}$_2$] with three equivalents of nitrous oxide is shown in **Scheme 5.1**.[3] It resulted in a compound containing two four-membered disiloxane rings bridged by two oxygen atoms and one eight-membered Si_4O_4 ring. The disiloxane rings were found to be parallel to each other and the amidinate ligands were arranged orthogonally to these four-membered rings. This compound was the first of its class and demonstrated a singlet $^{29}Si\{^1H\}$ NMR resonance at δ -111.02 ppm, different from Driess' cyclodisiloxane [LSi(OH)(μ-O)$_2$SiL'] (L = [{N(Dip)C(Me)}$_2$HC], L' = L-H) (δ -60.7 and -119.2 ppm).[4] Formation of the former bridged species was proposed via a primary insertion of oxygen as a result of Si-Si bond cleavage. Thereafter, each lone pair of silicon centre was shown to react with nitrous oxide to give Si=O bonds, which further dimerised to give disiloxane rings-based bridged product [{PhC(NBu^t)Si(μ-O)}$_4$(μ-O)$_2$].

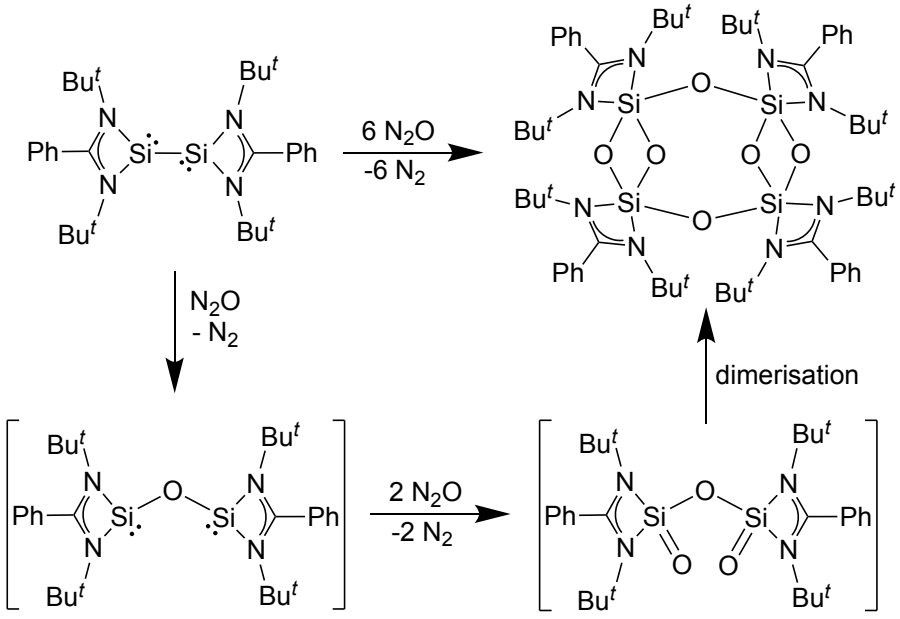

Scheme 5.1. Reaction of a silicon(I) dimer with N_2O.

In 2011, Baceiredo and Kato reported a singly bonded disilyne bisphosphine adduct that activated carbon dioxide by efficiently reducing it (**Scheme 5.2**).[5] The complex was shown to initially deoxygenate three molecules of carbon dioxide with the formation of three Si-O-Si moieties. This then reacted with an additional carbon dioxide molecule which inserted into one of the previously formed Si-O bonds, resulting in the formation of one bridged carbonate unit. This compound comprised a central tricyclic core with two Si-O-Si and one $Si(CO_3)Si$ groups with complete cleavage of Si-Si bond. Furthermore, both silicon centres possessed a distorted trigonal bipyramidal arrangement in which an oxygen and a silicon centre were at the apical position with O-Si-P bond angle of 173.27°.

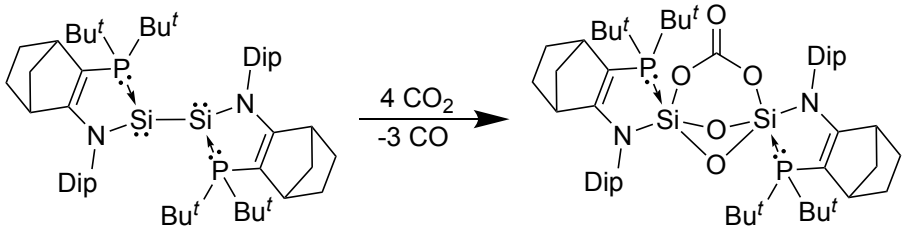

Scheme 5.2. Reaction of a disilyne with CO_2.

The reactivity of bidentate singly bonded silicon(I) dimers is limited to only a few small molecules. In this context, the reactivity of silicon(II) complexes based on bidentate amidinate and boryl-amide ligands is also worth mentioning.[6]

Since the first reported dihydrogen activation by $[\{(^{Dip}Ar)Ge\}_2]$ (^{Dip}Ar = 2,6-$(Dip)_2Ph$, Dip = 2,6-Pr^i_2Ph) in 2005,[7] various main group element complexes have been explored for the same purpose.[8] In 2012, a room temperature stable silylene $[Si\{B(NDipCH)_2\}\{N(SiMe_3)Dip\}]$ was isolated and shown to undergo facile oxidative addition of dihydrogen to give a dihydrosilane in quantitative yield.[9] This was the first experimentally observed dihydrogen activation by a silylene, and the single activation product could be achieved even at low temperature as 0 °C (**Scheme 5.3**). The reaction was strongly exergonic (ΔG = -122.2 kJ/mol) in accordance with the experimentally observed irreversibility. Further, a parallel reaction of the silylene with HD, that gave an analogous reaction product, was also confirmed to proceed by concerted bimolecular process using DFT calculations. The transition state calculations for dihydrogen addition revealed a side-on approach with a perpendicular B-Si-N plane (99.4°). This resulting electrophilic nature was reminiscent of the dihydrogen activation by transition metals.[10]

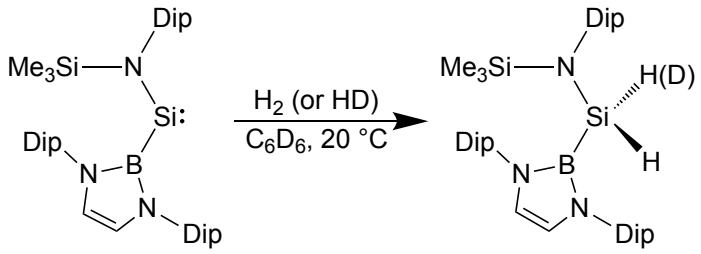

Scheme 5.3. Dihydrogen activation by a silicon(II) compound.

Activation of carbon monoxide has been a focus of synthetic chemists for catalytic applications in C-C bond formation, for example in well-known Fischer-Tropsch synthesis.[11] This has been dominated by transition metals owing to the high dissociation energy of the C≡O bond (BDE = 1077 kJ/mol).[12] In contrast, main group mediated activations of carbon monoxide remains scarce due to its limited oxidation states.

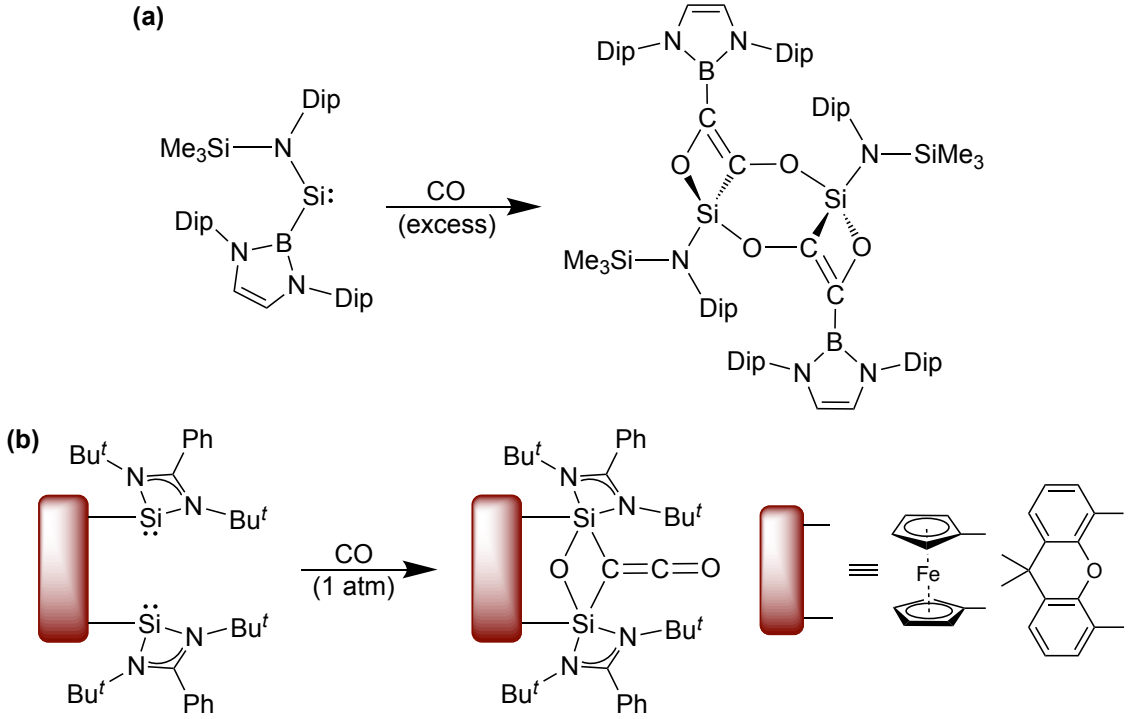

Scheme 5.4. Carbon monoxide activation by silylene complexes.

Aldridge and co-workers reported a reductive coupling of two equivalents of carbon monoxide with a boryl ligand stabilised silylene [Si{B(NDipCH)$_2$}{N(SiMe$_3$)Dip}] (**Scheme 5.4**).[13] The reaction generated four- and six-membered ethynediolate rings via inter- and intramolecular Si-O interactions. This molecular skeleton formed as a result of C≡C insertion of the ethyne diolate anion $[OCCO]^{2-}$ into the Si-B bonds of the silylene units. Notably, this type of carbon monoxide coupling to give ethynediolate dianions is

precedented for alkali, d- and f-block metal systems (the formation of ethynediolate by carbon monoxide coupling).[14–20] Further, both silicon centres, in +4 oxidation states, were tetra-coordinated and linked as part of the six-membered $Si_2C_2O_2$ ring.

In addition to that, Driess' amidinate ligand stabilised bis(silylene) complexes [$(LSi)_2$linker] (linker = Xant, Fc; Xant = 9,9-dimethylxanthene-4,5-diyl, Fc = 1,1'-ferrocenyl; L = [$PhC(NBu^t)_2$]) reacted with carbon monoxide at room temperature and one atmosphere pressure.[21] The reactions gave two corresponding ketenes [linker$(LSi)_2(\mu\text{-}O)(\mu\text{-}CCO)$] in high yields as a result of deoxygenative reductive homocoupling of carbon monoxide (**Scheme 5.4**). The $^{29}Si\{^1H\}$ NMR spectra depicted a remarkable upfield shift at δ -91.4 and -84.8 ppm as compared to the bis(silylene) precursor (δ 17.3 ppm) due to the change in the oxidation state of silicon from Si^{II} to Si^{IV}. These compounds featured a four-membered Si_2OC ring where the Si---Si distance was found to be 2.6692(13) Å, confirming no bonding interaction between the silicon centres. DFT calculations revealed a unique binding mechanism for these reactions. The initial step involves a cooperative interaction of silicon lone pairs of silylenes with two π*-orbitals of carbon monoxide, resulting in an intermediate in which carbon monoxide acts as a Lewis acid and silylene centres as Lewis bases. This intermediate reacts with another carbon monoxide molecule to afford [linker$(LSi)_2(\mu\text{-}CO)_2$], in which a OC-CO homocoupling occurs, followed by several rearrangement steps to finally get the desired ketenes.

5.1.1.2 Reactivity Towards Unsaturated Substrates

The reactivity of group 14 element(I) dimers especially ditetrelenes with unsaturated hydrocarbons containing C=C and C≡C bonds often results in irreversible cycloaddition reactions.[22] Yeong et al. reported the reaction of the singly bonded bidentate ligand stabilised the silicon(I) dimer [$\{PhC(NBu^t)Si\}_2$] with PhC≡CH and PhC≡CPh in toluene (**Scheme 5.5**).[23] These reactions resulted in highly air and moisture sensitive compounds [cis-$\{PhC(NBu^t)Si\}_2(\mu\text{-}PhC{=}CH)$] and [$\{PhC(NBu^t)Si(\mu\text{-}PhC{=}CPh)\}_2$] in 13.6 % and 47 % yields, respectively. The reactions proceeded via a [1+2] cycloaddition at one silicon centre with one alkyne molecule which then undergoes an insertion with another silicon centre to form the bridged species. The compound [cis-$\{PhC(NBu^t)Si\}_2(\mu\text{-}PhC{=}CH)$] had a trigonal pyramidal geometry at each silicon centre with N-Si-C bond angles 95.54(7)° and 98.48(7)°. These angles also indicated the presence of

stereochemically active lone pair of electrons at both silicon centres, which is similar to the earlier reported three-coordinate chlorosilylene [PhC(NBu$^t_2$)SiCl].[24]

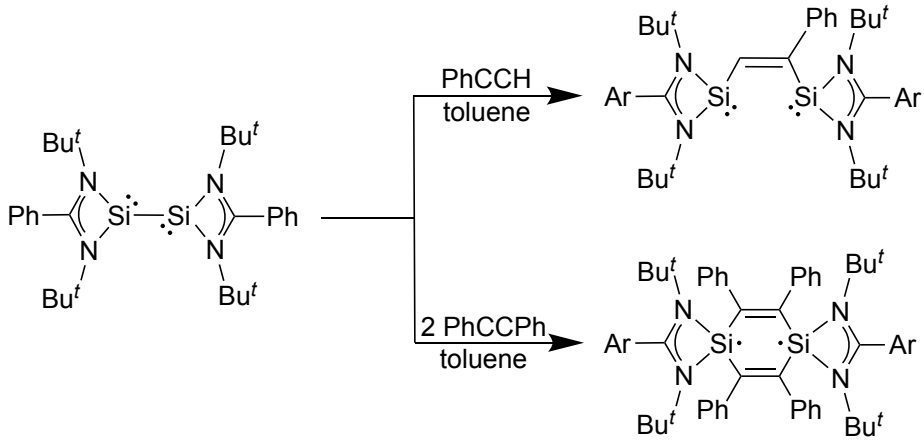

Scheme 5.5. Reactivity of silicon(I) dimer with PhC≡CH and PhC≡CPh.

In case of reaction with PhC≡CPh, after the insertion of one molecule, reaction with another molecule of PhC≡CPh affords a biradicaloid species. This compound contains a planar "Si(μ-C_2Ph_2)$_2$Si" ring, which is tilted by 5.98° angle from the *N,N'*-chelated amidinate rings. This radical species is stabilised by the amidinate ligand and delocalisation within the six-membered "Si(μ-C_2Ph_2)$_2$Si" ring. The compound exhibits a singlet peak at δ -51.0 ppm in the ^{29}Si{^{1}H} NMR spectrum, in contrast to the (μ-PhC=CH) bridged species which showed two singlets at δ 15.1 and 29.5 ppm for non-equivalent centres.

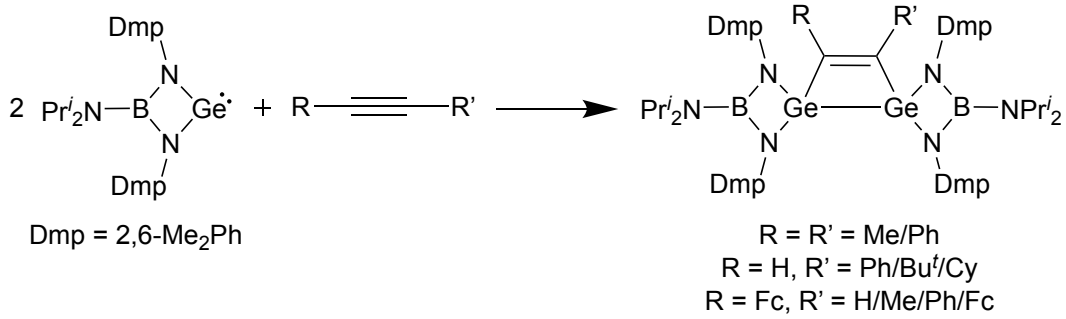

Scheme 5.6. Reactivity of a germanium(II) complex with substituted alkynes.

Reactions of amidinate stabilised germanium(I) dimer with unsaturated hydrocarbons are not reported in literature till date. However, a similar reaction was observed by the treatment of a boraguadinato stabilised germylene complex with several alkynes (**Scheme 5.6**).[25] The reaction led to a formal [2+2+2] cyclisation to afford the substituted

1,2-digermacyclo-but-3-enes, which demonstrated C=C stretching vibrations in the range of 1511-1549 cm^{-1} in Raman spectra.

These above-mentioned examples represent how the steric encumbrance of the applied alkynes affects the final product. Multiple studies have shown that these reactions follow a certain pathway which is similar for most of the cycloaddition reactions of alkynes (**Scheme 5.7**).[8] In case of addition of one hydrocarbon molecule, initially a three-membered ring is formed at one element centre which rearranges to a cycloaddition product. On adding another hydrocarbon molecule, a similar three-membered ring is generated at the other element centre which further rearranges to give the desired 1,2- or 1,4-diteteral benzenes.

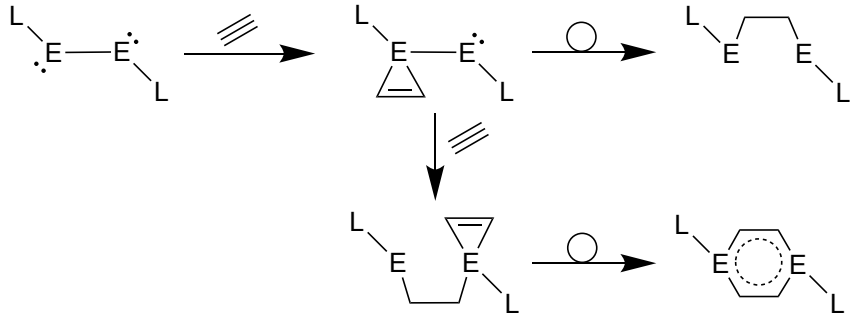

Scheme 5.7. General reaction pathway for cycloaddition reactions of ditetrelenes with alkynes.

Further, a particular amidinate ligand stabilised diradicaloid complex was synthesised in 2012 by stirring three equivalents of disilylene [{PhC(NBu^t)$_2$Si}$_2$] with two equivalents of aromatic carbodiimide DipN=C=NDip for 12 hours at room temperature in toluene.[26] The reaction afforded a mixture of products containing yellow crystals of silylenylsilamine [LSi(=NDip)-SiL] (L = [PhC(NBu^t)$_2$]) (major product) and yellow brown coloured crystals of singlet delocalised 2,4-diimino-1,3-disilacyclobutanedinyl [LSi(μ-CNDip)$_2$SiL] (minor product) (**Scheme 5.8**).

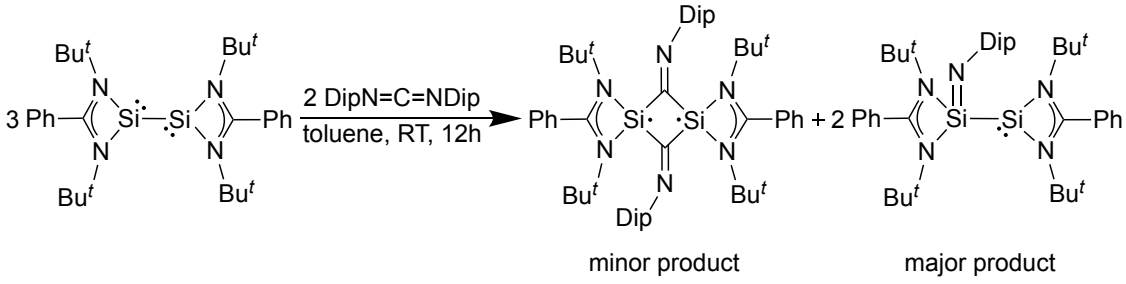

Scheme 5.8. Reaction of a silicon(I) dimer with DipN=C=NDip.

The minor product comprised a four-membered Si_2C_2 ring with each silicon centre adopting a tetrahedral geometry. The bond distance between the two silicon centres is 2.553(2) Å which is significantly longer than the covalent radii of Si-Si single bond (2.34 Å). Theoretical studies revealed a singlet diradicaloid character with a considerable delocalisation over the central four-membered Si_2C_2 ring and exocyclic C=N bonds. Furthermore, the compound showed no EPR signal and only a singlet resonance was seen in its $^{29}Si\{^1H\}$ spectrum at δ -39.9 ppm. These observations also confirmed a singlet ground state. In contrast, the major product had a three-coordinate silicon(I) centre with distorted tetrahedral geometry at one side which is in good agreement with the presence of stereoactive lone pair of electrons. The other side showed a silaimine substituent with a Si=N bond. A proposed mechanism for major and minor product formation involved a [1+2] cycloaddition reaction, which initially formed a bis(silaaziridimine) intermediate, followed by two nitrene (:N-Dip) eliminations to yield [1.1.0]butane-2,4-diimine. This reacted with another silylene molecule to form the major product, while homolytic Si-Si bond cleavage in [1.1.0]butane-2,4-diimine resulted in the minor product.

5.1.1.3 Reactivity Towards Transition Metals

Prior studies of silylenes have shown unusual reactivity towards various transition metal species.[27–29] Silylenes stabilise transition metal complexes that feature interesting coordination modes. Amidinate stabilised disilylenes contain two available reactive sites when treated with transition metals viz. (**i**) Si-Si bond and (**ii**) silicon lone pairs.

The singly bonded dimers were expected to behave as Lewis bases on reacting with transition metals, due to the presence of a lone pair of electrons on each element centre. However, only one example of the reactivity of bidentate ligand stabilised singly bonded germanium(I) dimer with a transition metal is known. The reaction of two equivalents of $Fe_2(CO)_9$ with $[\{PhC(NBu^t)_2Ge\}_2]$ resulted in the formation of a Lewis acid-base adduct $[\{PhC(NBu^t)_2GeFe(CO)_4\}_2]$ (**Scheme 5.9**).[30] Interestingly, in this compound the Ge-Ge bond (2.55(5) Å) was retained, with a shorter bond length as compared to the starting material (2.57(5) Å). Each germanium centre was coordinated with one $Fe(CO)_4$ unit, two nitrogens of monoanionic ligand and another germanium(I) centre. Each iron centre was five-coordinated and showed a distorted trigonal bipyramidal geometry. The Fe-Ge bond length was 2.34(4) Å which is comparable to the earlier $[LGe(OH)Fe(CO)_4]$ (L= $[HC(CMeNDip)_2]$) (2.33(1) Å) complex.[31]

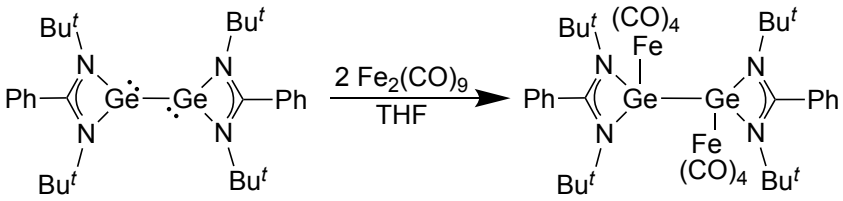

Scheme 5.9. Reaction of a germanium(I) dimer with $Fe_2(CO)_9$.

Further, Tacke and co-workers found that amidinate and bis(guanidinate) ligand stabilised silicon(II) compounds react with transition metal carbonyls as a nucleophile, resulting in transition metal silylene complexes. These compounds form Si-M bonds on addition of the transition metal carbonyls $Fe(CO)_5$ and $M(CO)_6$ (M = Cr, Mo, W) in toluene (**Scheme 5.10**).

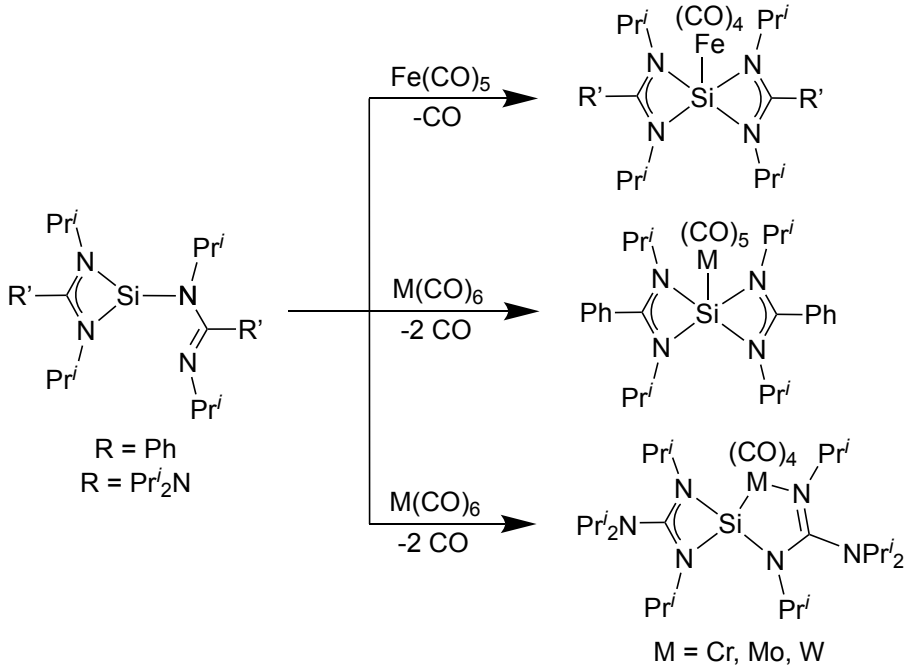

Scheme 5.10. Reactions of amidinate and guanidinate stabilised silylenes with $Fe(CO)_5$ and $M(CO)_6$ (M = Cr, Mo, W).

In this context, the reaction of amidinate and guanidinate stabilised disilylenes with $Fe(CO)_5$ gave four-coordinate silicon(II) complexes $[\{PhC(NDip)_2Si(NMe_2)\}_2Fe(CO)_4]$ and $[\{Pr^i_2NC(NDip)_2Si(NMe_2)\}_2Fe(CO)_4]$ in more than 60 % yield.[32,33] Whereas, the treatment of guanidinate and amidinate stabilised silylenes with $M(CO)_6$ leads to different products. In the case of amidinate stabilised silylene, only one of the CO group was replaced with silylene and both amidinate moieties bind in a *N,N'*-chelating fashion. With the guanidinate stabilised silylene, substitution of two carbonyl groups occurred,

leading to *N,N'*-chelation of one guanidinate ligand to silicon centre and the second guanidinate ligand bridged between silicon and a transition metal atom. These complexes encompass a four-membered SiN_2C and a five-membered $MSiN_2C$ rings.

The treatment of amidinate ligand stabilised germanium(II) complexes with $Fe_2(CO)_9$ resulted in four-coordinate germanium centred complexes after the elimination of $Fe(CO)_5$. As a result, the complexes $[Bu^tC(NPr^i)_2Ge(Cl)Fe(CO)_4]$ and $[PhC(NBu^t)_2Ge(Cl)Fe(CO)_4]$ were isolated in 78 % and 92 % yields, respectively (**Scheme 5.11**).[34] The iron centres displayed distorted trigonal bipyramidal geometries with the germylene occupying the axial position.

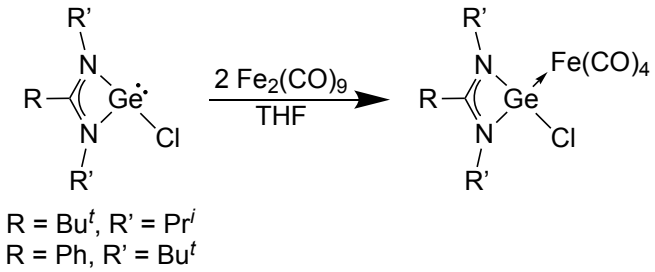

Scheme 5.11. Synthesis of amidinate stabilised germylene iron complexes.

5.2 Research Proposal

As can be gleaned from the literature, amidinate stabilised group 14 element(I) dimers have received significant attention over the last two decades, due to being isoelectronic to alkynes. The isolation of these complexes is dependent on the steric encumbrance of the ligand framework, which in turn leads to diverse reactivity on slight variations. Currently, there are only two amidinate ligand stabilised silicon(I) dimers $[\{PhC(NBu^t)_2Si\}_2]$ and $[\{(Butiso)Si\}_2]$ (Butiso = $[\{4\text{-}Bu^tPhC(NDip)_2\}^-]$), which are reported by Roesky and co-workers and our group, respectively. The reactivity of Roesky's dimer has been well explored, however, that of the latter is still unknown. It was therefore thought that the reactivity of the amidinate stabilised silicon(I) dimer $[\{(Butiso)Si\}_2]$ would add to our understanding in the rapidly developing area of main group chemistry.

Hence, our goal was to explore the reactivity of the amidinate ligand stabilised silicon(I) dimer $[\{(Butiso)Si\}_2]$ towards small molecules such as CO, H_2, CO_2, N_2O. Further, we also aimed to study the reactivity of the disilylene with unsaturated substrates like C_2H_4, Bu^tNC (isolobal to CO) and transition metal complexes ($Fe(CO)_5$ and $Mo(CO)_6$).

Additionally, to draw a comparison, the reactivity of literature reported germanium(I) dimer [{(Butiso)Ge}$_2$] utilising the similar ligand system was also explored.

5.3 Results and Discussion

The first target of this study was the synthesis of the known silicon(I) and germanium(I) dimers, which were carried out by following the procedures reported in literature.[2] The reaction of the silicon(IV) complex [(Butiso)SiCl$_3$] and germanium(II) complex [(Butiso)GeCl] with 1.5 and one equivalents of magnesium(I) dimer [{(^{Mes}Nacnac)Mg}$_2$] (^{Mes}Nacnac = [HC{N(Mes)C(Me)}$_2$]$^-$; Mes = 2,4,6-Me$_3$Ph), respectively, in toluene resulted in the formation of silicon(I) and germanium(I) dimers **1** and **2**, [{(Butiso)E}$_2$] (E = Si, Ge) (**Figure 5.1**).

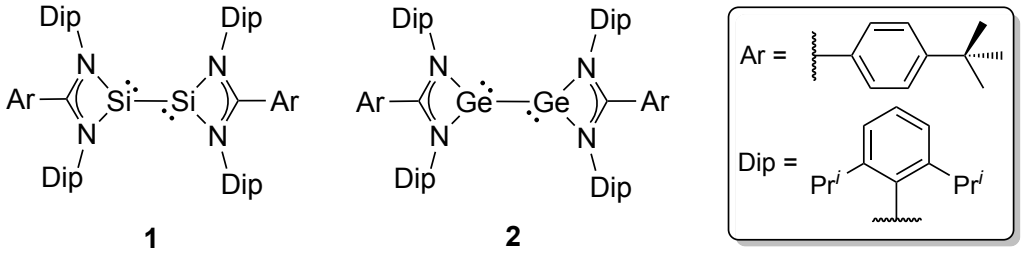

Figure 5.1. Butiso ligand stabilised reported silicon(I) and germanium(I) dimers.

5.3.1 Reactivity of Silicon(I) Dimer

5.3.1.1 Reaction with Carbon Monoxide

The initial reactivity of **1** was conducted with carbon monoxide gas. Exposure of a pentane solution of **1** to excess carbon monoxide at room temperature and pressure for 12 hours resulted in a change in colour from purple to orange (**Scheme 5.12**). ^{1}H NMR measurements of the reaction mixture predicted the conversion to a new species **3** with the formation of 10 % protonated ligand. Product **3** was characterised by two downfield resonances at δ -12.2 ppm, 35.2 ppm from δ 96.9 ppm (for **1**) in the ^{29}Si{^{1}H} NMR spectrum. The two silicon peaks ascertained the presence of two distinct silicon centres. **3** also showed a characteristic peak at δ 182.8 ppm in ^{13}C{^{1}H} NMR spectrum, associated with the reacting CO. This was verified by reacting dimer **1** with ^{13}CO gas in an NMR tube.

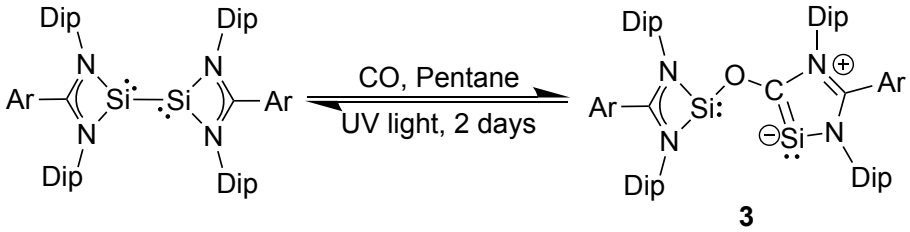

Scheme 5.12. Reactivity of silicon(I) dimer **1** with carbon monoxide.

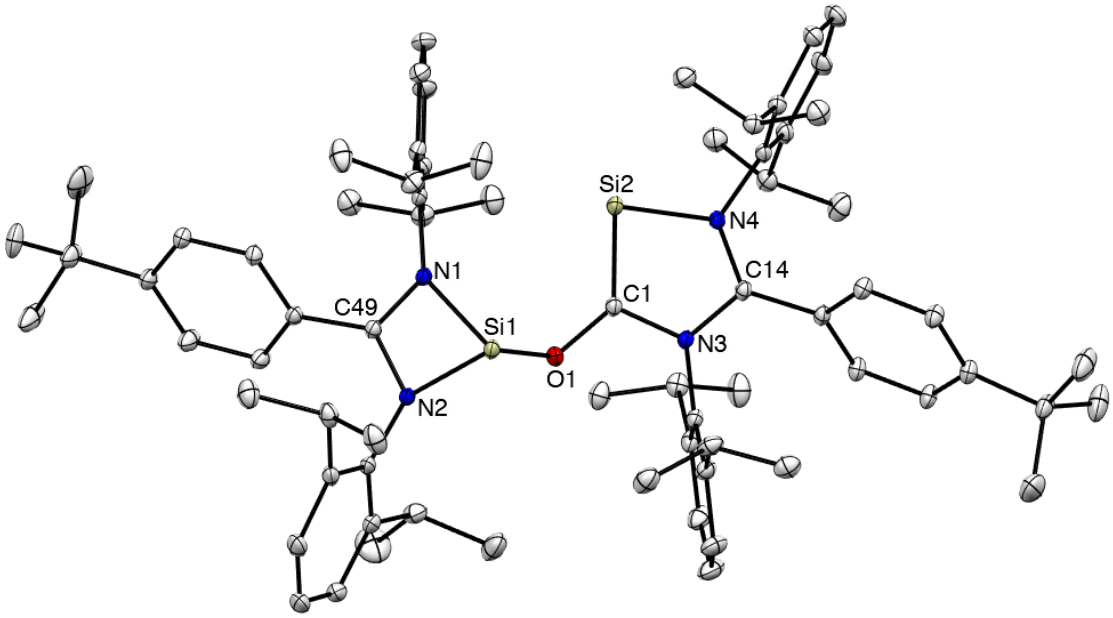

Figure 5.2. Molecular structure of [(Butiso)SiOCSi(Butiso)] (**3**) (thermal ellipsoids shown at 20 % probability). Hydrogen atoms omitted for clarity. Selected bond lengths (Å) and angles (°): Si1-O1 1.7126(12), O1-C1 1.3778(19), N3-C1 1.4042(19), Si2-C1 1.8093(17), Si2-N4 1.8282(13), Si1-N1 1.9053(13), Si1-N2 1.9142(14), N1-C49 1.322(2), N2-C49 1.347(2), N3-C14 1.357(2), N4-C14 1.351(2), C1-O1-Si1 110.42(10), C1-Si2-N4 83.41(7), C14-N4-Si2 117.38(11), N4-C14-N3 111.00(13), C14-N3-C1 114.34(13), N1-Si1-N2 68.47(6), N1-C49-N2 107.27(13).

Compound **3** was crystallised from a concentrated pentane solution and the X-ray crystal structure is depicted in **Figure 5.2**. The molecular structure of **3** reveals an insertion of CO between two silylene fragments. The oxygen of CO is bonded to the silicon centre of a silylene unit, while the carbon inserts between the Si-N bond of the other silylene fragment forming a planar five-membered SiNCNC ring. The N4-C14 (1.357(2) Å) and N3-C14 (1.351(2) Å) bonds are almost identical. The Si2-C1 bond length is 1.8093(17) Å, which is slightly longer than the Si=C bond length in [{(Trip)$_2$Si(SiTrip)$_2$CO}$_2$] (Trip = 2,4,6-Pr$^i_3$Ph) (1.771(4) Å).[22] Further, the Si2-N4 (1.8282(13) Å), C1-N3 (1.4042(19) Å) bond lengths are shorter than reported single bonds.[35] Hence, these bond lengths

confirm the compound's delocalisation of electrons within the ring. The silicon centre Si1 is three-coordinate with *N,N'*-chelated amidinate and oxygen, giving a trigonal pyramidal geometry, whereas two-coordinate Si2 is ligated to a carbon and a nitrogen.

The above-mentioned bond lengths in the structure reveal that a Lewis description of the compound will prove challenging. The most obvious of these are the nearly similar N-C bond lengths in the five-membered heterocycle. Therefore, the compound must contain at least two resonance structures with electron delocalisation around this ring. However, unlike an amidinate, the five-membered ring of **3** shows a zwitterionic structure. The average resonance structure hypothesised is shown in **Figure 5.3**.

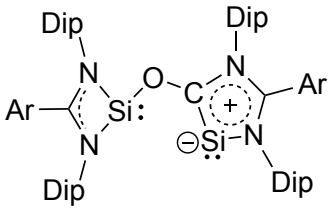

Figure 5.3. Proposed average resonance structure for **3**.

A geometry optimisation of **3** was performed by C. Smith using density functional theory (DFT) calculations at B3PW91, 6-31+G(d) level of theory. The calculated and experimental geometries of the compound gave a close match of key bond lengths and bond angles within the five-membered SiNCNC ring. The Si-N bond lengths in four-membered ring are slightly overestimated by 1.89 % and 2.04 %. Furthermore, the frontier orbitals analysis of **3** (**Figure 5.4**) reveals that the HOMO largely comprises the C-Si π-bond, whereas the LUMO represents the antibonding parts of Si-O which delocalises over the ligand backbone.

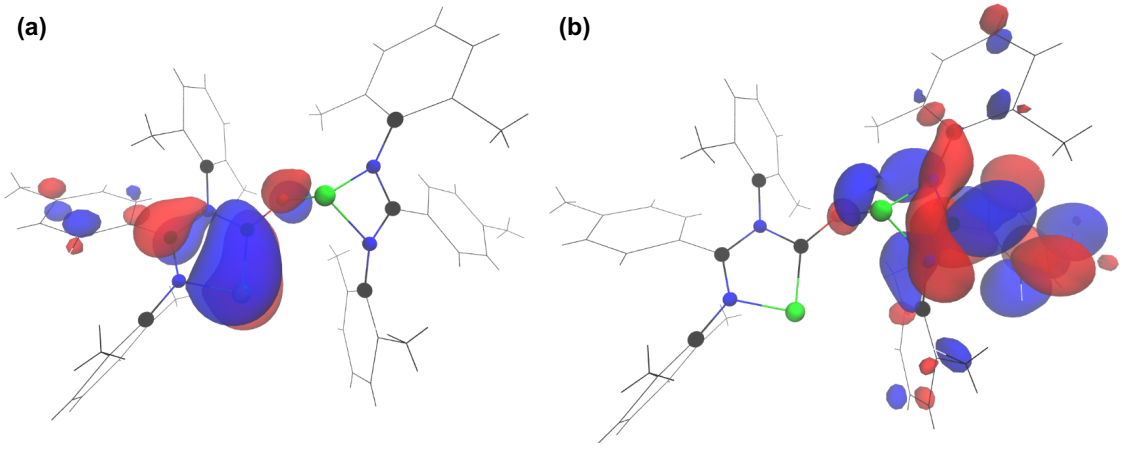

Figure 5.4. HOMO (**a**) and LUMO (**b**) of **3**.

The mechanism for the addition of carbon monoxide has also been studied using DFT analysis on a sterically reduced model **1A**, which produces near-identical bond lengths to the full molecule. Additionally, both the HOMO and LUMO show the same key features as in the full model. It was found that the primary reaction step involves the formation of a CO adduct on interaction with silicon centre, forming an Si-C bond in an end-on geometry. After this, an insertion of oxygen atom occurs into the Si-Si bond, followed by an additional insertion of C1 into the Si2-N3 bond. This results in weaking of C=O bond and formation of a heterocyclic transition state. Finally, a rearrangement step strengthens both the N3-C1 and CO bonds while breaking the two weaker Si-O bonds due to a relatively large barrier to the lower energy product **3A** (**Figure 5.5**).

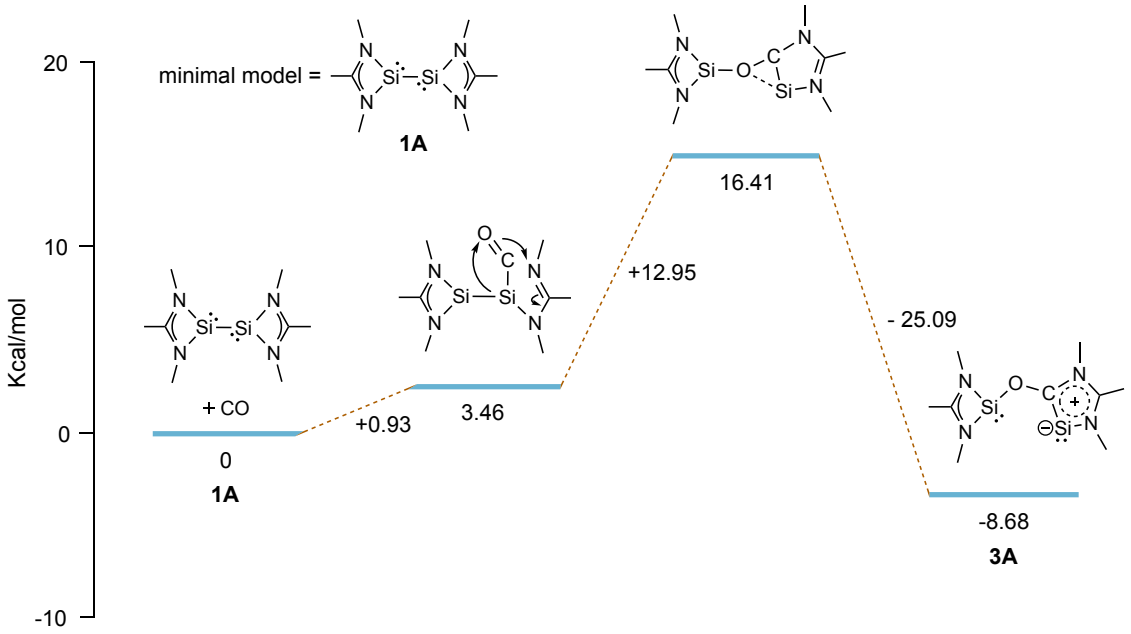

Figure 5.5. Calculated reaction profile for carbon monoxide activation with **1A**.

Further, upon photoactivation of compound **3** in C_6D_6 by irradiating with ultraviolet light (λ = 370 nm, 43W LED lamp), the orange colour of the solution began to disappear, and a green coloured solution was formed, which turned darker at longer exposure (two days). The ^{1}H NMR spectrum of the reaction mixture showed a subsequent 90 % conversion to silicon(I) dimer **1** within 2 days. This strongly suggested the reversible nature of the reaction under UV light. The progress of the reaction was also consistently monitored by ^{1}H NMR spectroscopy (**Figure 5.6**). To the best of our knowledge, this finding represents the first example of reversible carbon monoxide activation by silicon(I) dimer.

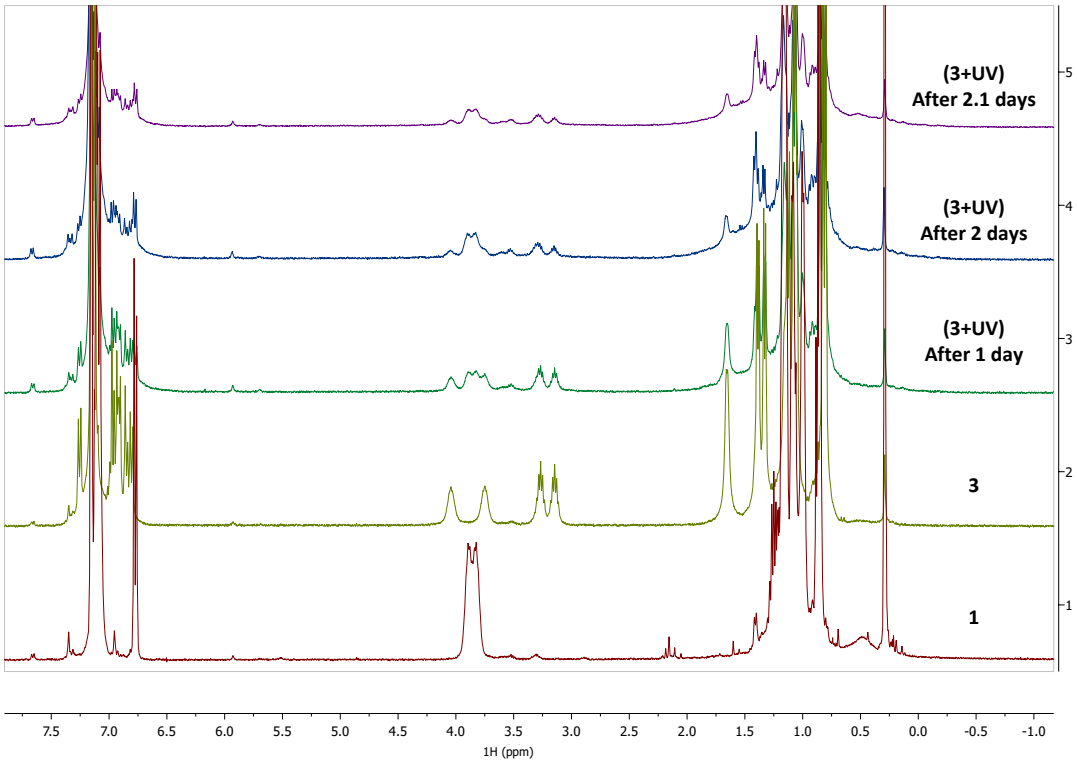

Figure 5.6. ^{1}H NMR spectra of solutions of **3** irradiated with ultraviolet light.

According to hard and soft acid-base concept, **3** can be considered as a soft base.[36,37] To validate this hypothesis, the reaction with Lewis acids was proposed to evaluate if **3** can form a Lewis acid-base adduct. **3** was reacted with transition metal complexes $Fe(CO)_5$ and $Mo(CO)_6$/$[Mo(CO)_4(nbd)]$ in benzene. The reactions did not proceed at room temperature or even after heating the solutions up to 70 °C. However, on irradiating the solutions with ultraviolet light, disappearance of the yellow colour solution of **3** occurred, leading to distinct products (**Scheme 5.13**). Slow evaporation of pentane solutions of both reaction mixtures afforded brown and orange coloured crystals of the Lewis acid-base adducts $[(Butiso)Si\{\mu\text{-}Fe(CO)_3\}]_2$ **4** and $[(Butiso)Si\{\mu\text{-}Mo(CO)_4\}(OC)Si(Butiso)]$ **5**, respectively.

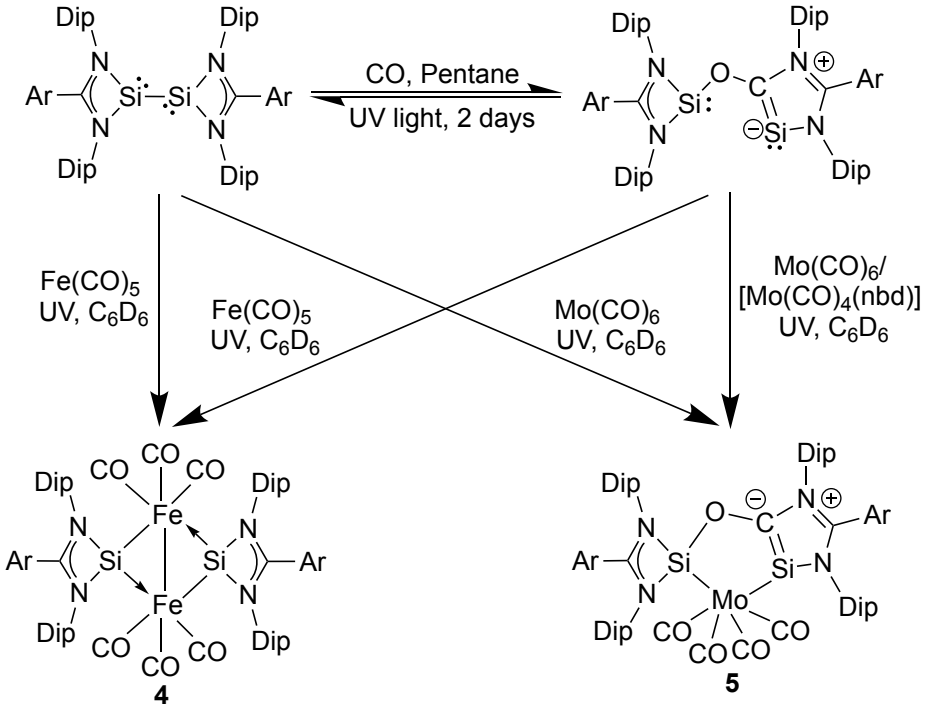

Scheme 5.13. Reactions of complexes **1** and **3** with CO, $Fe(CO)_5$, $Mo(CO)_6$ and $[Mo(CO)_4(nbd)]$.

It is worth nothing that complex **4** does not contain an N-Si inserted CO unit. In fact, two $Fe(CO)_3$ units were found to be inserted between two silicon centres. This observation strongly supports the reversibility of complex **3** under ultraviolet light. To test this further, when solutions of **1** and $Fe(CO)_5$ or $Mo(CO)_6$ were irradiated with ultraviolet light, these reactions resulted in similar products **4** and **5**, as confirmed by NMR spectroscopic techniques.

The X-ray structure of **4** (**Figure 5.7**) reveals two $Fe(CO)_3$ units bridged between the two silicon centres where silylene fragments act as σ-donors to bind these moieties. A similar reactivity has also been observed for Power's germanium(I) and tin(I) dimers with group 6 metal carbonyls under ultraviolet light.[38] The Si---Si (3.205 Å) distance in **4** is more than the sum of covalent radii of single Si-Si bond (2.22 Å), suggesting the absence of any covalent interaction. The bonding distance between two iron atoms (Fe-Fe = 2.7852(3) Å) is considerably longer than the previously reported similar $[Fe(CO)_3]_2$ bridged compounds (Fe-Fe = 2.4875(9) Å-2.666(3) Å).[39–42] Each iron centre displays an octahedral coordination by three carbonyl ligands, two silylene centres and one other $Fe(CO)_3$ group. The average Si-Fe bond distance (2.2305 Å) resembles those reported for $[Me_2NC(NDip)(NBu^t)Si(H)Fe(CO)_4]$ (2.234(1) Å) and $[PhC(NBu^t)_2Si(OBu^t)Fe(CO)_4]$ (2.237(7) Å).[43,44] Moreover, **5** is reminiscent of carbene

ligand stabilised [{LSi{μ-Fe(CO)$_3$}}$_2$(μ-CO)] (L = [:C{N(Dip)CH}$_2$]), isolated by Robinson and co-workers.[41]

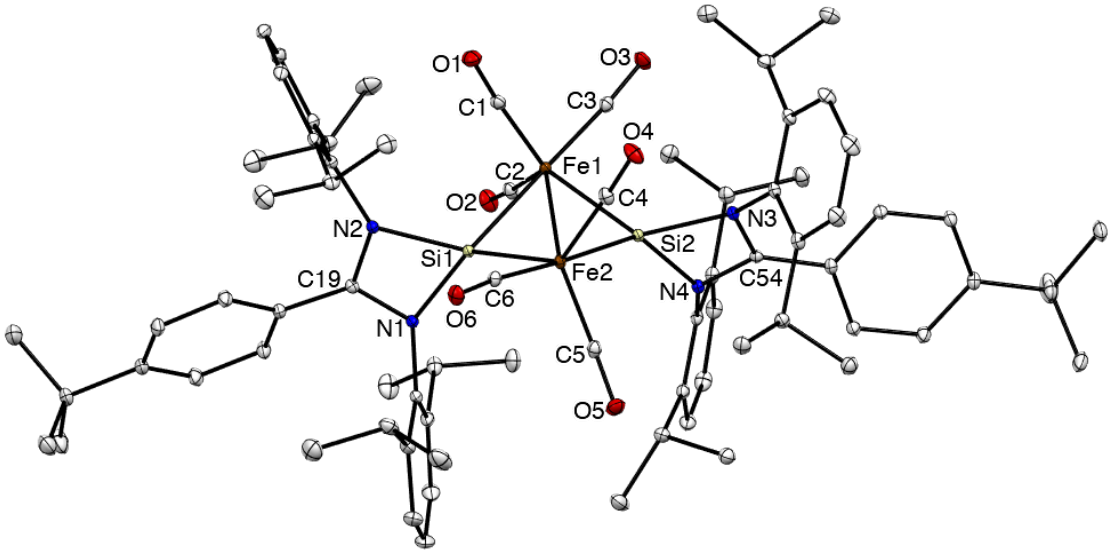

Figure 5.7. Molecular structure of [(Butiso)Si{μ-Fe(CO)$_3$}]$_2$ (**4**) (thermal ellipsoids shown at 20 % probability). Hydrogen atoms omitted for clarity. Selected bond lengths (Å) and angles (°): Fe1-Fe2 2.7852(3), Si1---Si2 3.205, Si1-N1 1.8510(12), Si1-N2 1.8686(12), Fe1-Si1 2.2488(4), Fe2-Si1 2.2105(4), Fe1-C1 1.8068(16), O1-C1 1.146(2), N1-Si1-Fe1 135.42(4), N1-Si1-Fe2 129.36(4), N2-Si1-Fe1 119.38(4), N2-Si1-Fe2 134.21(4), N1-Si1-N2 70.78(5), Fe1-Si2-Fe2 77.229(14), Si2-Fe1-Si1 92.080(15), Si1-Fe1-Fe2 50.737(11), O1-C1-Fe1 176.21(14).

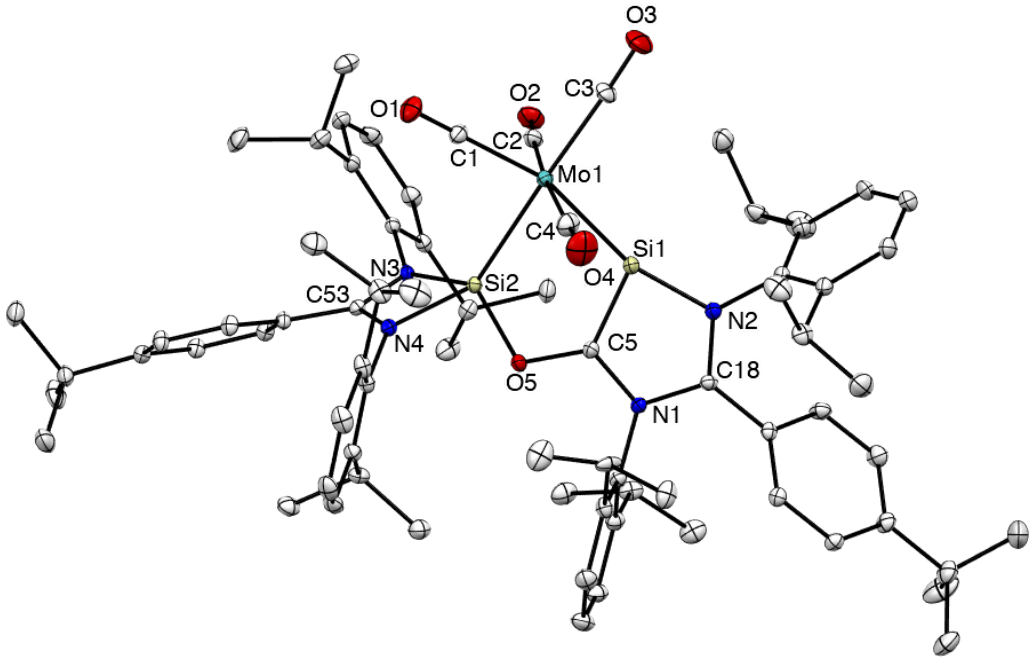

Figure 5.8. Molecular structure of [(Butiso)Si{μ-Mo(CO)$_4$}(OC)Si(Butiso)] (**5**) (thermal ellipsoids shown at 20 % probability). Hydrogen atoms omitted for clarity. Selected bond lengths (Å) and angles (°): Mo1-C1 2.005(7), O1-C1 1.136(8), Mo1-Si1 2.4735(18), Mo1-Si2

2.5177(16), Si2-O5 1.717(4), O5-C5 1.373(7), Si1-C5 1.767(6), N1-C5 1.379(8), N1-C18 1.379(8), N2-C18 1.354(7), Si1-N2 1.779(5), Si2-N3 1.882(5), Si2-N4 1.862(5), Si1---Si2 2.965, Si1-Mo1-Si2 72.87(5), O1-C1-Mo1 176.6(6), C5-O5-Si2 109.2(4), C5-Si1-N2 85.4(3), C18-N2-Si1 116.1(4), N2-C18-N1 111.1(5), C5-N1-C18 113.0(5), N1-C5-Si1 114.3(4), N3-C53-N4 106.9(5), N4-Si2-N3 70.6(2).

The molecular structure of **5** showed a similar CO activated silylene core as **3**, with one chelated $Mo(CO)_4$ unit (**Figure 5.8**). It contains a six-coordinate molybdenum atom with four carbonyl ligands and two silylene centres at cis positions, affording a distorted octahedral coordination at molybdenum. The C-Mo1-Si, C-Mo1-C and Si-Mo1-Si angles vary from 72.87(5)° to 102.8(3)°. Further, two Si-Mo bonds in **5** are 2.4735(18) Å and 2.5177(16) Å which are shorter than the sum (2.65 Å) of the covalent radii of Si and Mo. These Si-Mo bond lengths are also in the range of earlier reported Si-Mo interactions in compounds $[\{PhC(NPr^{i})_2\}_2Mo(CO)_5]$ and $[\{1,2\text{-}H_2C\text{-}CH_2(NBu^{t})_2\}_2\{\mu\text{-}Mo(CO)_4\}]$.[45,46] The inter core distances of $CN_2SiOCSiN_2C$ in **5** are slightly shorter and the bond angles are narrower than in **3**, possibly due to electronic and steric properties of the chelated $Mo(CO)_4$ unit.

While the formation of **4** and **5** occurs via the silicon(I) dimer species, the relevant mechanisms remain unclear. In contrast to **4**, which exhibited only a singlet resonance (δ 225.8 ppm) in the $^{29}Si\{^{1}H\}$ NMR spectrum, **5** showed two upfield signals at δ 68.4 ppm and δ 88.4 ppm, which suggest that **5** has an unsymmetrical structure not only in solid-state but also in solution. It should be noted that the terminal carbonyl groups at transition metal centres in **4** and **5** showed four stretching frequencies in the range of 1898-1999 cm^{-1} and 1835-2005 cm^{-1}, respectively in their infrared spectra, which is consistent with their corresponding C2 symmetry and cis-$ML_2(CO)_4$ geometry. Further, the $^{13}C\{^{1}H\}$ NMR singlet resonance for carbonyl groups in **4** is at δ 219.5 ppm, while **5** displays one singlet peak at δ 189.0 ppm for bridging CO group and four singlets for terminal carbonyls for molybdenum at δ 211.0, 211.4, 218.0, 222.2 ppm.

During one particular crystallisation of **5**, yellow coloured crystals of [(Butiso)C(O)OSi(μ-O){μ-$Mo(CO)_4$}Si(Butiso)] **6** were isolated, but no spectroscopic data could be obtained due to the very low yield. The mechanism of formation of **6** is unclear, however it seemed to form as a result of the reaction of a benzene solution of **1** and $Mo(CO)_6$ with advantageous oxygen from the solvent under ultraviolet light irradiation (**Scheme 5.14**).

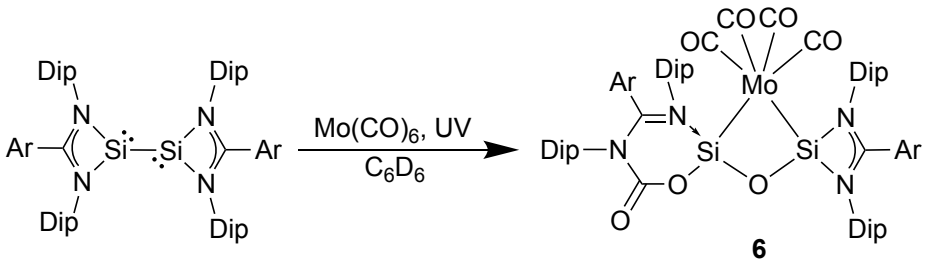

Scheme 5.14. Synthesis of **6**.

The molecular structure of **6** is depicted in **Figure 5.9** and displays an oxygen and a $Mo(CO)_4$ unit bridged between two silicon centres. The molybdenum atom shows a distorted octahedral geometry with Si1-Mo1-Si2 bond angle of 72.87(5)°, also confirming a cis configuration. The Si-Mo bond lengths (2.4917(8) Å and 2.5175(8) Å) are slightly longer, and Si-O bond lengths are (1.695(2) Å and 1.690(2) Å) comparatively shorter, than the respective bond lengths in the earlier reported compound $[CpMo(CO)_3(SiMe_2)_2OMe]$ (Si-Mo = 2.4804(9) Å, 2.4795(9) Å and Si-O = 1.782(2) Å, 1.788(3) Å).[47] Further, a OC(O) unit is found inserted between Si1 and N1 centres, resulting in a six-membered SiNCNCO core. The terminal C5-O5 bond is double, with bond length 1.201(4) Å, while the other C5-O6 (1.313(4) Å) has a single bond with a length shorter than the single bond in carboxylic acids (1.36 Å), due to a partial double bond character.

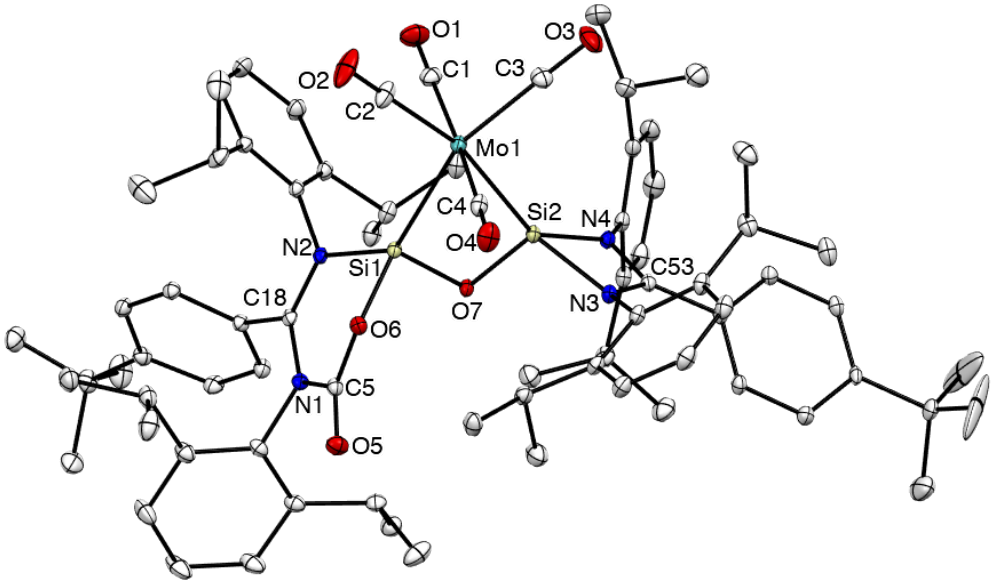

Figure 5.9. Molecular structure of [(Butiso)C(O)OSi(μ-O){μ-$Mo(CO)_4$}Si(Butiso)] (**6**) (thermal ellipsoids shown at 20 % probability). Hydrogen atoms omitted for clarity. Selected bond lengths (Å) and angles (°): Mo1-C1 2.038(4), O1-C1 1.141(4), Mo1-Si1 2.5175(8), Mo1-Si2 2.4917(8), Si1-O7 1.695(2), Si1-O6 1.721(2), O6-C5 1.313(4), O5-C5 1.201(4), N1-C5 1.433(4), N1-C18

1.370(4), N2-C18 1.312(4), Si1-N2 1.891(2), Si2-N4 1.852(2), Si2-N3 1.880(2), N3-C53 1.345(4), N4-C53 1.337(4), Si1---Si2 2.551, Si2-O7 Si1 97.83(11), Si2-Mo1-Si1 61.24(3), O1-C1-Mo1 176.3(3), C5-O6-Si1 128.72(19), O6-C5-N1 116.3(2), C18-N1-C5 124.4(2), N2-C18-N1 122.3(3), C18-N2-Si1 123.4(2), N4-Si2-N3 70.28(11), N4-C53-N3 106.4(2).

5.3.1.2 Reaction with Bu^{t}NC

Next, the silicon(I) dimer **1** was proposed to react with Bu^{t}NC, which is isolobal to carbon monoxide. The reaction of **1** with two equivalents of Bu^{t}NC in pentane at room temperature over 30 minutes afforded the complete conversion to the diradicaloid species [{(Butiso)Si(μ-CNBu^t)}$_2$] **7** with a concomitant colour change to dark reddish-orange (**Scheme 5.15**). Generation of only a single product is in stark contrast to the previously reported reaction of [{PhC(NBu^t)$_2$Si}$_2$] with DipN=C=NDip.[26] Compound **7** was crystallised as dichromic orange yellow crystals in 50.1 % yield.

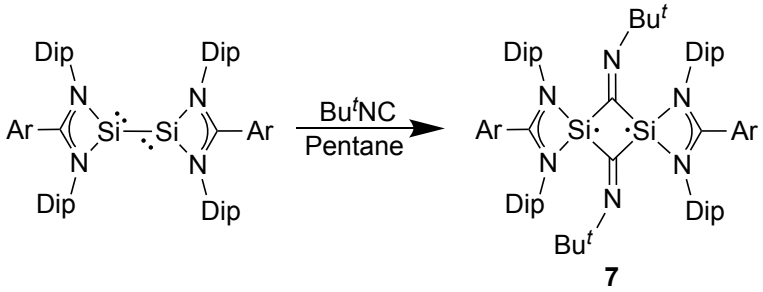

Scheme 5.15. Reaction of silicon(I) dimer **1** with Bu^{t}NC.

The molecular structure of **7** was determined by X-ray crystallographic analysis, and two independent molecules were found with almost identical bond lengths and angles in the unit cell (**Figure 5.10**). Here, only one of them will be discussed for simplicity. Each silicon centre is four-coordinate and exhibits a distorted tetrahedral configuration. Both silicon centres incorporate two bridging CNBu^t fragments, as well as two *N,N'*-chelated amidinate moieties. As a result, a planar four-membered Si_2C_2 ring is formed. All Si-C (1.834(3) Å, 1.845(3) Å, 1.840(3) Å, 1.836(3) Å) bonds of this ring and C-N(Bu^t) (1.310(3) Å, 1.312(4) Å) bonds are almost identical and intermediate between that of single and double Si-C, Si=C and C=N, C-N(sp^2) bonds.[35,48] These bond lengths indicate a possible electronic delocalisation. The Si1---Si2 bond length (2.5017(9) Å) is found to be longer than a typical Si-Si single bond (2.34 Å). Further, the Si_2C_2 core is titled at an angle of 80.49° with respect to Si1-N3-C23-N4 unit. All other metrical parameters were found to be similar to the earlier reported diradicaloid species mentioned in section **5.1.1.2**.

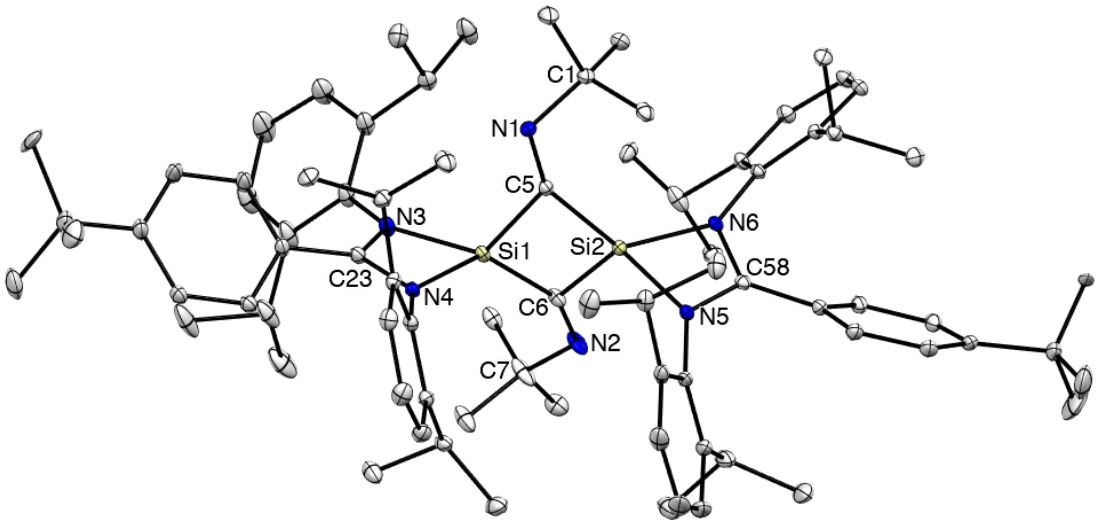

Figure 5.10. Molecular structure of [{(Butiso)Si(μ-CNBu^t)}$_2$] (**7**) (thermal ellipsoids shown at 20 % probability). Hydrogen atoms omitted for clarity. Selected bond lengths (Å) and angles (°): Si1---Si2 2.502, Si1-C5 1.845(3), Si2-C5 1.840(3), N1-C5 1.310(3), N1-C1 1.482(3), Si1-N3 1.894(2), Si1-N4 1.876(2), N3-C23 1.353(3), N4-C23 1.333(3), C6-Si2-C5 92.71(12), Si2-C5-Si1 85.53(11), C5-N1-C1 119.9(2), N4-Si1-N3 69.57(10), N4-C23-N3 106.4(2), C5-Si1-N3 121.80(11), C5-Si1-N4 111.89(10).

Compound **7** showed a signal at δ -46.3 ppm in its ^{29}Si{^{1}H} NMR spectrum, which lies slightly upfield from that for the earlier reported diradicaloid species [{PhC(NBu^t)$_2$Si(μ-CNDip)}$_2$] (δ = -39.9 ppm) and [RSi(μ-NAr)] (R = [{(Me$_3$Si)$_2$CH}$_2$Pr^{i}Si], Ar = 3,5-Me$_2$Ph) (δ(skeleton silicon) = 19.4 ppm).[26,49] In the ^{1}H NMR spectrum at room temperature, the expected number of aliphatic resonances were not observed. This could be because of the delocalisation of unpaired electrons and additional conjugation with the central exo-cyclic CN double bonds. To overcome this problem, a variable temperature ^{1}H NMR study was proposed which could restrict this delocalisation of radical electrons (**Figure 5.11**). Interestingly, at -40 °C and -60 °C, eight sets of isopropyl methyl and four sets of methine protons were seen, which equates to the solid-state structure of **7**. On increasing the temperature, the aliphatic signals start to broaden and finally merge. From this observation, it could be inferred that possible rotation of the -NBu^t unit is frozen at low temperature.

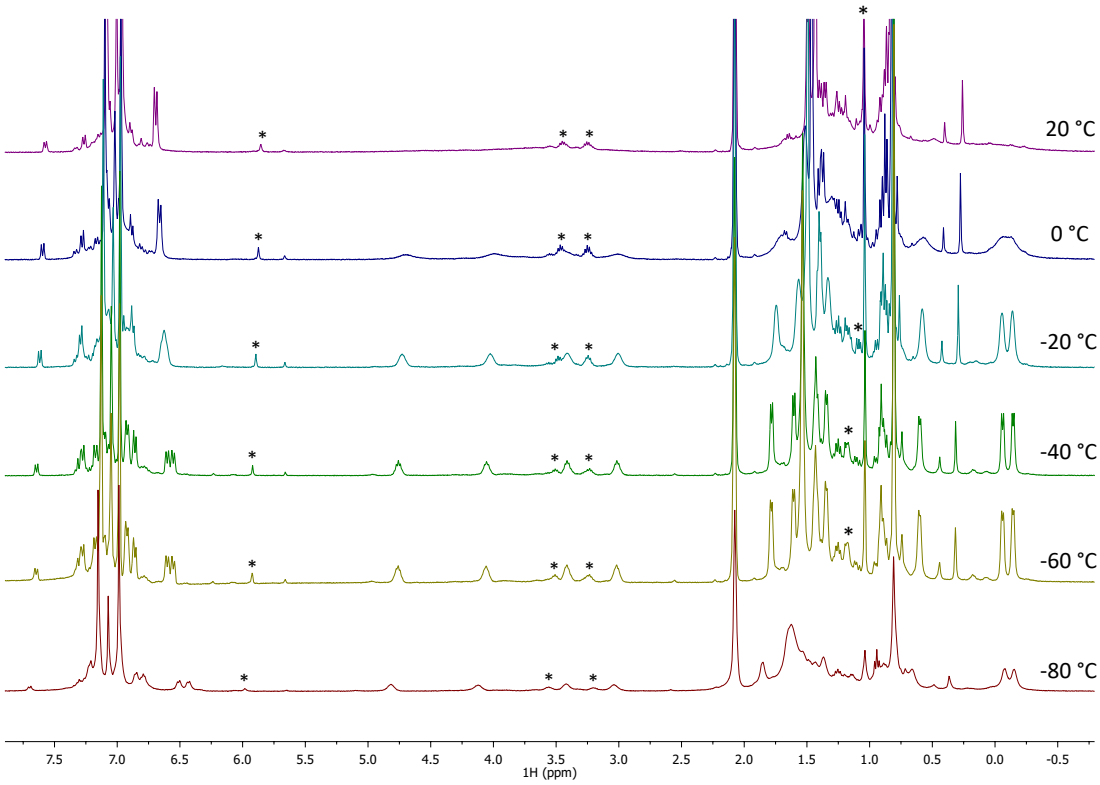

Figure 5.11. ^{1}H NMR spectrum (400 MHz, toluene-d_8) of **7** from 20° C to -80° C, * = LH.

Compound **7** was also studied using DFT by C. Smith. Calculations were performed on the full model **7A** and optimised geometries of singlet and triplet states were compared with that of the crystal structure. All metrical parameters match very closely with the singlet state rather than those for the triplet state (**Table 5.1**).

Table 5.1. Bond lengths in optimised singlet, triplet geometries and crystals structure of **7**.

Bonds/bond lengths (Å)	Singlet	Triplet	Crystal structure
Si-C	1.829	1.857	1.836
Si-C	1.830	1.858	1.839
C=N	1.302	1.296	1.319
C-Si-C	94.09	89.59	92.73
Si-C-Si	84.79	89.53	85.70
Si-N	1.868	1.807	1.881
Si-N	1.875	1.809	1.883
Si-Si	2.467	2.615	2.501

The major difference arises in the geometry of the central Si_2N_2 ring, where the triplet state is a near-square structure. On the other hand, both X-ray and singlet state calculated structures show a distorted geometry, shortening the distance between the silicon atoms.

Moreover, on comparing the energy difference of both optimised structures, the singlet state is found to be more stable than the triplet state by 9.00 kcal/mol. Further, an analysis of the frontier molecular orbitals of both states reveals a preference for the singlet state over the triplet state (**Figure 5.12**). The HOMO of the singlet state resembles the lower SOMO of the triplet state. This orbital represents a delocalisation of electrons throughout the Si_2N_2 ring resulting in a stronger bonding interaction for the singlet state as compared to the triplet state. The singlet LUMO resembles the higher triplet SOMO and consists of the electron delocalisation in the amidinate ligand framework, hence the presence of an electron in this orbital leads to a stronger Si-N interaction in the triplet state thereby increasing the energy of the system.

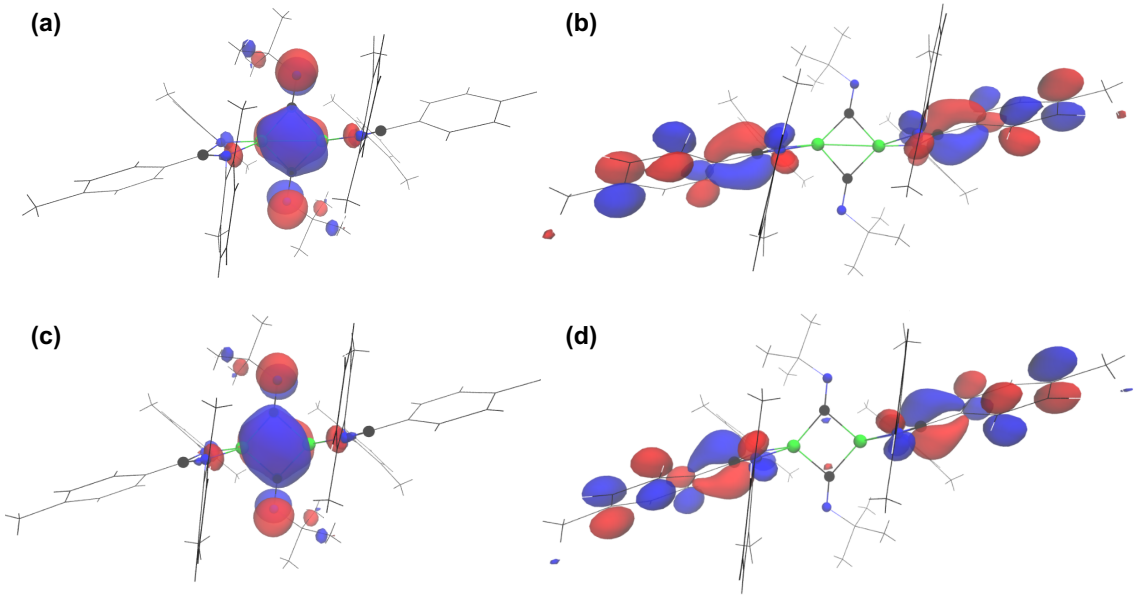

Figure 5.12. HOMO and LUMO of singlet state (**a**) and (**b**), lower SOMO and higher SUMO of triplet state (**c**) and (**d**).

The reactivity of silicon radicals is well studied.[50] Nucleophilic silyl radicals undergo halogen abstraction reactions with alkyl or aryl halides.[51] The diradicaloid species **7** was found to be highly reactive, and was halogenated when treated with 1,2 dibromoethane, to form the corresponding dihalide species **8** in 62 % yield (**Scheme 5.16**). Compound **8** was crystallised from toluene/pentane solution in 15:85. It was further characterised by ^{1}H and $^{13}C\{^{1}H\}$ NMR spectroscopy, however due to the low solubility in normal

deuterated solvents (C_6D_6 and THF-d_8), $^{29}Si\{^1H\}$ NMR spectroscopic data could not be obtained.

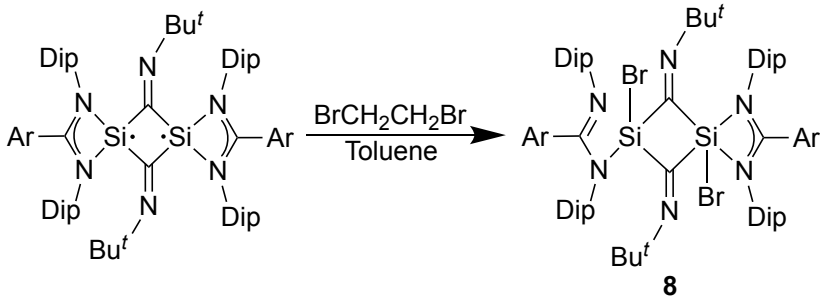

Scheme 5.16. Reaction of **7** with $BrCH_2CH_2Br$.

The molecular structure of **8** is given in **Figure 5.13**. Similar to **7**, compound **8** maintains a planar Si_2C_2 ring with comparable C-N bond distances, although the Si-C bond distances are longer. This also indicates unlikely delocalisation over Si_2C_2 fragment. Further, each silicon centre incorporates a terminal bromide ligand. In contrast to **7**, the amidinate ligands show *N,N'*-chelation with Si1 centre and a possible π-donor interaction with Si2 centre.

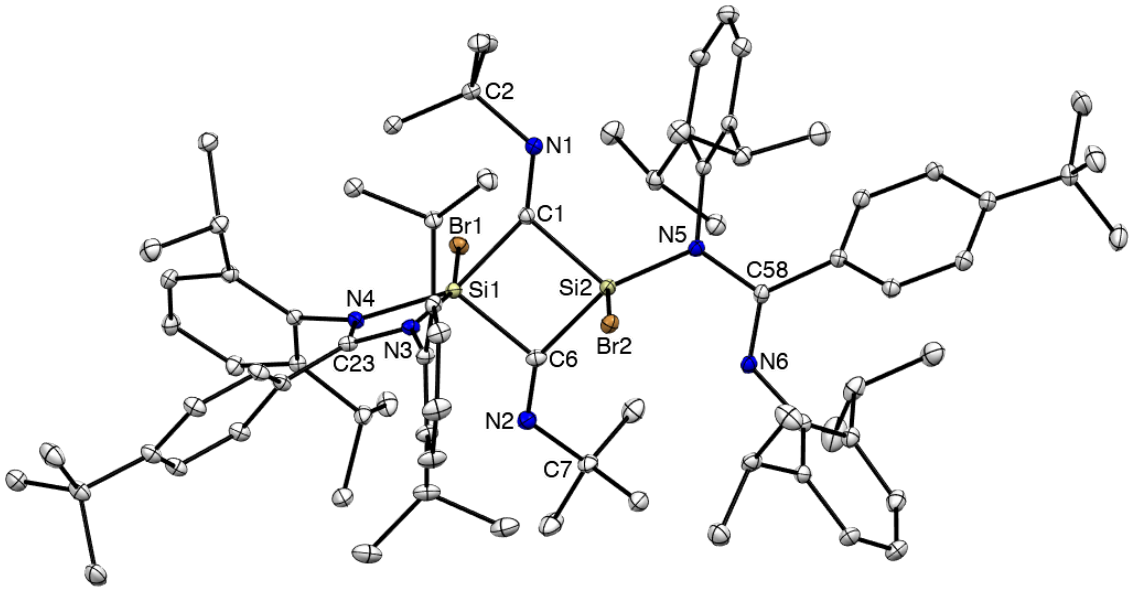

Figure 5.13. Molecular structure of [{(Butiso)SiBr(μ-CNBu^t)}$_2$] (**8**) (thermal ellipsoids shown at 20 % probability). Hydrogen atoms omitted for clarity. Selected bond lengths (Å) and angles (°): Si1---Si2 2.7960(8), Br1-Si1 2.3804(6), Si2-Br2 2.2286(14), Si1-C1 1.933(2), Si2-C1 1.926(2), Si2-C6 1.955(2), Si1-C6 1.918(2), N1-C1 1.263(3), N2-C6 1.274(3), Si1-N3 2.0452(18), Si1-N4 1.8238(18), Si2-N5 1.7742(18), N5-C58 1.416(3), N6-C58 1.276(3), C6-Si1-C1 87.26(9), C1-Si2-C6 86.43(9), Si2-C1-Si1 92.86(9), Si1-C6-Si2 92.42(9), N3-C23-N4 107.69(18), N6-C58-N5 115.04(18), N4-Si1-N3 67.82(7), C1-Si1-Br1 90.52(6), C1-Si2-Br2 101.72(7), N3-Si1-Br1 160.31(6), N4-Si1-Br1 93.31(6), N5-Si2-Br2 108.46(8).

5.3.1.3 Reactions with H_2, CO_2 and N_2O

Due to the difference in electronics between **1** and Roesky's previously reported disilylene, we sought to investigate its reactivity with dihydrogen, carbon dioxide and nitrous oxide. The reaction of **1** with dihydrogen was unsuccessful even after heating to 80 °C or irradiating it with ultraviolet light.

In case of carbon dioxide and nitrous oxide, placing a solution of **1** under an atmosphere of the respective excess gases caused dissipation of purple colour within 20 minutes at ambient temperature (**Scheme 5.17**). **1** reacted with five molecules of carbon dioxide and four molecules of nitrous oxide. ^{1}H NMR spectroscopic analyses showed the formation of new products **9** and **10** with small quantities (~5 %) of free ligand. Subsequent filtration and concentration of reaction mixtures yielded colourless crystalline blocks of **9** and **10**.

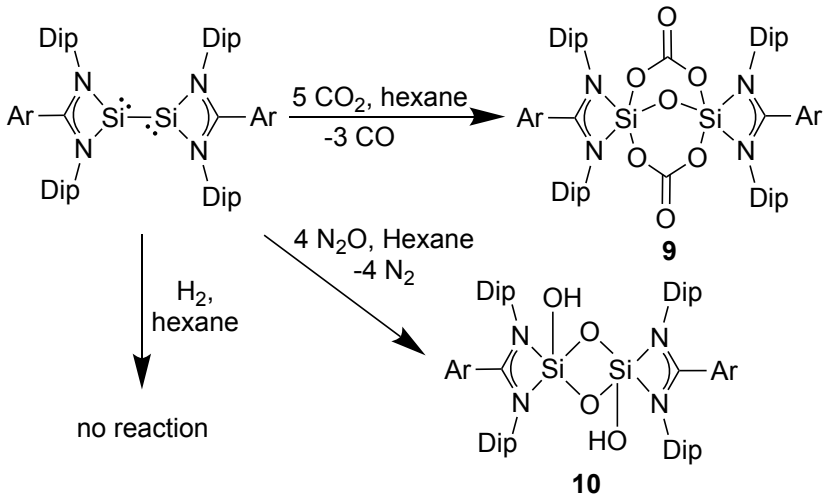

Scheme 5.17. Reaction of **1** with H_2, CO_2 and N_2O.

For the carbon dioxide reaction, it is assumed that the disilylene **1** initially reacts with three carbon dioxide molecules to form three oxo bridged bonds between silicon centres. These Si-O-Si units further react with two more molecules of carbon dioxide to result in a central Si(μ-CO_3)$_2$(μ-O)Si core. However, nitrous oxide being an ideal source of atomic oxygen, results in the elimination of four N_2 molecules with the insertion of two oxygen atoms between silicon atoms and two terminal hydroxo groups at each silicon centre. It is possible that the reaction progresses via the formation of two oxo bridges and two terminal oxy groups, which further abstract the hydrogen atoms from the solvent to form the terminal hydroxy groups (**Scheme 5.18**).

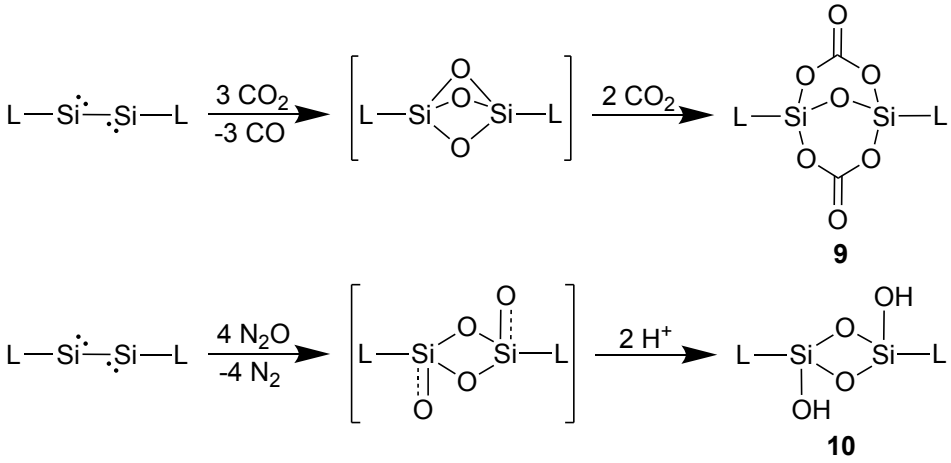

Scheme 5.18. Possible reaction pathways for the formation of **8** and **9**.

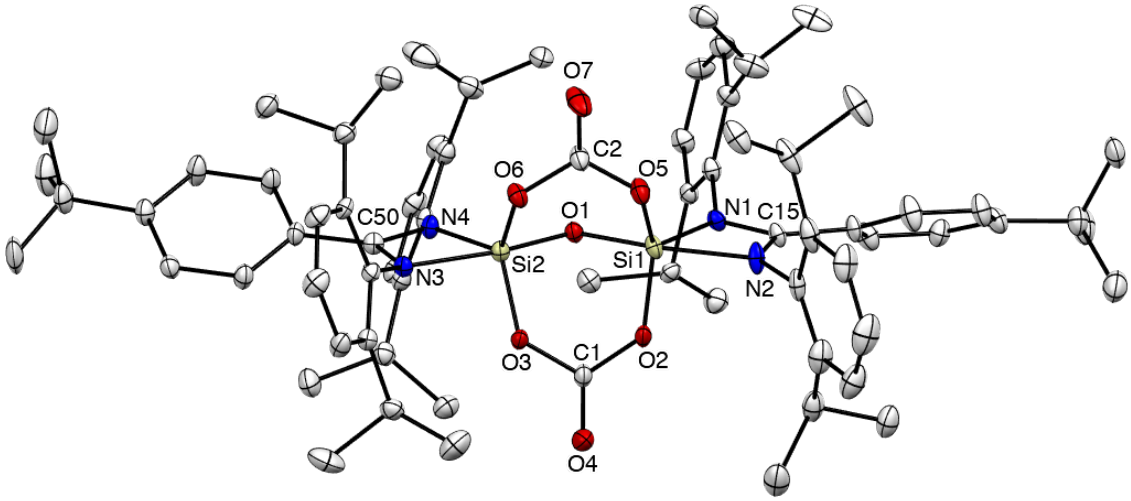

Figure 5.14. Molecular structure of [{(Butiso)Si(μ-CO_3)}$_2$(μ-O)] (**9**) (thermal ellipsoids shown at 20 % probability). Hydrogen atoms omitted for clarity. Selected bond lengths (Å) and angles (°): Si1---Si2 , Si1-O1 1.660(5), Si1-O2 1.678(5), Si2-O3 1.677(5), O2-C1 1.327(7), O3-C1 1.354(7), O4-C1 1.189(8), Si1-N1 1.809(5), Si1-N2 1.984(6), N1-C15 1.354(8), N2-C15 1.311(8), Si2-O1-Si1 116.4(3), N1-Si1-N2 68.9(2), N2-C15-N1 107.6(5), O1-Si1-O2 98.0(2), O-Si1-O5 96.5(2), O5-Si1-O2 115.9(3), C1-O2-Si1 128.3(4), C1-O3-Si2 129.5(4), O2-C1-O3 115.5(6), O4-C1-O3 120.5(6), O4-C1-O2 123.8(6).

The molecular structure of **9** (**Figure 5.14**) shows it to be a symmetrical mixed oxide bridged dimeric species with the presence of a central Si(μ-CO_3)$_2$(μ-O)Si tricyclic core linked by planar amidinate groups. This core contains two CO_3 units and one oxygen atom bridged between two silicon centres, which has occurred as a result of the cleavage of Si-Si single bond. Both five-coordinate silicon centres arrange in distorted trigonal bipyramidal geometry with nitrogen N1 and oxygen O1 at apical positions (N1-Si1-O1 = 170.2(3)°) and O5, O2 and N2 at equatorial positions. The equatorial bond distances (Si1-N1 = 1.809(5) Å, Si1-O5 = 1.666(5) Å, Si1-O2 = 1.678(5) Å) are much shorter than

the apical ones (Si1-N2 = 1.984(6) Å, Si1-O1 = 1.660(5) Å) which is similar to the previously reported carbon dioxide activation of a disilyne bis(phosphine).[5] The non-bonded Si-Si distance in **9** (Si---Si = 2.820(2) Å) is shorter than that observed in [{LSi(O)}$_2${μ-CO$_3$(O)}] (L = [:C{N(Dip)CH}$_2$]) (Si---Si = 2.944 Å).[52] The other C-O and Si-O distances compares well with this known complex.

The spectroscopic data of **9** are consistent with its solid-state structure. A singlet silicon resonance was observed in the ^{29}Si{^{1}H} NMR spectrum at δ -121.0 ppm, which is δ 30 ppm upfield compared to the reported mixed oxide compound [{LSi(O)}$_2${μ-CO$_3$(O)}]. The C=O stretch of carbonate unit is at 1756 cm^{-1}, which is close to other bridged silicon carbonate species (1780 cm^{-1}).[53]

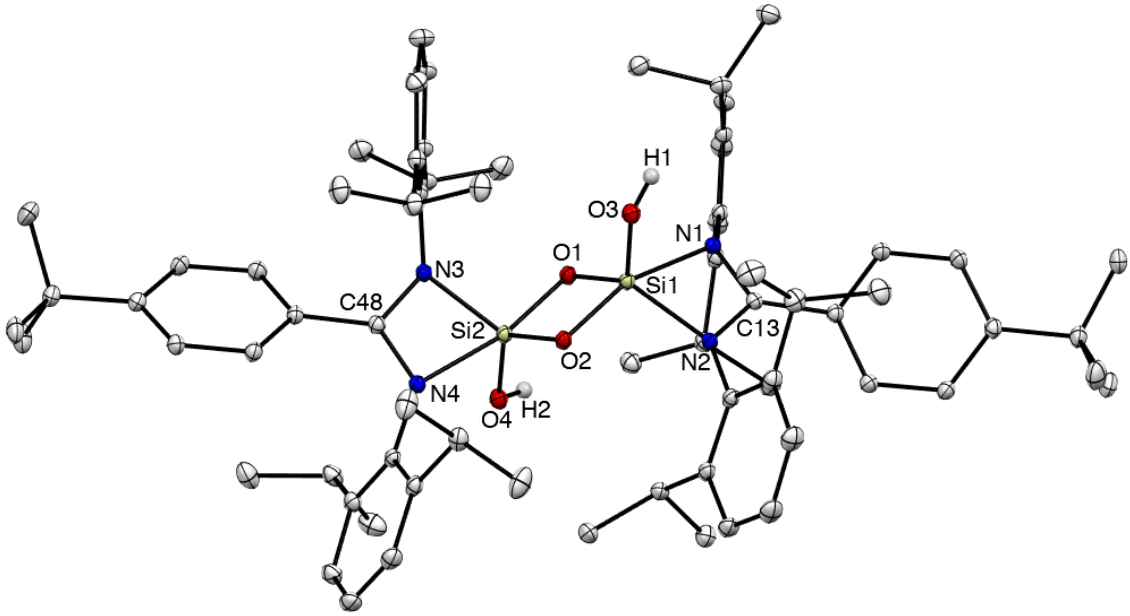

Figure 5.15. Molecular structure of [{(Butiso)Si(OH)(μ-O)}$_2$] **(10)** (thermal ellipsoids shown at 20 % probability). Hydrogen atoms except H1 and H2 omitted for clarity. Selected bond lengths (Å) and angles (°): Si1-N1 2.0077(12), Si1-N2 1.8297(13), Si2-N3 1.8098(13), Si2-N4 1.9979(13), Si1-O1 1.6509(12), Si1-O2 1.7119(11), Si1-O3 1.6465(13), Si1---Si2 2.4477(6), O2-Si2-O1 86.62(5), Si1-O1-Si2 93.26(5), O1-Si1-N1 91.95(5), O1-Si1-N2 128.16(6), O2-Si1-N1 160.29(6), O2-Si1-N2 97.75(5), O3-Si1-O1 120.10(6), O3-Si1-O2 101.08(6), O3-Si1-N1 96.54(6), O2-Si1-N2 97.75(5), N2-Si1-N1 67.74(5).

Compound **10** crystallises in the triclinic space group *P*-1 (**Figure 5.15**). Each silicon atom is five-coordinate and comprises *N,N'*-amidinate chelation, two bridging oxygen atoms and one hydroxy group owing to its distorted trigonal bipyramidal geometry. The four-membered central Si_2O_2 ring is planar and contains two types of Si-O bond lengths. The average longer bond length is 1.714 Å and the shorter one is 1.653 Å, which is

comparable to oxo bridged dimers [{PhC(NBu^t)$_2$Si(X)(μ-O)}$_2$] (X = PPh$_2$, NPh$_2$, NMe$_2$, OBu^t, Bu^t).[54,55] Each silicon is bound in a trans fashion to the hydroxy group with respect to the central Si$_2$O$_2$. Both Si-O(H) bond lengths (Si-O(H) = 1.6465(13) Å and 1.6534(13) Å) are similar but shorter than the other Si-O bonds. These bond lengths are also in the range of reported Si-OH bonds.[56] The average Si-O-Si and O-Si-O bond angles are 93.27° and 86.73°, respectively.

Compound **10** is stable indefinitely in solid-state, however it decomposes to give free protonated ligand after two days in solution under inert gas atmosphere. The ^{29}Si{^{1}H} NMR spectrum of **10** showed an upfield singlet resonance at δ -102.4 ppm compared to **1** (δ = -96.9 ppm), due to the shielding of silicon atom upon attachment of oxygen to its silicon centres. Further, the OH groups displayed a broad singlet peak at δ 2.64 ppm in the ^{1}H NMR spectrum.

5.3.1.4 Reaction with C_2H_4

Reaction of a hexane solution of **1** with ethylene at one atmosphere pressure and ambient temperature readily yielded an orange coloured solution of **11** (**Scheme 5.19**). Removal of volatiles did not result in any colour change, suggesting an irreversible reaction (cf. reversible ethylene addition to [{(^{Dip}Ar)Ge}$_2$]; ^{Dip}Ar = 2,6-(Dip)$_2$Ph).[57] Compound **11** was crystallised from pentane as orange solid in 60 % yield.

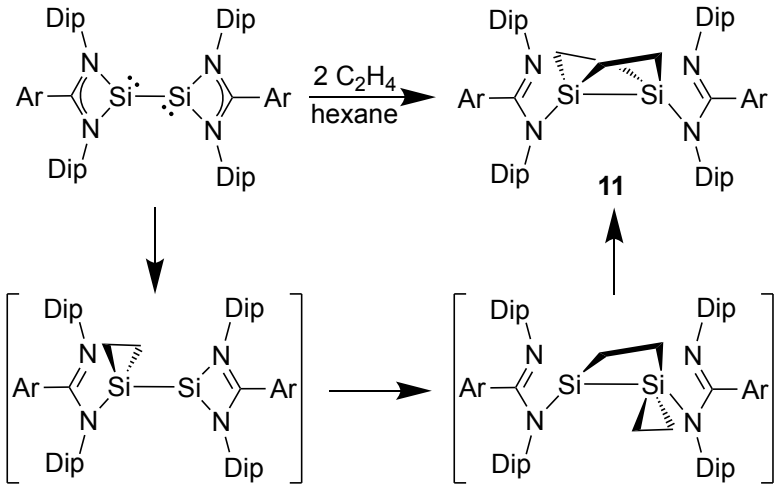

Scheme 5.19. Reactivity of **1** with ethylene and the proposed mechanism.

The reaction mechanism is likely to be similar to that proposed for [{(^{Dip}Ar)E(μ-C$_2$H$_4$)}$_2$] (E = Ge, Sn),[57] i.e. the C-C bond of each ethylene interacts with silicon centres of dimer **1** (via 1+2 cycloaddition), to give an intermediate with two three-membered EC$_2$ rings.

This intermediate further rearranges to give **11**. The ^{1}H NMR spectrum of **11** exhibits broad resonances for the two bridging C_2H_4 groups which hints at a fluxional process occurring in solution.

X-ray analysis of **11** revealed it to be a doubly C_2H_4-bridged disilabicylo [2.2.0]hexane compound, which can be viewed as a [2+2+2] cycloaddition adduct of silylene with two molecules of ethylene (**Figure 5.16**). Compound **11** is found to be very similar to that of [LGe(μ-C_2H_4)$_2$GeL] (L = ^{DBu}L and ^{iPr}L†; ^{DBu}L = NDip(Bu^{t}); 2,6-Pr$^{i}_2$Ph, ^{iPr}L† = Pr$^{i}_3$SiAr*N, Ar* = 2,6-(Ph$_2$CH)$_2$-4-Pr^{i}Ph) reported in our group.[58,59] It has a puckered bicyclic Si_2C_4 ring with dihedral angles 68.26° between its Si_2C_2 least square planes. The amidinate ligand is coordinated to silicon centres in a κ^1 coordination mode, leaving the other nitrogen site free. The Si-Si (2.3720(8) Å), average Si-C (1.871 Å, 1.916 Å) and Si-N (1.7886 Å) bond distances are in the normal single bond range and similar to those in the [5,6-acenaphthene{PhC(NBu^{t})$_2$Si}$_2$(μ-C_2H_4)].[60]

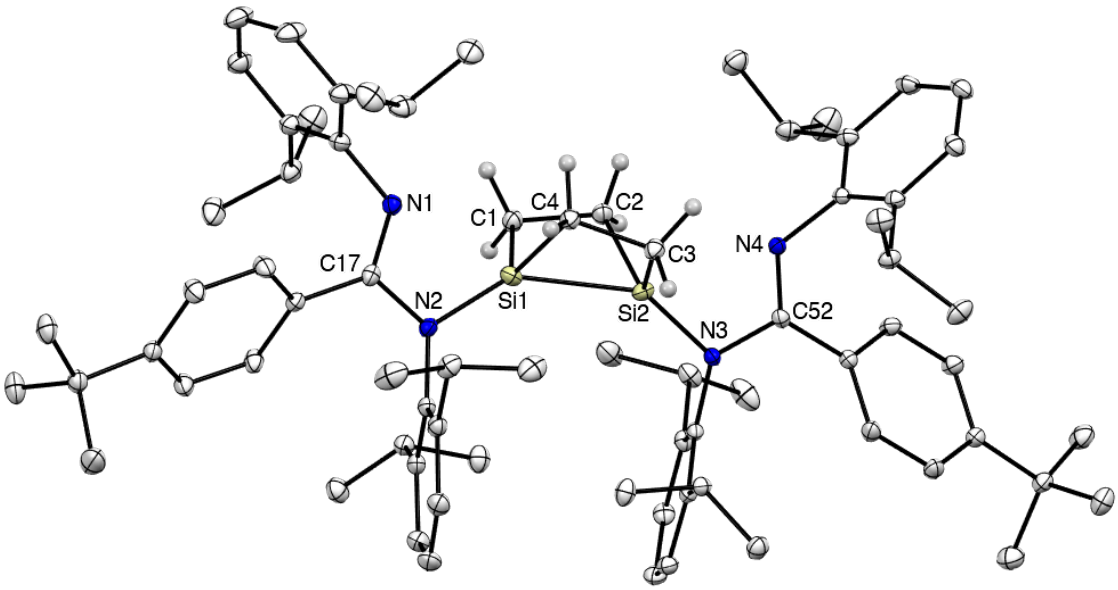

Figure 5.16. Molecular structure of [{(Butiso)Si(μ-C_2H_4)}$_2$] (**11**) (thermal ellipsoids shown at 20 % probability). Hydrogen atoms except that on C1, C2, C3 and C4 omitted for clarity. Selected bond lengths (Å) and angles (°): Si1-C1 1.874(2), Si2-C2 1.915(2), C1-C2 1.567(3), Si2-Si1 2.3720(8), Si1-N2 1.7872(16), Si2-N3 1.7899(16), N1-C17 1.293(3), N2-C17 1.386(2), C1-Si1-C4 108.07(10), C2-C1-Si1 97.67(13), C1-C2-Si2 104.57(13), C17-N2-Si1 108.97(13), N1-C17-N2 112.65(16), C1-Si1-Si2 80.25(7), C2-Si2-Si1 73.75(6).

5.3.2 Reactivity of Germanium(I) Dimer

Following the reactivity studies of **1**, we focused our attention to study some related reactivity of **2**. The initial reactivity of **2** towards H_2, CO and C_2H_4 was analysed by

placing a NMR sample of **2**/C_6D_6 in an environment of the respective gas at ambient temperature and atmospheric pressure (**Scheme 5.20**). Monitoring the reactions by ^{1}H NMR spectroscopy showed that in case of H_2 and CO, the only signals present were those for the starting material **2**. When these reactions were heated to 70 °C, no reaction occurred.

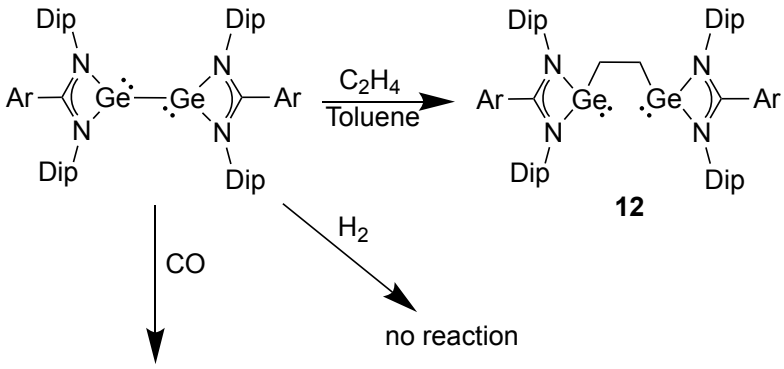

Scheme 5.20. Reactivity of **2** with H_2, CO, C_2H_4.

Upon reacting **2** with C_2H_4, the red-purple colour of the solution faded to light yellowish-brown over the course of a few hours and new signals appeared in the ^{1}H NMR spectrum. Consequently, the reaction was scaled up with a continuous stirring of the solution in toluene, which resulted in reaction completion after 1 hour. On working up the reaction mixture, a C_2H_4 inserted complex **12** was obtained as light-yellow coloured crystals. The formation of **12** can be explained by a similar mechanism used to describe the reaction of silicon(I) dimer with ethylene. Unlike **11**, **12** showed only one C_2H_4 ligand bridged between two germanium centres. This difference in reactivity could be due to the more reactive nature of silylenes, relative to germylenes. Further, **12** showed a symmetrical ligand environment in its ^{1}H NMR spectrum, with a singlet resonance for bridging $(C_2H_4)^{2-}$ group at δ 1.67 ppm, four sets of isopropyl methyl and two sets of methine protons.

Compound **12** was crystallographically characterised and the molecular structure is displayed in **Figure 5.17**. **12** crystallises in the centrosymmetric space group *P*-1 and reveals a non-planar structure with no Ge---Ge interaction. The two amidinate groups are oriented in opposite directions with involvement of *N,N'*-chelation to both germanium centres. The C36-C36' bond length of bridged C_2H_4 group is 1.549(4) Å which is reminiscent of the amide ligand stabilised complex [{($^{i\text{Pr}}$L†)Ge}$_2$(μ-C_2H_4)] (1.554(6) Å).[61] The Ge-C (2.000(2) Å) bond lengths are slightly longer and Ge-C36-C36' (106.08°)

bond angle is slightly shorter than the respective bond lengths and angles of [{($^{i\text{Pr}}$L†)Ge}$_2$(μ-C_2H_4)] (1.973(4) Å, 109.58°).

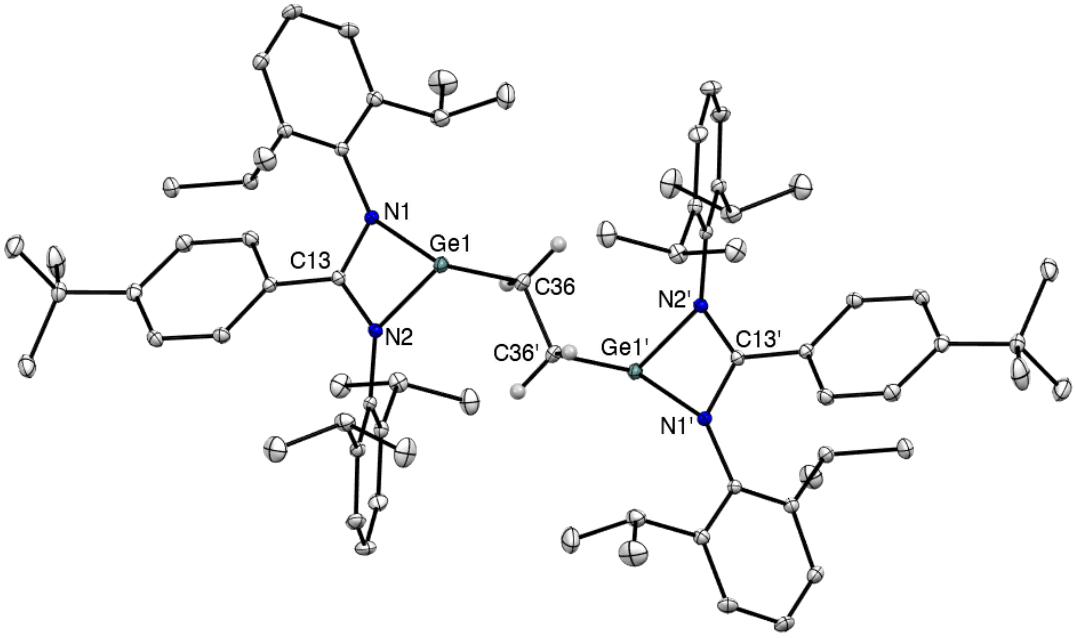

Figure 5.17. Molecular structure of [{(Butiso)Ge}$_2$(μ-C_2H_4)] (**12**) (thermal ellipsoids shown at 30 % probability). Hydrogen atoms except that on C36 and C36' omitted for clarity. Selected bond lengths (Å) and angles (°): Ge1-C36 2.000(2), C36-C36' 1.549(4), Ge1-N1 2.0389(15), Ge1-N2 2.0273(15), N1-C13 1.339(2), N2-C13 1.330(2), N2-Ge1-N1 64.54(6), N2 C13 N1 108.90(16), C36-Ge1-N2 94.39(7), C36-Ge1-N1 101.28(7), C36'-C36-Ge1 105.74(18).

5.4 Conclusion

To summerise, the amidinate ligand stabilised silicon(I) dimer [{(Butiso)Si}$_2$] has been shown to be effective in activation of a wide range of compounds. This includes various small molecules such as carbon monoxide, carbon dioxide and nitrous oxide. The reaction with carbon monoxide showed reversible coordination under ultraviolet light and is of fundamental interest. The bonding in the carbon monoxide activation product **3** is yet to be fully explored, however the reaction of this product with transition metal carbonyls $Fe(CO)_5$ and $Mo(CO)_6$ confirmed its Lewis basicity.

Further, we have studied reactions of silicon(I) and germanium(I) species towards various unsaturated substrates such as Bu^{t}NC and C_2H_4, and their reactivities are similar to previously reported examples. This includes the formation of a silicon diradicaloid species and cycloaddition reactions of ethylene with both dimers.

5.5 Experimental

[(Butiso)SiOCSi(Butiso)] (3). A solution of [{(Butiso)Si}$_2$] (150 mg, 0.14 mmol) in pentane (10 mL) was stirred under an atmosphere of dry CO at room temperature overnight. All the volatiles were subsequently removed from the reaction mixture *in vacuo* and the residue was extracted in pentane (8 mL). The extract was filtered and then concentrated to ca. 2 mL under reduced pressure (in order to remove the free ligand formed). Storage at room temperature for 3 days led to the deposition of [(Butiso)SiOCSi(Butiso)] as dark-yellow colored crystals (74 mg, 48.0 %). M.p. 160 °C (decomp.); ^{1}H NMR (600 MHz, C_6D_6, 298 K) δ = 0.80 (s, 9H, C(C*H*$_3$)$_3$), 0.82 (s, 9H, C(C*H*$_3$)$_3$), 1.05-1.08 (m of three overlapping d, m, 18H, CH(C*H*$_3$)$_2$), 1.12 (d, $^3J_{HH}$ = 6.9 Hz, 6H, CH(C*H*$_3$)$_2$), 1.16 (d, br, $^3J_{HH}$ = 4.8 Hz, 6H, CH(C*H*$_3$)$_2$), 1.33 (d, $^3J_{HH}$ = 6.6 Hz, 6H, CH(C*H*$_3$)$_2$), 1.39 (d, $^3J_{HH}$ = 6.7 Hz, 6H, CH(C*H*$_3$)$_2$), 1.65 (d, br, $^3J_{HH}$ = 6.6 Hz, 6H, CH(C*H*$_3$)$_2$), 3.15 (sept, $^3J_{HH}$ = 6.7 Hz, 2H, C*H*(CH$_3$)$_2$), 3.27 (sept, $^3J_{HH}$ = 6.7 Hz, 2H, C*H*(CH$_3$)$_2$), 3.75 (sept, br, 2H, C*H*(CH$_3$)$_2$), 4.04 (sept, br, 2H, C*H*(CH$_3$)$_2$), 6.81 (d, $^3J_{HH}$ = 8.5 Hz, 2H, Ar-*H*), 6.84-7.12 (m, 16H, Ar-*H*), 7.26 (d, $^3J_{HH}$ = 8.6 Hz, 2H, Ar-*H*); ^{13}C{^{1}H} NMR (151 MHz, C_6D_6, 298 K) δ = 23.0, 23.1, 23.2, 23.8, 25.2, 25.7, 27.0, 27.10 (CH(*C*H$_3$)$_2$), 28.7, 28.8, 29.0, 29.6 (*C*H(CH$_3$)$_2$), 30.7, 30.8 (C(*C*H$_3$)$_3$), 34.2, 34.7 (*C*(CH$_3$)$_3$), 123.7, 123.9, 124.0, 124.3, 125.2, 126.0, 126.7, 127.1, 127.5, 127.6, 128.4, 128.5, 2×129.8, 130.3, 134.6, 137.6, 138.4, 140.3, 144.7, 144.9, 145.5, 146.9, 150.2 (Ar-*C*), 155.1, 166.5 (N*C*N) 182.8 (*C*O); ^{29}Si{^{1}H} NMR (80 MHz, C_6D_6, 298 K) δ = -12.2, 35.2; IR ν/cm^{-1} (Nujol): 3059 (w), 2958(vs), 1607 (w), 1564 (w), 1493 (w), 1446 (vs), 1385 (s), 1262 (m),1229 (s), 1179 (s), 1129 (m), 1102 (s), 1055 (m), 971 (m), 935 (m), 849 (w), 827 (vs), 779 (s), 745 (vs), 703 (m), 659 (m); anal. calc. for $C_{71}H_{94}N_4OSi_2$: C 79.27 %, H 8.81 %, N 5.21 %, found: C 79.20 %, H 8.89 %, N 5.20 %.

[(Butiso)Si{μ-Fe(CO)$_3$}]$_2$ (4). To a solution of [{(Butiso)Si}$_2$] (100 mg, 0.10 mmol) in toluene (15 mL), Fe(CO)$_5$ (28 μL, 0.21 mmol) was added at room temperature. The reaction mixture was stirred under UV light for 2 hours. All volatiles were subsequently removed from the reaction mixture *in vacuo* and the residue washed with cold pentane 2×3 mL to yield a very dark red colored pure compound **4** (46 mg, 45.4%). Storage of a dilute pentane solution of **4** at room temperature led to the deposition of [(Butiso)Si{μ-Fe(CO)$_3$}]$_2$ as very dark red colored crystals. M.p. > 260 °C; ^{1}H NMR (400 MHz, C_6D_6, 298 K) δ = 0.72 (s, 18H, C(C*H*$_3$)$_3$), 1.00 (d, $^3J_{HH}$ = 6.8 Hz, 24H, CH(C*H*$_3$)$_2$), 1.44 (d, $^3J_{HH}$ = 6.7 Hz, 24H, CH(C*H*$_3$)$_2$), 4.05 (sept, $^3J_{HH}$ = 6.7 Hz, 8H, C*H*(CH$_3$)$_2$), 6.84 (d, $^3J_{HH}$ = 8.4

Hz, 4H, Ar-*H*), 7.06-7.14 (m, 12H, Ar-*H*), 7.45 (d, $^{3}J_{HH}$ = 8.4 Hz, 4H, Ar-*H*); $^{13}C\{^{1}H\}$ NMR (151 MHz, C_6D_6, 298 K) δ = 24.2, 25.9 (CH(*C*H$_3$)$_2$), 29.0 (*C*H(CH$_3$)$_2$), 30.4 (C(*C*H$_3$)$_2$), 34.9 (*C*(CH$_3$)$_3$), 123.0, 125.1, 125.6, 128.9, 132.1, 135.3, 146.7, 157.7 (Ar-*C*), 169.8 (N*C*N), 219.5 (*C*O); $^{29}Si\{^{1}H\}$ NMR (80 MHz, C_6D_6, 298 K) δ = 225.8; IR ν/cm^{-1} (Nujol): 3062 (w), 2955 (vs), 1999 (s, CO), 1958 (vs, CO), 1921 (vs, CO), 1898 (vs, CO), 1608 (m), 1564 (w), 1443 (s), 1427 (s), 1384 (s), 1286 (w), 1263 (w), 1201 (w), 1097 (w), 1043 (m), 1020 (m), 985 (w), 935 (w), 853 (w), 833 (m), 785 (s), 750 (w), 706 (w), 673 (m); anal. calc. for $C_{76}H_{94}Fe_2N_4O_6Si_2$: C 68.77 %, H 7.14 %, N 4.22 %, found: C 68.89 %, H 7.26 %, N 4.07 %.

[(Butiso)Si{μ-Mo(CO)$_4$}(OC)Si(Butiso)] (5). To a mixture of [{(Butiso)Si}$_2$] (100 mg, 0.10 mmol) and Mo(CO)$_6$ (38 mg, 0.14 mmol), benzene (15 mL) was added at room temperature. The reaction mixture was stirred under UV light for 2 hours. All the volatiles were subsequently removed from the reaction mixture *in vacuo* and the residue extracted in pentane (10 mL). The extract was filtered and the solution was concentrated to ca. 6 mL. Storage at -30 ºC for two days led to the deposition of **5** as orange colored crystals (63 mg, 51.3 %). M.p. 210 °C (decomp.); ^{1}H NMR (600 MHz, C_6D_6, 298 K) δ = 0.08 (d, $^{3}J_{HH}$ = 6.7 Hz, 3H, CH(C*H*$_3$)$_2$), 0.20 (d, $^{3}J_{HH}$ = 6.6 Hz, 3H, CH(C*H*$_3$)$_2$), 0.24 (d, $^{3}J_{HH}$ = 6.6 Hz, 3H, CH(C*H*$_3$)$_2$), 0.56 (d, $^{3}J_{HH}$ = 6.8 Hz, 3H, CH(C*H*$_3$)$_2$), 0.72 (d, $^{3}J_{HH}$ = 6.8 Hz, 3H, CH(C*H*$_3$)$_2$), 0.78 (s, 9H, C(C*H*$_3$)$_3$), 0.83 (s, 9H, C(C*H*$_3$)$_3$), 0.88 (d, $^{3}J_{HH}$ = 6.3 Hz, 3H, CH(C*H*$_3$)$_2$), 1.25 (d, $^{3}J_{HH}$ = 6.9 Hz, 3H, CH(C*H*$_3$)$_2$), 1.43 (d, $^{3}J_{HH}$ = 6.9 Hz, 6H, CH(C*H*$_3$)$_2$), 1.50 (d, $^{3}J_{HH}$ = 6.8 Hz, 3H, CH(C*H*$_3$)$_2$), 1.59 (d, $^{3}J_{HH}$ = 6.8 Hz, 3H, CH(C*H*$_3$)$_2$), 1.61 (d, $^{3}J_{HH}$ = 6.7 Hz, 3H, CH(C*H*$_3$)$_2$), 1.73 (d, $^{3}J_{HH}$ = 6.5 Hz, 3H, CH(C*H*$_3$)$_2$), 1.77 (2 overlapping d, $^{3}J_{HH}$ = 6.7 Hz, 6H, CH(C*H*$_3$)$_2$), 1.80 (d, $^{3}J_{HH}$ = 6.8 Hz, 3H, CH(C*H*$_3$)$_2$), 2.79-2.90 (m of two overlapping sept, 2H, C*H*(CH$_3$)$_2$, 3.00 (sept, $^{3}J_{HH}$ = 6.8 Hz, 1H, C*H*(CH$_3$)$_2$), 3.09 (sept, $^{3}J_{HH}$ = 6.8 Hz, 1H, C*H*(CH$_3$)$_2$), 3.28 (sept, $^{3}J_{HH}$ = 6.6 Hz, 1H, C*H*(CH$_3$)$_2$), 3.75 (sept, $^{3}J_{HH}$ = 6.8 Hz, 1H, C*H*(CH$_3$)$_2$), 4.13 (sept, $^{3}J_{HH}$ = 6.7 Hz, 1H, C*H*(CH$_3$)$_2$), 5.09 (sept, $^{3}J_{HH}$ = 6.7 Hz, 1H, C*H*(CH$_3$)$_2$), 6.69-7.31 (m, 20H, Ar-*H*); $^{13}C\{^{1}H\}$ NMR (151 MHz, C_6D_6, 298 K) δ = 22.0, 22.3, 22.5, 23.0, 23.2, 23.4, 23.6, 23.7, 24.6, 24.9, 25.2, 25.6, 26.2, 26.5, 27.6, 28.0 (CH(*C*H$_3$)$_2$), 28.6, 28.7, 28.9, 2×29.2, 2×30.3 (*C*H(CH$_3$)$_2$), 30.5, 30.8 (C(*C*H$_3$)$_2$), 31.1 (*C*H(CH$_3$)$_2$), 34.3, 34.9 (*C*(CH$_3$)$_3$), 123.8, 2×124.1, 2×124.2, 124.4, 124.5, 124.6, 124.9, 125.8, 2×126.0, 126.9, 127.6, 127.7, 128.4, 2×128.5, 130.1, 130.2, 131.3, 131.6, 134.0, 134.8, 135.0, 135.2, 137.4, 144.5, 144.9, 2×145.0, 145. 6, 146.0, 146.1, 148.1, 150.6 (Ar-*C*), 157.4 172.7 (N*C*N), 189.0

(*C*O), 211.0, 211.4, 218.0, 222.2 (Mo*C*O); ^{29}Si{^{1}H} NMR (80 MHz, C_6D_6, 298 K) δ = 68.4, 88.4; IR ν/cm^{-1} (Nujol): 3062 (w), 2957 (s), 2078 (w), 2005 (s, CO), 1915 (s, CO), 1900 (vs, CO), 1870 (vs, CO), 1835 (s, CO), 1607 (m), 1561 (w), 1449 (s), 1382 (m), 1292 (w), 1270 (w), 1260 (w), 1233 (w), 1189 (m), 1137 (w), 1097 (m), 1057 (w), 1045 (w), 986 (m), 935 (m), 853 (w), 831 (m), 801 (w), 784 (vs), 753 (s), 735 (s), 709 (m), 694 (m), 679 (m), 659 (s); anal. calc. for $C_{75}H_{95}Mo_1N_4O_5Si_2$: C 70.12 %, H 7.45 %, N 4.36 %, found: C 69.36 %, H 7.29 %, N 4.16 %.

[{(Butiso)Si(μ-CNBu^t)}$_2$] (7). To a solution of [{(Butiso)Si}$_2$] (100 mg, 0.10 mmol) in pentane (10 mL), Bu^{t}NC (23 μL, 0.20 mmol) was added at room temperature. The reaction mixture was stirred for 30 minutes and concentrated to ~5 mL. Storage at room temperature for 2 days led to the deposition of [{(Butiso)Si(CNBu^t)}$_2$] as dark-red colored crystals (58 mg, 50.1 %). M.p. 130 °C (decomp.); ^{1}H NMR (400 MHz, toluene-d_8, 233 K) δ = -0.18 (d, $^{3}J_{HH}$ = 6.3 Hz, 6H, CH(CH_3)$_2$), -0.10 (d, $^{3}J_{HH}$ = 6.6 Hz, 6H, CH(CH_3)$_2$), 0.56 (d, $^{3}J_{HH}$ = 6.7 Hz, 6H, CH(CH_3)$_2$), 0.77 (s, 18H, C(CH_3)$_3$), 1.31 (d, $^{3}J_{HH}$ = 6.5 Hz, 6H, CH(CH_3)$_2$), 1.39 (2 overlapping d, 12H, CH(CH_3)$_2$), 1.49 (s, 18H, CNC(CH_3)$_3$), 1.57 (d, $^{3}J_{HH}$ = 6.7 Hz, 6H, CH(CH_3)$_2$), 1.74 d, $^{3}J_{HH}$ = 6.4 Hz, 6H, CH(CH_3)$_2$), 2.98 (m, 2H, CH(CH$_3$)$_2$), 3.37 (m, 2H, CH(CH$_3$)$_2$), 4.01 (m, 2H, CH(CH$_3$)$_2$), 4.72 (m, 2H, CH(CH$_3$)$_2$), 6.51 (d, $^{3}J_{HH}$ = 8.4 Hz, 2H, Ar-*H*), 6.56 (d, $^{3}J_{HH}$ = 8.4 Hz, 2H, Ar-*H*), 6.82 (d, $^{3}J_{HH}$ = 7.8 Hz, 4H, Ar-*H*), 6.88 (d, $^{3}J_{HH}$ = 8.2 Hz, 4H, Ar-*H*), 7.03-7.27 (m, 7H, Ar-*H*), 7.60 (d, $^{3}J_{HH}$ = 8.1 Hz, 1H, Ar-*H*); ^{13}C{^{1}H} NMR (151 MHz, C_6D_6, 298 K) δ = 28.1, 29.1 (CH(*C*H$_3$)$_2$), 30.3, 30.7 (*C*H(CH$_3$)$_2$), 30.8 (C(*C*H$_3$)$_3$), 31.0 (CNC(*C*H$_3$)$_3$), 34.8 (*C*(CH$_3$)$_3$), 55.3 (CN*C*(CH$_3$)$_3$), 124.1, 125.7, 127.7, 128.4, 128.5, 130.9, 146.3, 152.7 (Ar-*C*), 155.8 (N*C*N), 172.0 (*C*NC(CH$_3$)$_3$); ^{29}Si{^{1}H} NMR (80 MHz, C_6D_6, 298 K) δ = -46.3; IR ν/cm^{-1} (Nujol): 3062 (w), 2957 (s), 1606 (w), 1565 (w), 1437 (vs), 1381 (s), 1290 (m), 1267 (w), 1226 (w), 1183 (s), 1132 (w), 1115 (w), 1072 (w), 1020 (m), 982 (m), 933 (m), 840 (vs), 801 (w), 777 (vs),751 (m), 696 (s), 676 (s); anal. calc. for $C_{80}H_{112}N_6Si_2$: C 79.15 %, H 9.30 %, N 6.92 %, found: C 79.50 %, H 9.07 %, N 6.30 %.

[{(Butiso)SiBr(μ-CNBu^t)}$_2$] (8). To a solution of [{(Butiso)Si}$_2$] (80 mg, 0.08 mmol) in toluene (15 mL), Bu^{t}NC (18 μL, 0.16 mmol) was added at room temperature and stirred for 30 minutes. The reaction mixture was cooled to -30 °C and 1,2-dibromoethane (8 μL, 0.09 mmol) was added. The mixture was warmed to room temperature, stirred for 1.5

hours and filtered. The solution was concentrated to ca. 5 mL and layered with pentane. Storage at room temperature for 5 days led to the deposition of orangish-yellow coloured crystals and analytically pure yellow powder (65 mg, 62.0 %). M.p. 170 °C (decomp.); ^{1}H NMR (600 MHz, C_6D_6, 298 K) δ = 0.07 (d, $^{3}J_{HH}$ = 5.5 Hz, 3H, CH(CH_3)$_2$), 0.22 (br, 6H, CH(CH_3)$_2$), 0.25 (d, $^{3}J_{HH}$ = 6.1 Hz, 3H, CH(CH_3)$_2$), 0.78 (s, 9H, C(CH_3)$_3$), 0.88 (s, 9H, C(CH_3)$_3$), 1.15 (d, $^{3}J_{HH}$ = 5.1 Hz, 3H, CH(CH_3)$_2$), 1.24 (d, $^{3}J_{HH}$ = 5.3 Hz, 3H, CH(CH_3)$_2$), 1.28 (d, $^{3}J_{HH}$ = 5.5 Hz, 3H, CH(CH_3)$_2$), 1.31 (d, $^{3}J_{HH}$ = 6.0 Hz, 3H, CH(CH_3)$_2$), 1.33 (s, 9H, CNC(CH_3)$_3$), 1.40 (d, $^{3}J_{HH}$ = 6.5 Hz, 3H, CH(CH_3)$_2$), 1.43 (d, $^{3}J_{HH}$ = 5.6 Hz, 3H, CH(CH_3)$_2$), 1.46 (d, $^{3}J_{HH}$ = 5.8 Hz, 3H, CH(CH_3)$_2$), 1.51 (d, $^{3}J_{HH}$ = 6.0 Hz, 3H, CH(CH_3)$_2$), 1.53 (d, $^{3}J_{HH}$ = 5.1 Hz, 3H, CH(CH_3)$_2$), 1.62-1.65 (two br overlapping d, 6H, CH(CH_3)$_2$), 1.76 (s, 12H, CH(CH_3)$_2$, CNC(CH_3)$_3$) {signal of CH(CH_3)$_2$ and CNC(CH_3)$_3$ overlaps}, 3.06 (br m, 1H, CH(CH$_3$)$_2$), 3.10-3.16 (two br overlapping m, 2H, CH(CH$_3$)$_2$), 3.22 (br m, 1H, CH(CH$_3$)$_2$), 3.79 (br m, 1H, CH(CH$_3$)$_2$), 4.19 (br m, 1H, CH(CH$_3$)$_2$), 4.47 (br m, 1H, CH(CH$_3$)$_2$), 4.75 (br m, 1H, CH(CH$_3$)$_2$), 6.77 (d, $^{3}J_{HH}$ = 8.5 Hz, 4H, Ar-*H*), 6.89-7.29 (m, 15H, Ar-*H*), 7.43 (d, $^{3}J_{HH}$ = 7.7 Hz, 1H, Ar-*H*); ^{13}C{^{1}H} NMR (151 MHz, C_6D_6, 298 K) δ = 22.5, 22.7, 23.1, 23.5, 24.0, 24.1, 24.7, 24.9, 25.0, 25.1, 2×25.3, 25.7, 26.2, 27.3, 27.6 (CH(*C*H$_3$)$_2$), 27.9, 28.1, 28.2, 28.4, 28.6, 28.7, 28.9, 29.1 (*C*H(CH$_3$)$_2$), 30.5, 30.9 (C(*C*H$_3$)$_3$), 2×31.1 (CNC(*C*H$_3$)$_3$), 34.3, 34.7 (*C*(CH$_3$)$_3$), 60.3, 61.6 (CN*C*(CH$_3$)$_3$), 123.5, 123.6, 2×123.9, 124.0, 124.4, 2×124.6, 124.9, 125.0, 125.3, 125.9, 127.3, 127.5, 2×127.6, 128.4, 2×128.5, 128.8, 129.1, 132.3, 136.0, 137.6, 139.7, 141.7, 142.0, 144.5, 144.7, 145.6, 145.9, 146.3, 149.2, 149.3, 151.7, 156.2 (Ar-*C*), 160.3, 171.1 (N*C*N), 185.7, 192.3 (*C*NC(CH$_3$)$_3$); ^{29}Si{^{1}H} NMR (80 MHz, C_6D_6, 298 K) δ = Due to low solubility of compound, ^{29}Si NMR peak could not be observed; IR ν/cm^{-1} (Nujol): 2957 (s), 1609 (s), 1587 (m), 1499 (m), 1440 (s), 1421 (m), 1262 (s), 1239 (m), 1206 (m), 1168 (w), 1136 (w), 1117 (m), 1095 (w), 1076 (vs), 1046 (w), 1017 (m), 981 (m), 950 (m), 934 (m), 865 (m), 835 (s), 802 (s), 785 (vs), 777 (s), 767 (s), 755 (m), 743 (w), 728 (s), 700 (s), 688 (m), 663 (s); A reproducible microanalysis could not be obtained for the compound.

[{(Butiso)Si(μ-CO$_3$)}$_2$(μ-O)] (9). A solution of [{(Butiso)Si}$_2$] (100 mg, 0.10 mmol) in toluene (10 mL) was stirred under an atmosphere of dry CO_2 at room temperature for 1.5 hours. All the volatiles were subsequently removed from the reaction mixture *in vacuo* and the residue was extracted in hexane (10 mL). The extract was filtered and the solution was concentrated to ca. 8 mL. Storage at -30 ºC for two days led to the deposition of

[{(Butiso)Si(μ-CO_3)}$_2$(μ-O)] as colourless crystals. These were isolated and a second crop was obtained from the mother liquor (75 mg, 66.3 %). M.p. > 260 °C; ^{1}H NMR (400 MHz, C_6D_6, 298 K) δ = 0.74 (s, 18H, C(C*H*$_3$)$_3$), 0.99 (d, $^3J_{HH}$ = 6.8 Hz, 12H, CH(C*H*$_3$)$_2$), 1.33 (d, $^3J_{HH}$ = 6.7 Hz, 12H, CH(C*H*$_3$)$_2$), 3.79 (sept, $^3J_{HH}$ = 6.8 Hz, 4H, C*H*(CH$_3$)$_2$), 6.80 (d, $^3J_{HH}$ = 8.7 Hz, 4H, Ar-*H*), 6.99-7.09 (m, 12H, Ar-*H*), 7.28 (d, $^3J_{HH}$ = 8.7 Hz, 4H, Ar-*H*); ^{13}C{^{1}H} NMR (101 MHz, C_6D_6, 298 K) δ = 23.7, 25.3 (CH(*C*H$_3$)$_2$), 29.1 (*C*H(CH$_3$)$_2$), 30.5 (C(*C*H$_3$)$_3$), 34.8 (*C*(CH$_3$)$_3$), 122.6, 124.7, 125.3, 128.2, 131.3, 135.4, 146.0, 147.8 (Ar-*C*), 157.3 (N*C*N), 173.6 (N*C*O); ^{29}Si{^{1}H} NMR (80 MHz, C_6D_6, 298 K) δ = -121.1; IR ν/cm^{-1} (Nujol): 3063 (w), 2960 (s), 2336 (w), 1756 (vs), 1581 (s), 1510 (m), 1418 (s), 1296 (w), 1220 (vs), 1133 (m), 1099 (w), 1072 (s), 992 (m), 933 (w), 880 (vs), 822 (m), 785 (s), 755 (m), 726 (s); anal. calc. for $C_{72}H_{94}N_4O_7Si_2$: C 73.06 %, H 8.00 %, N 4.73 %, found: C 72.67 %, H 8.20 %, N 4.66 %.

[{(Butiso)Si(OH)(μ-O)}$_2$] (10). A solution of [{(Butiso)Si}$_2$] (100 mg, 0.10 mmol) in hexane (15 mL) was stirred under an atmosphere of dry N_2O at room temperature for 2 hours. The reaction mixture was filtered and the solution was concentrated to ca. 8 mL. Storage at -30 ºC for 2 days led to the deposition of [{(Butiso)Si(OH)(μ-O)}$_2$] as colourless crystals (50 mg, 47.0 %). M.p. 198 °C (decomp.); ^{1}H NMR (400 MHz, C_6D_6, 298 K) δ = 0.80 (s, 18H, C(C*H*$_3$)$_3$), 1.00 (d, $^3J_{HH}$ = 6.8 Hz, 24H, CH(C*H*$_3$)$_2$), 1.32 (d, $^3J_{HH}$ = 6.7 Hz, 24H, CH(C*H*$_3$)$_2$), 2.64 (s, 2H, O*H*), 3.89 (sept, $^3J_{HH}$ = 6.8 Hz, 8H, C*H*(CH$_3$)$_2$), 6.77 (d, $^3J_{HH}$ = 8.7 Hz, 4H, Ar-*H*), 7.08-7.14 (m, 12H, Ar-*H*), 7.33 (d, $^3J_{HH}$ = 8.6 Hz, 4H, Ar-*H*); ^{13}C{^{1}H} NMR (101 MHz, C_6D_6, 298 K) δ = 23.8, 25.1 (CH(*C*H$_3$)$_2$), 28.8 (*C*H(CH$_3$)$_2$), 30.7 (C(*C*H$_3$)$_3$), 34.7 (*C*(CH$_3$)$_3$), 124.2, 124.8, 125.2, 126.9, 130.9, 137.2, 145.4, 155.6 (Ar-*C*), 170.6 (N*C*N); ^{29}Si{^{1}H} NMR (80 MHz, C_6D_6, 298 K) δ = -102.4; IR ν/cm^{-1} (Nujol): 3685 (w, OH), 3653 (m, OH), 3059 (w), 2959 (s), 1609 (m), 1573 (s), 1542 (w), 1498 (w), 1425 (m), 1383 (s), 1289 (m), 1256 (w), 1200 (w), 1175 (w), 1132 (w), 1099 (m), 1052 (m), 985 (m), 932 (m), 865 (s), 835 (s), 804 (vs), 781 (s), 750 (s), 725 (vs), 696 (s); anal. calc. for $C_{70}H_{96}N_4O_4Si_2$: C 75.49 %, H 8.69 %, N 5.03 %, found: C 74.97 %, H 8.65 %, N 5.01 %.

[{(Butiso)Si(μ-C_2H_4)}$_2$] (11). A solution of {(Butiso)Si}$_2$ (150 mg, 0.14 mmol) in hexane (10 mL) was stirred under an atmosphere of dry C_2H_4 at room temperature for 1.5 hours. All volatiles were subsequently removed from the reaction mixture *in vacuo* and the residue was extracted in pentane (10 mL). The extract was filtered and the

solution was concentrated to ca. 8 mL. Storage at room temperature for 1 day led to the deposition of [{(Butiso)Si(μ-C_2H_4)}$_2$] as light-orange colored crystals. These were isolated and a second crop was obtained from the mother liquor (95 mg, 60.1 %). M.p. 122 °C (decomp.); ^{1}H NMR (400 MHz, C_6D_6, 298 K) δ = 0.62-0.67 (two overlapping t, 2H, SiC*H*$_2$), 0.83 (s, 18H, C(C*H*$_3$)$_3$), 0.95 (d, $^3J_{HH}$ = 6.7 Hz, 12H, CH(C*H*$_3$)$_2$), 1.08 (d, br, $^3J_{HH}$ = 6.6 Hz, 12H, CH(C*H*$_3$)$_2$), 1.21 (d, br, $^3J_{HH}$ = 6.2 Hz, 12H, CH(C*H*$_3$)$_2$), 1.35 (d, $^3J_{HH}$ = 6.7 Hz, 12H, CH(C*H*$_3$)$_2$), 1.76 (s, 2H, SiC*H*$_2$), 1.95 (d, br, $^3J_{HH}$ = 8.5 Hz, 2H, SiC*H*$_2$), 2.19 (d, br, $^3J_{HH}$ = 8.4 Hz, 2H, SiC*H*$_2$), 3.58 (overlapping sept, 4H, C*H*(CH$_3$)$_2$), 3.64 (overlapping, 4H, C*H*(CH$_3$)$_2$) 6.79-7.11 (m, 20H, Ar-*H*); ^{13}C{^{1}H} NMR (101 MHz, C_6D_6, 298 K) δ = -2.6, 7.3, 22.5 (Si*C*H$_2$), 23.2, 23.5, 25.3, 25.6 (CH(*C*H$_3$)$_2$), 25.7 (Si*C*H$_2$), 28.8, 28.9 (*C*H(CH$_3$)$_2$), 30.8 (C(*C*H$_3$)$_2$), 34.5 (*C*(CH$_3$)$_3$), 124.0, 124.8, 126.1, 127.1, 130.1, 139.3, 143.6, 153.6 (Ar-*C*), 164.9 (N*C*N); ^{29}Si{^{1}H} NMR (80 MHz, C_6D_6, 298 K) δ = -74.8; IR ν/cm^{-1} (Nujol): 3059 (w), 3019 (w), 2959 (vs), 1583 (vs), 1513 (m), 1410 (m), 1286 (m), 1253 (w), 1200 (w), 1178 (m), 1129 (s), 1095 (s), 1056 (s), 1022 (w), 978 (m), 961 (s), 932 (w), 862 (w), 837 (vs), 788 (s), 766 (m), 747 (s), 723 (w), 701 (w), 663 (s); anal. calc. for $C_{74}H_{102}N_4Si_2$: C 80.52 %, H 9.31 %, N 5.08 %, found: C 79.53 %, H 9.21 %, N 4.89 %.

[{(Butiso)Ge}$_2$(μ-C_2H_4)] (12). A solution of [{(Butiso)Ge}$_2$] (80 mg, 0.07 mmol) in toluene (15 mL) was stirred under an atmosphere of dry C_2H_4 at room temperature for 2 hours. All the volatiles were subsequently removed from the reaction mixture *in vacuo*. The residue was extracted in toluene (5 mL), filtered, concentrated to ca. 3 mL and layered with hexane. Storage at room temperature for 6-7 days led to the deposition of [{(Butiso)Ge}$_2$(μ-C_2H_4)] as light orange colored crystals (45 mg, 54.9 %). M.p. 172 °C (decomp.); ^{1}H NMR (600 MHz, C_6D_6, 298 K) δ = 0.84 (s, 18H, C(C*H*$_3$)$_3$), 0.93 (d, $^3J_{HH}$ = 6.8 Hz, 12H, CH(C*H*$_3$)$_2$), 1.08 (d, $^3J_{HH}$ = 6.9 Hz, 12H, CH(C*H*$_3$)$_2$), 1.18 (d, $^3J_{HH}$ = 6.8 Hz, 12H, CH(C*H*$_3$)$_2$), 1.44 (d, $^3J_{HH}$ = 6.8 Hz, 12H, CH(C*H*$_3$)$_2$), 1.67 (s, 4H, GeC*H*$_2$), 3.71 (sept, $^3J_{HH}$ = 6.8 Hz, 4H, C*H*(CH$_3$)$_2$), 4.01 (sept, $^3J_{HH}$ = 6.8 Hz, 4H, C*H*(CH$_3$)$_2$), 6.83 (d, $^3J_{HH}$ = 8.7 Hz, 4H, Ar-*H*), 7.00-7.06 (m, 12H, Ar-*H*), 7.18 (d, $^3J_{HH}$ = 8.6 Hz, 4H, Ar-*H*); ^{13}C{^{1}H} NMR (151 MHz, C_6D_6, 298 K) δ = 2×23.1 (CH(*C*H$_3$)$_2$), 26.1 (CH(*C*H$_3$)$_2$), 26.2 (Ge*C*H$_2$), 26.5 (CH(*C*H$_3$)$_2$), 28.8, 28.9 (*C*H(CH$_3$)$_2$), 30.8 (C(*C*H$_3$)$_3$), 34.6 (*C*(CH$_3$)$_3$), 124.0, 124.1, 125.1, 126.1, 127.6, 128.4, 128.5, 130.1, 139.4, 143.9, 144.4, 153.7, (Ar-*C*), 163.3 (N*C*N); IR ν/cm^{-1} (Nujol): 2958 (w), 2958 (s), 1617 (s), 1512(w), 1260 (s),

1192 (m), 1096 (s), 1019 (s), 965 (w), 800 (vs), 778 (s), 691 (s); A satisfactory reproducible microanalysis could not be obtained.

5.6 References

1 S. S. Sen, A. Jana, H. W. Roesky and C. Schulzke, *Angew. Chem., Int. Ed.*, 2009, **48**, 8536–8538.

2 C. Jones, S. J. Bonyhady, N. Holzmann, G. Frenking and A. Stasch, *Inorg. Chem.*, 2011, **50**, 12315–12325.

3 S. S. Sen, G. Tavčar, H. W. Roesky, D. Kratzert, J. Hey and D. Stalke, *Organometallics*, 2010, **29**, 2343–2347.

4 S. Yao, Y. Xiong, M. Brym and M. Driess, *J. Am. Chem. Soc.*, 2007, **129**, 7268–7269.

5 D. Gau, R. Rodriguez, T. Kato, N. Saffon-Merceron, A. De Cózar, F. P. Cossío and A. Baceiredo, *Angew. Chem., Int. Ed.*, 2011, **50**, 1092–1096.

6 C. Shan, S. Yao and M. Driess, *Chem. Soc. Rev.*, 2020, **49**, 6733–6754.

7 G. H. Spikes, J. C. Fettinger and P. P. Power, *J. Am. Chem. Soc.*, 2005, **127**, 12232–12233.

8 F. Hanusch, L. Groll and S. Inoue, *Chem. Sci.*, 2021, **12**, 2001–2015.

9 A. V. Protchenko, K. H. Birjkumar, D. Dange, A. D. Schwarz, D. Vidovic, C. Jones, N. Kaltsoyannis, P. Mountford and S. Aldridge, *J. Am. Chem. Soc.*, 2012, **134**, 6500–6503.

10 G. D. Frey, V. Lavallo, B. Donnadieu, W. W. Schoeller and G. Bertrand, *Science*, 2007, 439–441.

11 R. Kalescky, E. Kraka and D. Cremer, *J. Phys. Chem. A*, 2013, **117**, 8981–8995.

12 A. Y. Khodakov, W. Chu and P. Fongarland, *Chem. Rev.*, 2007, **107**, 1692–1744.

13 A. V. Protchenko, P. Vasko, D. C. H. Do, J. Hicks, M. Á. Fuentes, C. Jones and S. Aldridge, *Angew. Chem., Int. Ed.*, 2019, **58**, 1808–1812.

14 P. A. Bianconi, I. D. Williams, M. P. Engeler and S. J. Lippard, *J. Am. Chem. Soc.*, 1986, **108**, 311–313.

15 P. W. Lednor and P. C. Versloot, *J. Chem. Soc., Chem. Commun.*, 1983, **983**, 284–285.

16 R. N. Vrtis, C. P. Rao, S. G. Bott and S. J. Lippard, *J. Am. Chem. Soc.*, 1988, **110**, 7564–7566.

17 J. D. Protasiewicz and S. J. Lippard, *J. Am. Chem. Soc.*, 1991, **113**, 6564–6570.

18 A. S. Frey, F. G. N. Cloke, P. B. Hitchcock, I. J. Day, J. C. Green and G. Aitken, *J. Am. Chem. Soc.*, 2008, **130**, 13816–13817.

19 P. L. Arnold, Z. R. Turner, R. M. Bellabarba and R. P. Tooze, *Chem. Sci.*, 2011, **2**, 77–79.

20 S. M. Mansell, N. Kaltsoyannis and P. L. Arnold, *J. Am. Chem. Soc.*, 2011, **133**, 9036–9051.

21 Y. Wang, A. Kostenko, T. J. Hadlington, M. P. Luecke, S. Yao and M. Driess, *J. Am. Chem. Soc.*, 2019, **141**, 626–634.

22 M. J. Cowley, Y. Ohmori, V. Huch, M. Ichinohe, A. Sekiguchi and D. Scheschkewitz, *Angew. Chem., Int. Ed.*, 2013, **52**, 13247–13250.

23 H. X. Yeong, H. W. Xi, K. H. Lim and C. W. So, *Chem. - Eur. J.*, 2010, **16**, 12956–12961.

24 C. W. So, H. W. Roesky, J. Magull and R. B. Oswald, *Angew. Chem., Int. Ed.*, 2006, **45**, 3948–3950.

25 J. Böserle, G. Zhigulin, P. Štěpnička, F. Horký, M. Erben, R. Jambor, A. Růžička, S. Ketkov and L. Dostál, *Dalton Trans.*, 2017, **46**, 12339–12353.

26 S. H. Zhang, H. W. Xi, K. H. Lim, Q. Meng, M. B. Huang and C. W. So, *Chem. - Eur. J.*, 2012, **18**, 4258–4263.

27 R. Azhakar, R. S. Ghadwal, H. W. Roesky, H. Wolf and D. Stalke, *J. Am. Chem. Soc.*, 2012, **134**, 2423–2428.

28 W. Wang, S. Inoue, S. Yao and M. Driess, *J. Am. Chem. Soc.*, 2010, **132**, 15890–15892.

29 T. Iwamoto and S. Ishida, in *Organosilicon Compounds: Theory and Experiment (Synthesis)*, Elsevier Inc., 2017, pp. 361–532.

30 S. S. Sen, D. Kratzert, D. Stern, H. W. Roesky and D. Stalke, *Inorg. Chem.*, 2010, **49**, 5786–5788.

31 L. W. Pineda, V. Jancik, J. F. Colunga-Valladares, H. W. Roesky, A. Hofmeister and J. Magull, *Organometallics*, 2006, **25**, 2381–2383.

32 F. M. Mück, D. Kloß, J. A. Baus, C. Burschka and R. Tacke, *Chem. - Eur. J.*, 2014, **20**, 9620–9626.

33 K. Junold, J. A. Baus, C. Burschka, T. Vent-schmidt, S. Riedel and R. Tacke, *Inorg. Chem.*, 2013, **52**, 11593–11599.

34 M. El Ezzi, T. G. Kocsor, F. D'Accriscio, D. Madec, S. Mallet-Ladeira and A.

Castel, *Organometallics*, 2015, **34**, 571–576.

35 *As determined from a survey of the Cambridge Crystallographic Database, January, 2021.*

36 R. G. Pearson, *Science*, 1966, **151**, 172–177.

37 R. G. Pearson, *J. Am. Chem. Soc.*, 1963, **85**, 3533–3539.

38 M. L. McCrea-Hendrick, C. A. Caputo, J. Linnera, P. Vasko, C. M. Weinstein, J. C. Fettinger, H. M. Tuononen and P. P. Power, *Organometallics*, 2016, **35**, 2759–2767.

39 N. S. Nametkin, B. I. Kolobkov, V. D. Tyurin, A. N. Muratov, A. I. Nekhaev, M. Mavlonov, A. Y. Sideridu, G. G. Aleksandrov, A. V. Lebedev, M. T. Tashev and H. B. Dustov, *J. Organomet. Chem.*, 1984, **276**, 393–397.

40 R. B. King, F.-J. Wu, N. D. Sadanani and E. M. Holt, *Inorg. Chem.*, 1985, **24**, 4449–4450.

41 H. P. Hickox, Y. Wang, Y. Xie, M. Chen, P. Wei, H. F. Schaefer and G. H. Robinson, *Angew. Chem., Int. Ed.*, 2015, **54**, 10267–10270.

42 M. Elder, *Inorg. Chem.*, 1969, **8**, 2703–2708.

43 W. Yang, H. Fu, H. Wang, M. Chen, Y. Ding, H. W. Roesky and A. Jana, *Inorg. Chem.*, 2009, **48**, 5058–5060.

44 B. Blom, M. Pohl, G. Tan, D. Gallego and M. Driess, *Organometallics*, 2014, **33**, 5272–5282.

45 T. A. Schmedake, M. Haaf, B. J. Paradise, A. J. Millevolte, D. R. Powell and R. West, *J. Organomet. Chem.*, 2001, **636**, 17–25.

46 K. Junold, J. A. Baus, C. Burschka, T. Vent-Schmidt, S. Riedel and R. Tacke, *Inorg. Chem.*, 2013, **52**, 11593–11599.

47 K. Ueno, A. Masuko and H. Ogino, *Organometallics*, 1999, **18**, 2694–2699.

48 N. Wiberg, G. Wagner and G. Müller, *Angew. Chem., Int. Ed.*, 1985, **24**, 229–230.

49 K. Takeuchi, M. Ichinohe and A. Sekiguchi, *J. Am. Chem. Soc.*, 2011, **133**, 12478–12481.

50 C. Chatgilialoglu and H. Schiesser, C., in *The Chemistry of Organic Silicon Compounds,* Vol. 3, 1990, pp. 341–390.

51 C. Chatgilialoglu, *Chem. Rev.*, 1995, **95**, 1229–1251.

52 Y. Wang, M. Chen, Y. Xie, P. Wei, H. F. Schaefer and G. H. Robinson, *J. Am. Chem. Soc.*, 2015, **137**, 8396–8399.

53 M. Santoro, F. Gorelli, J. Haines, O. Cambon, C. Levelut and G. Garbarino, *Proc. Natl. Acad. Sci. U. S. A.*, 2011, **108**, 7689–7692.

54 R. Azhakar, K. Pröpper, B. Dittrich and H. W. Roesky, *Organometallics*, 2012, **31**, 7586–7590.

55 R. Azhakar, R. S. Ghadwal, H. W. Roesky, H. Wolf and D. Stalke, *Chem. Commun.*, 2012, **48**, 4561–4563.

56 R. Siefken, M. Teichert, D. Chakraborty and H. W. Roesky, *Organometallics*, 1999, **18**, 2321–2325.

57 Y. Peng, B. D. Ellis, X. Wang, J. C. Fettinger and P. P. Power, *Science*, 2009, **325**, 1668–1670.

58 T. J. Hadlington, J. Li, M. Hermann, A. Davey, G. Frenking and C. Jones, *Organometallics*, 2015, **34**, 3175–3185.

59 J. A. Kelly, M. Juckel, T. J. Hadlington, I. Fernández, G. Frenking and C. Jones, *Chem. - Eur. J.*, 2019, **25**, 2773–2785.

60 A. Kostenko and M. Driess, *J. Am. Chem. Soc.*, 2018, **140**, 16962–16966.

61 T. J. Hadlington, M. Hermann, G. Frenking and C. Jones, *Chem. Sci.*, 2015, **6**, 7249–7257.

Appendix I

General Synthetic Considerations

All manipulations were carried out using standard Schlenk and glove box techniques under an atmosphere of high purity dinitrogen. Diethyl ether and pentane were distilled over Na/K alloy (25:75), while THF, hexane and toluene were distilled over molten potassium. Dichloromethane was distilled over CaH_2. Benzene-d_6 and toluene-d_8 were stored over a sodium mirror and activated molecular sieves 4 Å, respectively and degassed three times via freeze-pump-thawing before use. ^{1}H, $^{13}C\{^{1}H\}$, $^{29}Si\{^{1}H\}$, $^{119}Sn\{^{1}H\}$ and $^{7}Li\{^{1}H\}$ NMR spectra were recorded on either Bruker Advance III 400 or Bruker Advance III 600 spectrometers and were referenced to the resonances of the solvent used, external $SiMe_4$, $SnMe_4$, or LiCl (1 M in D_2O). Mass spectra were run using an Agilent Technologies 5975D inert MSD with a solid-state probe. FTIR spectra were collected for solid samples or Nujol mulls on an Agilent Cary 630 attenuated total reflectance (ATR) spectrometer. Irradiations were carried out using UV (λ = 370 nm, 43W) light LED lamps, with the reaction vessel placed approximately 2 cm from the light source, whilst being cooled by an external fan. Melting points were determined in sealed glass capillaries under dinitrogen and are uncorrected. Microanalyses were carried out at the Science Centre, London Metropolitan University or using a PerkinElmer- 2400 CHNS/O Series II System. H_2, CO, ^{13}CO, CO_2, N_2O and C_2H_4 were dried over P_2O_5 prior to use. Bu^{t}NC was dried over activated molecular sieves 3 Å. All other reagents were used as received.

Appendix II

Crystallographic Data

For full crystallographic data, in the form of .cif files, please find the attached DVD. X-ray diffraction studies were performed on a Bruker X8 APEX CCD using a graphite monochromator with Mo Kα radiation (λ = 0.71073 Å), an Oxford Gemini Ultra diffractometer using a graphite monochromator with Mo Kα radiation (λ = 0.71073 Å) or Cu Kα radiation (1.54180 Å), Rigaku Xtalab Synergy Dualflex using a graphite monochromator with Mo Kα radiation (0.71073 Å) or Cu Kα radiation (1.54180 Å), or the MX1 and MX2 beamlines of the Australian Synchrotron. The software package Blu-Ice[1] was used for synchrotron data acquisition, while the program XDS[2] was employed for synchrotron data reduction. All structures were solved by direct methods and refined on F2 by full matrix least squares (SHELX-16[3]) using all unique data.

References

1 T. M. Mcphillips, S. E. Mcphillips, A. E. Cohen, A. M. Deacon, J. Paul, E. Garman, A. Gonzalez, K. Nicholas, R. P. Phizackerley and S. Michael, *J. Synchrotron Rad.*, 2002, **9**, 401–406.

2 W. Kabsch, *J. Appl. Crystallogr.*, 1993, **26**, 795–800.

3 G. M. Sheldrick, *SHELX-16, University of Göttingen,* 2016.

Appendix III

Computational Studies

All structure optimisation in chapter 2 were obtained using DFT calculations at bvp86/def2svp theory level. Computational studies in chapter 5 were performed by C. Smith at the B3PW91/6-31+G(d) level of theory, unless otherwise stated.

Appendix IV

Publications in Support of this Thesis

s- and p-Block Dinuclear Metal(loid) Complexes Bearing 1,4-Phenylene and 1,4-Cyclohexylene Bridged Bis(amidinate) Ligands; P. Garg, D. Dange and C. Jones, *Eur. J. Inorg. Chem.*, 2020, **2020**, 4037–4044.

Bulky Arene-Bridged Bis(amide) and Bis(amidinate) Complexes of Germanium(II) and Tin(II); P. Garg, D. Dange and C. Jones, *Dalton Trans.*, 10.1039/D1DT01642C, *Accepted for publication.*

Reversible Activation of Carbon Monoxide with Amidinate supported Silicon(I) Dimer, P. Garg et al., *manuscript under preparation*.

A Comparative Study of Steric Bulk: Towards the Chlorogermylenes and Digermynes, P. Garg et al., *manuscript under preparation*.